

Aus der Klinik für Frauenheilkunde und Geburtshilfe
der Charité Campus Virchow-Klinikum
(Direktor: Prof. Dr. med. W. Lichtenegger)
Medizinische Fakultät der Humboldt-Universität zu Berlin

MOLECULAR GENETIC ALTERATIONS IN OVARIAN CANCER
The Role of the p53 Tumor Suppressor Gene and the mdm2 Oncogene

Habilitationsschrift
zur Erlangung der Venia legendi
für das Fach

Gynäkologie und Geburtshilfe

vorgelegt von

Dr. med. Angela Reles

Präsident: Prof. Dr. rer. nat. J. Mlynek

Dekan: Prof. Dr. med. Joachim W. Dudenhausen

Eingereicht im: 28.03.2001

Öffentlich-wissenschaftlicher Vortrag: 04.12.2001

Gutachter: 1. Frau Prof. Dr. med. M. Kiechle
2. Herr Prof. Dr. med. D. Kieback

TABLE OF CONTENTS

ABBREVIATIONS	v
1. INTRODUCTION.	1
1.1 Clinical and histopathological aspects of ovarian tumors	1
1.1.1 Diagnosis and clinical aspects	1
1.1.2 Histological classification of epithelial ovarian tumors	2
1.1.3 Therapeutic aspects of epithelial ovarian tumors	2
1.1.4 Clinical course and prognosis	5
1.2 Molecular genetic alterations in ovarian tumors	6
1.2.1 Hereditary ovarian tumors	6
1.2.2 Sporadic ovarian tumors	8
1.2.3 Gene therapy	11
1.3 The <i>p53</i> tumor suppressor gene	13
1.3.1 <i>p53</i> domains: structure and function	13
1.3.2 <i>p53</i> response to cellular stress: Upstream events	15
1.3.3 Downstream mediators of <i>p53</i> -dependent cell cycle arrest	18
1.3.4 Mechanisms of <i>p53</i> -dependent apoptosis	20
1.3.5 <i>p53</i> and genomic stability	21
1.3.6 The role of <i>p53</i> in tumorigenesis	22
1.3.7 Clinical implications	23
1.3.8 <i>p53</i> and efficacy of chemotherapeutic agents	24
1.4 The <i>mdm2</i> (murine double minute 2) gene	26
1.4.1 Molecular structure of the <i>mdm2</i> gene	26
1.4.2 <i>mdm2</i> expression in tumors	27
1.4.3 The MDM2/ <i>p53</i> autoregulatory feedback-loop	28
1.4.4 Clinical implications of <i>mdm2</i> alterations	36
2. OBJECTIVES	34
3. PATIENTS, MATERIALS, AND METHODS	35
3.1 Patients and clinical data	35
3.1.1 Asservation and storage of tissue	35
3.1.2 Study population and surgical therapy	35
3.1.3 FIGO-stage, histology and grade of differentiation	35
3.1.4 Adjuvant chemotherapy	36
3.1.5 Clinical follow-up information	36
3.2 Materials	37
3.2.1 Plastic ware, chemicals, and consumables	37
3.2.2 Standard buffers and solutions	37
3.2.3 Standard gel electrophoresis components	39
3.2.4 Chemicals	39
3.2.5 Radio-chemicals	42
3.2.6 Standard kits.	42
3.2.7 Monoclonal and polyclonal antibodies	42
3.2.8 Laboratory equipment and other materials	43

3.3	Methods	43
3.3.1	Immunohistochemistry	43
3.3.1.1	<i>Sections of tissues and control cell lines</i>	43
3.3.1.2	<i>Incubation with primary and secondary antibodies</i>	44
3.3.1.3	<i>Peroxidase-antiperoxidase reaction</i>	44
3.3.1.4	<i>Microscopic evaluation</i>	44
3.3.2	Molecular biology techniques	44
3.3.2.1	<i>Isolation of genomic DNA from frozen tumor tissue</i>	44
3.3.2.2	<i>Isolation of genomic DNA from paraffin embedded tissue</i>	45
3.3.2.3	<i>Polymerase chain reaction (PCR) for p53</i>	45
3.3.2.4	<i>Single strand conformation polymorphism (SSCP)</i>	47
3.3.2.5	<i>DNA sequence analysis</i>	48
3.3.2.6	<i>Automated DNA sequencing.</i>	50
3.3.2.7	<i>Isolation of total RNA from tumor tissue</i>	51
3.3.2.8	<i>Northern hybridization.</i>	51
3.3.2.9	<i>Southern hybridization</i>	52
3.3.2.10	<i>cDNA synthesis</i>	53
3.3.2.11	<i>Polymerase chain reaction (PCR) with nested primers</i>	54
3.3.2.12	<i>Subcloning of cDNA into a TA cloning vector.</i>	56
3.3.2.13	<i>Growth and storage of bacteria</i>	57
3.3.2.14	<i>Generation of electro-competent bacteria.</i>	58
3.3.2.15	<i>Small scale (mini-prep) and medium scale preparation (midi-prep) of plasmid DNA</i>	59
3.3.2.16	<i>Restriction enzyme digestion of plasmid DNA and PCR product</i>	60
3.3.2.17	<i>Sequencing of DNA fragments cloned into the pCR™2.1 vector</i>	60
3.3.2.18	<i>Gel extraction of PCR products for sequencing</i>	60
3.3.2.19	<i>Sequencing of cDNA PCR products after gel purification</i>	61
3.3.2.20	<i>Primer design and PCR for in vitro protein expression using the pcDNA3 vector</i>	61
3.3.2.21	<i>Purification and restriction enzyme digestion of PCR product and pcDNA3 vector</i>	63
3.3.2.22	<i>Ligation of mdm2 splice variant DNA into the pcDNA3 expression vector</i>	64
3.3.2.23	<i>Transformation of pcDNA3/cDNA constructs into electro-competent E.coli bacteria.</i>	65
3.3.2.24	<i>Restriction enzyme digestion of the pcDNA3 vector containing the cDNA insert</i>	65
3.3.2.25	<i>Transient transfection of HeLa-cells with the cDNA containing plasmid</i>	66
3.3.3	Biochemical techniques	68
3.3.3.1	<i>Preparation of cell lysates for SDS-polyacrylamide gel electrophoresis (SDS-PAGE)</i>	68
3.3.3.2	<i>SDS-polyacrylamide gel electrophoresis (SDS-PAGE)</i>	68
3.3.3.3	<i>Western blotting of p53 and MDM2 proteins fractionated by SDS-PAGE</i>	69
3.4	Statistical tests	70
4.	RESULTS	72
4.1	Alterations of the p53 tumor suppressor gene in ovarian cancer	72
4.1.1	<i>p53 mutations</i>	72
4.1.2	<i>p53 polymorphisms and intron alterations</i>	80
4.1.3	<i>Confirmation of p53 polymorphisms in normal tissue DNA</i>	83

4.1.4	p53 protein overexpression.	83
4.1.5	Comparison of p53 overexpression with <i>p53</i> mutations	88
4.1.6	<i>p53</i> polymorphisms and p53 protein overexpression	88
4.1.7	Correlation of <i>p53</i> alterations with histopathological and clinical data	90
4.1.8	<i>p53</i> alterations and response to chemotherapy	90
4.1.9	<i>p53</i> alterations as a predictor of time to progression and overall survival	92
4.1.10	Univariate and multivariable analysis of prognostic factors	95
4.2	Alterations of the <i>mdm2</i> gene in ovarian cancer	101
4.2.1	Expression and absence of amplification of <i>mdm2</i> in ovarian cancer	101
4.2.2	<i>mdm2</i> alternative and aberrant RNA splicing in ovarian cancer	102
4.2.3	Loss of p53 binding sequence in <i>mdm2</i> splice variants	109
4.2.4	<i>mdm2</i> splice sites and repeat sequences	109
4.2.5	<i>mdm2</i> alterations in ovarian cystadenomas and borderline tumors	111
4.2.6	<i>mdm2</i> alterations in normal ovarian tissue	113
4.2.7	In vitro expression of p53 and MDM2 splice variant proteins	115
4.2.8	Correlation of <i>mdm2</i> and <i>p53</i> alterations	116
4.2.9	Correlation of <i>mdm2</i> alterations with histopathological and clinical data	118
4.2.10	<i>mdm2</i> alterations and clinical outcome in ovarian cancer	120
5.	DISCUSSION	125
5.1	Alterations of the <i>p53</i> tumor suppressor gene in ovarian cancer	125
5.1.1	<i>p53</i> mutations	125
5.1.2	<i>p53</i> mutations in evolutionary highly conserved domains	127
5.1.3	<i>p53</i> polymorphisms and intron alterations	128
5.1.4	p53 protein overexpression	132
5.1.5	Correlation of p53 overexpression with <i>p53</i> mutations	133
5.1.6	<i>p53</i> alterations and response to chemotherapy	133
5.1.7	<i>p53</i> alterations as a predictor of time to progression and overall survival	136
5.2	Alterations of the <i>mdm2</i> gene in ovarian cancer	138
5.2.1	<i>mdm2</i> expression and absence of amplification in ovarian cancer	138
5.2.2	<i>mdm2</i> alternative and aberrant RNA splicing in ovarian cancer	139
5.2.3	Loss of p53 binding sequence in <i>mdm2</i> splice variants	141
5.2.4	<i>mdm2</i> splice sites and repeat sequences	143
5.2.5	<i>mdm2</i> alterations in ovarian cystadenomas and borderline tumors	144
5.2.6	<i>mdm2</i> alterations in normal ovarian tissue	144
5.2.7	In vitro expression of p53 and MDM2 splice variant proteins	146
5.2.8	Correlation of <i>mdm2</i> and <i>p53</i> alterations	147
5.2.9	Correlation of <i>mdm2</i> alterations with histopathological and clinical data	148
5.2.10	<i>mdm2</i> alterations and clinical outcome in ovarian cancer	148
6.	SUMMARY AND CONCLUSIONS	150
7.	REFERENCES	154
	ACKNOWLEDGEMENTS .	179

ABBREVIATIONS

aa	amino acid
Ab	antibody
APS	ammoniumpersulfat
Asn	antisense
bp	basepair
BPB	bromophenol blue
BSA	bovine serum albumine
DEPC	diethyl-pyrocabonate
ddH ₂ O	double distilled H ₂ O
ddATP	2',3'-dideoxy-adenine-5'triphosphate
ddCTP	2',3'-dideoxy-cytosine-5'triphosphate
ddGTP	2',3'-dideoxy-guanine-5'triphosphate
ddTTP	2',3'-dideoxy-thymine-5'triphosphate
DNA	deoxyribonucleic acid
DNA-PK	DNA-activated protein kinase
dNTP	2'-deoxynucleoside-5'triphosphate
DTT	dithiotreitol
ECL	enhanced chemiluminescence
EDTA	ethylenediamine-tetraacetate
EtBr	ethidiumbromide
FCS	fetal calf serum
FIGO	Fédération Internationale de Gynécologie et d'Obstétrique
GTB	glycerol tolerant buffer
HA	hemagglutinine
HEPES	(N-[2-hydroxyethyl]piperazine-N'-[2-ethanesulfonic acid])
HRPO	horse radish peroxidase
Ig	immunoglobuline
Im	immunostaining
kB	kilo base
kD	kilo Dalton
LMP	low malignant potential tumor
LOH	loss of heterozygosity
<i>mdm2</i>	murine double minute 2 gene
MDM2	90 kD protein of the <i>mdm2</i> gene
MOPS	3-[N-morpholino]propane sulfonic acid
Mut	Mutation
MW	molecular weight

NER	nucleotide excision repair
NES	nuclear export signal
OD	optical density
<i>p53</i>	p53 tumor suppressor gene
p53	53 kD protein of the <i>p53</i> gene
PAGE	polyacrylamide gel electrophoresis
PCNA	proliferating cell nuclear antigen
PCR	Polymerase Chain Reaction
PIG	p53-induced gene
PMSF	phenylmethylsulfonylfluoride
RNA	ribonucleic acid
RT	room temperature
RT-PCR	reverse transcriptase polymerase chain reaction
SDS	sodium dodecyl sulfate
sec	seconds
Sn	sense
SF	serum free
SSCP	single strand conformation polymorphism
SST	sequence specific transactivation
TAE	buffer containing Tris-Acetate and EDTA
TBE	buffer containing Tris, boric acid, EDTA
TEMED	N,N,N',N'-tetramethylethylenediamine
UV	ultra violet
WT	wild type
XC	xlenecyanol
X-gal	5-bromo-4-chloro-3-indolyl- β -D-galactopyranoside

1. INTRODUCTION

1.1 Clinical and histopathological aspects of ovarian tumors

1.1.1 Diagnosis and clinical aspects

Ovarian cancer is the leading cause of death from gynecologic malignancies, and the fifth most common malignant condition among women in the United States, with an annual incidence of 25.400 and approximately 14.500 deaths each year (Landis et al. 1998). The majority of women, approximately 70%, present with advanced stage disease with either regional or distant metastases at the time of diagnosis (Landis et al. 1998).

The incidence of ovarian cancer increases with age and peaks in the eighth decade. The rate increases from 15.7/100,000 in the 40 to 44 age group to a peak rate of 54/100,000 in the 75 to 79 age group. The median age at diagnosis is 61 years (Averette et al. 1995). The risk of developing ovarian cancer in a lifetime is only 1.4% in women with negative family history, but can increase to 14.6%- 32.2% in women with a family history and germline mutations of the *BRCA1* gene at the age of 60 years (Tortolero-Luna et al. 1994, Laplace-Marieze et al. 1999, Whittemore et al. 1997).

Epidemiologic studies have shown weak or mixed degrees of correlation with increased risk for ovarian cancer for tobacco smoke, radiation exposure, talc in genital hygiene, psychotropic medication, the mumps virus, high level physical activity, and dietary factors (as reviewed by Holschneider and Berek, 2000). Infertility has been found to be a significant risk factor for ovarian cancer, while parity, lactation, and oral contraceptive use have a protective effect (as reviewed by Holschneider and Berek, 2000). This supports the „incessant ovulation,, hypothesis for ovarian cancer. According to this hypothesis, ovarian cancer develops from an aberrant repair process of the surface epithelium which is ruptured and repaired during each ovulatory cycle (Fathalla, 1971). Long term use of oral contraceptives reduces the risk of developing ovarian cancer by 50% (Whittemore et al. 1992).

The diagnosis of ovarian cancer is mainly based on bimanual palpation and transvaginal sonography. CT and MRT can be useful to obtain information about the spread of the disease, lymph node involvement and liver metastases. The ultrasound criteria of an adnexal mass suspicious for malignancy are the presence of cystic or polycystic tumors with solid structures, completely solid structures, thick irregular septae, ascites, and evidence of infiltration into adjacent organs (Reles et al. 1997, 1998). The sensitivity of transvaginal ultrasound for the diagnosis of ovarian cancer in this tumor cohort was as high as 95% and specificity was found to be 82% (Reles et al.

1998). Transvaginal color Doppler sonography is also routinely used for the diagnosis of ovarian cancer since the blood vessel resistance in malignant ovarian tumors is significantly lower than in benign tumors due to tumor neovascularization. The value of the method though is limited by a relatively low specificity of 69% (Reles et al. 1998).

1.1.2 Histological classification of epithelial ovarian tumors

Malignant epithelial ovarian tumors, including tumors of borderline malignancy, account for almost 90% of all ovarian carcinomas (Scully, 1979). The tumors of "common epithelial origin,, arise from the surface epithelium of the ovary. During embryonic life the celomic cavity forms and is lined by a layer of mesothelium, parts of which become specialized to form the serosal epithelium covering the gonadal ridge. By a process of invagination, this same mesothelial lining gives rise to the müllerian ducts, from which arise the fallopian tube, uterus, and vagina (Kurman, 1987).

As the ovary develops, the surface epithelium extends into the ovarian stroma to form inclusion glands and cysts (Clement, 1987). The epithelium, in becoming malignant, exhibits a variety of müllerian type differentiations: serous (resembling fallopian tube), mucinous (resembling the endocervix), endometrioid (resembling endometrium), and clear cell (cells resembling endometrial glands in pregnancy) tumors. The ovarian surface epithelium, within its repertoire of differentiation, can also exhibit urothelial differentiation in the form of transitional cells. Table 1 presents the histologic classification scheme which has been developed and continuously updated under the auspices of WHO, International Federation of Gynecology and Obstetrics (FIGO), International Society of Gynecologic Pathologists, and Society of Gynecologic Oncologists (Scully, 1979).

1.1.3 Therapeutic aspects of epithelial ovarian tumors

The standard of care for newly diagnosed advanced ovarian cancer currently includes cytoreductive surgery, followed by combination chemotherapy with platinum and paclitaxel. Optimal tumor debulking is critical in the management of ovarian carcinoma and residual disease has been shown to be one of the most important factors influencing survival in patients with advanced ovarian carcinoma (Makar et al. 1995, Eisenkop et al. 1998). Patients in stage IIIc and IV ovarian carcinoma have a

Table 1: Histologic classification of common epithelial tumors of the ovary**SEROUS TUMORS**

Benign:	Cystadenoma and papillary cystadenoma Surface papilloma
Borderline:*	Adenofibroma and cystadenofibroma Cystadenoma and papillary cystadenoma Surface papilloma
Malignant:	Adenofibroma and cystadenofibroma Papillary adenocarcinoma and papillary cystadenocarcinoma Surface papillary carcinoma Malignant adenofibroma and cystadenofibroma

MUCINOUS TUMORS

Benign:	Cystadenoma Adenofibroma and cystadenofibroma
Borderline:	Cystadenoma Adenofibroma and cystadenofibroma
Malignant:	Adenocarcinoma and cystadenofibroma Malignant adenofibroma and cystadenofibroma

ENDOMETRIOID TUMORS

Benign:	Adenoma and cystadenoma Adenofibroma and cystadenofibroma
Borderline:	Adenoma and cystadenoma Adenofibroma and cystadenofibroma
Malignant:	Adenocarcinoma Adenoacanthoma Adenosquamous carcinoma Malignant adenofibroma and cystadenofibroma
Epithelial-stromal and stromal:	Adenosarcoma Stromal sarcoma Mesodermal (müllerian) mixed tumors, homologous and heterologous

CLEAR CELL (MESONEPHROID) TUMORS

Benign:	Adenofibroma
Borderline	
Malignant:	Adenocarcinoma (carcinoma)

TRANSITIONAL CELL TUMORS

Benign	Brenner Tumor
Borderline:	Proliferating Brenner Tumor
Malignant	Malignant Brenner tumor Transitional cell carcinoma

MIXED EPITHELIAL TUMORS

Benign
Borderline
Malignant

UNDIFFERENTIATED CARCINOMA**UNCLASSIFIED EPITHELIAL TUMORS**

*Tumors of borderline malignancy / Carcinoma of low malignant potential (LMP)

significantly better survival if postoperatively no residual tumor remains as compared to those who have a residual tumor of 10 mm or more (Eisenkop et al. 1998).

As a standard surgical approach a midline incision extending from the symphysis to above the umbilicus or to the xiphoid is performed. After obtaining histological confirmation by frozen section, bilateral salpingo-oophorectomy, hysterectomy, infragastric omentectomy, and pelvic and paraaortic lymphadenectomy are performed. Appendectomy is optional. Resection of the small intestine, colon, peritoneal surfaces, partial gastrectomy, partial liver resection, and urinary tract surgery are performed as necessary, depending on the extent of metastasis. Diffuse peritoneal spread of the carcinoma is treated by infrared light thermocoagulation. The incidence of lymph node metastasis has been reported to be as high as 64%-75% in advanced stage carcinomas, but even in stage I carcinomas, lymph node metastasis have been found in up to 24% of the cases (Burghardt et al. 1991, Petru et al. 1994). Pelvic and paraaortic lymphadenectomy is therefore routinely performed at the Department of Gynecology, Charité Campus Virchow-Klinikum as part of the primary surgery. The aim of surgery is optimal debulking with resection of all visible tumor.

Surgery is followed by adjuvant combination chemotherapy in all cases of FIGO-stage Ic-IV. In stage Ia and Ib disease, the decision depends on the histologic grading of the tumor. Stage Ia/Ib ovarian carcinomas with grade I do not need to receive adjuvant chemotherapy while patients with G3 tumors would be treated with chemotherapy. In stage Ia/Ib, grade II tumors, decision should be made individually.

The standard combination chemotherapy for adjuvant treatment of primary tumors is Carboplatin and Paclitaxel. Application of Cisplatin (75 mg/m²) and Paclitaxel (135 mg/m², 24h infusion) has been shown to be superior to Cisplatin in combination with Cyclophosphamide (750 mg/m²) (McGuire et al. 1996). Because of the toxicity profile of Cisplatin, especially nephro- and neurotoxicity, and similar reponse rates of Cisplatin and Carboplatin, the present regimen for most hospitals as first line treatment of ovarian cancer is Carboplatin AUC 6 and Paclitaxel 175 mg/m² (3-h-infusion). However, resistance to chemotherapy remains a complex problem. Despite high overall clinical response rates of up to 80% including a high proportion of complete reponses achieved with platinum-based therapy, most patients subsequently relapse and require additional treatment (McGuire and Ozols, 1998).

A consensus for the treatment of recurrent ovarian cancer has not been established so far. Patients with late recurrency (>12 months after completion of primary chemotherapy) benefit from surgical tumor debulking in terms of median survival and response to a second line chemotherapy. In a multidisciplinary approach in a team of gynecologists, surgeons and urologists we try to achieve optimal tumor debulking by surgery for recurrent disease followed by second line chemotherapy.

Patients who were initially sensitive to platinum-based chemotherapy have demonstrated relatively high response rates (40%-50%) to second-line platinum-based therapy (Markman et al. 1991).

Promising results have been found for Topotecan, a topoisomerase I inhibitor (Hycamtin, SmithKline Beecham Pharmaceuticals, Philadelphia, PA) with response rates of up to 31% in recurrent ovarian cancer, depending on initial response to platinum-based chemotherapy (ten Bokkel Huinink et al. 1997). Another substance that may play an important role for second line chemotherapy in the future is Gemcitabine, a novel nucleoside analog, which has been shown to have response rates as high as 19% in patients with recurrent ovarian cancer who had been resistant to previous first line Cisplatin chemotherapy (Lund et al. 1994).

Other substances for chemotherapy of recurrent ovarian cancer include Etoposide, Treosulfan, pegylated liposomal Doxorubicin, and Docetaxel. The primary goal of therapy in relapsed ovarian cancer is to extend survival time by maximizing all available therapies while minimizing side effects and preserving quality of life.

1.1.4 Clinical course and prognosis

Although relative 5-year survival is 83%- 88% in stage FIGO I, and 59-64% in FIGO II, the more advanced stages III and IV have a survival of approximately only 30% and 18% respectively (Kosary, 1994). Overall, earlier diagnosis by vaginal ultrasound, radical debulking surgery and chemotherapy have contributed to a significant improvement in the 5-year survival rate from 36% in 1974-1976 to 47% in the years 1986-1993 (Landis et al. 1998).

Established prognostic factors of ovarian cancer are FIGO stage, residual tumor after surgery, histological grading, lymph node status, age, and amount of ascites in primary surgery (Kosary, 1994, Makar et al. 1995, Eisenkop et al. 1998, Reles et al. 2001, as reviewed by Holschneider and Berek, 2000). The role of the histological type as a prognostic factor remains controversial (Kosary, 1994, Makar et al. 1995). Other factors such as DNA-ploidy, decline of CA125 level after surgery, expression of oncogenes and growth factor receptors (*Her-2/neu*, EGFR), and alterations of tumor suppressor genes (*p53*, *Rb*) are currently under investigation.

Within FIGO-stages, grade and lymph node status have a large impact on survival. Survival declines from 94.6% for well differentiated FIGO stage I tumors to 69.7% for poorly differentiated. For FIGO stage II, this decline is from 78.3% to 48.2%, for FIGO stage III from 76.2% to 23.9%, and for FIGO stage IV from 50.2% to 13.8% (Kosary, 1994). For patients diagnosed with stage I ovarian tumors, 5-year survival is 85.1% without lymph node metastasis, but survival drops to 51.9%, if

lymph node metastasis are present. Age also has a strong impact on survival. A women at age 40 with stage IV ovarian cancer has a 50% 5-year survival probability, while this declines to 7.7% in stage IV for a patient >70 years of age (Kosary, 1994).

Multivariate analysis usually reveals stage as well as residual tumor after surgery, and in some studies histological grade of differentiation and age as independent prognostic factors in epithelial ovarian cancer (Eisenkop et al. 1998, Reles et al. 2001).

1.2 Molecular genetic alterations in ovarian tumors

1.2.1 Hereditary ovarian tumors

Approximately 10% of ovarian cancers are thought to be due to autosomal dominant hereditary syndromes (Lynch et al. 1978). The risk of ovarian cancer in first and second degree relatives of women with ovarian cancer is increased 3.6- and 2.9-fold respectively, compared to women who have no family history of ovarian cancer (as reviewed by Berchuck et al. 1999). Three syndromes have been recognized so far (Table 2):

Table 2: Genetic alterations in hereditary ovarian cancer syndromes

Hereditary ovarian cancer syndrome	Gene affected by mutation
Site specific ovarian cancer	<i>BRCA1, BRCA2</i>
Hereditary breast and ovarian cancer (HBOC)	<i>BRCA1, BRCA2</i>
Hereditary Non-Polyposis Colon Carcinoma (HNPCC)	<i>MSH2, MLH1, PMS1, PMS2</i> (DNA mismatch repair genes)

(1) site-specific ovarian cancer syndrome (familial predisposition to ovarian cancer only), (2) hereditary breast and ovarian cancer (HBOC) (predisposition to both breast and ovarian cancers), and (3) hereditary non-polyposis colorectal cancer syndrome (HNPCC), also known as Lynch II syndrome (predisposition in men for colorectal, cancer and in women for breast, colorectal, endometrial and ovarian cancer) (as reviewed by Berchuck et al. 1999).

It has been estimated that the breast-ovarian cancer syndrome accounts for the majority of hereditary ovarian cancer cases (65-75%), out of which, approximately 10-15% are site specific. Site-specific and breast-ovarian cancer syndromes have been linked to mutations in the *BRCA1* and *BRCA2* gene.

The *BRCA1* gene is located on chromosome 17q21-12 and it is thought to act as a tumor suppressor gene (Hall et al. 1990, Miki et al. 1994). Initial studies in families selected on the basis of strong family history and early age of onset, suggested that germline mutations in *BRCA1* were responsible for about 50% of hereditary breast cancers and 90% of hereditary ovarian cancers (Ford et al. 1995). Constitutional mutations in *BRCA1* were found in 34-58% of hereditary ovarian cancer families from North American and European origin (as reviewed by Aunouble et al. 2000). In families with *BRCA1* mutations, the lifetime risk of developing ovarian cancer was estimated to be as high as 60% (Easton et al. 1995). More recently it has been suggested that initial estimates of *BRCA1* penetrance may have been too high because of selection bias. Population-based case-control studies estimated a cumulative risk of 14.6% respectively, 32.2% for *BRCA1* mutation carriers to develop ovarian cancer at the age of 60 years (Laplace-Marieze et al. 1999, Whittemore et al. 1997).

The second major breast/ovarian cancer susceptibility gene, *BRCA2*, was identified on chromosome 13q12 (Wooster et al. 1995), and may account for 10% to 35% of hereditary ovarian cancer. *BRCA2* mutations were found in 7-14.5 % high risk families (as reviewed by Aunoble et al. 2000), and the penetrance of the gene was estimated to be 27% by age 70 (Ford et al. 1998). Approximately 80-90% of *BRCA1* and *BRCA2* mutations result in truncated protein products, while missense mutations are rare (as reviewed by Berchuck et al. 1999).

The HNPCC syndrome (Hereditary Non-Polyposis Colon Cancer) is suspected to account for 10-15% of the hereditary ovarian cancer cases. Affected families typically present with colon and endometrial carcinomas, but some ovarian cancers occur too. HNPCC is associated with germline mutations in a family of genes involved in DNA repair (*MSH2*, *MLH1*, *PMS1*, *PMS2*) (as reviewed by Berchuck et al. 1999).

At present, testing for *BRCA1* and *BRCA2* mutations is recommended, if two individuals in a family either had ovarian cancer at any age, or breast cancer before age 50, and are first or second degree relatives. When these conditions are met, there is a 10% to 20% probability of finding a mutation. The most notable founder mutations described thus far are the *BRCA1* 185delAG, the *BRCA1* 5382insC and the *BRCA2* 6174delT mutations (as reviewed by Berchuck et al. 1999).

Besides genetic testing, ultrasound and Doppler screening as well as serum CA125 marker testing are prevention tools for high risk families. Prophylactic oophorectomy followed by hormonal replacement therapy in women in their late 30s

or 40s is believed to be a reasonable intervention to consider in *BRCA1* and *BRCA2* mutation carriers. However, it has been noted that approximately 2% of these women develop primary peritoneal papillary serous carcinoma after oophorectomy (Piver et al. 1993). Oral contraceptive use (six years or more) by women out of families with hereditary ovarian cancer decreases the risk by as much as 60% and therefore seems an attractive alternative for cancer prevention (Narod et al. 1998).

In general, genetic counseling and testing, as well as the decision about the best strategy for prevention or early detection of ovarian cancer in high risk families, requires a multidisciplinary approach by geneticists, gynecologists, and psychologists. Health care, family planning, psychological aspects, and potential health insurance problems are important considerations for these patients.

1.2.2 Sporadic ovarian tumors

Molecular genetic alterations are frequent in sporadic ovarian cancers and these alterations include chromosomal deletion, oncogene amplification and overexpression, mutation of tumor suppressor genes, and alternative and aberrant RNA splicing. Some alterations have been found to correlate with tumor histopathological criteria and clinical outcome.

Loss of heterozygosity (LOH) is defined as a deletion of a portion of a chromosome that contains a putative tumor suppressor gene. LOH implies loss of the normal polymorphism present at a given locus. Tumor DNA has a propensity to lose one of its two alleles of various genes, compared with DNA from normal cells of the same patient. LOH has been frequently identified in ovarian carcinomas. Several investigators reported that chromosomes 17p, 17q, and 6q show high frequencies of LOH, as high as 31%-83%, 39%-74%, and 39%-74% respectively, in ovarian carcinomas (as reviewed by Chuaqui et al. 1997). Other loci potentially important in ovarian carcinogenesis are chromosomes 4p, 7p, 12p, 12q, 18q, and 19p (as reviewed by Chuaqui et al. 1997).

Several oncogenes have been found to be altered in ovarian cancer, including *HER-2/neu*, *k-ras*, *fms*, *c-myc*, and *c-fos*. Most important among these are *HER-2/neu*, *k-ras*, and *c-myc*. The *HER-2/neu* gene maps to 17q21-22 and encodes a 185-kd transmembrane glycoprotein receptor (p185^{HER2}), which has partial homology with the epidermal growth factor receptor. It has tyrosine kinase activity and promotes cell proliferation and differentiation. The p185^{HER2} protein is a member of the family of growth factor receptors, which include also EGF-R, HER-3, and HER-4.

In an early study by Slamon et al. 1989, *HER-2/neu* was found to be amplified and overexpressed in 26% of ovarian carcinomas. The number of gene copies

significantly correlated with clinical outcome, >5 gene copies giving the poorest outcome. The prognostic value of *HER-2/neu* overexpression still remains controversial though. Only one author has reported an independent correlation with survival in 275 cases (Meden et al. 1994), while others found correlations only in univariate analysis or no correlation at all, including 174 cases analyzed at the Department of Gynecology, Charité-Campus Virchow-Klinikum (as reviewed by Aunoble et al. 2000, Schmider, 1999).

Table 3: Molecular genetic alterations in sporadic ovarian cancer

Structure	Type of Alteration	Affected Chromosomes or Genes
Chromosomes	Loss of heterozygosity (LOH)	17p, 17q, 6q 4p, 7p, 12p, 12q, 18q, 19p 6q, 13q, 19q (serous ovarian tumors)
Oncogenes	Amplification/Overexpression Mutation	<i>HER-2/neu</i> , <i>c-myc</i> , <i>c-fos</i> <i>k-ras</i>
Tumor suppressor genes	Mutation Protein overexpression	<i>p53</i> , <i>BRCA1</i> , <i>BRCA2</i> <i>Rb</i>
Other growth regulatory genes	Alternative splicing Overexpression/Polymorphisms	<i>mdm2</i> <i>p21</i> ^{<i>WAF1/CIP1</i>}

More important than the prognostic value is the fact that this protein is used as a therapeutic target for a recombinant humanized anti-HER2 monoclonal antibody (rhuMAb HER2 [trastuzumab]). RhuMAb HER2 has achieved an objective response rate of 15% as a single agent in patients with HER-2/neu overexpressing metastatic breast cancer who had received extensive prior therapy (Cobleigh et al. 1999). The therapy was well tolerated and the most common adverse effects were infusion-associated fever and chills. Several protocols of a combination therapy of trastuzumab with chemotherapeutic agents are currently under investigation. The results of the rhuMAb HER2 clinical trials demonstrate that a better understanding of genetic alterations in cancer can lead to new targeted approaches to cancer treatment.

The *c-myc* oncogene is located on chromosome 8q24 and is involved in cell cycle regulation by activation or inhibition of several genes including cyclins (A,D or E) and *p53* (Dang, 1999). Amplification and/or overexpression of the wild-type sequence has been demonstrated in 26-37% of ovarian cancer, but a correlation to survival has only been demonstrated in one study in co-expression with HER-2/neu and p21^{ras} (as reviewed by Aunoble et al. 2000).

K-ras was localized to 12p12.1 and is a member of the family of ras genes which code for serine/threonine protein kinases. Mutated K-ras protein loses the ability to become inactivated and thus stimulates growth and differentiation autonomously (as reviewed by Aunoble et al. 2000). In ovarian cancer, mutations of the *K-ras* oncogene have been detected in 11-75% in mucinous and 5-36% in nonmucinous tumors (as reviewed by Aunoble 2000 et al.). These results suggest that *K-ras* mutational activation is an early event of mucinous ovarian tumorigenesis. Little is known about the prognostic value of *K-ras*. While most studies find no correlation, only one study showed a significant relationship between *K-ras* alterations and poor clinical outcome (Scambia et al. 1997).

Among the tumor suppressor genes which are altered in sporadic ovarian cancer, *p53* plays the most important role, while *BRCA1* and *BRCA2* are only rarely mutated. *p53*, located at 17p13.1, codes for a 53 kilodalton transcription factor which regulates cell cycle control and apoptosis. It has been found to be mutated in approximately 40-80% and overexpressed in 32%-84% of epithelial ovarian cancers (as reviewed in chapter 1.3.7). The value of *p53* mutations and protein overexpression as prognostic markers are controversial (as reviewed in chapter 1.3.7). Since efficacy of platinum-based chemo-therapy is believed to depend on p53-induced apoptosis (reviewed in chapters 1.3.8 and 5.1.7), restoration of p53 function has become an attractive target for gene therapy (as reviewed in chapter 1.2.3).

Further genes that are frequently altered in ovarian cancer are the *mdm2* gene, which tightly regulates p53 function (as reviewed in chapter 1.4.3), and the *CIP1/WAF1* gene, which mediates p53 induced G1 cell cycle arrest. (see chapter 1.3.3). The *CIP1/WAF1* gene was shown to have no mutations but an AGC→AGA (serine→arginine) polymorphism at codon 31 was detected in 15% of ovarian cancer cases (Lukas et al. 1997). We found overexpression of the p21 protein in 61% of ovarian carcinomas, and high overexpression (>50% of the nuclei) was correlated significantly with early stage and favourable prognosis of ovarian cancer (Schmider et al. 2000).

The *Rb/cyclin D1/p16* pathway may also be involved in ovarian carcinogenesis, but the mechanisms remain to be further analyzed. Sequence alterations of the retinoblastoma gene are rare, but pRb expression was found in 71% of ovarian carcinomas as opposed to 41% of benign tissues (Dong et al. 1997). Mutations of the

p16ink4A tumor suppressor gene which encodes a cyclin-dependent kinase inhibitor are infrequent in ovarian cancers, but methylation of the gene has been noted in 4% of ovarian cancers (Wong et al. 1999). Recently aberrant RNA splicing of the *p16ink4A* gene has been described in ovarian cancer (Suh et al. 2000).

As opposed to hereditary ovarian cancer, alterations of the *BRCA1* and *BRCA2* tumor suppressor gene are rare in sporadic ovarian cancer. Although LOH at the *BRCA1* and *BRCA2* locus is seen in 80% respectively more than 50% of sporadic ovarian carcinomas, mutations of *BRCA1* have been found in only 5%, and mutations of *BRCA2* in only 4.6% respectively 8% of these tumors (as reviewed by Aunoble et al. 2000).

1.2.3 Gene therapy

Because *p53* is a central regulator in cell cycle control and mutations of the *p53* gene are the most frequent abnormalities identified in human tumors, restoration of *p53* function has become a major focus of research for gene replacement therapy. Re-introduction of wild-type *p53* gene into cells that have lost normal *p53* function can induce either growth arrest or apoptosis (El-Deiry et al. 1993, Yonish-Rouach et al. 1991, Wills et al. 1994, Nielsen and Maneval, 1998).

For the delivery of tumor suppressor genes into cancer cells, adenovirus vectors (Ad) have been shown to be most efficient. Adenoviruses can be produced in high titers and can infect both dividing and non-dividing cells at high efficiencies, thus resulting in high levels of transgene expression. Adenovirus vectors do not normally integrate into the host genome, so transgene expression is transient (as reviewed by Pützer 2000).

In vitro studies of cell cultures derived from various human malignancies have shown that delivery of wild-type *p53* in cells previously mutant or null for *p53* results in a dose-dependent inhibition of cell proliferation, usually associated with cell death via apoptosis (Wills et al. 1994, Yonish-Rouach et al. 1991, Nielsen and Maneval, 1998, Hirai et al. 1999). *p53* tumor suppressor gene therapy, applied to an intraperitoneal model of ovarian cancer in mice, demonstrated an increase in survival in the treated compared to the control group (Mujoo et al. 1996, Kim et al. 1999).

Considering the short half-life of wild-type *p53* and the fact that only a small percentage of tumor cells can be transduced, some of the growth suppressing effect of adenovirus mediated *p53* gene therapy is thought to be due to the so-called bystander effects. These effects possibly include transfer of metabolic products through gap junctions, phagocytosis of apoptotic vesicles containing dead tumor cells that mediate

apoptosis, induction of an immune response against the tumor, and inhibition of angiogenesis (as reviewed by Pützer 2000).

Cell culture experiments have shown that the sensitivity of tumor cells to various chemotherapeutic agents such as adriamycin, etoposide, doxorubicin, cisplatin and others depends on the efficient induction of apoptosis mediated by a functional p53 protein. Therefore, loss of p53 can enhance resistance to chemotherapy (Lowe et al. 1993, Vasey et al. 1996, Vikhanskaya et al. 1997). In addition to the anti-tumor effect of *p53* tumor suppressor gene transduction, sensitization to chemotherapy by re-introduction of wt *p53* may play an important role for gene therapy. Other potential targets for gene therapy include the *WAF1/CIP1*, a universal inhibitor of the cyclin dependent kinases, the *mdm2* gene and other genes which are involved in cell cycle regulation.

A synergistic efficacy of adenovirus-mediated *p53* gene therapy and chemotherapy, both for Cisplatin and Paclitaxel, have been demonstrated in xenograft models of colon, ovarian, prostate and breast cancer (Ogawa et al. 1997, Nielsen et al. 1998, Gurnani et al. 1999).

Promising results have been found in the first clinical *p53* gene therapy study (Schering Plough Research Institute/ Essex Pharma) for ovarian carcinomas with *p53* mutations. In a phase I clinical trial, re-introduction of wild-type *p53* via a recombinant adenovirus was investigated in recurrent ovarian cancer. Intraperitoneal administration of Ad *p53* resulted in successful *p53* gene transfer and expression as well as objective tumor response in part of the cases (I.B. Runnebaum, personal communication).

Currently, the Department of Gynecology of the Charité-Campus Virchow-Klinikum participates in a multinational, multicenter, randomized phase II/III trial of chemotherapy alone (Taxol/Carboplatin) versus chemotherapy plus *p53* gene therapy in newly diagnosed stage III ovarian cancer and primary peritoneal cancer with ≤ 2 cm residual disease following surgery, which is conducted by the Schering-Plough Research Institute (Project Director: Jo Ann Horowitz, M.D., USA).

The present data suggests that gene replacement therapy provides a potentially effective anti-tumor strategy. The increasing knowledge about regulation of cell division and apoptosis opens new perspectives for treatment strategies. By means of molecular genetic techniques such as the chip technology for analyzing mutations and gene expression patterns, a precise genetic characterization of tumor cells and an individual choice of the most efficient therapy may be possible in the future.

1.3 The *p53* tumor suppressor gene

1.3.1 *p53* domains: structure and function

The *p53* gene is a tumor suppressor gene and has been named "the guardian of the genome,, (Lane, 1992) or the "cellular gatekeeper of growth and division,, (Levine, 1997). The *p53* protein is a transcription factor which plays a central role in the regulation of cell cycle arrest and apoptosis following DNA damage.

The *p53* gene contains eleven exons which encode for a 2.8 kb mRNA, translated into a 53kD protein (Matlashewski et al. 1984, Harlow et al. 1985). Exon 1 is always non-coding. In human *p53*, a very large intron of 10 kb with unknown biological function is located between exon 1 and exon 2 (Soussi and May, 1996).

Functional region

Transactivation	SH3		DNA binding domain		Tetramerization	Regulatory domain
aa 1-50	63-97		102-292		323-356	363-393



Conserved region

aa	12-23		117-142		171-181		234-258	270-286
----	-------	--	---------	--	---------	--	---------	---------



DNA interacting region

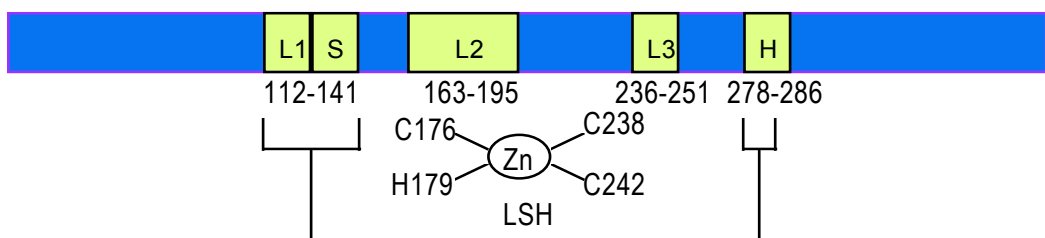


Fig. 1: Structural and functional regions of the *p53* protein (redrawn from May and May, 1999) Functional regions and corresponding amino acid residues are shown on top. In the middle, evolutionary highly conserved domains I-V are shown. The bottom represents the tertiary structure of the site-specific DNA-binding. L1, L2, L3 indicate loops, and LSH indicates a loop-sheet-helix structure. The tertiary structure is shown in more detail in Fig. 2.

The human *p53* protein contains 393 amino acids and can be divided into three regions: 1) the amino-terminal region, which contains the transcriptional trans-activation domain, 2) the carboxy-terminal region, which contains the functional regions for nuclear localization, tetramerization, and both non-specific DNA-binding

and recognition of primary DNA damage, and 3) the central region of the protein (amino acid residues 102 to 292), which contains most of the sequence specific DNA binding domains (Soussi and May, 1996) (Fig. 1).

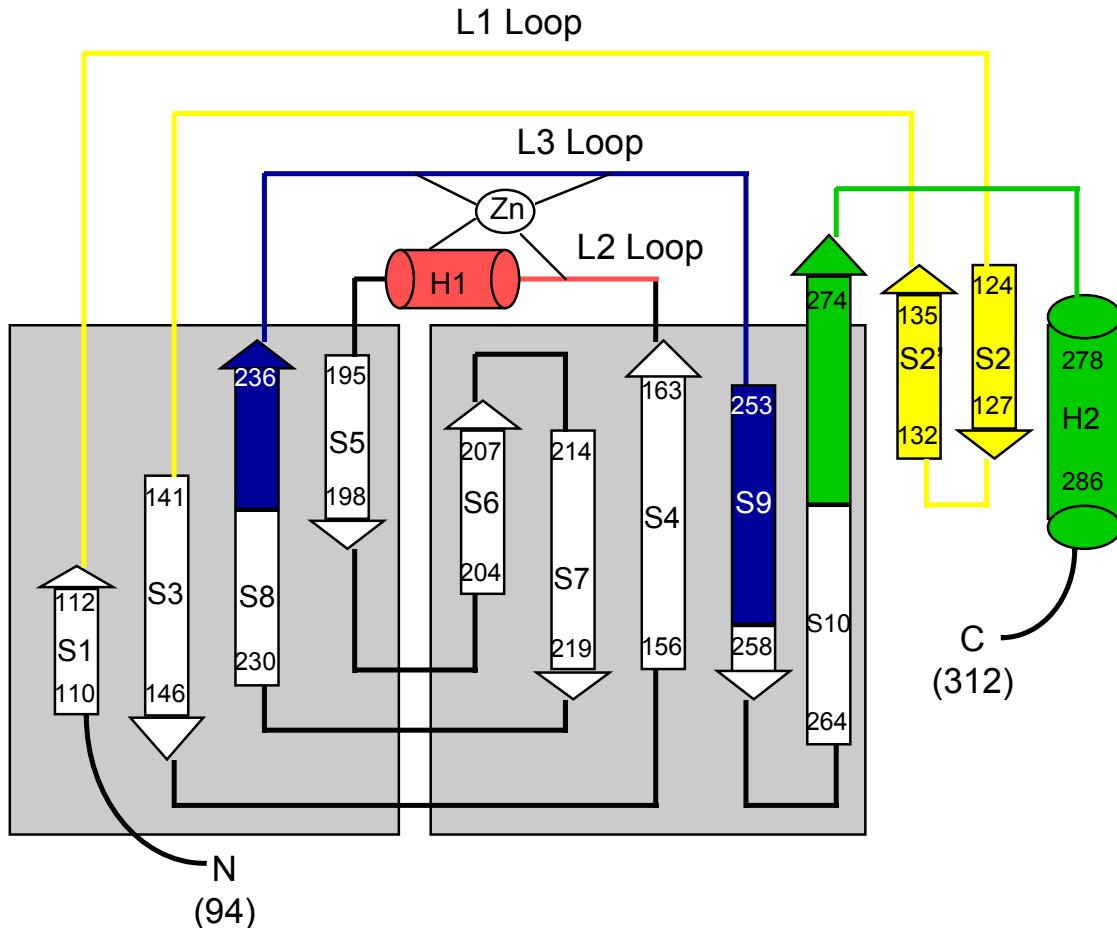


Fig. 2: Topological diagram of the secondary structure elements of the core domain of the p53 protein (redrawn from Cho et al. 1994). The residues at the start and the end of each secondary structure element are indicated. The DNA-binding regions of the protein (L1-S2-S', L2, L3, S10-H2) correspond to the conserved regions of the p53 gene and are colored yellow for region II (residue 117-142), red for region III (residue 171-181), blue for region IV (residue 234-258) and green for region V (residue 270-286). The boundaries of the two β -sheets that make up the β -sandwich are shaded. The scaffolding regions are white.

The functional form of the p53 protein is a tetramer, which is assembled by the amino acid residues 323-356 of the carboxy-terminal region of the protein (Wang et al. 1994). It has been shown that some p53 mutants exhibit a dominant negative phenotype and are able to associate with the wild-type p53 protein, which is expressed by the remaining wild-type allele, to induce the formation of an inactive heterooligomer (Soussi and May, 1996).

Within the *p53* sequence five regions have been identified, which have been highly conserved throughout evolution (Soussi et al. 1990). The conserved domain I (amino acid residues 12-23) is located within the aminoterminal region and corresponds to the binding site of the MDM2 protein. The conserved domains II (residues 117-142), III (residues 171-181), IV (residues 234- 258) and V (residues 270-286) are located in the central region of the protein and are almost identical to the DNA interactive regions of the protein as described in the crystallographic structure of the p53 protein by Cho et al. (1994) (Fig 2).

The crystallographic analysis of the p53 protein has revealed the following motifs in the central region of the gene: 1) two antiparallel β -sheets composed of four and five β -strands that hold the other elements, 2) a loop-sheet-helix-motif (LSH) containing three β -strands, an α -helix, and the L1 loop (residues 112-141), 3) an L2 loop containing a small helix (residues 163-195), and 4) an L3 loop composed mainly of turns (residues 236-251) (Cho et al. 1994) (Fig 2). The LSH motif and the L3 helix are involved in direct DNA interaction (Cho et al. 1994).

There is remarkable correspondence between these structural elements and the conserved domains II-V of the gene. More than 90% of the missense mutations in the *p53* gene have been found clustered in so-called "hotspots,, in the highly conserved regions of the II-IV of the gene, which have also been identified as the DNA binding regions (Greenblatt and Harris, 1994). It has been suggested to distinguish between class I mutations, which affect amino acid residues directly involved in the protein-DNA interaction (residues in LSH and L3), and class II mutations, which affect amino acids involved in the stabilization of the tertiary structure of the protein (residues in L2) (Soussi and May, 1996). While class I mutations result in defective contacts with the DNA and loss of the ability of p53 to act as a transcription factor, class II mutations disrupt the structural basis of the p53 core domain and may, therefore, indirectly affect its function.

1.3.2 p53 response to cellular stress: upstream events

Under normal conditions, the p53 protein is present in extremely small quantities in most cells and displays a rapid turnover rate which is on the order of minutes. Rapid degradation of p53 in normal cells is critical to efficiently dampen p53 activity and is regulated in large part by MDM2 via ubiquitin-mediated proteolysis (Maki and Howley, 1997, Haupt et al. 1997, Kubbutat and Vousden, 1998).

In its role as a tumor suppressor gene, *p53* serves as a "guardian of the genome,, (Lane, 1992). The amount of p53 protein increases in response to a variety of signals mediated by cellular stresses, such as DNA damage produced by γ -irradiation

or ultraviolet radiation (Guidos et al. 1996), oncogene activation, hypoxia (Graeber et al. 1996), nucleotide depletion (Linke et al. 1996), and metabolic and pH changes (Fig. 3). The p53 protein level increases proportionally to the extent of DNA damage through a prolonged half-life of the protein (Levine, 1997). Furthermore, the DNA-binding activity of p53 is increased. p53 stabilization and enhanced activity are regulated by several mechanisms.

1) p53 protein stabilization can occur through N-terminal phosphorylation and decreased MDM2-binding, for example after exposure to DNA-damaging ionizing radiation or the topoisomerase inhibitor etoposide (Siliciano et al. 1997). Two candidate kinases for p53 phosphorylation have been identified. The ATM gene which recognizes DNA damage phosphorylates p53 on serine 15, and DNA-PKs (DNA-activated protein kinase) which phosphorylates p53 at both serine 15 and serine 37 (Woo et al. 1998, Siliciano et al. 1997, Canman et al. 1998, Shieh et al. 1997). Phosphorylation of p53 at serines 15 and 37 impairs the ability of MDM2 to inhibit p53-dependent transactivation, most likely due to a conformational change of p53 (Shieh et al. 1997).

Shieh et al. (1999) have also shown that in addition to serine 15, serine 20 is phosphorylated in response to DNA damage. Recently it has been shown that mutation of serine-20 renders p53 less stable and more prone to MDM2 mediated degradation. p53 peptides phosphorylated at serine-20 are less efficient competitors of the p53/MDM2 interaction than non-phosphorylated peptides (Unger et al. 1999). These observations are particularly interesting, given that serine-20 resides in the region of p53 which binds to MDM2 (Kussie et al. 1996, Picksley et al. 1994). p53 protein that has been phosphorylated at the N-terminus binds poorly to MDM2 and is, therefore, stabilized through a decrease in its degradation rate.

2) Acetylation of the C-terminal domain of p53 which occurs on lysine 382 by p300 or lysine 320 by PCAF causes a conformational change at the C-terminus and activates p53-dependent DNA-binding (Sakaguchi et al. 1998).

3) C-terminal dephosphorylation of p53 at serine 376 creates a consensus binding site for interaction with *14-3-3* σ , which enhances the ability of p53 to bind to DNA (Waterman et al. 1998). A phosphorylation-acetylation cascade model has been discussed. It suggests that following DNA damage, N-terminal phosphorylation directs C-terminal acetylation to activate p53 (Sakaguchi et al. 1998). This would result in both higher stability of the p53 protein as well as increased DNA binding ability.

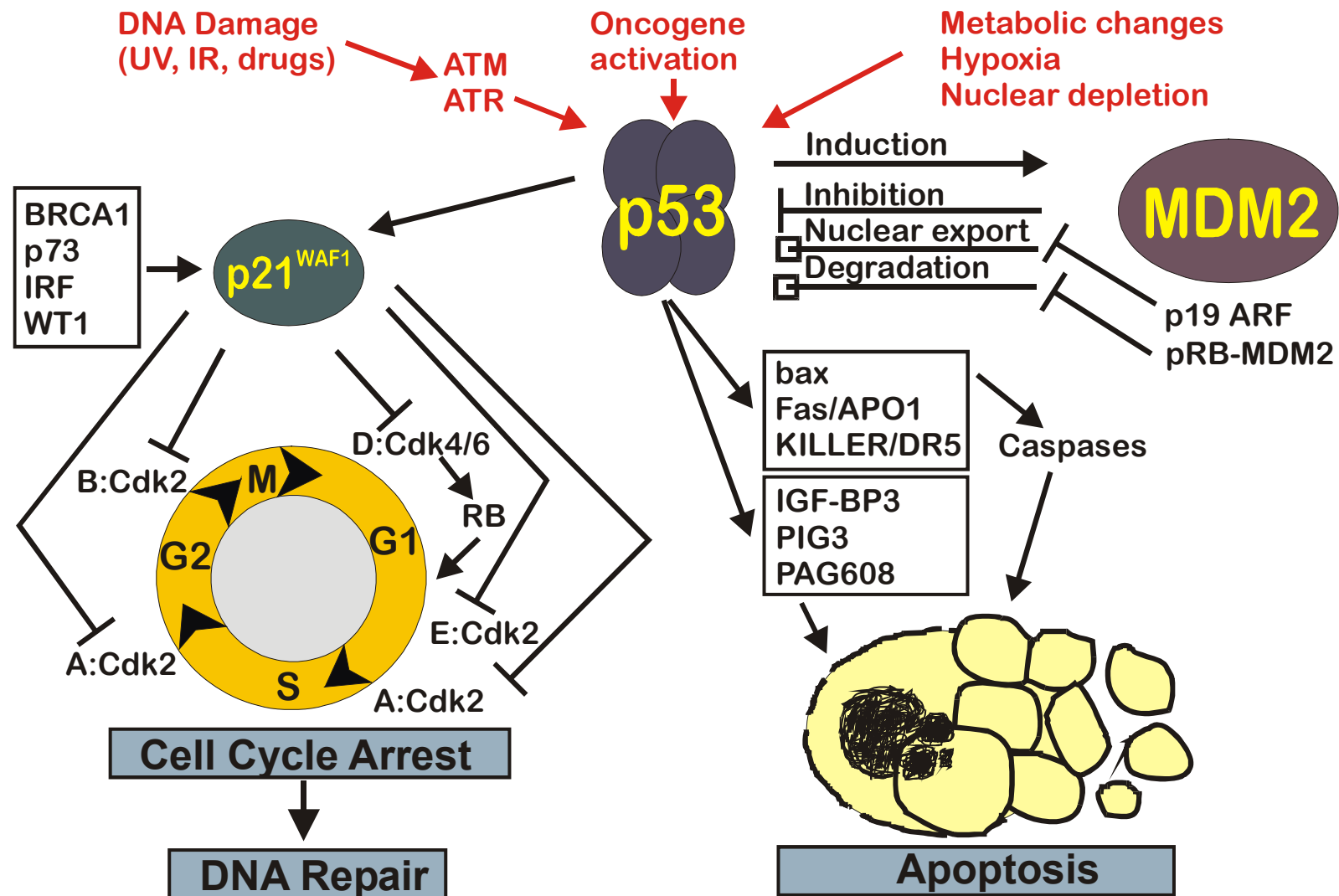


Fig. 3: p53 pathways. Upstream activators are shown above in red. Multiple downstream effectors of p53 which play a role for cell cycle arrest and apoptosis are shown. Arrows indicate a positive effect, while a flat line indicates inhibition. Quadrangles indicate specific functions in p53/MDM2 interaction.

1.3.3 Downstream mediators of p53-dependent cell cycle arrest

The downstream events mediated by p53 play a major role for cell cycle arrest, apoptosis, and genomic stability. The growth controlling functions of p53 include cell cycle arrest, apoptosis, senescence and antiangiogenesis (Fig. 4). The transcriptional activating function of p53 is a major component of its biological effects and a substantial number of target genes have been identified. These include *WAF1/CIP1*, *GADD45*, *14-3-3 σ* , *bax*, *FAS/APO1*, *KILLER/DR5*, *PIG3*, *Tsp1*, *IGF-BP3* and others (as reviewed by El-Deiry 1998). It has been suggested, that there may be as many as 200-400 p53 target genes or perhaps even more (El-Deiry et al. 1992).

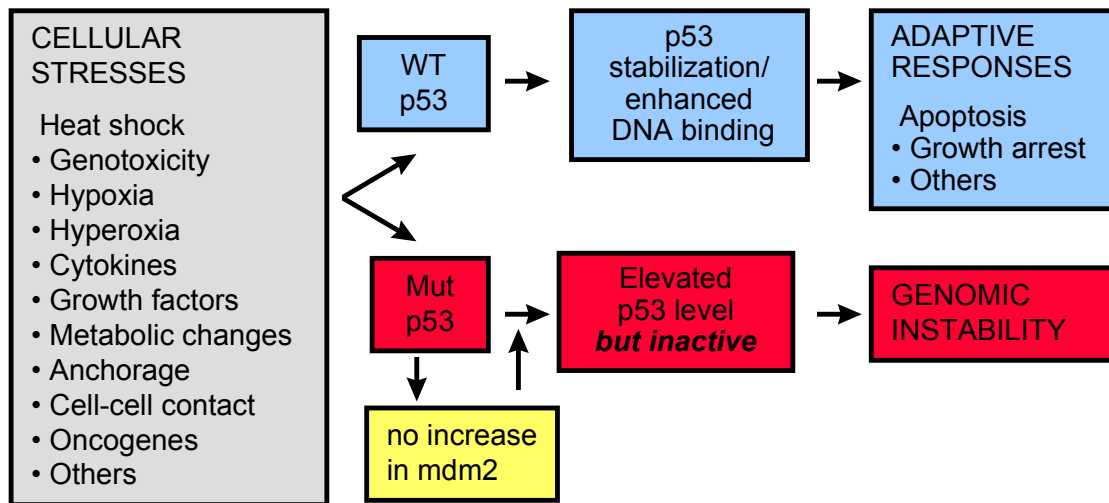


Fig. 4: Response to cellular stresses in cells with wildtype p53 versus cells with mutated p53

The G₁ checkpoint

p53 directly regulates the expression of p21^{WAF1/Cip1}, a universal inhibitor of the cyclin dependent kinases (Cdk) (Fig.3) (El-Deiry et al. 1993). This 21 kilodalton protein forms a quaternary complex found in normal cells with cyclin/Cdks and the DNA polymerase processivity factor PCNA (Xiong et al. 1993). It binds to the cyclin-Cdk complexes cyclin D1-Cdk4, cyclin E-Cdk2, cyclin A-Cdk2 and cyclin A-Cdc2 and inhibits their kinase activity (Fig. 3). One molecule of p21 per complex appears to permit Cdk activity, while two molecules inhibit its activity and block cell cycle progression (Zhang et al. 1994). The available evidence suggests that p21 acts on cyclin-Cdk complexes and PCNA such that it blocks DNA replication. p21 binds with its greatest affinity to G1 cyclin-CDK complexes, and binds poorly to cyclin B/cdc2. p21 appears to be required for G1 arrest following DNA damage (Waldmann et al. 1995).

The G₂ checkpoint

While it is clear that *p53*-deficiency leads to defective cell cycle arrest in G₁, the role of *p53* in G₂ arrest is less clear. Deregulation of the G₂ checkpoint is one of the hallmarks of malignant transformation. The G₂ checkpoint is the last barrier before the perpetuation of mutations and therefore, very important for the maintenance of genomic stability. Overexpression of wildtype *p53* protein has been found to arrest cells in G₂ and inhibit entry into mitosis (Stewart et al. 1994). This property of *p53* is important in a novel cell cycle checkpoint that controls entry into mitosis when DNA synthesis is blocked. *p53*^{-/-} cells do not arrest in response to spindle inhibitors, but undergo multiple rounds of DNA synthesis without DNA segregation. This results in the formation of tetraploid and octaploid cells (Cross et al. 1995).

The *GADD45* (growth arrest and DNA-damage inducible gene #45) was initially discussed to play a role in G₁ arrest. The gene is induced when cells are subjected to DNA damage, leading to arrest in the G₁ phase of the cell cycle (Kastan et al. 1992). The *GADD45* protein was found to interact with the replication and repair factor PCNA and to inhibit the entry of cells into the S-phase (Smith et al. 1994). More recent evidence has suggested that cyclin B/*cdc2* may be bound and inhibited by *GADD45*, thereby leading to G₂ arrest (Zhan et al. 1999). The *cdc2* kinase-cyclin B1 complex, termed Mitosis Promoting Factor (MPF), serves as the primary mediator of the signal for G₂-mitosis transition (Zhan et al. 1999).

The 14-3-3 σ proteins have also been suggested to be involved as mediators of *p53*-dependent G₂-arrest. These 14-3-3 σ proteins have been shown to bind to the non-functional phosphorylated form of the *cdc25c* phosphatase, which in turn, prevents the dephosphorylation of the *cdc2* kinase, thus resulting in non-functional MPF and inducing G₂ arrest (Conklin et al. 1995). The 14-3-3 σ gene has been shown to be upregulated by *p53* (Hermeking et al. 1997).

Another gene which may play a role as a mediator of cell cycle arrest is *B99*. It is a *p53* target gene, which is induced by DNA damage and is specifically upregulated in the G₂-phase, during which its protein is localized in the microtubule network. Ectopic overexpression of *B99* in *p53*-null fibroblasts leads to G₂ arrest (Utrera et al. 1998).

The present knowledge about *p53* suggests, that even though *p53* can cause an arrest or prolongation of G₂ to enable sufficient repair of DNA defects before the onset of mitosis, *p53* also contributes to the efficiency of DNA repair and therefore reduces the G₂ delay (as reviewed by Schwartz and Rotter 1998).

The spindle checkpoint

p53 is associated with centrosomes and thus may affect centrosome duplication directly (Brown et al. 1994). Embryo fibroblasts from *p53*-null mice acquire more than two centrosomes, leading to mitosis with more than two spindle poles and frequent mitotic failure (Fukasawa et al. 1996). *p53*^(-/-) cells have also been found to show aberrant DNA replication, termed endoreduplication. Polyploid giant cells were the result. Therefore, this checkpoint prevents the formation of aneuploid cells that are destined to harbor an unstable genome (Cross et al. 1995).

1.3.4 Mechanisms of p53-dependent apoptosis

Overexpression of wild-type p53 can result in a rapid loss of cell viability by a manner characteristic of apoptosis (Yonish-Rouach et al. 1991). Apoptosis is defined as a programmed form of cell death in which the cell "commits suicide,, by disintegrating into membrane vesicles. The determinants of whether a cell undergoes a viable cell cycle arrest or apoptosis in response to p53 activation are not fully understood. The extent of the DNA damage and the levels of p53 have been shown to affect the choice between cell cycle arrest and apoptosis (Chen X. et al. 1996).

Other factors of influence include expression of the retinoblastoma gene (*Rb*), the transcription factor E2F1, viral protein expression and growth factor availability. The Rb/E2F1 pathway may play a central role in determining the balance between cell cycle arrest and apoptosis. Loss of *Rb* function by expression of viral proteins or by homozygous gene disruption has been correlated with loss of G₁ arrest after DNA damage and apoptosis (Slebos et al. 1994, Howes et al. 1994, Morgenbesser et al. 1994). Inactivation of pRb by either E2F-1 overexpression (Qin et al. 1994) or by caspase-mediated cleavage of p21^{WAF1} has also been shown to induce apoptosis (Levkau et al. 1998). Furthermore, overexpression of *Rb* blocks p53-mediated apoptosis (Haupt et al. 1995).

p53-mediated apoptosis is thought to occur through a combination of sequence-specific transactivation-dependent and independent mechanisms acting in concert. Several target genes, such as *bax*, *Fas/APO1*, *KILLER/DR5*, *PIG* genes, *PAG608*, and *Pidd* are induced by p53 through sequence specific transactivation (SST) and have been identified to participate in the induction of apoptosis.

The *bax* gene encodes a 21-kD protein of the Bcl-2 family and has been found to possess potent pro-apoptotic properties (Oltvai et al. 1993, Miyashita and Reed 1995). The ratio of p21 Bax: Bcl-2 has been suggested as a criteria to determine whether cells live or die (Oltvai et al. 1993). Furthermore, the downregulation of Bcl-

2, which normally enhances cell survival, further promotes apoptosis (Miyashita et al. 1994). Thus p21 Bax may be an important target mediator of p53-dependent apoptosis.

The cell surface death receptor gene *CD95/Fas/Apo-1* is a potent inducer of apoptosis (as reviewed by Nagata 1997). Once cell surface death receptors bind death ligands, they transmit rapid apoptotic signals. However, the role of CD95/FAS/APO1 seems to be cell-type and signal-dependent (as reviewed by Gottlieb and Oren 1998). p53 stimulates the expression of another death-receptor, *KILLER/DR5*, which is activated by the death ligand TRAIL (as reviewed by Gottlieb and Oren 1998).

PIGs (p53-induced genes) cause disruption of mitochondrial integrity and subsequent apoptosis through stimulating reactive oxygen species formation (Polyak et al. 1997). Other putative pro-apoptotic target genes of p53 are *PAG608* (Israeli et al. 1997), the genes which encode IGF-BP3 (Buckbinder et al. 1995) and p85 (Yin et al. 1998). Recently, *Pidd*, a new gene regulated by p53, was identified and found to induce apoptosis (Lin et al. 2000).

Inactivation of p53 function may provide a selective advantage for clonal expansion of preneoplastic and neoplastic cells. Of particular interest is the fact that hypoxia can activate p53 and promote p53-dependent apoptosis. A hypoxic environment occurs frequently within the central portion of tumors, particularly prior to sufficient neoangiogenesis. This would explain the hypoxia-driven selection for cells with diminished apoptotic potential within solid tumors and would provide an attractive explanation for the loss of p53 function in tumors (Graeber et al. 1996).

The p53-dependent apoptotic pathway has not only been demonstrated to be critical to the development of tumors but also to their treatment, since the effectiveness of various chemotherapeutic agents depends on the ability of p53 to induce apoptosis (as reviewed in chapter 1.3.8).

1.3.5 p53 and genomic stability

Inactivation of p53 can lead to an increase of mutation frequency resulting from inefficient nucleotide excision repair (NER). Poor NER causes genomic instability. The instability is manifested as gene amplification, aneuploidy, and chromosomal aberrations, associated with malignant progression. p53 can bind to several DNA helicases, which are part of the basal transcription factor TFIIH (Wang et al. 1995). One functional outcome of such interaction may be modulation of nucleotide excision repair (NER) by p53 (Wang et al. 1995).

A model has been proposed in which p53 binds the damaged DNA and stimulates DNA repair (Wang et al. 1996). Upon successful completion of DNA repair, it has been proposed that p53 would be phosphorylated and then released from

the DNA (Lu et al. 1997). If repair is not carried out successfully, it is assumed that p53 fails to be released and its extended interaction with DNA helicases triggers apoptosis (Wang et al. 1996).

Furthermore, p53 can recognize several forms of damaged DNA including the mismatched DNA (Lee et al. 1995) and the single-stranded DNA ends (Obersler et al. 1993, Bakalkin et al. 1994). p53 may act as a sensor that binds to damaged DNA regions and recruits the NER machinery by trapping TFIIH, a major component of the repair complex, at sites where it is needed. This p53-TFIIH complex in turn may facilitate the formation of a functional „repairosome,, (Wang and Harris, 1997).

p53's function is frequently lost during the process of tumorigenesis and in the spontaneous immortalization of primary cells. This indicates that loss of p53's function promotes genomic instability.

1.3.6 The role of p53 in tumorigenesis

The *p53* gene plays a crucial role for cell cycle control, induction of apoptosis, DNA repair, and genomic stability, all of which are central to the prevention of human carcinogenesis. Inactivation of the wild-type p53 function is thought to be a common event during the development of cancer. Several mechanisms of functional inactivation of p53 such as mutation, inhibition, nuclear export, degradation through the MDM2 protein, or aberrant transcription are known.

Mutations which inactivate some or all of p53's functions as a tumor suppressor gene have been found in over 50% of all human tumors (Hollstein et al. 1994). Over 85% of these mutations are missense mutations that encode altered forms of the protein with a prolonged half-life. Missense mutations are predominantly located in the DNA-binding regions of the protein and therefore affect the DNA-binding ability of the p53 protein (Cho et al. 1994). As a consequence, p53 can not activate the target genes that regulate cell cycle arrest. p53 protein alterations due to mutations therefore provide a selective advantage for clonal expansion of neoplastic cells (Vogelstein 1994).

In addition to failure to elicit a tumor suppressor response, these mutant p53s are also unable to activate expression of MDM2. As a result, these mutant p53 proteins are unusually stable and accumulate to high levels in the tumor cells (Kubbutat and Vousden, 1998). However, wildtype p53 may also be inactivated through amplification of the *mdm2* gene in some tumors, especially sarcomas, since the MDM2 protein rapidly degrades and inhibits p53 by binding to the protein (Oliner et al. 1992, Kubbutat et al. 1997, Haupt et al. 1997).

The function of p53 may also be abolished through mechanisms that prevent its entry into the nucleus, or promote nuclear exclusion, and keep it localized in the cytoplasm, as has been described for some breast tumors and neuroblastomas (Moll et al. 1995, Roth et al. 1998, Stommel et al. 1999).

Furthermore in a number of human tumors transcription of p53 has been shown to be reduced or absent. This could result from cis-acting mutations in the regulatory regions of the gene or hypermethylation of the promoter as has been shown for other tumor suppressor genes (Counts and Goodman, 1995, Baylin, 1997).

More common than loss of expression, is elevated expression of p53 due to mutation. The *myc*-oncogene may play an important role for high p53 expression. C-myc has been found to be elevated as an early event in oncogenesis and is thought to subsequently induce p53 expression, which then leads to cell cycle arrest. A cell population with mutant *p53* would not undergo growth suppression as expected but would have a growth advantage under these conditions. Clonal selection of these cells would therefore be favored (as reviewed by Reisman and Loging 1998).

Humans with germline mutations, who are heterozygotes for the wild-type allele of *p53*, have a very high frequency of developing cancer (90-95%) at an early age (*Li-Fraumeni-Syndrom*). The tissue distribution of these cancers is, however, not random (sarcomas, breast, adrenal carcinomas) and it is not clear what this means for the p53 function (Li and Fraumeni, 1969).

1.3.7 Clinical implications

Ovarian cancer, like most other adult malignancies, is thought to result from accumulation of mutations in multiple genes, which are important for normal function. The *p53* tumor suppressor gene is the most frequently mutated gene in human cancers (Greenblatt and Harris, 1994) and plays a critical role in the regulation of cell cycle and apoptosis. It has been found to be mutated in approximately 40-80% of epithelial ovarian cancers (Mazars et al. 1991, Kihana et al. 1992, Milner et al. 1993, Kohler et al. 1993b, Kupryjanczyk et al. 1993, Wertheim et al. 1994, Zheng et al. 1995, Kappes et al. 1995, Casey et al. 1996, Righetti et al. 1996, Skilling et al. 1996, Schuyer et al. 1998). In a previous study of 105 ovarian cancer patients we found mutations in 57% of the cases (Wen et al. 1999). It is thought that p53 protein alterations due to missense mutations, nonsense or frameshift mutations, provide a selective advantage for clonal expansion of neoplastic cells (Vogelstein, 1994).

Only few studies have analyzed the entire open reading frame of the gene (Kihana et al. 1992, Kupryjanczik et al. 1993, 1995, Casey et al. 1996, Skilling et al. 1996, Sood et al. 1997, Angelopoulou et al. 1998, Wen et al. 1999) and have found

mutations in 50% - 79% of the cases. 5%-20% of these mutations were outside exon 5-8 (Kupryjanczik et al. 1993, Skilling et al. 1996, Casey et al. 1996, Wen et al. 1999). Therefore a study which is limited to exons 5-8 will miss a substantial number of mutations.

Though p53 protein expression has been studied extensively by immunohistochemistry in ovarian cancer. In those studies which used frozen ovarian carcinoma specimens for immunohistochemical analysis of p53, the percentage of cases with p53 overexpression was 32%-84% with an overall average of 51% (Marks et al. 1991, Kihana et al. 1992, Eccles et al. 1992, Kohler et al. 1993a, Kiyokawa et al. 1994, Henriksen and Oberg 1994, Sheridan et al. 1994, Lee et al. 1995, Casey et al. 1996, Skilling et al. 1996, Buttitta et al. 1997, Geisler et al. 1997, Schuyer et al. 1998, Wen et al. 1999).

The role of p53 alterations as a prognostic factor remains controversial. Several studies have identified p53 overexpression as a prognostic factor (Bosari et al. 1993, Henriksen et al. 1994, Hartmann et al. 1994, van der Zee et al. 1995, Klemi et al. 1995, Levesque et al. 1995, Herod et al. 1996, Viale et al. 1997, Eltabakkah et al. 1997, Geisler et al. 1997, Röhlke et al. 1997, Werness et al. 1999, Anttila et al. 1999), and few studies as an independent prognostic factor of overall survival in multivariate analysis (Klemi et al. 1995, Herod et al. 1996, Geisler et al. 1997, Röhlke et al. 1997, Anttila et al. 1999). *p53* mutations have been found to be associated with a significantly shorter overall survival compared to the wildtype p53 sequence in only one study (Wen et al. 1999).

1.3.8 p53 and efficacy of chemotherapeutic agents

Cell culture experiments have shown that the sensitivity of tumor cells to various chemotherapeutic agents depends on the efficient induction of apoptosis mediated by a functional p53 protein. Therefore loss of p53 can enhance resistance to chemotherapy (Lowe et al. 1993, Vasey et al. 1996, Vikhanskaya et al. 1997). It is well documented that drugs such as Adriamycin, Etoposide, Doxorubicin, Cisplatin, and others induce DNA damage and p53-dependent apoptosis.

The wildtype p53-expressing A2780 human ovarian cancer cell line acquired cross resistance to Cisplatin and Doxorubicin by transfection with a dominant negative mutant *p53* gene, while it retained sensitivity to Taxol (Vasey et al. 1996). In another study Cisplatin caused strong induction of p53, WAF1, and Bax in the Cisplatin sensitive A2780 cell line, while there was no such effect in a Cisplatin resistant cell line A2780-DX3, which furthermore showed a significant proportion of potentially inactive p53 protein located in the cytoplasm instead of the nucleus (Vikhanskaya et

al. 1997). Other studies suggest that Cisplatin-resistance in the 2780CP ovarian cancer cell line is caused by a defect in the signal transduction pathway for p53 induction following cisplatin-induced DNA damage (Siddik et al. 1998).

Further strong evidence for the importance of a functional p53 protein for the efficacy of Cisplatin and Carboplatin is given by a database of the National Cancer Institute on drug activity in cell lines which shows a strong correlation between *p53* wildtype sequence respectively p53 function and efficacy of Cisplatin and Carboplatin (Weinstein et al. 1997). In contrast to this, antimetabolic tubulin-active agents such as Taxol show a strong negative correlation between *p53* wildtype as well as p53 function and activity of the drug (Weinstein et al. 1997). Sensitivity to Taxol has been found enhanced through the absence of functional p53 protein because of increased G2M arrest and p53 independent apoptosis (Wahl et al. 1996, Vikhanskaya et al. 1998).

Since dysfunctional p53 can not mediate the apoptotic process, tumors with *p53* mutations or altered p53 protein may become resistant to platinum-based chemotherapy (Lowe et al. 1994). This has been initially demonstrated in two clinical studies which showed that patients with FIGO III/IV ovarian cancer had a poor response to platinum-based chemotherapy if their tumors had p53 overexpression (Buttitta et al. 1997) or *p53* missense mutations (Righetti et al. 1996). In a further study which analyzed 168 primary stage III-IV ovarian carcinomas, p53 overexpression was significantly correlated with resistance to a platinum based chemotherapy (Ferrandina et al. 1999).

The hypothesis that ovarian cancer cells with functional p53 are more sensitive to Cisplatin is further supported by the findings of gene therapy studies. Introduction of wildtype p53 protein via adenovirus gene transfer into A2780/CP Cisplatin resistant cells significantly sensitized these cells to platinum cytotoxicity, indicating that p53 was involved in resistance to cisplatin (Song et al. 1997). Similar results were reported for p53-deleted SK-OV-3 ovarian cancer cells (Kanamori et al. 1998).

Since the efficacy of a platinum-based chemotherapy may depend in part on a functional *p53* gene, the introduction of a p53 wildtype sequence into ovarian cancer cells via an adenovirus has become a major focus of research (see chapter 1.2.3). Furthermore, molecular genetic analysis of ovarian tumors might in the future identify those patients who are most likely to respond to a chemotherapy.

1.4 The *mdm2* (murine double minute 2) gene

1.4.1 Molecular structure of the *mdm2* gene

The *mdm2* (murine double minute) gene was initially described as a proto-oncogene and is amplified and overexpressed in human soft tissue sarcomas and gliomas. It was originally identified in a spontaneously transformed Balb/cT3 fibroblast murine cell line (Cahilly-Snyder et al. 1987). In these cells *mdm2* is localized on double minute chromosomes and is amplified approximately 50-fold (Fakharzadeh et al. 1991).

In humans, the gene is located on chromosome 12q13-14 (Oliner et al. 1992). The full length mRNA encodes for a 90 kD protein of 491 amino acids. The mouse *mdm2* gene contains 12 exons, of which exon 3-12 comprise the coding region (Montes de Oca Luna et al. 1996). Comparison of the gene in different species reveals four major conserved regions (as reviewed by Piette et al. 1997 and Freedman et al. 1999) (Fig. 5).

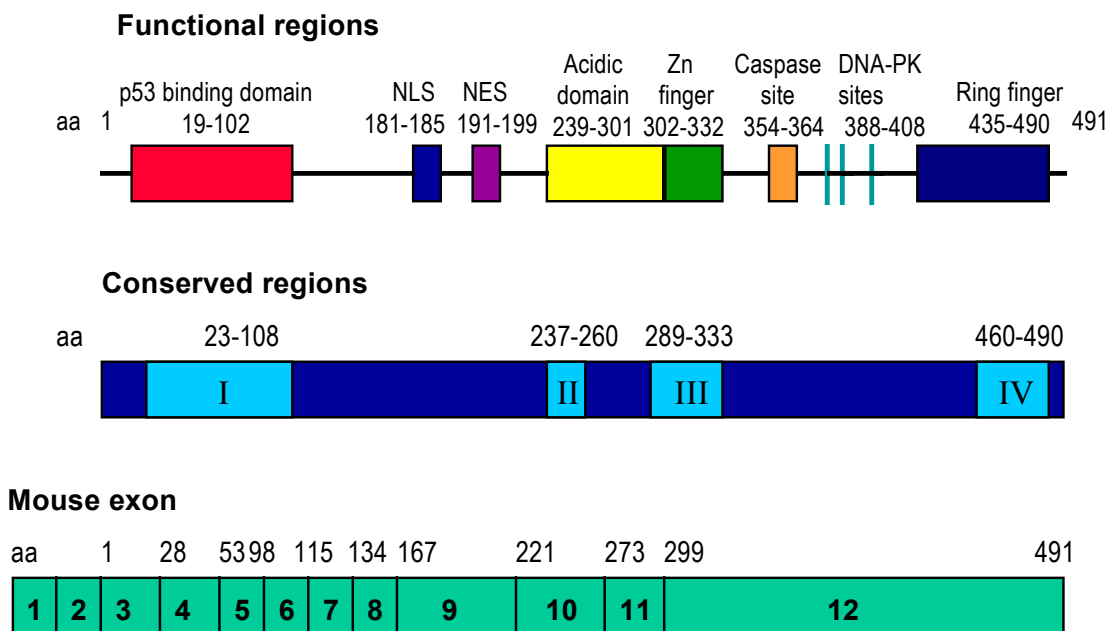


Fig. 5: Structure and functional regions of the MDM2 protein. Above functional domains with corresponding amino acid residues are shown (see Freedman et al. 1999). DNA-PK sites comprise aa 388/389, 395/396 and 407/408. The p53 binding domain and conserved region I are almost identical. Since the human *mdm2* exon boundaries are not fully known yet, mouse exons 1-12 are shown with the first codon of each exon indicated. Exon 1 and 2 are noncoding (Montes de Oca Luna et al. 1996).

Region I contains 90 aa of the N-terminus and corresponds closely to the p53 binding site (aa 19-102) (Chen et al. 1993). In a crystal structure analysis of the 109-residue amino-terminal domain of MDM2 bound to a 15-residue transactivation domain peptide of p53, it was shown that MDM2 has a deep hydrophobic cleft, on which the p53 peptide binds as an amphiphatic α helix (Kussie et al. 1996).

The region II of MDM2 protein contains a central acidic domain, which was shown to interact with the ribosomal L5 protein and its associated 5S rRNA (Marechal et al. 1994, Elenbaas et al. 1996). This suggests a possible function in ribosome biosynthesis or in translational regulation.

Between region I and II, a putative nuclear localization signal has been suggested to be located at amino acid 181 (Fakharzadeh et al. 1991). Recently, a conserved nuclear export signal (NES) sequence has been localized to amino-acid residues 191-199 and mediates the ability of MDM2 to shuttle between the nucleus and the cytoplasm and back (Roth et al. 1998). Region III contains a central zinc-fingerlike sequence of unknown function.

Region IV, which is highly conserved between species, contains a c-terminal RING finger domain, which has been shown to specifically bind to RNA. This suggests a role for MDM2 in translational regulation in a cell (Elenbaas et al. 1996). Sequence analysis defined the RING finger domain as the most conserved region of MDM2. Recently it was shown that the RING finger domain is essential for MDM2 targeted degradation of p53 (Kubbutat et al. 1999). The C-terminal region may also play an important role for the suppression of MDM2 function since it has recently been shown that ARF binds to MDM2 at the C-terminus and degrades the MDM2 protein. Thereby, MDM2's inhibition of p53 is indirectly neutralized (Zhang et al. 1998, Pomerantz et al. 1998).

RING finger domains have been hypothesized to participate in protein-protein interactions or DNA-binding, but for MDM2 it has been shown that the RING finger interacts specifically with RNA in vitro (Elenbaas et al. 1996). This means that the RNA-binding activity of MDM2 is likely to be an important function of MDM2. Recently the RING finger of MDM2 was shown to play a role in cell cycle regulation which was independent of p53 degradation (Argentini et al. 2000).

1.4.2 *mdm2* expression in tumors

The *mdm2* gene has been found amplified and overexpressed mainly in tumor cells of non-epithelial origin, especially in those derived from the mesenchyme. *mdm2* amplification has been found in approximately 20% of soft tissue tumors including osteosarcomas, liposarcomas, and malignant fibrous histiocytomas, and furthermore, in

about 9% of gliomas, 12% of testicular germ cell tumors (as reviewed by Momand and Zambetti 1997). In carcinomas, except for esophageal tumors, amplification is rare (as reviewed by Momand and Zambetti 1997) and has not been found in any case of ovarian cancer (Foulkes et al. 1995). In primary sarcomas and cell lines that were characterized in more detail, amplification of the *mdm2* gene correlated with overexpression of the MDM2 protein (Oliner et al. 1992).

Overexpression has been found in some tumors independently of amplification. In human leukemia samples, *mdm2* mRNA was dramatically upregulated while a normal DNA copy number was maintained (Momand and Zambetti, 1997). MDM2 protein overexpression has been found despite normal levels of *mdm2* mRNA, most likely due to enhanced translation efficiency (Landers et al. 1994).

Evidence of different sizes of mRNA transcripts in tumors was noted when *mdm2* was initially cloned (Oliner et al. 1992) and, later, altered mRNAs resulting from alternative splicing were described in bladder and ovarian carcinomas (Sigalas et al. 1996). These alternatively spliced *mdm2* mRNAs were correlated with advanced stage and poor differentiation in ovarian carcinomas and transfection of NIH 3T3 cells with the splice variants showed transforming ability of the RNA transcripts (Sigalas et al. 1996). Smaller protein variants of sizes between 78 kD and 12kD have been noted in non-small cell lung cancer, and are also thought to be derived by differential splicing (Maxwell, 1994).

The finding of these alterations in human tumors indicates that *mdm2* acts as a proto-oncogene that promotes the tumorigenicity of a cell through inactivation of the p53 tumor suppression function and possibly by other, as yet unidentified, mechanisms.

1.4.3 The MDM2/p53 autoregulatory feedback-loop

mdm2 has several characteristics of a cellular proto-oncogene and the mechanism by which it promotes the tumorigenicity of a cell became clearer when MDM2 was discovered to bind to the p53 protein and inhibit p53 mediated transactivation (Momand et al. 1992). MDM2 is a potent inhibitor of p53. It binds to the transcriptional activation domain of p53 and blocks its ability to regulate target genes (Picksley et al. 1994, Chen J. et al. 1996) and to exert antiproliferative effects (Chen, C.-Y. et al. 1994, Haupt and Oren, 1996, Chen, J. et al. 1996). *Mdm2* expression is upregulated by p53 in an autoregulatory feedback loop (Gottlieb and Oren, 1998).

Several mechanisms of MDM2/p53 interaction are presently known: 1) counteracting the induction of cell cycle inhibitory genes 2) a protective role of

MDM2 against apoptosis 3) nuclear export and 4) rapid degradation of the p53 protein by MDM2 (Fig. 6).

1) MDM2 was shown to inhibit p53-transcriptional activation by „concealing,, the acidic activation domain of p53 from the transcriptional machinery (Oliner et al. 1993). Other experiments suggested that p53 protein, if it is bound in a complex with MDM2, no longer binds to p53 target DNA (Zauberman et al. 1993). The binding site of MDM2 to p53 has been located to amino-acid 18-23 at the N-terminus of the p53 protein by mapping studies (Chen et al. 1993). Only the amino-terminal end of MDM2 is necessary to bind and inhibit p53, suggesting that the full-length protein may carry out additional functions. The binding site for p53 has been localized to aa 19-102 of

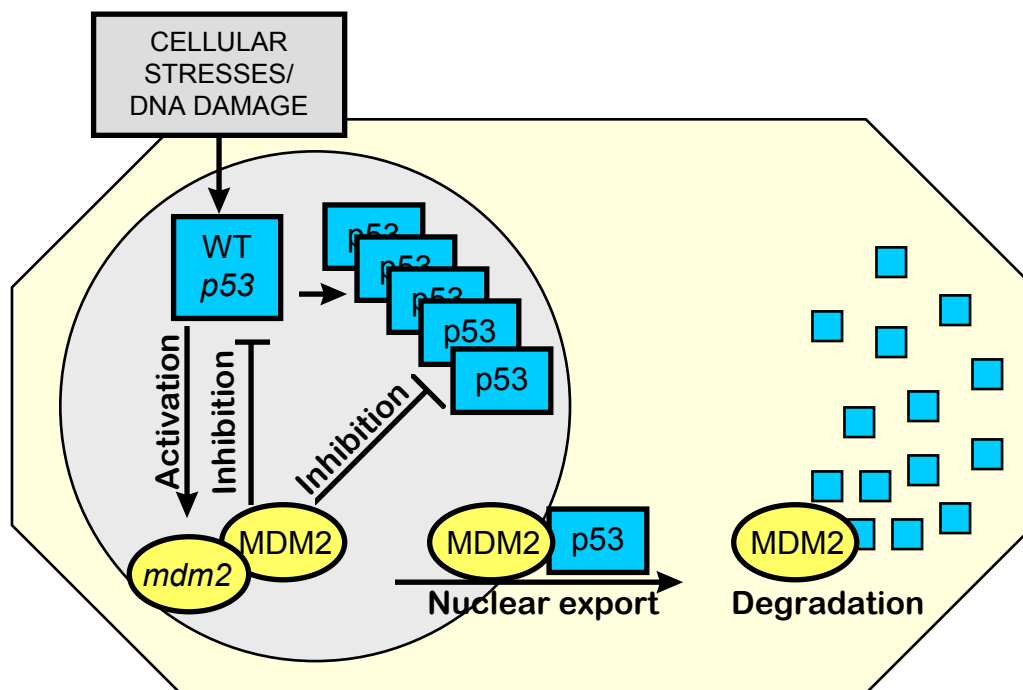


Fig. 6: Autoregulatory feedback loop of the p53 tumor suppressor gene and the *mdm2* gene. p53 at basal and at increased levels activates the *mdm2* gene. The MDM2 protein binds to p53, inhibits its DNA binding ability, and promotes nuclear export and protein degradation.

the *mdm2* gene (Chen et al. 1993). MDM2 residues G58, D68, V75 and C77 have been shown to be critical for MDM2 interaction with p53. Mutation of these residues prevents MDM2 interaction with p53 in vitro and MDM2's regulation of p53's transcriptional activity in vivo (Freedman et al. 1997).

Recent reports also indicate that MDM2 may have a second mechanism to inhibit p53-dependent transcriptional activation at a promoter. In these experiments, deletion mutants of MDM2 defective in p53 binding are able to repress both p53-

activated and basal transcription when brought to a promoter by fusion to a DNA-binding domain (Thut et al. 1997).

MDM2 is upregulated in response to p53 activation and has been shown to inhibit p53-dependent G1 arrest in response to irradiation (Chen et al. 1994, Chen J. et al. 1996). Control of p53 activity by MDM2 also plays an important role during embryonic development. The expression of the xenopus laevis homolog *xmd2* of *mdm2* increases during early embryogenesis from oocyte stage I/II to reach its maximum in oocyte stage V/VI in unfertilized eggs and then becomes undetectable (Marechal et al. 1997). Earlier studies had already demonstrated that the *mdm2*-null genotype leads to embryonic lethality while mice deficient for both *mdm2* and *p53* develop normally and are viable (Montes de Oca Luna et al. 1996, Jones et al. 1995). These results strongly suggest a primary developmental role for MDM2 in negative regulation of p53 function.

2) The role of MDM2 in protecting against apoptosis is less clear, but several studies have shown evidence for this function of MDM2. p53 dependent apoptosis induced by *c-myc* overexpression was inhibited by MDM2 (Chen et al. 1996) and protection from apoptosis required formation of a p53- MDM2 complex in human H1299 cells (Haupt et al. 1997). Rb can overcome the antiapoptotic effect of MDM2 on p53-induced apoptosis by preventing MDM2 from targeting p53 for degradation. Rb-MDM2 interaction, though, does not prevent inhibition of p53-mediated transcription (Hsieh et al. 1999). Recently, experiments with fibroblasts from *p53/mdm2* null mice, which were transfected with a retroviral vector carrying temperature-sensitive p53, have shown that loss of *mdm2* can induce the p53-dependent apoptotic pathway in vivo (de Rozières et al. 2000).

3) MDM2 has been shown to contain a nuclear export signal (NES) and to be able to shuttle across the nuclear membrane in both directions (Fig. 6) (Roth et al. 1998). The findings suggest that MDM2 binds to p53 in the nucleus and transports it to the cytoplasm for degradation (Roth et al. 1998, Tao and Levine, 1999). Cytoplasmic distribution of p53 is thought to result from efficient export of nuclear p53 in combination with MDM2-mediated degradation (Lu et al. 2000).

4) MDM2 was shown to promote rapid degradation of the p53 protein (Haupt et al. 1997, Kubbutat et al. 1997, Kubbutat and Vousden, 1998). MDM2 downregulates the amount of p53 protein but does not reduce *p53* mRNA levels (Haupt et al. 1997, Kubbutat et al. 1997). These results indicate that p53 levels are regulated by MDM2 through a post-transcriptional mechanism. Once shuttled out of the nucleus, p53 is thought to be transported to a cytoplasmic proteasome for ubiquitin mediated degradation (Roth et al. 1998, Tao and Levine, 1999). Amino-acids 92-112 of p53 have been identified to function as a degradation signal (Gu et al. 2000).

Degradation of p53 by MDM2 depends directly on the ability of MDM2 to shuttle from the nucleus to the cytoplasm (Tao and Levine, 1999). Expression of p19ARF was shown to block the nucleo-cytoplasmic shuttling of MDM2 and could therefore stabilize p53 by protecting it from MDM2 mediated degradation (Tao and Levine, 1999).

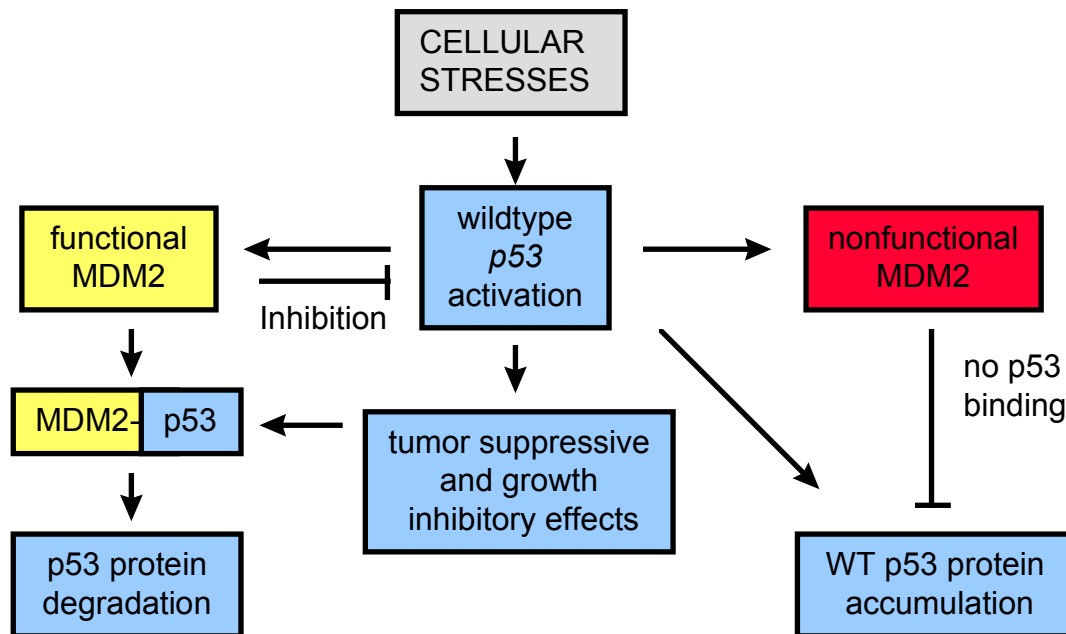


Fig. 7: Hypothetic model about the effects of impaired MDM2 function on p53 protein accumulation in the cell. Cellular stresses cause p53 activation, which is downregulated by functional MDM2 in an autoregulatory feedback loop. In case of nonfunctional MDM2, wildtype p53 accumulates in the nucleus.

The MDM2/p53 autoregulatory feedback loop, as described above, can be abolished by p53 as well as MDM2 alterations (Fig. 7). Firstly, *p53* mutations have been shown to cause accumulation of p53 protein which is frequently seen in tumors due to a lack of p53-mediated MDM2 induction (Haupt et al. 1997, Kubbutat et al. 1997). Secondly, a dysfunctional MDM2, as it is seen in some forms of alternative splicing, can cause p53 accumulation due to the loss of p53 binding ability (Kubbutat et al. 1997, Kraus et al. 1999).

Physiologically, the MDM2 protein itself is degraded by ARF, which means that p53 cell cycle regulatory functions can be restored by ARF/MDM2 binding (Zhang et al. 1998, Pomerantz et al. 1998). Despite other, as yet not fully understood, functions of MDM2 the MDM2/p53 interaction seems to play a crucial role in cell cycle regulation. MDM2 ensures effective reduction and termination of the p53 signal

after DNA damage induced p53 activation to reverse cell cycle arrest and allow the re-entry of the cell into the cell cycle.

1.4.4 Clinical implications of *mdm2* alterations

mdm2 amplification has been frequently noted in tumors of mesenchymal origin, and overexpression, which is present in approximately 20% of soft tissue sarcomas, has been found associated with poor prognosis (Cordon-Cardo et al. 1994). *mdm2* alternative mRNA splicing has been found to be associated with poor differentiation and advanced stage in ovarian carcinomas (Sigalas et al. 1996). Since MDM2 controls p53 function in an autoregulatory feedback loop, it plays a major role in tumorigenesis.

It was hypothesized that tumors expressing abnormally high levels of *mdm2* could be treated by means of peptides derived from the p53 interaction domain. By binding to MDM2 and preventing its interaction with p53, such peptides could restore p53 function to the tumor cells, presumably preventing further growth (Oliner et al. 1993). Microinjection of a monoclonal antibody against the p53-binding domain of MDM2, 3G5, (Chen et al. 1993) blocks the p53/MDM2 interaction and leads to p53-dependent activation of reporter genes in cell lines that have wild-type *p53* (as reviewed by Freedman et al. 1999).

Since MDM2 is assumed to counteract the induction of apoptosis by p53, it may also play a role for the response of tumors to DNA-damaging chemotherapeutic agents. Overexpression of *mdm2* was found to decrease the susceptibility of human glioblastoma cells to apoptosis induced by Cisplatin, while expression of antisense *mdm2* increased their susceptibility (Kondo et al. 1995). Lowering the levels of *mdm2* in cell lines that overexpress p53 also appears to activate the wild-type p53 protein present in such cells. By using antisense oligonucleotides to the *mdm2* message in a choriocarcinoma cell line which has wild-type *p53* and *mdm2* gene amplification, *p53* reporter genes can be activated and the cells induced to undergo apoptosis (Chen et al. 1998). Following intraperitoneal administration of anti-*mdm2* antisense oligonucleotides, in vivo antitumor activity was observed in nude mice bearing osteosarcoma and choriocarcinoma xenografts (Wang et al. 1999). An *mdm2* antisense phosphorothioate oligodeoxynucleotide was identified that effectively inhibits *mdm2* expression in tumor cells containing *mdm2* gene amplification. Antisense inhibition of *mdm2* was associated with a decrease in MDM2/p53 complex formation, increase in p53-inducible gene expression, increase in p53 transcriptional activity and apoptosis (Chen et al. 1998). Recently a novel mechanism of MDM2 degradation by the protein ARF has been identified, which can neutralize the inhibition of p53 by MDM2 and restore

the p53 function for cell cycle control and apoptosis (Zhang et al. 1998, Pomerantz et al. 1998).

Further understanding of the functions and regulatory mechanisms in which *mdm2* is involved will give important new insights in tumorigenesis and resistance to chemotherapy. Disruption of the MDM2/p53 wildtype interaction and perhaps Rb, E2F1, and DP1 might be important goals for cancer therapy.

2. OBJECTIVES

The *p53* gene is a tumor suppressor gene which has been named the "guardian of the genome", (Lane 1992). It is activated in response to cellular stresses and DNA damage and regulates cell cycle arrest and apoptosis. It has been found to be mutated in more than 50% of human carcinomas and the loss of its function through mutation is thought to be one of the major steps in carcinogenesis (Hollstein et al. 1994). The *mdm2* (murine double minute 2) gene was initially described as a proto-oncogene and is amplified and overexpressed in human soft tissue sarcomas and gliomas (Oliner et al. 1992). Most importantly though, MDM2 was found to be activated by p53 and subsequently inhibit p53 in an autoregulatory feedback-loop and promote its nuclear export and rapid degradation (Momand et al. 1992, Haupt et al. 1997, Kubbutat et al. 1997, Roth et al. 1998). Thereby it allows the cell to re-enter the cell cycle after repair of DNA damage.

In this investigation we analyzed frozen tumor tissue of a series of 178 ovarian carcinoma patients with long term follow-up data for alterations of the *p53* and *mdm2* gene and their impact on response to chemotherapy and survival. *p53* mutations and polymorphisms were characterized by screening the entire coding region of the gene (exon 2-11) with PCR/SSCP (Single Strand Conformation Polymorphism) and DNA sequence analysis. Overexpression of p53 was analyzed by immunohistochemistry in frozen tissue.

Since MDM2 promotes the rapid degradation of p53 protein, alterations of MDM2 are expected to cause p53 stabilization and accumulation, as it is seen in a number of ovarian carcinomas with wildtype *p53* sequence. We therefore analyzed *mdm2* for amplification and overexpression by Southern and Northern hybridization and for RNA alternative splicing by RT-PCR and cDNA sequencing. The frequency and the type of alternative *mdm2* RNA splice variants were also analyzed in ovarian tumors of borderline malignancy, benign cystadenomas, and normal ovarian tissue to identify patterns of splicing which may be involved in carcinogenesis.

Results of *p53* and *mdm2* alterations were statistically evaluated for correlations to clinical and histopathological parameters, response to platinum-based chemotherapy, time to relapse or progression of disease, and overall survival. Furthermore p53 mutation and overexpression were analyzed in correlation to *mdm2* alterations to clarify whether loss of the p53 binding domain in *mdm2* splice variants would cause stabilization and accumulation of p53 protein in the absence of mutations.

3. PATIENTS, MATERIALS, AND METHODS

3.1 Patients and clinical data

3.1.1 Asservation and storage of tissue

During exploratory laparotomy both ovaries were examined for tumor involvement and salpingo-oophorectomy was performed in a typical manner. The ovary which was suspected of being tumorous or, if both were involved, the ovary which had the greater tumor mass was sent to the Pathology Department for frozen section diagnosis, where a tissue block of at least 1 cm³ was excised and immediately snap frozen in liquid nitrogen. The tissue was stored in plastic containers (Althor Products, Bethel, Connecticut, USA) at -80° C. Ninety-eight cases were collected at the Department of Gynecology of the Charité, Campus Virchow-Klinikum, Humboldt-University in Berlin. Eighty cases were available from the USC frozen tissue resource of the Principal Investigator Michael F. Press MD, PhD and had mainly been collected at the M.D. Anderson Cancer Center in Houston, Texas, USA.

3.1.2 Study population and surgical therapy

The study population consisted of a total of 178 patients with invasive epithelial ovarian carcinoma who had undergone surgery between 1972 and 1995 at the Department of Gynecology of the Charité, Campus Virchow-Klinikum, Humboldt-University in Berlin (n=98) or at the M.D. Anderson Cancer Center in Houston, Texas, USA (n=80). The clinical and histopathological characteristics of the patients are demonstrated in Table 12. Patient age ranged from 23 to 84 years with a median age of 57 years. The racial-ethnic groups represented were: White 92%, African-American 5%, Hispanic 3% and Asian 1%.

Each patient underwent exploratory laparotomy with bilateral salpingo-oophorectomy, hysterectomy, and infracolic omentectomy as part of her treatment for ovarian cancer. In 61 of the patients pelvic lymphadenectomy and in 29 patients additional paraaortic lymphadenectomy was performed as part of the primary surgery.

3.1.3 FIGO-stage, histology and grade of differentiation

All patients were staged according to the 1986 guidelines of the International Federation of Gynecologists and Obstetricians (FIGO) (Pettersson 1991). For purposes of statistical analysis, patients who had undergone surgery before 1986 were restaged according to the 1986 guidelines. At the time of diagnosis, 21% of the patients were diagnosed as FIGO stage I, 5% as stage II, 61% as stage III and 13% as stage IV (Table 12). Complete surgical resection of the tumor was possible in 71 cases (46%) and optimal debulking with a residual tumor mass of less than 2 cm was achieved in 48 cases (31%), but a residual tumor mass of more than 2 cm was left *in situ* in 34 cases (22%).

All tumors were classified and graded according to the criteria defined by the World Health Organization. The 178 epithelial ovarian carcinomas studied for p53 alterations included 111 (62%) serous, 30 (17%) endometrioid, 8 (5%) mucinous, 6 (3%) clear cell, 1 (0.6%) malignant Brenner tumor, 10 (6%) undifferentiated, 10 (6%) mixed epithelial and 2 (1%) unclassified epithelial tumor.

The tumors were graded as well differentiated in 28 (16%) cases, moderately differentiated in 52 (29%) and poorly differentiated in 98 (55%) cases. The evaluation of differentiation was based on the degree of histologic differentiation with the formation of papillary, tubular, glandular or cystic structures versus solid structures.

One hundred and three cases included in this study had been previously characterized for DNA ploidy and S-phase fraction with a Cell Analysis System Image Analyzer (CAS 200, Becton-Dickinson). Fifty-four percent of the ovarian carcinomas were found to be diploid, 38% aneuploid and 8% tetraploid. The S-phase-fraction was low ($< 5\%$) in 27%, intermediate (5% - 14.5%) in 47% and high ($\geq 14.5\%$) in 26% of the patients (Reles et al. 1998).

3.1.4 Adjuvant chemotherapy

Adjuvant chemotherapy was given to 115 (76%) of the patients with tumor stages Ib-IV. Among these, 54 (47%) of the patients were treated with Cisplatin / Cyclophosphamide, 20 patients (17%) with Carboplatin / Cyclophosphamide and 41 (36%) of the patients with other chemotherapy-regimens. 36 patients (24%) were not treated with adjuvant chemotherapy because of early stage disease, old age, or because they refused treatment. In 27 patients, information about chemotherapy treatment was insufficient (Table 12).

The response to chemotherapy was defined 1) as platinum refractory, if there was no change or progressive disease during therapy, 2) as platinum resistant, if the patient responded initially but relapsed or progressed within 6 months after the last cycle of chemotherapy and 3) as platinum sensitive, if no relapse or progression was noted within six months after the last cycle of chemotherapy.

3.1.5 Clinical follow-up information

Clinical follow-up and overall survival information was available for all 178 patients and information about progression of the disease was available for 138 (78%) patients. The majority of patients were seen at the outpatient clinics of the Charité, Campus Virchow-Klinikum, Berlin and the MD Anderson Cancer Center, Houston, respectively for follow-up. Additional information was available from physicians in private practice. Follow-up ranged from 1 month to 12 years with a median follow-up of 31 months in the total cohort and 52 months for the survivors.

During the time of follow-up 117 (66%) deaths occurred. 104 patients died from ovarian cancer, 6 patients by intercurrent disease or accident, and one patient died from a complication of surgery. Sixty (34%) patients were alive and in 7 cases, no information about the cause of death was available. At the time of last contact, 48 patients (27%) showed no evidence of disease. 76 patients (43%) had been documented to have recurrent disease, three patients had

known residual disease with steady state, 11 patients (6%) had primarily progressive disease and in 29 (16%) patients, who died from the tumor, the date of relapse was not available from the patient charts. In 11 patients, the disease status was not sufficiently documented.

3.2 Materials

3.2.1 Plastic ware, chemicals, and consumables

If not otherwise specified, sterile disposable plastic ware for molecular biology experiments was purchased from CLP (Continental Lab Products) and Falcon Labware (Oxnard, CA, USA). PCR tubes were purchased from CLP (Continental Lab Products). Chemicals were obtained from Sigma (St. Louis, MO, USA) and Amersham Life Science (Arlington Heights, IL, USA). Restriction enzymes were ordered from Gibco BRL (Gaithersburg, MD, USA) or NEB (Beverly, CA, USA). Length standards for DNA and RNA were purchased from Gibco BRL (Gaithersburg, MD, USA). Molecular biology products were obtained from Pharmacia (Uppsala, Sweden), Stratagene (La Jolla, CA, USA) or NEB (Beverly, CA, USA). Tissue culture plastic ware was purchased from Falcon Labware (Oxnard, CA, USA) and additives for tissue culture and media from Gibco BRL (Gaithersburg, MD, USA) or Difco (Detroit, MI, USA).

3.2.2 Standard buffers and solutions

TE	10 mM Tris/Cl, pH 7.4 1 mM EDTA
TAE	40 mM Tris / acetate, pH 8,0 1mM EDTA
TBE	89 mM Tris 89 mM boric acid 2 mM EDTA pH 8.3
PBS	137 mM NaCl 2.7 mM KCl 8 mM Na ₂ HPO ₄ 1.5 mM KH ₂ PO ₄ pH 7.2

GTB 20x 250 ml ready mix	Tris base	54g
	Taurine	18 g
	Na ₂ -EDTA	1g
MOPS	200 mM MOPS	
	50 mM Na Acetate 3.H ₂ O	
	10 mM Na ₂ -EDTA	
SSC	150 mM NaCl	
	15 mM Na-citrate	
DEPC-H ₂ O (Diethyl-pyrocbonat)	0.1% v/v DEPC in H ₂ O	
Stop Solution for SSCP	95% v/v Formamide	
	20 mM EDTA	
	0.25% w/v Bromophenol Blue	
	0.25% w/v Xylene Cyanol	
Dye for RNA/DNA gel electrophoresis	1 mM EDTA, pH 8.0	
	50% v/v Glycerol	
	0.25% w/v Bromophenol blue	
	0.25% w/v Xylene cyanole	
Loading buffer RNA gels (1ml)	10x MOPS	100 µl
	Formamide	500 µl
	Formaldehyde	174 µl
	10 x dye	100 µl
	EtBr (10mg/ml)	10 µl
0.1 M sodium acetate buffer pH 4.0	0.2 M acetic acid	82 ml
	0.2 M sodium acetate	18 ml
	deionized H ₂ O	<u>100 ml</u> 200 ml
Ethyl Green solution	Ethyl Green	0.5g
	0.1 M sodium acetate buffer	100 ml

3.2.3 Standard gel electrophoresis components

1.2% Agarose Gel (100 ml)	0.5x TBE	100 ml
	Agarose	1.2g
	EtBr (10mg/ml)	2 µl
0.5 x MDE Gel for SSCP (100 ml)	MDE Gel Solution	25 ml
	10 x TBE	6 ml
	Glycerol 10%	5 ml
	deionized H ₂ O	64 ml
	TEMED	40 µl
	10 % APS	400 µl
6% Acrylamide Gel for Sequencing (100 ml)	Sequagel™ Concentrate	24 ml
	Sequagel™ Diluent	66 ml
	10 x GTB buffer	10 ml
	TEMED	40 µl
	10% APS	800 µl
1% Agarose gel for Northern (500 ml)	Agarose	5g
	DEPC H ₂ O	365 ml
	10 x MOPS	50 ml
	Formaldehyde	85 ml

3.2.4 Chemicals

Table 4: List of all chemicals used in the experiments

Chemical	Company	Catalog #
Acetic Acid	Sigma	A 5640
Acetone	Sigma	A 4206
Acrylamide	Sigma	A 8887
Ammonium Persulfate	Sigma	A-3678
Ampicillin	Sigma	A 9393
Aprotinin	Sigma	A 1153
Bisacrylamide	Sigma	M 7256
Bromophenol Blue	Sigma	B 0126
Chloroform	Sigma	C 5312
DAB	Abbott (ER Kit)	2A08-18

Deoxycholate	Sigma	D 5670
dNTP (Ultrapure dNTP Set)	Pharmacia Biotech	27-2035-01
dNTP mix 10mM	Gibco	18427
DNA ladder 1Kb	Gibco	15615-016
DTT (Dithiotreitol)	Gibco	15508-013
ECL Western blotting detection reagent	Amersham	RPN 2109
E. coli pulser cuvettes 0.1 cm	BIO-RAD	165-2089
EDTA	Sigma	E 7889
Epicurian Coli® XL1-Blue Electroporation-Competent Cells	Stratagene Cloning Systems	200228
Ethidiumbromide	Biorad	161-0433
Ethyl Green	Sigma	M 8884
Exonuclease I	Amersham Life Sciences	US 72050
Fetal calf serum	Omega	FB 01
Gene Clean Kit	Bio 101	1001-600
L-Glutamine (cell culture)	Gibco	21051-016
Glycerol	Amersham Life Sciences	US 16374
Glycine	Sigma	G 7403
GTB Glycerol Tolerant Buffer	Amersham Life Sciences	US 71949
Hepes	Gibco	11344-033
Hybridization membrane Hybond ECL	Amersham Life Sciences	RPN 68D
Hybridization membrane Hybond XL	Amersham Life Sciences	RPN 82S
Isopropanol	Sigma	405-7
Kanamycin	Sigma	K 4000
Kcl (Potassium Chloride)	Sigma	P 9333
Kodak X-OMAT AR	Eastman Kodak Company	1651454
Kodak Biomax MS film	Eastman Kodak Company	1435726
Kodak Biomax MR film	Eastman Kodak Company	8715187
Kodak Biomax MR2 film	Eastman Kodak Company	IB8952855
LB Agar tablets	Sigma	L 7025
LB Broth	Sigma	L 3022
Leupeptin	Sigma	L 2023
Lipofectamine™ Reagent	Gibco BRL	18324-020
MDE™ Mutation Detection Gel Solution	AT Biochem	1-500-00
Megaprime™ DNA labelling system	Amersham Life Science	RPN1604/5/6/7
Methanol	Sigma	M 1775
MicroSpin Columns S-400 HR	Pharmacia	27-5140-01
Mineral oil (PCR)	Sigma	M 8662
M-MLV Reverse Transcriptase	Gibco BRL	28025-013
NaCl (Sodium Chloride)	Sigma	S 7653

NaF (Sodium Fluoride)	Sigma	S 7920
Nonidet P40 (Octylphenoxy Polyethoxy Ethanol) (Igepal CA 630)	Sigma	I 3021
oligo (dT) ₁₅ primer	Promega	C 1101
pcDNA3.1 Expression vector	Invitrogen	V 790-20
Penicillin/Streptomycin	Gibco	043-05140
Pepstatin A	Sigma	P 5318
Permout	Fisher	SP15-500
Phenol/chloroform/isoamyl alcohol (25:24:1)	Boehringer Mannheim	101 001
Plasmid Maxi Protocol kit	Qiagen	12162
PMSF (PhenylmethylsulfonylFluoride)	Sigma	P 7626
Protein G sepharose beads	Pharmacia	17-0618-01
Proteinase K	Sigma	P 6556
Pwo DNA Polymerase	Boehringer Mannheim	1644947
Qiagen Plasmid Midi Protocol Kit	Qiagen	12143
Qiagen Plasmid Purification Kit (Mini-Prep)	Qiagen	12123
Qiaquick Gel Extraction Kit	Qiagen	28704
Qiaquick PCR Purification Kit	Qiagen	28104
Quick Spin TM Columns	Boehringer Mannheim	1273 922
Rapid-hyb buffer	Amersham Life Science	RPN 1635
Restriction enzyme		
AscI	NEB	558S
Bam HI	NEB	136S
BglII	NEB	143S
Eco RI	Gibco	15202-013
HindIII	NEB	104S
MluI	NEB	198L
NcoI	Gibco	15421-019
Sal I	Gibco	15217-011
RNAguard®	Pharmacia	27-0816-01
RNA ladder 0.24-9.5 Kb	Gibco	15620-016
RPMI medium 1640	Gibco	21870-092
Salmon sperm DNA	Gibco	15632-011
SDS (Sodium Dodecyl Sulfate)	Pharmacia	US75832
SDS-PAGE Standards, broad range, prestained	BIO-RAD	161-0318
Sequagel TM Sequencing System, Concentrate	National Diagnostics	EC 830
Sequagel TM Sequencing System, Diluent	National Diagnostics	EC 840
Shrimp Alkaline Phosphatase	Amersham Life Sciences	US 70173
Sodiumacetate (NaOAc)	Sigma	S 7670
SEA Spray	CLP	5455

TA Cloning® kit (INVαF' One Shot Kit)	Invitrogen	K2000-01
Taq DNA Polymerase 500 units	Promega	M 1865
TEMED (N,N,N,N'-Tetramethyl-Ethylenediamine)	Sigma	T 8133
T4 DNA Ligase 500 units	Boehringer Mannheim	481220
Tris base	Sigma	T 6791
Trizol Reagent	Gibco	15596-026
Tween-20	Sigma	P 7949
Whatman 3 MM Chromatography paper	Fisher	057163W
X-Gal	Gibco	15520-034
Xylene cyanole	Fisher	X3P-IGAL

3.2.5 Radio-chemicals

[α - ³² P]dCTP (10 mCi/ml - 3000 Ci/mmol)	Amersham	# AA 0005
[α - ³³ P]dATP (10 mCi/mmol - 2000 Ci/mmol)	Dupont	# NEG/613 H
[α - ³³ P]dCTP (10 mCi/mmol - 2000 Ci/mmol)	Dupont	# NEG/612 H
[α - ³³ P]ddATP (450 μ Ci/ml - 1500 Ci/mmol)	Amersham	Kit # 188403
[α - ³³ P]ddATP (450 μ Ci/ml - 1500 Ci/mmol)	Amersham	Kit # 188403
[α - ³³ P]ddATP (450 μ Ci/ml - 1500 Ci/mmol)	Amersham	Kit # 188403
[α - ³³ P]ddATP (450 μ Ci/ml - 1500 Ci/mmol)	Amersham	Kit # 188403

3.2.6 Standard kits

The Qiaquick PCR Purification Kit (Qiagen, Hilden, Germany) was used for purification of PCR products for cloning and the Qiaquick Gel Extraction Kit (Qiagen, Hilden, Germany) and the GeneClean kit (BIO 101) were used for extraction of DNA from agarose gels. DNA sequencing was performed with the Thermo Sequenase radiolabeled terminator cycle sequencing kit (Amersham Life Science). Purification of plasmid DNA was performed with the Qiagen Plasmid Purification Kit (Qiagen, Hilden, Germany) for mini- and midi-preps. The TA cloning kit (Invitrogen, INVαF'One Shot Kit) was used for cloning cDNA into a TA vector. For detection of proteins in Western blotting we used the ECL Kit (Amersham).

3.2.7 Monoclonal and polyclonal antibodies

Monoclonal Antibodies

Clone	origin	Company	Catalog #
DO7	mouse anti-human p53 protein	DAKO Inc.	M7001
3F10	rat anti human influenza virus HA	Boehringer Mannheim	1867423
9E10	mouse IgG1 anti human c-myc	Boehringer Mannheim	1667149
12CA5	mouse IgG1 anti HA	Boehringer Mannheim	15833816

Polyclonal Antibodies

normal mouse IgG	Zymed Laboratories	08-6599
rabbit anti-mouse IgG	Zymed Laboratories	61-6500
mouse peroxidase anti-peroxidase antibody	Sternberger Meyer	405
goat anti-mouse IgG-HRPO	BIO-RAD	172-1011
rabbit anti-rat IgG-HRPO	DAKO	P0162

3.2.8 Laboratory equipment and other materials

For DNA and RNA extraction a tissue homogenizer (VWR) was used and centrifugation steps were carried out in an Eppendorf 5415 table centrifuge. The optical density of DNA and RNA were measured with a Beckman DU-600 spectrophotometer. PCR reactions were performed in either a Perkin Elmer Cetus DNA Thermal Cycler 480 or an MJ Research PC 100/96V Thermal Cycler.

For SSCP and sequencing, gel electrophoresis was carried out in a 38x50 cm Sequi-Gen GT Sequencing Cell (Biorad), using a Power Pac 3000 Power Supply (Biorad). For sequencing a Vinyl Sharktooth Comb of 0.4 mm thickness and 30 cm length with 97 wells was used to separate lanes. Gels were dried in a Savant gel drier (GDS 100 - SGD 2000 - GP 110).

Tissue sections for immunohistochemistry were cut with a Tissue Tek II Cryostat, mounted on Fisher slides and encircled with a PAP pen (Kiyota International Inc.). Staining results were evaluated with an Olympus BH2 microscope.

For Southern and Northern hybridization radioactivity of the probe was measured in a Scintillation Counter Tri-Carb 2100TR (Packard Instruments) and hybridization was carried out in a Micro Hybridization Incubator Model 2000 (Robbins Scientific).

For DNA cloning into the pcDNA3 expression vector a Biorad E. coli pulser apparatus 120 V was used for transformation of bacteria. Western blotting of expressed proteins was carried out with a Transblot Electrophoretic Transfer Cell (BIO-RAD Laboratories, Hercules, CA, USA).

3.3 Methods

3.3.1 Immunohistochemistry

3.3.2.1 Sections of tissues and control cell lines

Frozen tissue samples were embedded in OCT compound, sectioned at 4 μ m in a TissueTek II cryostat, thaw-mounted on glass slides and fixed immediately in acetone for 10 minutes. The initial tissue section, stained with hematoxylin and eosin, was used to confirm that an ovarian tumor of the appropriate histopathologic type was present in the frozen specimen. Subsequent tissue sections were immunostained for p53 or used as a negative control section.

Frozen cell pellets of human breast cancer cell lines known to have mutant *p53* (SK-BR-3 and T47D, American Type Culture Collection) were used as positive control specimens for the immunohistochemistry. After fixation in acetone, sections were transferred to PBS buffer and subsequently, endogenous peroxidase was bleached off by incubation with 0.5% H₂O₂ in PBS for 15 minutes.

3.3.1.2 *Incubation with primary and secondary antibodies*

After rinsing in PBS for 2 x 5 minutes, unspecific antigen activity was blocked by incubation with 10% normal rabbit serum for 20 minutes. Tissue sections were encircled with a PAP pen. *p53* immunostaining was performed by successive incubation in a primary mouse monoclonal *p53* antibody (DO-7, 0.95 microgm/ml [1:100 dilution], DAKO Corp.) for 1 hour and after rinsing in PBS a bridging secondary rabbit antimouse IgG antibody (Zymed Laboratories) for 30 minutes.

A negative control was prepared for each unknown tissue by substituting normal mouse IgG (2.5 microgm/ml [1:1000 dilution], Zymed Laboratories, Inc. Cat# 08-6599) for the primary *p53* antibody.

3.3.1.3 *Peroxidase-antiperoxidase reaction*

After rinsing in PBS, the peroxidase anti-peroxidase antibody (Sternberger Meyer #405) was applied in a 1:50 dilution for 30 minutes at room temperature and slides were subsequently rinsed in PBS again for 3 x 5 minutes. A DAB solution (Abbott Kit #2A08) was prepared, filtered through a 0.22 µm millipore filter and applied to the slides for 7 minutes at room temperature after blotting off excess saline.

Slides were counterstained by rinsing in 0.1 M sodium acetate buffer for 10 minutes, staining in ethyl green solution for 10 minutes, rinsing in deionized H₂O for 2x 10 dips and 1x 30 seconds, and dehydrating in butanol with 2x 10 dips, 1x 3 minutes and xylene 3x for 2 minutes each. Slides were subsequently mounted with Permount (Fisher).

3.3.1.4 *Microscopic evaluation*

Nuclear immunostaining patterns were evaluated by three observers (Angela Reles, Wen H. Wen, Michael F. Press). The immunoreactivity for *p53* antibody was scored as the percentage of positively stained nuclei by counting 100-200 (minimum 100) tumor cells. Tumors with 10% or more nuclei showing immunostaining were considered to have *p53* overexpression.

3.3.2 **Molecular biology techniques**

3.3.2.1 *Isolation of genomic DNA from frozen tumor tissue*

Frozen tissue sections stained with hematoxylin and eosin were used to confirm that the majority of the tissue selected for analysis was composed of tumor cells. To isolate genomic DNA, 10-20 serial frozen tissue sections (10 microns thick) of the tumor were collected in Eppendorf tubes and incubated in 300 µl extraction solution consisting of 10mM Tris Hcl pH 7.5, 25mM EDTA, 100mM NaCl, 0.5% SDS and Proteinase K (0.1 mg/ml) overnight at 50°C.

After complete digestion 300 µl of phenol:chloroform:isoamyl alcohol (50:49:1) were added and DNA was purified by centrifugation following deproteinization at 14.000 rpm for 5 min. The DNA containing supernatant was placed in a new tube and DNA was precipitated with 2.5 volumes of 100% ethanol and 0.1 volume 3M Na-Acetate pH 6.0 overnight at -20° C. After centrifugation at 14.000 rpm for 30 min and removing the supernatant the pellet was washed with 75% ethanol, airdried and resuspended in 20 µl TE buffer. The DNA yield was measured by spectrophotometry at OD 260 and the concentration was determined according to the formula: DNA concentration (µg/ µl) = (OD 260 x 50 x dilution factor) : 1000

3.3.2.2 *Isolation of genomic DNA from paraffin embedded tissue*

Formalin-fixed, paraffin-embedded tissue stained with hematoxylin and eosin was used to confirm that the majority of the tissue selected for analysis was composed of tumor cells. Three serial sections of 8-10 microns were collected into Eppendorf tubes and deparaffinized by subsequent treatment with Xylene for 5 min, 100% ethanol for 3 min and 95% ethanol for 3 min, each step followed by 5 min centrifugation at 14.000 rpm and removal of the supernatant. The tissue was airdried for 1 hour and then placed in 400 µl of an extraction solution at pH 8.0 containing:

- 100 mM Tris/Cl
- 4mM EDTA
- 500 µg/ml proteinase K

for 3 to 4 days at 50°C. After complete digestion 400 µl of phenol:chloroform:isoamyl alcohol (50:49:1) were added and DNA was purified by centrifugation following deproteinization at 14.000 rpm for 5 min. The DNA containing supernatant was placed in a new tube and DNA was precipitated with 2.5 volumes of 100% ethanol and 0.1 volume 3M Na-Acetate pH 6.0 overnight at -20° C. After centrifugation at 14.000 rpm for 30 min and removing the supernatant the pellet was washed with 75% ethanol, airdried and resuspended in 20 µl TE buffer. The DNA yield was measured by spectrophotometry at OD 260 and the concentration was determined according to the formula: DNA concentration (µg/ µl) = (OD 260 x 50 x dilution factor) : 1000

3.3.2.3 *Polymerase Chain Reaction (PCR) for p53*

The PCR was used 1) to amplify each of the exons contributing to the open reading frame of the *p53* gene (exon 2-11) of all ovarian cancer cases for the mutation screening by SSCP (Single Strand Conformation Polymorphism) and 2) to reamplify those exons which had shown abnormal band patterns in SSCP to detect mutations by DNA sequencing. Sense and antisense primers for exon 2-11 of the *p53* gene were designed and analyzed for sequence homologies by using the DNAsis software package on a Macintosh computer and the NCBI (National Center of Biotechnology Information, website: www.ncbi.nlm.nih.gov) sequence data base available through the internet. Primers were usually of 20-21 bases length with a G/C-content ranging between 40-60%.

Table 5: Primers and PCR conditions for amplification of p53 exon 2-11

<i>p53</i> exon	primer sequence	spans nucleotides	PCR pro- duct	Mg ⁺⁺ mM	tempe- rature
ex 2 Sn	5' CAGGGTTGGAAGCGTCTCAT 3'	11642-11661	224 bp	1.6	63°C
ex 2 Asn	5' CTTCCCACAGGTCTCTGCTA 3'	11865-11846			
ex 3 Sn	5' TAGCAGAGACCTGTGGGAAGC 3'	11846-11866	159 bp	0.6	63°C
ex 3 Asn	5' AGAGCAGTCAGAGGACCAGGT 3'	12004-11984			
ex 4 Sn	5' CGTTCTGGTAAGGACAAGGG 3'	11921-11940	445 bp	0.8	63°C
ex 4 Asn	5' AAGAAATGCAGGGGGGATACGG 3'	12366-12346			
ex 5 Sn	5' CTGTTCACTTGTGCCCTGAC 3'	13004-13023	271 bp	0.7	60°C
ex 5 Asn	5' AACCAGCCCTGTCGTCTCTC 3'	13275-13256			
ex 6 Sn	5' GCTGGAGAGACGACAGGGCT 3'	13252-13271	228 bp	0.7	60°C
ex 6 Asn	5' CAACCACCCTTAACCCCTCC 3'	13480-13461			
ex 7 Sn	5' CTTGCCACAGGTCTCCCCAA 3'	13941-13960	237 bp	1.6	70°C
ex 7 Asn	5' AGGGGTCAGCGGCAAGCAGA 3'	14158-14177			
ex 8 Sn	5' TTCCTTACTGCCTCTTGCTT 3'	14411-14430	231 bp	1.2	65°C
ex 8 Asn	5' AGGCATAACTGCACCCTTGG 3'	14622-14641			
ex 9 Sn	5' AGCAAGCAGGACAAGAAGCG 3'	14592-14611	264 bp	1.4	66°C
ex 9 Asn	5' GCAAATGCCCCAATTGCAGG 3'	14836-14855			
ex 10 Sn	5' CGATGTTGCTTTTGATCCGTCA 3'	17465-17486	257 bp	1.6	63°C
ex 10 Asn	5'ATCCTATGGCTTTCCAACCTAG3'	17722-17743			
ex 11 Sn	5' TCCCGTTGTCCCAGCCTTAG 3'	18491-18510	383 bp	0.6	63°C
ex 11 Asn	5' GGTATGTCCTACTCCCCATC-3'	18874-18894			

One pair of primers was used for each exon except exon 4 for which in part of the cases two pairs of oligonucleotide primers were used as previously published (Wen et al. 1999). The sequence of the primers for exon 7 and exon 8 was used as described by Kohler et al. (1993b). Each of the oligonucleotide primer pairs were designed to span not only the exon of interest, but also sufficient flanking intron sequence so that splice junction mutations would be included for analysis. The 3' oligonucleotide primer of exon 11 was not outside of the splice junction but was 196 nucleotides downstream of the translation termination-codon.

The annealing temperature was determined according to the NCBI information and the Mg⁺⁺ concentration was optimized for each primer pair. The sequence for each primer pair, the nucleotides spanned by the primer, the expected PCR fragment size, the optimal Mg⁺⁺ concentration and the annealing temperature were as shown in table 5.

Primers were chemically synthesized by the University of Southern California core lab. The primers which were obtained in dried form were diluted in ddH₂O. The concentration was determined by measuring the absorbance at $\lambda=260$ nm (A_{260}) and aliquots of 20 μ l with a concentration of 50 pmol were stored at -20°C. 2-5 μ l of the tumor DNA samples were diluted to a concentration of 100 ng/ μ l in TE buffer.

The PCR reaction with a total volume of 25 μ l was set up as follows:

- 1 μ l DNA (100 ng)
- 1 μ l dNTP mix (conc 100 μ M)
- 0.6-1.6 μ l Mg⁺⁺ (conc 25 mM)
- 0.25 μ l primer sense (conc 50 pmol)
- 0.25 μ l primer antisense (conc 50 pmol)
- 2.5 μ l Mg⁺⁺ free buffer
- 0.2 μ l Taq polymerase (1U) (Promega)
- 17.9-19.2 μ l H₂O to a total volume of 25 μ l
- for SSCP 0.15 μ l 33P-labeled-dATP and 0.15 μ l 33P-labeled-dCTP were added

For each PCR run, a reaction mix with H₂O instead of DNA was used as a negative control. For SSCP specimens containing known mutations were processed as positive control samples for exons 5-8 and normal ovarian tissue DNA was used as a normal control. The reactions were set up on ice in 0.5 ml PCR tubes (CLP) and the mixtures were overlaid with one drop of mineral oil to prevent evaporation during repeated heating and cooling during the PCR. After short spinning at 12,000 rpm the PCR reaction was carried out in a DNA thermal Cycler (Perkin-Elmer Cetus, Norwalk, CT, USA) at the following conditions:

1 cycle	94°C	2 min (initial denaturing of template DNA)
35 cycles	94°C	1 min (denaturing of template DNA)
	60-70°C	1 min (annealing temperature, depending on primers)
	72°C	2 min (elongation)
1 cycle	72°C	2 min (elongation)

After completion of the PCR reaction, samples were cooled to 4°C and, if not used immediately, stored at -20°C.

3.3.2.4 *Single Strand Conformation Polymorphism (SSCP)*

The PCR products were checked on an agarose gel for the amount and correct size of DNA. 5 μ l of the PCR reaction were mixed with 5 μ l dd H₂O and 2 μ l 10x DNA dye and run on a 1.2% agarose gel (50 ml 0.5x TBE buffer, 0.6g Agarose and 1 μ l EtBr) with 0.5x TBE as running buffer at 70 volt for 1 hour.

Conformational differences in the PCR products were resolved on a non-denaturing, 0.5x MDE (mutation detection enhancement) polyacrylamide gel with the addition of 5% glycerol at room temperature (Spinardi et al. 1991). A total volume of 100 ml of the gel was mixed out of the following components:

- MDE Gel Solution 25 ml
- 10 x TBE 6 ml
- Glycerol 10% 5 ml
- dd H₂O 64 ml
- TEMED 40 µl
- 10 % APS 400 µl

The gel mix was cast between two glass plates of a Biorad sequencing apparatus and allowed to polymerize after insertion of a 0.4 mm thick 97 well comb for at least 1 hour at room temperature. A 0.6x TBE solution was used as running buffer. 5 µl of the PCR product of each sample were mixed with 7 µl of stop solution (as described above), and denatured at 94°C for 2 min, followed by immediate cooling on ice for 10 min, except for a normal DNA double-stranded control. Forty-five samples including the single-stranded normal DNA control, the double-stranded normal DNA control and the positive control were loaded on the gel and run at 21 W at room temperature for a time period between 8 hours (exon 3) and 20 hours (exon 4), on average 14-16 hours, depending on the expected size of the PCR product. After the DNA had migrated far enough through the gel to allow separation of the DNA strands, the gel was dried on Whatman 3 MM paper and subsequently exposed to a Kodak Biomax MR film for 12-48 hours.

3.3.2.5 *DNA sequence analysis*

DNA segments identified as having altered mobility by SSCP were evaluated by conventional DNA sequence analysis methods (Sanger et al. 1977, Slatko, 1996). Both the sense and anti-sense strands were analyzed by the dideoxynucleotide chain termination technique with PCR sense and anti-sense primers using the ThermoSequenase radiolabeled terminator cycle sequencing kit (Amersham Life Science, Arlington Heights, IL, USA).

a) Preparation of the sequencing gel:

- two big glass plates of a Biorad sequencing apparatus were cleaned twice with ddH₂O, once with 100% ethanol, once with acetone and subsequently prepared with SEA spray
- both plates were mounted with 0.4 mm spacers shortly before the gel was cast
- a 6% acrylamide gel was prepared with
 - 24 ml Sequagel™ Concentrate
 - 66 ml Sequagel™ Diluent
 - 10 ml 10x GTB buffer
- 40 µl TEMED and 800 µl 10% APS were added to start polymerization
- the gel was immediately cast with a syringe into the mounted glass plates and a comb with 0.4 mm width was inserted upside down to create a gel free space. Polymerization was allowed at 4°C for 2 hours or overnight

b) Sequencing reaction

- the ThermoSequenase kit included the following solutions:
- Thermo Sequenase DNA polymerase 4U/ μ l, Thermoplasma acidophilum inorganic pyrophosphatase, 50mM Tris-HCl, pH 8.0, 1mM dithiothreitol (DTT), 0.1mM ethylenediamine tetraacetic acid (EDTA), 0.5% Tween®-20, 0.5% Nonidet® P-40, 50% glycerol
- Reaction buffer (concentrate): 260mM Tris-HCl, pH 9.5, 65mM $MgCl_2$
- dGTP termination master mix: 7.5 μ M dATP, dCTP, dGTP, dTTP
- Stop solution: 95% formamide, 20mM EDTA, 0.05% bromophenol blue, 0.05% xylene cyanol FF
- Glycerol tolerant gel buffer: powdermix 54g Tris base, 18gm Taurine, 1gm $Na_2EDTA \cdot 2H_2O$, H_2O to 250ml for a 20x buffer concentrate
- ^{33}P labeled terminators:

ddATP, 0.3 μ M [α - ^{33}P]ddATP (1500Ci/mmol, 450 μ Ci/ml) 11.25 μ Ci
 ddCTP, 0.3 μ M [α - ^{33}P]ddCTP (1500Ci/mmol, 450 μ Ci/ml) 11.25 μ Ci
 ddGTP, 0.3 μ M [α - ^{33}P]ddGTP (1500Ci/mmol, 450 μ Ci/ml) 11.25 μ Ci
 ddTTP, 0.3 μ M [α - ^{33}P]ddTTP (1500Ci/mmol, 450 μ Ci/ml) 11.25 μ Ci

The sequencing reaction was set up according to the following protocol (Mok et al.1993):

Ovarian carcinoma template DNA was reamplified with the appropriate PCR primer pair as described previously. 5 μ l of the amplified PCR product were pretreated with 1 μ l (2U) of shrimp alkaline phosphatase (Amersham) and 1 μ l (10U) of exonuclease I (Amersham) at 37°C for 15 min in a thermal cycler followed by inactivation of the enzyme at 80°C for 15 min.

For each case two sets of PCR tubes (for the sense and the antisense primer) were labelled as A,C,G,T and a termination mix was set up on ice as follows:

- A 2 μ l dGTP termination master mix + 0.5 μ l [α - ^{33}P]ddATP
- C 2 μ l dGTP termination master mix + 0.5 μ l [α - ^{33}P]ddCTP
- G 2 μ l dGTP termination master mix + 0.5 μ l [α - ^{33}P]ddGTP
- T 2 μ l dGTP termination master mix + 0.5 μ l [α - ^{33}P]ddTTP

Subsequently a reaction mix of 20 μ l volume was set up on ice for each case as follows:

- pretreated PCR product 3 μ l
- reaction buffer 2 μ l
- ddH₂O 12 μ l
- primer 2.5 pmol/ μ l 1 μ l
- Thermosequenase 2 μ l

4.5 µl of this reaction mix were added to each A,C,G,T termination mix tube (total volume 7 µl) on ice. The sequencing reaction was carried out in a thermal cycler (MJ research) which was preheated to 95°C under the following conditions for 30 cycles:

- 95°C 30 sec
- 55°C 30 sec
- 72°C 90 sec

followed by cooling to 0°C. Subsequently 4 µl of stop solution were added to each of the reactions and the samples were stored at -20°C overnight.

c) Gel electrophoresis:

- the glasplates containing the gel were fixed into a sequencing gel apparatus (Biorad) and the upper and lower chambers were filled with 1x glycerol tolerant buffer. The comb was removed and inserted for lane separation. The gel spaces were carefully cleaned from gel residues and urea.
- pre-electrophoresis was carried out with 2 µl of stop solution in each lane at a power of 120 watts until the gel warmed up to a temperature of 50-55°C.
- the stopped sequencing reactions were denatured at 80°C for 3 min and placed on ice for loading
- 2 µl of the samples were loaded per lane in the order of A,C,G,T for each case and electrophoresis was carried out at 120 watts until either the BPB or the XC marker had migrated far enough through the gel (depending on the region of interest), assuming that BPB migrates at a length of 26 bases and XC at a length of 106 bases of the DNA sequence in a 6% acrylamide gel
- after electrophoresis the glasplates were separated after cooling to room temperature
- the gel was removed from the glasplate by application of 3 MM Whatman paper and dried at 80°C for 60 min in a vacuum gel drier
- the DNA sequence was revealed by autoradiography by exposure of the dried gel to a Biomax MR film at RT for 12-48 hrs

3.3.2.6 Automated DNA sequencing

Automated DNA sequencing was used 1) to identify *p53* mutations in ovarian cancer cases which had not shown SSCP alterations and 2) to compare the normal tissue DNA sequence of tumor cases with suspected *p53* polymorphisms.

Forty-two ovarian carcinoma cases which had no mobility shift identified by SSCP screening were subjected to complete DNA sequence analysis of exon 2-11 by automated DNA sequence analysis, to identify those mutations which SSCP failed to identify, as described elsewhere (Wang-Gohrke et al.1998, Wen et al. 1999). The automated sequencing was performed in the Molecular Biology Laboratory of Prof. Dr. R. Kreienberg at the Department of Gynecology and Obstetrics at the University of Ulm, Germany, using an A.L.F. Express Sequencer (Pharmacia Biotech, Uppsala, Sweden) (Wang-Gohrke et al. 1998).

For automated sequencing of normal tissue controls for *p53* polymorphisms a PCR reaction of 50 µl volume was set up with 400 ng of DNA, 40 µmoles dNTP, 25pmol of each of the appropriate primers, Mg^{++} concentration as described in table 5 and 2U of Taq DNA polymerase. The PCR product was analyzed by gel electrophoresis on a 1.2% agarose gel (Seakem) made up with 0.5x TAE buffer and 160 µg/l ethidium bromide. The PCR product of the expected size was extracted from the gel with a DNA gel extraction kit (Qiagen, Chatsworth, CA).

150 ng of each purified PCR product and 5 pmol of each of the appropriate primers as used for the PCR reaction were submitted to automated sequencing on a Perkin Elmer 377 ABI prism automated sequencer. DNA sequencing was performed with a dye-based (Big Dye) Applied Biosystems procedure incorporating 3' fluorescent-labeled dideoxynucleotide triphosphates (dye terminators) into the extension of the PCR products (asymmetric PCR). The specific emissions were detected and analyzed by a PC program which counts the fluorescence label excitements produced by laser lights.

3.3.2.7 *Isolation of total RNA from tumor tissue*

Total RNA was extracted from frozen tissue by using the TRIzol reagent and extraction protocol (Gibco BRL). Frozen tissue sections stained with hematoxylin and eosin were used to confirm that the majority of the tissue selected for analysis was composed of tumor cells. To isolate total RNA an adjacent piece of frozen tissue (50 mg) of the tumor was collected in an Eppendorf tube placed on dry ice. Subsequently 1 ml of TRIzol reagent was added to the tube, immediately followed by homogenization with a tissue homogenizer (VWR) at maximum speed. The homogenized samples were incubated 5 min at room temperature to permit complete dissociation of nucleoprotein complexes. After adding 0.2 ml of chloroform, tubes were vigorously shaken by hand for 15 sec and then incubated at room temperature for 3 min, followed by centrifugation at 12.000 rpm for 15 min at 4°C. The RNA-containing upper aqueous phase was transferred to a fresh tube and precipitated with 0.5 ml isopropyl alcohol, incubated for 10 min at room temperature and then centrifuged at 12.000 rpm for 10 min at 4°C. After centrifugation the supernate was removed and the RNA pellet was washed with 1 ml of -20°C cold 75% ethanol, mixed by vortexing and centrifuged at 10.000 rpm for 5 min at 4°C. Subsequently the RNA pellet was airdried and redissolved in DEPC-H₂O. The RNA yield was measured by spectrophotometry at OD 260 and the concentration was determined according to the formula: RNA conc. (µg/ µl) = (OD 260 x 40 x dilution factor) : 1000
RNA preparations were stored at -70°C.

3.3.2.8 *Northern hybridization*

Total RNA from tumor tissue and a control cell line (SA1 osteosarcoma cell line) was fractionated, blotted on nylon membranes and hybridized according to the following protocol:

a) RNA fractionation:

- 15 µg of total RNA dissolved in DEPC-H₂O were added to DEPC- H₂O to a total volume of 15 µl; 10 µg of an RNA ladder (Gibco) were used as a length standard

- a 1% agarose gel containing 1% MOPS and 17% formaldehyde was cast
- 45 µl of a denaturing buffer containing 5 µl MOPS (10x), 25.8 µl formamide, 8.7 µl formaldehyde (37% solution), 5 µl 10x dye (1mM EDTA, 0.25% bromophenol blue, 0.25% xylene cyanol, 50% glycerol) and 0.5 µl EtBr was added to the RNA
- the samples were denatured at 65°C and afterwards kept on ice
- the samples were loaded on the gel and electrophoresis was carried out at 40 volt for approximately 16 hours, until the bromophenol-blue marker had reached the end of the gel

b) Immobilization of the fractionated RNA on nylon filters:

- after completion of electrophoresis, the gel was photographed with a fluorescent scale next to the RNA ladder under UV-illumination
- the gel was then washed in DEPC-H₂O for 2x 30 minutes and in 10x SSC for 2x 30 minutes
- a nylon membrane (BioRad) was cut to the exact size of the gel and soaked in DEPC-H₂O
- a glasplate was placed on top of a 35 mm dish in a tray which was filled with 10x SSC
- a long sheet of 3MM Whatman paper was laid on top of the glasplate in such a way, that both ends reached into the buffer tank
- the gel was laid on top of the Whatman paper, the nylon membrane was placed on the gel and covered with two sheets of Whatman paper of the same size, soaked in DEPC-H₂O
- a pile of paper towels was placed on top of the gel-nylon-membrane stack and weighted down with a book; the Whatman paper surrounding the gel stack was covered with plastic foil
- the transfer was carried out for 14 hours overnight
- after the transfer the RNA was crosslinked at 1200 in a stratalinker.

c.) Hybridization

- the blot was transferred into a hybridization tube and was pre-hybridized for 2 hours at 65°C in 10 ml rapid hyb buffer (Amersham)
- 25 ng of a 1.7 kb *mdm2* cDNA probe (kindly provided by B. Vogelstein, John Hopkins Oncology Center, Baltimore, USA) were radioactively labeled (Megaprime labeling kit, Amersham) with p32 dCTP (Amersham) at an activity of 1-3 x 10⁶ cpm/ml
- the probe was purified from unincorporated p32 in a quick spin column (Boehringer Mannheim 100400)
- for hybridization, the probe was mixed with 100 µl salmon sperm DNA, boiled for 10 min, iced for 10 min, mixed with 10 ml rapid hyb buffer and added to the blot; hybridization was then carried out under the same conditions as prehybridization
- after hybridization, the blot was washed 1) in 2x SSC, 0.1% SDS for 15 min at rt, 2) in 0.5x SSC, 0.1% SDS for 15 min at rt and 3) in 0.1x SSC, 0.1% SDS for 10 to 20 min at 65°C
- blots were wrapped into plastic foil and x-ray autoradiography was carried out at -70°C on Biomax MS film overnight

3.3.2.9 *Southern hybridization*

Genomic DNA from tumor tissue and cell lines was fractionated, blotted on nylon membranes and hybridized according to the following protocol:

a) DNA fractionation:

- 15 µg of genomic DNA were diluted in TE buffer to a total volume of 40 µl; 15 µl (1.5 µg) of a 1 kb DNA ladder (Gibco) were used as a length standard
- DNA samples were digested with EcoRI (3 units/ µg DNA) for 4 hrs at 37°C
- 500 ml of a 1% agarose gel (prepared with 0.5x TBE buffer) were cast
- after completion of digestion, 5.5 µl 10x dye (1mM EDTA, 0.25% bromophenol blue, 0.25% xylene cyanol, 50% glycerol) was added to the DNA samples
- the samples were loaded on the gel and electrophoresis was carried out at 40 volt for approximately 16 hours, until the bromophenol-blue marker had migrated 10 cm through the gel

b) Immobilization of the fractionated DNA on nylon filters:

- after completion of electrophoresis, the gel was photographed with a fluorescent scale next to the DNA ladder under UV-illumination
- the gel was then washed 1) in 0.25 M HCl until the dye turned yellowish 2) washed in 0.5M NaOH, 1.5M NaCl until the dye changed back to blue, 3) rinsed in ddH₂O 4) neutralized by 2x 30 min washing in 0.5 M Tris, 3M NaCl, pH 7.4
- a nylon membrane (BioRad) was cut to the exact size of the gel and transfer was carried out as described for Northern blotting

c.) Hybridization

- 25 ng of a DNA probe were radioactively labeled (Megaprime labeling kit, Amersham) and hybridization was carried out as described for Northern hybridization
- after hybridization, the blot was washed twice in 2x SSC for 5 min at rt and twice in 0.1x SSC, 0.1% SDS for 30 min at 65°C
- blots were wrapped into plastic foil and x-ray autoradiography was carried out at -70°C on Biomax MS film overnight

3.3.2.10 *cDNA synthesis*

cDNA synthesis was performed with the following reaction mix:

- 2 µg total RNA
- add H₂O to a volume of 7 µl
- 0.5 µl oligo dT primer

were heated to 70°C for 10 min and then immediately cooled to 0°C in ice water for 5 min; the following reagents were mixed on ice:

- 1 µl M-MLVRT (200U/µl)
- 5 µl RT buffer
- 2 µl dNTP mix (containing 10mM of each dNTP)
- 1 µl MgCl (25mM)
- 1 µl DTT
- 1µl RNA guard
- 2 µl H₂O

and the total volume of 13 µl was added to each tube. The cDNA synthesis was carried out at 39°C for 1 hour and stopped by heating to 95°C for 5 min, followed immediately by cooling the samples in ice water; 2 µl of the cDNA were used for RT-PCR; the cDNA was stored at -70°C.

3.3.2.11 Polymerase Chain Reaction (PCR) for *mdm2* with nested primers

a) Nested PCR for amplification of *mdm2* cDNA

cDNA which had been synthesized by reverse transcription from total RNA was used as a template for a nested PCR protocol. cDNA was amplified by a set of external *mdm2* primers spanning the entire coding region of the *mdm2* gene spanning exon 3 to exon 12. Since *mdm2* is expressed at low levels the PCR product was then subjected to a second run of PCR with internal primers. The primer sequence we used had been previously published (Sigalas et al. 1996). The internal sense primer has a gap of eight nucleotides.

The annealing temperature was determined to be 58° C according to a formula based on the nucleotide content. The Mg⁺⁺ concentration was chosen as 1.4 mMol according to previous protocols (Sigalas et al. 1996).

Table 6: *mdm2* external and internal primers for nested PCR

Primer	Primer sequence	spans nucleotides of coding region
ext Sn	5' CTGGGGAGTCTTGAGGGACC 3'	248-267
ext Asn	5' CAGGTTGTCTAAATTCCTAG 3'	1831-1851
int Sn	5' CGCGAAAACCCCGGGCAGGCAAATGTGCA 3'	280-293, 302-318
int Asn	5' CTCTTATAGACAGGTCAACTAG 3'	1784-1805

Primers were obtained from the University of Southern California core lab. The concentration of the primers dissolved in ddH₂O was determined by measuring the absorbance at λ=260 nm (A₂₆₀). Primers were diluted to a concentration of 50 pmol. 2 µl of the cDNA, which had been reverse transcribed from total RNA, were used as a template for the external PCR run and 2 µl of the resulting product were used for the internal primer PCR run.

The PCR reaction was set up for the external primer run to a total volume of 25 µl as follows. For the internal primer run a volume of 50 µl was set up to have a greater DNA yield for sequencing analysis.

- 2 µl cDNA / 4 µl PCR product
- 1 µl / 2 µl dNTP mix (conc 400 µM)
- 1.4 µl / 2.8 µl Mg⁺⁺ (conc 25 mM)
- 0.25 µl / 0.5 µl primer sense (conc 50 pmol)
- 0.25 µl / 0.5 µl primer antisense (conc 50 pmol)
- 2.5 µl / 5 µl Mg⁺⁺ free buffer
- 0.2 µl (1U) / 0.4 µl (2U) Taq polymerase (Promega)
- 17.4 µl H₂O to a total volume of 25 µl / 34.8 µl to a total volume of 50 µl

For each PCR run, a reaction mix with H₂O instead of DNA was used as a negative control. The reactions were set up on ice in 0.5 ml PCR tubes (CLP) and the mixtures were overlaid with one drop of mineral oil to prevent evaporation during repeated heating and cooling during the PCR. After short spinning at 12.000 rpm the PCR reaction was carried out in a DNA thermal Cycler (Perkin-Elmer Cetus, Norwalk, CT, USA) at the following conditions for both external and internal primers:

1 cycle	94°C	2 min (initial denaturing of template DNA)
30 cycles	94°C	1 min (denaturing of template DNA)
	58°C	1 min (annealing temperature)
	72°C	2 min (elongation)
1 cycle	72°C	2 min (elongation)

After completion of the PCR reaction, samples were cooled to 4°C and, if not used immediately, stored at -20°C.

b) PCR of the β_2 microglobulin gene as a control

PCR amplification of the β_2 microglobulin gene was used as an internal control to confirm that the RNA used for reverse transcription was intact and that sufficient and equal amounts of cDNA had been synthesized. The β_2 -microglobulin gene is approximately 8Kb in size and consists of four exons and three introns. The complete mRNA comprises 945 nucleotides and codes for a polypeptide of 99 amino acids, which are mostly represented by the exon 2 sequence (93 amino acids). We designed a pair of primers which span 898 bp of cDNA. The sense primer was located close to the 5' end of exon 1 and the antisense primer close to the 3' end of exon 4. The sequence of the primers was:

sense: 5' TCCTGAAGCTGACAGCATTC 3' (nucleotides 855-874) and

antisense: 5' CCGTACCAACACCAATTAGA 3' (nucleotides 3983-4002).

Primers were obtained from the University of Southern California core lab. Primer concentration was determined by measuring the absorbance at $\lambda=260$ nm (A_{260}) and primers were diluted to 50 pmol/µl. 1 µl of the cDNA template was used for the reaction which was carried out at an annealing temperature of 62° and a Mg⁺⁺ concentration of 0.8 mmol. The PCR reaction with a total volume of 25 µl was set up as follows:

- 1 µl cDNA
- 1 µl dNTP mix (conc 400 µM)
- 0.8 µl Mg⁺⁺ (conc 25 mM)
- 0.25 µl primer sense (conc 50 pmol)
- 0.25 µl primer antisense (conc 50 pmol)
- 2.5 µl Mg⁺⁺ free buffer
- 0.2 µl Taq polymerase (1U) (Promega)
- 19 µl H₂O to a total volume of 25 µl

For each PCR run, a reaction mix with H₂O instead of DNA was used as a negative control. The reactions were set up on ice in 0.5 ml PCR tubes (CLP) and the mixtures were overlaid with one drop of mineral oil to prevent evaporation during repeated heating and cooling during the PCR. After short spinning at 12.000 rpm the PCR reaction was carried out in a DNA thermal Cycler (Perkin-Elmer Cetus, Norwalk, CT, USA) at the following conditions:

1 cycle	94°C	2 min (initial denaturing of template DNA)
35 cycles	94°C	1 min (denaturing of template DNA)
	62°C	1 min (annealing temperature)
	72°C	2 min (elongation)
1 cycle	72°C	2 min (elongation)

After the PCR reaction was completed, samples were cooled to 4°C and 10 µl of the reaction product was run on a 1% agarose gel. A single PCR product of approximately 900 bp size was detected for all cDNA samples.

3.3.2.12 Subcloning of cDNA into a TA cloning vector

For optimal ligation efficiencies, a fresh PCR reaction was run with the internal *mdm2* primers using the external primer PCR product as a template to provide sufficient single 3' A-overhangs. Ligation and transformation were performed by using the Original TA Cloning® Kit (Invitrogen), which contains the pCRTM 2.1 vector.

a) Ligation

- the amount of PCR product was estimated by the following formula to ligate with 50 ng (20 fmoles) of pCRTM 2.1 vector for a 1:1 vector:insert ratio

$$x \text{ ng PCR product} = \frac{(y \text{ bp PCR product})(50 \text{ ng pCR}^{\text{TM}} 2.1 \text{ vector})}{(\text{size in bp of the pCR}^{\text{TM}} 2.1 \text{ vector} \approx 3900)}$$

- the PCR product was purified with the QIAquick PCR Purification Kit (Quiagen) according to the manufacturers instructions

- the ligation reaction was set up as follows:

fresh PCR product	6 μ l
10x ligation buffer	1 μ l
pCR TM 2.1 vector (25ng/ μ l) (Invitrogen)	2 μ l
T4 DNA ligase (5U/ μ l) (Boehringer Mannheim)	1 μ l
Total volume	10 μ l

- the ligation reaction was carried out at 14°C overnight in a waterbath

b) Transformation

- the chemically competent E. coli bacteria (One ShotTM competent cells, strand DH 5 α) were used for transformation
- the vials containing the ligation reactions were centrifuged briefly and placed on ice
- one 50 μ l vial of frozen One ShotTM competent cells for each ligation was thawed and kept on ice
- 0.5 M β -mercaptoethanol was thawed and 2 μ l were pipetted into each vial of the competent cells, mixed gently by stirring
- 2 μ l of the ligation reaction were pipetted into each vial containing the competent cells, mixed gently by stirring and incubated for 30 minutes on ice
- the vials were heat shocked for exactly 30 seconds in a 42°C waterbath and placed on ice for 2 minutes
- 450 μ l of SOC medium from the kit (at room temperature) were added to each tube
- the vials were then shaken horizontally at 37°C for 1 hour at 225 rpm in a rotary shaking incubator; the vials with the transformed cells were placed on ice.
- 50 μ l of x-gal were spread on LB agar plates containing 50 μ g/ml kanamycin
- 100 μ l of each transformation were spread out evenly on the agar plates
- plates were then inverted and incubated at 37°C for at least 18 hours; plates were then shifted to 4°C for 2-3 hours to allow for proper color development
- 8-10 white or blue-white colonies were picked from each transformation and placed into 3 ml of LB-medium containing 50 μ g/ml kanamycin
- to check the size of the insert, the following PCR reaction was set up:

ddH ₂ O	13.64 μ l
Mg free buffer	2 μ l
dNTP 400 μ M	1 μ l
primer PR 126	1 μ l
primer PR 127	1 μ l
MgCl ⁺⁺	0.96 μ l

Taq polymerase	0.4 μ l
Total	20 μ l

- the PCR reaction was run at 1 cycle 94°C 5 min, 30 cycles 94°C 1 min, 57°C 1 min, 72°C 1 min, 1 cycle 72°C 5 min
- to check the size of the insert, 10 μ l of the PCR product were run on a 1% agarose gel.
- all clones which contained an insert were selected for sequencing

3.3.2.13 *Growth and storage of bacteria*

- bacteria from a single colony from a LB agar plate were used to inoculate 5 ml or 100 ml of LB broth for small scale or large scale preparation of plasmid DNA, respectively. The LB broth contained the appropriate antibiotic (concentration 50 μ g/ml for kanamycin, 50 μ g/ml for ampicillin). Bacteria were grown overnight at 37°C in a horizontally rotating shaker at 230 rpm.
- E.coli strains were stored as glycerol stocks at -70°C. Therefore 0.5 ml of an overnight culture of E. coli was vigorously mixed with 0.5 ml of a solution containing 50% LB broth with kanamycin at a concentration of 50 μ g/ml and 50% glycerol. The mixture was shock frozen in liquid nitrogen and the stocks were transferred to -70°C. To recover bacteria from frozen stocks, an inoculation loop was used to scrape off some bacteria which were subsequently streaked out on a LB agar plate containing the appropriate antibiotic.

3.3.2.14 *Generation of electro-competent bacteria*

Electro-competent bacteria of the strain DH10B were generated and tested according to the following protocol:

a) Growth of electro-competent bacteria

- 25ml of LB medium were inoculated with bacteria scraped off from a frozen stock and incubated at 37°C for 12-16 hrs, with vigorous shaking at 300 rpm
- 1 ml of the overnight culture was inoculated into 500 ml of LB supplemented with 20 mM of glucose
- the bacteria were grown at 37°C with vigorous shaking at 300 rpm, while taking OD measurements every 20 minutes until an OD₆₀₀ of 0.6-0.7 was reached
- the cultures were chilled on ice for 30 min and for the following steps kept ice cold
- the bacteria were transferred to four 400 ml centrifuge bottles and centrifuged at 3720 rpm for 20 min at 4°C
- the supernatant was poured off and the bacteria were resuspended in 8 ml of ddH₂O
- 250 ml of ddH₂O were added to each bottle, and the centrifugation and washing steps were repeated; the pellets of two bottles were collected in one
- after centrifugation, the pellet was resuspended in 50 ml of a H₂O/10% glycerol 1:1 solution and centrifuged at 3600 rpm at 4°C for 20 min
- the pellet was then resuspended in an equal volume of the H₂O/ 10% glycerol mix and frozen in 300 μ l aliquots in 1.5 ml screw cap tubes on dry ice and stored at -80°C

b) Transformation of electro-competent bacteria

- 1 µl of plasmid DNA was added to 30 µl of the E.coli and incubated 30-60 sec on ice
- the suspension was transferred into a 0.1 cm gap Gene pulse cuvette (Bio-Rad, Hercules, CA, USA)
- the bacteria were pulsed in a Bio-Rad gene pulser at 1.66 kV, usually resulting in a time constant of 4.5 -5 msec
- the bacteria were mixed with 1 ml of LB medium and incubated for 1h at 37°C with vigorous shaking
- 100 µl and 10 µl of the bacterial suspension were plated on agar plates containing 50 µg/ml ampicillin; the plates were incubated at 37°C for 12-16 hours
- colonies were counted on the 10 µl plate and efficiency was expressed in bacterial colonies per one µg of plasmid used

3.3.2.15 Small scale (mini-prep) and medium scale preparation (midi-prep) of plasmid DNA

Mini- and midi-preps of plasmid DNA were carried out with a Quiagen plasmid purification kit (Quiagen Inc, Chatsworth, CA, USA) according to the protocol supplied by the manufacturer:

- bacteria of a 5 ml (midi-prep: 50 ml) overnight culture were centrifuged at 10.000 g for 1-2 minutes, the supernatant was blotted off
- the bacterial pellet was resuspended in 0.3 ml (midi-prep 5 ml) of buffer P1
- 0.3 ml (midi-prep 5 ml) of buffer P2 lysis buffer was added, the sample was gently mixed and the bacteria were allowed to lyse for 5 min at room temperature
- 0.3 ml (midi-prep 5 ml) of ice-cold buffer P3 neutralization solution was added, the sample was gently mixed and incubated on ice for 10 min (midi-prep 20 min)
- bacterial debris was removed from the lysate by centrifugation in an Eppendorf Microfuge, 15 min, 12.000 rpm, 4°C (midi-prep: 20 min, 12000 rpm, 4°C in a Sorvall RC2-B centrifuge equipped with a SS34 rotor, Sorvall, Newton, CT, USA)
- a Quiagen-tip 20 (midi-prep: Quiagen-tip 100) ion-exchange resin was equilibrated with 1 ml (midi-prep: 5 ml) buffer QBT and the clear supernatant was applied to the Quiagen column
- to remove contaminating DNA from the ion-exchange resin, the quiagen column was washed 4x with 1 ml (midi-prep: 2x 12 ml) medium salt-buffer QC
- plasmid DNA was eluted from the column with 0.8 ml (midi-prep: 5 ml) high-salt buffer QF
- the plasmid DNA was precipitated with 0.7 volumes isopropanol kept at room temperature
- centrifugation 20 min, 12000 rpm, 4°C in an Eppendorf microfuge (midi-prep 30 min, 12.000 rpm, 4°C in a Sorvall-centrifuge with SS34-rotor)
- the DNA pellets were washed once with -20°C cold 70% ethanol, air-dried and dissolved in 10-20 µl TE (midi-prep: 150 µl, 300 µl for big pellets)
- the concentration of the sample was determined by measuring the absorbance at $\lambda=260$ nm (1 OD corresponds to 50 µg/ml plasmid DNA)

- buffers used:

P1:	50 mM Tris/Cl, 10 mM EDTA, 100 µg/ml RNaseA, pH 8.0
P2:	200 mM NaOH, 1% SDS
P3:	3.0 M potassium-acetate, pH 5.5
QBT:	50 mM MOPS, 750 mM NaCl, 15% EtOH, 15% Triton X-100, pH 7.0
QC:	50 mM MOPS, 1000 mM NaCl, 15% EtOH, pH 7.0
QF:	50 mM Tris/Cl, 1250 mM NaCl, 15% EtOH, pH 8.5

3.3.2.16 Restriction enzyme digestion of plasmid DNA and PCR product

- Restriction enzyme digestion of DNA was carried out in 20 µl volumes at conditions recommended by the manufacturer (NEB Biolabs) using the appropriate restriction enzyme buffer supplied with the enzyme. Digestion of plasmid DNA was usually checked during the reaction on a 0.8-1.5% agarose mini-gel containing 5 µg/ml ethidium bromide. Digestion was usually stopped by incubation at 65°C for 10 to 15 min, before the digested DNA was used for further experiments.

3.3.2.17 Sequencing of DNA fragments cloned into the pCRTM2.1 vector

- A PCR reaction of a total volume of 20 µl with the primers PR 126 and PR 127 (as supplied by the manufacturer) was set up as follows:

• ddH ₂ O	13.6 µl
• Mgfree buffer	2 µl
• dNTP 400µM	1 µl
• PR 126	1 µl
• PR 127	1 µl
• 25 mM MgCl	0.96 µl
• Taq polymerase	0.4 µl

- the reaction was run under the following conditions: 1 cycle 94°C 5 min, 30 cycles 94°C 1 min, 57°C 1 min, 72°C 1 min, and 1 cycle 72°C 5 min. The PCR product was checked on a 1% agarose mini-gel containing 5 µg/ml ethidium bromide.

- the PCR product was then pretreated and sequenced as described in chapter 3.2.5

3.3.2.18 Gel extraction of PCR products for sequencing

For further analysis of *mdm2* splice products, the PCR product, amplified from the cDNA, was extracted from a 1.2% agarose gel containing 5 µg ethidium bromide with a QIAquick Gel Extraction Kit (Quiagen Inc, Chatsworth, CA, USA) with the buffers supplied in the kit according to the manufacturers instructions:

- the DNA fragment was excised from the gel with a clean, sharp scalpel and weighed (100 mg ≈ 100 ml)

- buffer QX1 was added in a ratio of 3 volumes buffer: 1 volume gel
- the gel-buffer-mix was incubated at 50°C for 10 min with repeated flicking and inverting of the tube
- one gel volume of isopropanol was added and mixed
- the sample was loaded into a QIAquick spin column, which was placed on a 2 ml collection tube; the sample was centrifuged for 1 min at 12.000 g
- after discarding the flow-through, 0.5 ml of buffer QX1 was added to the column followed by centrifugation for 1 min at 12.000 g
- for washing, 0.75 ml of buffer PE were added to the column and centrifuged for 1 min
- the flow-through was discarded and the column was centrifuged for an additional 1 min at 10.000 g
- the column was placed in a clean 1.5 ml microfuge tube and the DNA was eluted with 30 µl TE buffer by centrifugation for 1 min at maximum speed

3.3.2.19 Sequencing of cDNA PCR products after gel purification

- the PCR product was enzymatically pretreated as described in chapter 3.2.5
- 3 µl of the gel-extracted DNA and 1 µl of the internal sense and the internal antisense *mdm2* primers were used for the sequencing reaction, which was carried out with the Amersham Thermosequenase kit as previously described (chapter 3.2.5)
- the sense and the antisense sequence were read and compared to homology with the *mdm2* sequence by using the MacDNAsis software and the database of the NCBI (National Center of Biotechnology) via the internet.

3.3.2.20 *Primer design and PCR for in vitro protein expression using the pcDNA3-Vector*

For in vitro protein expression of the *mdm2* splice variants, MDM2 full length protein and p53 protein, cDNA was cloned into the pcDNA3.1 expression vector (Invitrogen) (Fig. 8a). A variant of the pcDNA3 vector with a human myc epitope, respectively a human hemagglutinin (HA) epitope was kindly provided by Ulf Grawunder PhD.

The following set of sense and antisense primers for p53 and MDM2 protein expression containing restriction enzyme sites for BamHI and MluI was designed:

mdm2 sense: 5' CG GGATCC ATGGGCAATACCAACATGTCTGTACCTAC 3'
 BamHI *mdm2* sequence (T exchanged to G)

mdm2 antisense: 5' GCG ACGCGT GGGGGAAATAAGTTAGCACAATCATTG 5'
MluI *mdm2* sequence (G added for correct frame)

p53 sense: 5' CG GGATCC ATGGAGGAGCCGCAGTCAGATCCTAGC 3'
BamHI *p53* sequence

p53 antisense: 5' GCG ACGCGT GGTCTGAGTCAGGCCCTTCTGTCTTGAAC 5'
MluI *p53* sequence (*G* added for correct frame)

CMV promotor: bases 209-863
T7 promotor: bases 864-882
Polylinker: bases 889-994
Sp6 promotor: bases 999-1016
BHG poly A: bases 1018-1249
SV40 promotor: bases 1790-2115
SV40 origin of replication: bases 1984-2069
Neo^R ORF: bases 2151-2945
SV40 poly A: bases 3120-3250
pUC19 backbone: bases 3272-5446
Amp^R ORF: bases 4450-5310

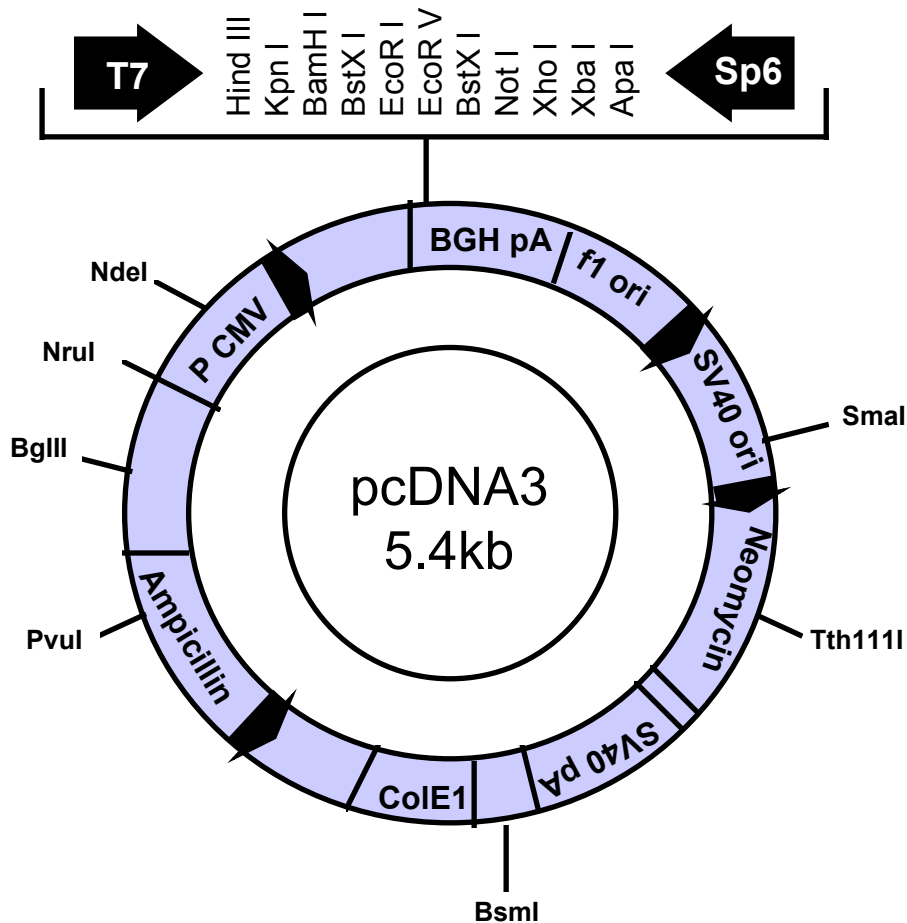


Fig. 8a: pcDNA3 expression vector (Invitrogen). cDNA of *p53*, full length *mdm2* and *mdm2* splice variants was ligated into the pcDNA3 expression vector.

To generate the insert with the correct sequence for protein expression, a PCR reaction was run with the pCRTM2.1 vector plasmid DNA containing the cDNAs of six different *mdm2* splice variants. The plasmid DNA was diluted 1:1000 in TE buffer. To obtain the PCR product containing the full length *mdm2* cDNA and the *p53* sequence, undiluted cDNA generated by reverse transcription from RNA of five different normal ovary tissues was used as a template. The following reaction was set up:

• ddH ₂ O	16.8 µl
• 10x buffer	3 µl
• dNTP 1mM	6 µl
• primer sense 10pmol	1.5 µl
• primer antisense 10pmol	1.5 µl
• Pwo polymerase	0.2 µl
• plasmid DNA diluted 1:1000 (respectively undiluted cDNA)	1 µl

The PCR product was run on a 1.2% agarose gel to check the size of the DNA.

3.3.2.21 Purification and restriction enzyme digestion of PCR Product and pcDNA3 vector

a) Purification of the PCR-product

The PCR products generated with the primers designed for protein expression were purified by using MicroSpin Columns S-400 HR, according to the manufacturers instructions:

- after vortexing and breaking off the tip, the columns were placed on Eppendorf tubes and centrifuged for 2 min at 3000 rpm
- the flow-through was discarded, the columns were placed on fresh tubes and 40 µl of the PCR product were loaded
- after centrifugation at 3000 rpm for 2 min, a yield of approximately 30 µl was obtained

b) Restriction enzyme digestion of PCR product and vector

- 20 µl of the PCR product were enzyme digested overnight at 37°C in a 40 µl reaction volume containing 4 µl BamHI buffer, 4 µl 10x BSA, 11 µl ddH₂O, 0.5 µl BamHI (20.000 U/ml) and 0.5 µl MluI (10.000 U/ml)
- 5 µl of the pcDNA3 vector (concentration 1 µg/µl) were enzyme digested overnight at 37°C in a 20 µl reaction volume containing 2 µl NEB buffer 4,2 µl 10x BSA, 10 µl ddH₂O, 0.5 µl BamHI (20.000 U/ml) and 0.5 µl AscI (10.000 U/ml)

c) Purification of PCR product and plasmid DNA

After enzyme digestion, the PCR products of the splice variants were run on a 1.5% agarose gel and the plasmid DNA, the *mdm2* full length, and *p53* PCR product were run on a 0.8% agarose gel. Both agarose gels were prepared with 1x TAE buffer and ethidiumbromide in a concentration of 1.2 µl/100ml gel. The DNA was then excised from the gel and purified with the Gene Clean kit (Bio 101), according to the manufacturers instructions:

- 3-3.5 volumes of sodium iodide were added to the gel slice (weight \cong volume)
- the gel was solubilized by incubation at 55°C for 5-10 min with repeated mixing
- 10 µl of glassmilk beads (20 µl for the pcDNA3 vector) were added to the PCR products, vortexed, incubated for 5-10 min at rt, repeatedly vortexed and centrifuged at 12.000 rpm for 20 sec
- the glassmilk bead pellet was washed 3x with 1.5 ml wash buffer; each washing step was followed by vortexing and centrifugation; the supernatant fluid was removed.
- the pellet was dried for 5-10 min in a speed vacuum
- the pellet was resuspended with 25 µl TE buffer (50 µl for the pcDNA3 vector) and incubated 5 min at rt
- the vials were centrifuged at 12.000 rpm for 20 sec to pellet the glassmilk beads
- the supernatant was transferred into fresh tubes
- a 1.2% agarose gel containing 1.2 µl EtBr/100ml gel was run with 2 µl of the purified DNA to check the amount of DNA; the concentration of the vector was estimated to be 200 ng/µl

3.3.2.22 Ligation of *mdm2* splice variant DNA into the pcDNA3 expression vector

To ligate the digested PCR products of the *mdm2* splice variants, the full length *mdm2* cDNA, and the full length *p53* cDNA into the pcDNA3 expression vector, the following reaction was set up:

• pcDNA3 vector + myc epitope	0.5 µl
• 10x ligase buffer	2 µl
• H ₂ O	6.5 µl
• T4 DNA ligase	1 µl
• <i>mdm2</i> cDNA template	10 µl
• total	20 µl
• pcDNA3 vector + HA epitope	0.5 µl
• 10x ligase buffer	2 µl
• H ₂ O	6.5 µl
• T4 DNA ligase	1 µl
• <i>p53</i> cDNA template	10 µl
• total	20 µl

Negative control I (no cDNA)

• pcDNA3 vector + myc epitope	0.5 µl
• pcDNA3 vector + HA epitope	0.5 µl
• 10x ligase buffer	2 µl
• H ₂ O	16 µl
• T4 DNA ligase	1 µl
• total	20 µl

Negative control II (no cDNA, no ligase)

• pcDNA3 vector + myc epitope	0.5 µl
• pcDNA3 vector + HA epitope	0.5 µl
• 10x ligase buffer	2 µl
• H ₂ O	17 µl
• total	20 µl

The ligation reaction was incubated for 30 min at room temperature.

3.3.2.23 Transformation of pcDNA3/cDNA constructs into electro-competent *E. coli* bacteria

- 40 µl of electro-competent *E. coli* bacteria (strain DH 10B) were thawed and pipetted into *E. coli* pulser cuvettes 0.1 cm (BIO-RAD)
- electroporation was performed in a BioRad® gene pulser at 1.66 kV with a time constant of 4.5-5 msec
- the bacteria were resuspended in 1 ml of LB medium and incubated at 37°C with vigorous shaking for 30-45 min
- 100 µl of the bacterial suspension were plated on agar plates containing 50 µg/ml ampicillin and incubated for 16 hours at 37°C
- six colonies per plate were picked and inoculated into 2 ml of LB medium containing 100 µg/ml ampicillin
- bacterial cultures were grown for 12-16 hrs at 37°C with vigorous shaking and plasmid DNA was subsequently prepared by mini-preps as previously described (chapter 3.3.2.15)

3.3.2.24 Restriction enzyme digestion of the pcDNA3 vector containing the cDNA insert

The pcDNA3 plasmid DNA containing the *mdm2* respectively *p53* insert was digested with the NcoI restriction enzyme in a reaction containing 2 µl template DNA, 1 µl 10x buffer, 1 µl 10x BSA, 5.8 µl H₂O, and 0.2 µl NcoI (10 U/µl) at 37°C overnight. The pcDNA3 vector contains three NcoI sites at positions 610, 1976 and 2711, which cut the plasmid into three expected sizes of 3345 bp (609+2736), 1366 bp and 735 bp (Figure 8a,b).

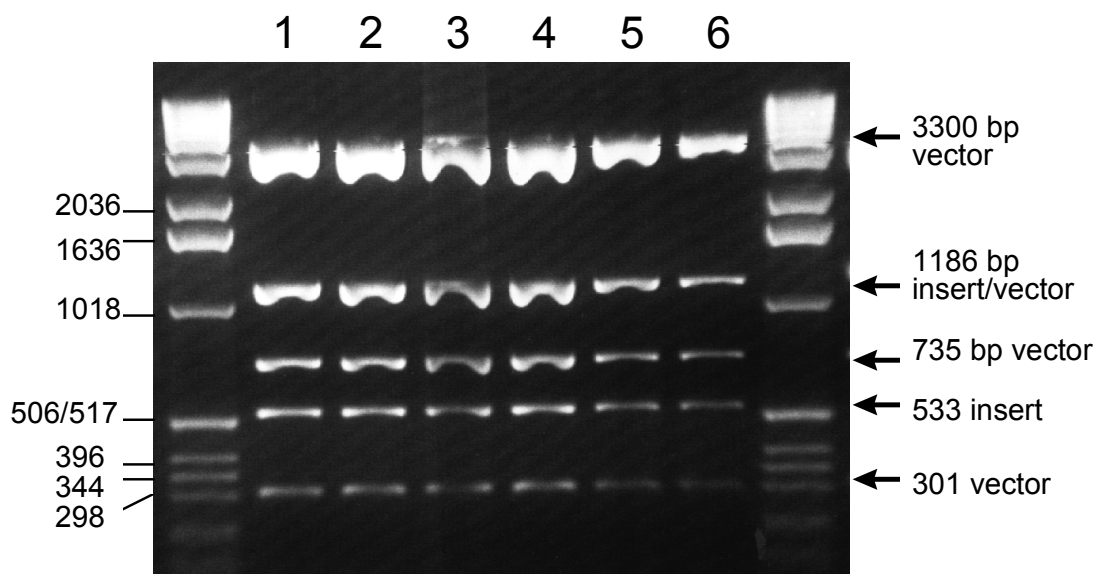


Fig. 8b: *mdm2* splice variant cDNA after NcoI restriction enzyme digestion of the pcDNA3 expression vector. The expression vector has three NcoI restriction sites at positions 610, 1976, and 2711 and the *mdm2* cDNA (654 bp) has one NcoI restriction site at position 533. The cDNA analyzed on the agarose gel shows three fragments of the vector and two fragments of the cDNA insert, one with additional vector sequence. All clones (lanes 1-6) contain the *mdm2* splice variant cDNA.

The site of the polylinker is between position 889 and 994. The primer designed for the protein expression contains a NcoI site. Therefore in cases with the expected insert, the plasmid was cut 301 bases from the first restriction site 610. The *mdm2* cDNA contains a NcoI site at position 1664, which has been spliced out in clones 49, 66, 68, 83, and 84, but not in clone 20. After restriction enzyme digestion, five bands of the correct size were seen in the *mdm2* full length clone and clone 20, while the other *mdm2* clones contained four bands of the correct size. The primer and the *p53* cDNA also contain one NcoI site each, so that the *p53* containing plasmid was cut into five pieces of DNA (Fig. 8b). The plasmid DNA of the clones containing the correct size inserts were phenol-chloroform extracted as previously described.

3.3.2.25 Transient transfection of HeLa-cells with the cDNA containing plasmid

We used a transient cytoplasmic expression system that relies on the synthesis of the bacteriophage T7 RNA polymerase in the cytoplasm of mammalian cells (Fig. 9) (Panicali and Paoletti, 1982, Mackett et al. 1982, Moss and Flexner, 1987). The *mdm2*-cDNA of interest, respectively the *p53*-cDNA, had been inserted into the pcDNA3 plasmid such that it came under the control of the T7 RNA polymerase promoter (p_{T7}) as previously described (chapter 3.3.2.22).

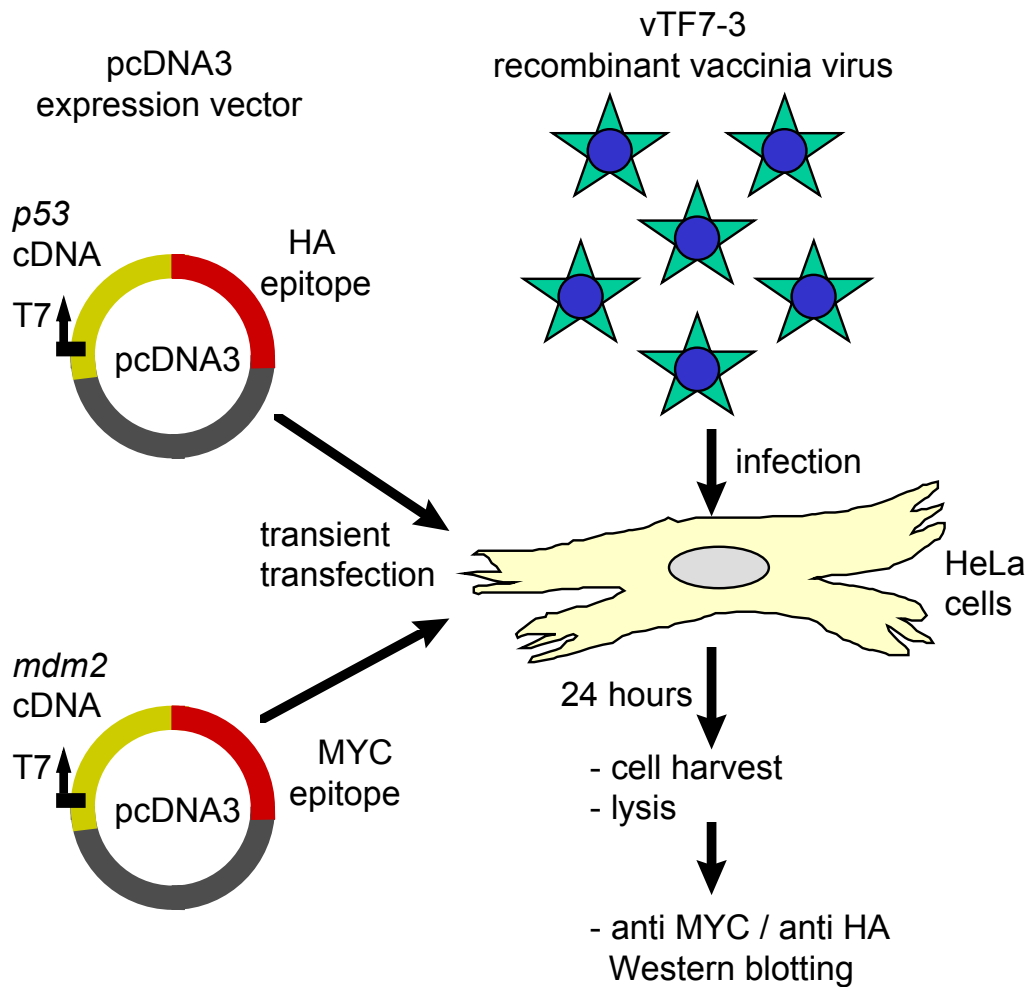


Fig. 9: Transient transfection of pcDNA constructs into vaccinia virus infected HeLa cells. The cDNA of interest was inserted into the pcDNA3 plasmid such that it came under the control of the T7 RNA polymerase promoter (p_{T7}). Using liposome-mediated transfection, this recombinant plasmid is introduced into the cytoplasm of HeLa-cells infected with the vTF7-3 strain, a recombinant vaccinia virus encoding bacteriophage T7 RNA polymerase. During incubation, the cDNA is transcribed with high efficiency by T7 RNA polymerase. Proteins were detected by immunoprecipitation and Western blotting.

Using liposome-mediated transfection, this recombinant plasmid is introduced into the cytoplasm of HeLa-cells infected with the vTF7-3, a recombinant vaccinia virus encoding bacteriophage T7 RNA polymerase. During incubation, the cDNA is transcribed with high efficiency by T7 RNA polymerase.

a) Infection of HeLa cells with the Vaccinia Virus vTF7-3

- HeLa cells (kindly provided by Ulf Grawunder PhD) were cultured in RPMI medium supplemented with 10% fetal calf serum, 50 μ M β -mercaptoethanol, 1x glutamine and 1x penicillin/streptomycin in a humidified incubator at 37°C, 10% CO₂ until 50% confluence

- cells were washed two times with serum free RPMI medium and after washing, 1 ml of serum was added to the plates
- Vaccinia-virus of the strain vTF-3 had been cultured on monkey BSC 40 cells, which each produced approximately 20-50 copies of the virus after infection; by shock freezing and thawing, the cell membranes had been destroyed and the virus was contained in the extracellular PBS supernatant; the virus stock was kindly provided by Ulf Grawunder PhD
- HeLa cells were infected with the virus by adding 20µl of the virus containing supernatant to the RPMI medium and incubating the cells at 37°C for 30 min

b) Transient transfection of HeLa cells

- 1 µg of the plasmid DNA (1-5 µl) is dissolved in 100 µl of RPMI medium
- 20 µl of LipofectAMINE™ (Gibco BRL Life Technologies) were added to each vial and incubated for 15 min at rt
- the plasmid-liposome complex was added to the HeLa cells and incubated in serum free medium for six hours at 37°C
- after 6 hours, 5 ml of full medium were added to the cell culture; the cell culture was grown overnight and harvested after 16 hours

3.3.3 Biochemical techniques

3.3.3.1 Preparation of cell lysates for SDS-polyacrylamide gel electrophoresis (SDS-PAGE)

- the transfected HeLa cells were harvested in 1 ml medium after 16 hrs by scraping off the cells from the cell culture plate and centrifugation at 12.000 rpm for 10 sec at room temperature
- cells were resuspended in 100 µl lysis buffer (1% NP-40, 50 mM Tris/Cl, pH 8.0, 150 mM NaCl, 0.5% deoxycholat, 0.1% SDS, 1 mM PMSF, 50 mM NaF, 0.02% Leupeptin, 0.02% Pepstatin A, 0.02% Aprotinin) and were incubated on ice for 30 min
- nuclei were separated from the cytoplasmic lysate by centrifugation at 12.000 rpm, 4°C, 15 min in an Eppendorf Microfuge

3.3.3.2 SDS-polyacrylamide gel electrophoresis (SDS-PAGE)

Cellular proteins either for Western blot analysis or after immunoprecipitation were electrophoretically fractionated by SDS-PAGE according to Laemmli (Laemmli, 1970). Therefore,

- two glassplates (10 cm x 8 cm) were cleaned once with H₂O, twice with 70% ethanol and once with absolute ethanol, before the plates were mounted with 1.2 mm spacers
- a separating gel was cast using the appropriate acrylamide concentration to separate proteins in the molecular-weight range of interest:

	<u>final acrylamide concentration:</u>				
	<u>10%</u>	<u>12.5%</u>	<u>15%</u>	<u>17.5%</u>	<u>20%</u>
MW-range (kd)	15-180	12-150	12-100	8-80	7-70
30% acrylamide	10 ml	12.5 ml	15ml	17.5 ml	20 ml
1% bis-acrylamide	3.9 ml	3.1 ml	2.6 ml	2.2 ml	2.0 ml

- 7.5 ml 1.5 M Tris/Cl pH 8.0, 150 µl 20% SDS, 10 µl TEMED and H₂O to a total volume of 30 ml were added before polymerization was started by addition of 100 µl 10% ammonium-persulfate
- the gel was cast immediately up to $\frac{3}{4}$ of the height of the glassplates and the acrylamide-solution was overlaid with a few ml of H₂O in order to prevent air-exposure of the acrylamide solution
- the gel was allowed to polymerize for at least 1 hour at room temperature
- after polymerization, the H₂O covering the gel was removed and the top-gel was prepared by mixing 1 ml 30% acrylamide, 1 ml 1% bis-acrylamide, 2.5 ml 0.5M Tris/Cl (pH 6.8), 5.35 ml H₂O, 50 µl 20% SDS, 5 µl TEMED and 100 µl 10% ammonium persulfate
- the top gel was cast immediately, a comb was inserted, and the gel was allowed to polymerize for an additional 2 hours at room temperature
- protein samples were mixed with 100 µl 2x reducing buffer containing
 - 125 mM Tris/Cl, pH 8.6
 - 20% glycerol
 - 0.2% SDS
 - 0.002% bromophenol-blue
 - 1.43 M 2-mercaptoethanol
- the samples were heated to 95°C for 10 min and 40 µl of each were loaded onto the gel
- the gel was subjected to electrophoresis for about 75 minutes at 120 volts using 0.025 M Tris base, 0.192 M glycine, 0.1% SDS as electrophoresis buffer

3.3.3.3 Western blotting of p53 and MDM2 proteins fractionated by SDS-PAGE

The expression of the MDM2 full length and splice variant proteins and the p53 protein was analyzed by Western blotting using antibodies directed against the myc- respectively HA- epitope followed by the use of secondary horseradish peroxidase (HRPO) labelled antibodies, which were detected by means of an ECL kit (Amersham Life Science, Arlington Heights, IL, USA).

- after the bromophenol-blue marker had reached the bottom of the gel, fractionated proteins were electro-blotted to a nitrocellulose membrane using a Bio-Rad Transblot-Cell (Bio-Rad Laboratories, Hercules, CA, USA)
- the nitrocellulose membrane, 4 Whatman 3MM papers and two foam pads were soaked in transfer buffer for 20 min
- the gel was laid on top of 2 Whatman 3MM papers, which had been placed on a foam pad

- the membrane was laid over the gel and covered with 2 Whatman 3MM papers and the second foam pad
- the assembly, as well as an ice-block for cooling, were put into the Transblot-Cell with the nitrocellulose membrane oriented to the anode
- transfer was carried out for 1 hour at 15 Watts in a blotting buffer containing
 - 0.025 M Tris-base
 - 0.192 M glycine
 - 20% methanol
- after electro-transfer the membrane was incubated in 100 ml blocking solution containing PBS buffer, 0.05% Tween-20, 10% nonfat dry milk powder for 2 hours or overnight on a shaker
- immunodetection of the proteins was performed by incubation of the membranes with anti-myc mouse monoclonal antibody clone 9E10 (Boehringer Mannheim) in a concentration of 1 µg/ml, respectively anti HA mouse monoclonal antibody clone 12CA5 (Boehringer Mannheim) in a concentration of 0.2 µg/ml in 50 ml PBS, 0.05% Tween-20 for 1 hour at room temperature
- the membranes were washed twice for 1 min and twice for 15 min in PBS, 0.05% Tween-20 at room temperature
- the membranes were then incubated with the polyclonal HRPO-labeled goat-anti-mouse antibody (Bio-Rad) diluted 1:2000 in 50 ml PBS, 0.05% Tween-20 for one hour at room temperature
- the membranes were washed twice for 1 min and twice for 15 min in PBS, 0.05% Tween-20 at room temperature
- specific binding of the HRPO-labeled antibodies was detected by incubation of the membrane in a 1:1 mixture of solution A and B of the ECL-kit for 1 min at room temperature
- chemiluminescence was detected by exposing the membranes to a Biomax MR film for 10 sec - 1 min at room temperature

3.4 Statistical tests

Statistical analyses were implemented using the SAS software packages. Overall survival was defined as the time from initial surgery following the diagnosis of ovarian cancer until death or the date of last follow-up, if the patient was still alive. All causes of death were counted as failures. Time to progression was defined as the time from initial surgery until documentation of disease progression. Patients who had not yet progressed were censored at the date of last follow-up in which the disease status was assessed; no patients died prior to progressing, unless they died from intercurrent disease. For 29 (16%) of the patients who died of their ovarian cancer, the date of progression was not documented. For those patients (n=83) who had progressed and whose date of progression was known, the median time from progression to death was calculated using the Kaplan-Meier estimator, to estimate the date of

progression (Kaplan and Meier 1958). This value, 273 days, was subtracted from the survival time of the patients whose date of recurrence was not documented. In 5 patients this value was greater than the time from surgery to death and in this situation, the time to progression was taken as one-half of the interval between surgery and death. In 11 cases, no follow-up regarding disease status was available; these patients were not included in the analysis of time to progression but were included in the summary of baseline characteristics.

Medians, quartiles and percentages were used to summarize the patient characteristics and to illustrate associations. Pearson's chi-square test for association and the Mantel-Haenszel test for trend (Mantel and Haenszel, 1959) were used to evaluate the strengths of the observed associations. Kaplan-Meier plots, relative risks and p-values derived from the partial likelihood ratio test based on Cox's proportional hazards model (Cox, 1972) were used to summarize the relationships; a stepwise forward selection algorithm was used to select a parsimonious subset of variables to classify patients into better or worse prognosis subsets.

Finally to further explore the association between p53 overexpression and outcome, an optimal cut-point for p53 nuclear staining was determined by adapting the maximally selected chi-square methods of Miller and Halpern (Miller and Siegmund 1982, Halpern 1982, Lausen and Schumacher 1992). To do this, we first applied the score function generated from the stepwise proportional hazards model to each patient. The logrank test statistic, stratified by the trichotomized scores, was used to compare overall survival for the two groups of patients (below or equal to the percentage of p53 staining value vs above the value). The percentage of p53 positive nuclei which yielded the largest stratified logrank test statistic (the maximal logrank statistic) was selected as the optimal cutpoint.

4. RESULTS

4.1 Alterations of the *p53* tumor suppressor gene in ovarian cancer

4.1.1 *p53* mutations

In a cohort of 178 ovarian carcinomas we found a total of 145 *p53* sequence alterations by PCR-SSCP and direct sequencing (66%) (Table 7). Among the sequence alterations, 100 *p53* mutations were identified in 99 cases, one of which had a mutation in both exon 7 and exon 8. In addition, four silent mutations without alteration of the amino acid sequence were identified and were considered polymorphisms. Forty-five of the sequence alterations were polymorphisms or intron alterations of undetermined significance.

Table 7: Summary of *p53* sequence alterations in 178 ovarian carcinomas

Type of sequence alteration	n	% cases
<u>Mutations with amino acid alterations in exon 2-11</u> (in 91 cases, double mutation in case #2341)	92	51.1
<u>Splice site mutations</u>	8	4.5
<u>Polymorphisms in exon 2-11</u>		
exon 4, codon 36	1	0.6
exon 4, codon 72	9	5.1
exon 6, codon 213	1	0.6
exon 6, codon 224	1	0.6
exon 7, codon 231	1	0.6
<u>Intron alterations (excluding splice site mutations)</u>		
intron 3 polymorphism (16 bp repeat)	24	13.5
intron 6 alteration (nt 13964)	2	1.1
intron 10 alteration (nt 17708)	2	1.1
intron 10 alteration (nt 18550)	4	2.3
Total number of sequence alterations (in 117 cases)	145	65.7

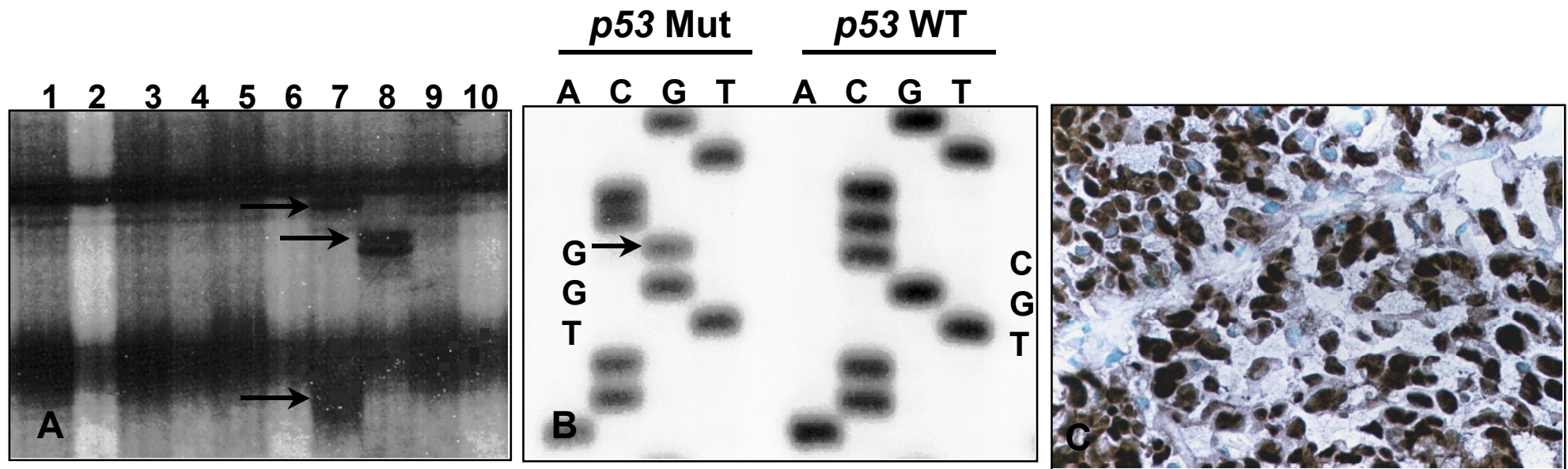


Fig. 10 A-C: p53 mutation and overexpression

A: Single Strand Conformation Polymorphism (SSCP) analysis of the *p53* gene, exon 5 in ovarian carcinomas. Arrows in lanes 7 and 8 indicate band shifts suspicious for mutations.

B: DNA sequence analysis of exon 5 of the *p53* gene in endometrioid ovarian carcinoma #2335. Missense mutation in codon 141, TGC to TGG (amino acid exchange cysteine to tryptophan).

C: Immunostaining shows overexpression of the p53 protein in the tumor nuclei (case #2335).

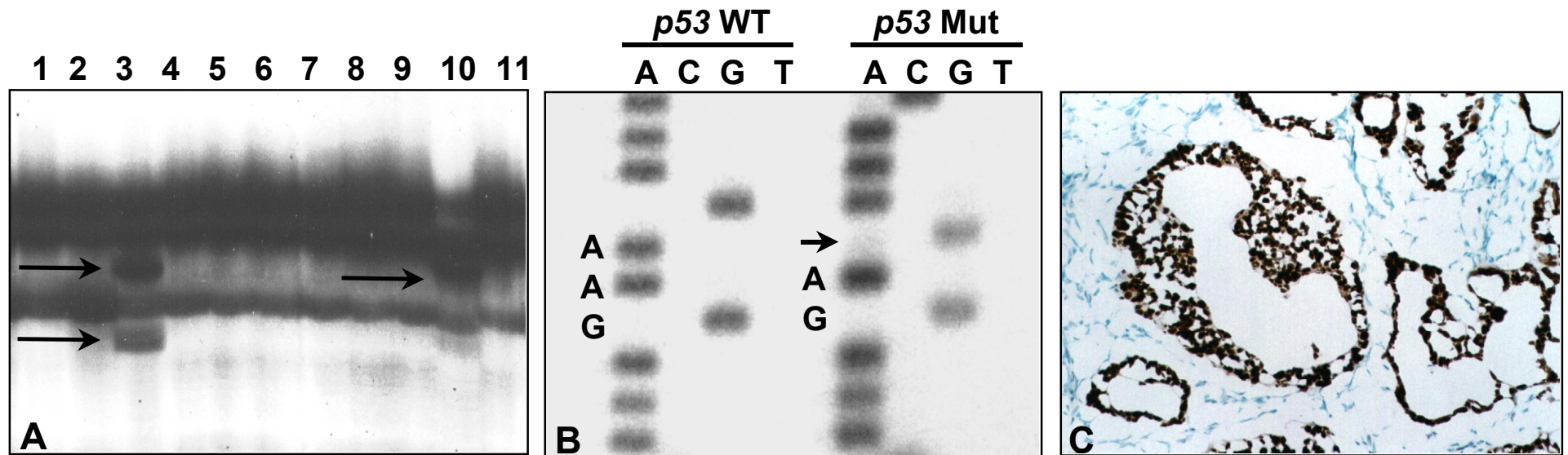


Fig. 11 A-C: p53 mutation and overexpression

A: Single Strand Conformation Polymorphism (SSCP) analysis of *p53*, exon 9 in ovarian carcinomas. Arrows in lanes 3 and 10 (case #3402) indicate band shifts suspicious for mutations.

B: DNA sequence analysis of exon 9 of the *p53* gene in endometrioid ovarian carcinoma #3402. A deletion mutation of one basepair in codon 320 causes a frameshift.

C: Immunostaining shows overexpression of the p53 protein in the tumor nuclei (case #2335.)

Thirteen of the *p53* sequence alterations considered polymorphisms were exon polymorphisms and 32 were intron alterations, some of which are known as polymorphisms. Nine sequence alterations, which are known as a Codon 72 Arg→Pro polymorphism, were found in exon 4.

One hundred *p53* mutations were identified by PCR-SSCP and direct sequencing in 99 ovarian cancer patients (56%) (Fig. 10-12, Table 8). 64 of these alterations have been previously described in a study of 105 ovarian carcinoma patients (Wen et al. 1999). One ovarian cancer patient had a mutation in exon 7 and exon 8, both with alteration of the amino acid sequence. The majority of mutations (86%) was found in exon 5 (22 mutations), exon 6 (12 mutations), exon 7 (26 mutations) and exon 8 (28 mutations) (Fig. 11, Table 8). However, 14% of the mutations were found outside codons 126-306 in exon 4 (3 mutations), exon 9 (3 mutations), intron 4 (3 splice junction mutations), intron 5 (1 splice junction mutation), intron 6 (1 splice junction mutation), intron 7 (2 splice site mutations), and intron 8 (1 splice junction mutations).

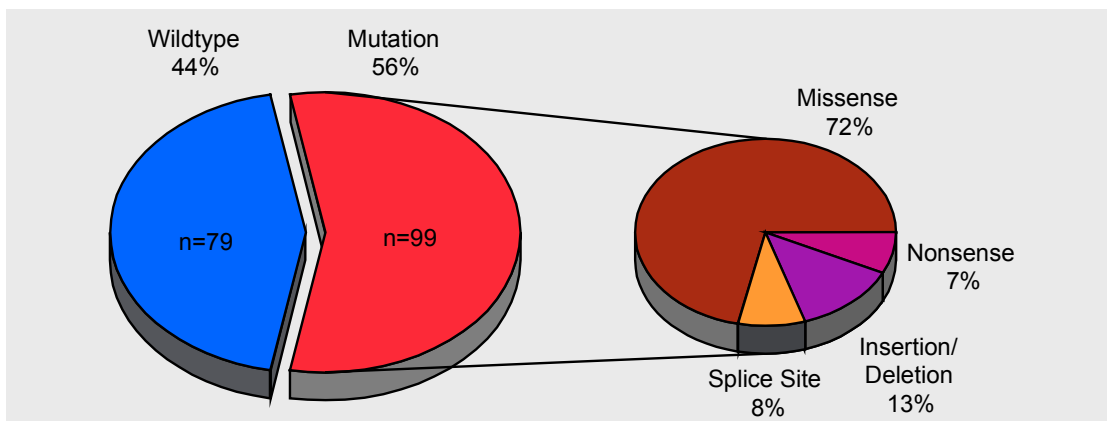


Fig. 12: *p53* mutations in ovarian cancer. Mutations of the *p53* gene were identified in 99/178 epithelial ovarian carcinomas. The majority of mutations were missense mutations.

Out of 100 mutations, 72% were missense mutations (Fig. 12), 7% were single base substitutions which resulted in the introduction of a premature stop codon, 3% were insertions of one to six basepairs, 10% were deletions of one to seven basepairs and 8% were splice junction mutations (Table 8). Four „silent,, DNA sequence alterations, which did not result in an amino acid alteration, were considered polymorphisms and were located in exon 4 (codon 36), exon 6 (codon 213 and 224), and exon 7 (codon 231).

Table 8: p53 mutations and protein overexpression in ovarian carcinomas

Case #	Histo-pathology	SSCP Result	Exon	Codon #	Amino Acids Cons*	DNA Sequence	Amino Acid Sequence	Mutation Type	Im** p53	TS/TV*** CpG
3379	Ser	+	4	36	NC	CCG to CCA	Pro / Pro	Polymorph	+	(TS)
2722	Ser	+	4	42	NC	GAT to TAT	Asp to Tyr	Missense	+	TV
3401	Ser	+	4	49, 50	NC	GAT ATT to GA...TT	frameshift	2 bp Del	-	-
715	Ser	-	4	73	NC	GTG to TTG	Val to Leu	Missense	+	TV
3391	Endo	+	4	nt 12301	Co	CGgt to CGga	intron 4	5' splice jun	-	TV
2658	Undiff	+	5	nt 13053	Co	agTA to ggTA	intron 4	3' splice jun	+	TS
3355	Endo	+	5	nt 13053	Co	agTA to ggTA	intron 4	3' splice jun	+	TS
1557	Ser	+	5	130	Co	CTC to GTC	Leu to Val	Missense	+	TV
3400	Ser	+	5	132	Co	AAG to AGG	Lys to Arg	Missense	+	TS
1282	Ser	+	5	132	Co	AAG to ACG	Lys to Thr	Missense	+	TV
ov 70	Ser	+	5	135	Co	TGC to TGG	Cys to Trp	Missense	+	TV
3367	Ser	+	5	136	Co	CAA to TAA	Gln to Stop	Nonsense	-	TS
687	Ser	+	5	136	Co	CAA to TAA	Gln to Stop	Nonsense	-	TS
2335	Endo	+	5	141	Co	TGC to TGG	Cys to Trp	Missense	+	TV
2745	Ser	+	5	151	NC	CCC to CAC	Pro to His	Missense	+	TV
3389	Mixed	+	5	158	NC	CGC to CCC	Arg to Pro	Missense	+	TV
824	Mixed	+	5	159	NC	GCC to GTC	Ala to Val	Missense	+	TS;CpG
704	Ser	+	5	160	NC	ATG to AAG	Met to Lys	Missense	+	TV
769	Ser	+	5	163	NC	TAC to TGC	Tyr to Cys	Missense	+	TS
2354	Brenner	+	5	163	NC	TAC to TGC	Tyr to Cys	Missense	+	TS
713	Ser	+	5	166	NC	TCA to TGA	Ser to Stop	Nonsense	-	TV
2650	Undiff	+	5	175	Co	CGC to CAC	Arg to His	Missense	+	TS;CpG
3371	Mixed	+	5	175	Co	CGC to CAC	Arg to His	Missense	+	TS;CpG
762	Ser	+	5	175	Co	CGC to CAC	Arg to His	Missense	+	TS;CpG
1270	Ser	+	5	175	Co	CGC to CAC	Arg to His	Missense	+	TS;CpG
3354	Ser	+	5	179	Co	CAT to GAT	His to Asp	Missense	+	TV
3529	Ser	+	5	179	Co	CAT to TAT	His to Tyr	Missense	+	TS
698	Adenoca	+	5	179	Co	CAT to CGT	His to Arg	Missense	+	TS
2716	Mixed	+	5	179	Co	CAT to CGT	His to Arg	Missense	+	TS
2721	Ser	+	5	nt 13240	-	TGgt to TGgc	intron 5	5'-splice jun	-	TS
3353	undiff	+	6	192	NC	CAG to TAG	Gln to Stop	Nonsense	-	TS
ov 59	Ser	+	6	193	NC	CAT to CGT	His to Arg	Missense	+	TS
2719	Ser	+	6	193-195	NC	CATCTTATC to GCCCCT	His,Leu,Ile to Ala, Pro	Del / Ins	+	-
2309	Undiff	+	6	195	NC	ATC to AAC	Ile to Asn	Missense	+	TV
805	Ser	+	6	201	NC	TTG to TTT	Leu to Phe	Missense	+	TV
2352	Ser	+	6	203	NC	GTG to TTG	Val to Leu	Missense	+	TV
2733	Ser	+	6	213	NC	CGA to CTA	Arg to Leu	Missense	-	TV
2340	Ser	+	6	213	NC	CGA to CGG	Arg / Arg	Polymorph	-	(TS)
2737	Ser	-	6	215	NC	AGT to GT	frameshift	1bp Del/Nonsense	-	-
2349	Ser	+	6	216	NC	GTG to TTG	Val to Leu	Missense	+	TV
241	Ser	-	6	220	NC	TAT to TGT	Tyr to Cys	Missense	+	TS
808	Clear	-	6	224	NC	GAG to GAA	Glu / Glu	Polymorph	-	(TS)
3373	Ser	+	7	nt 13999	-	agGT to agGT	intron 6	3' splice jun	+	TS
ov 49	Ser	+	7	227	NC	TCT to TCA	Asp to Ser	Missense	+	TV
2705	Mixed	+	7	231	NC	ACC to ACA	Thr / Thr	Polymorph	+	(TV)
3379	Ser	+	7	234	Co	TAC to TCC	Tyr to Ser	Missense	+	TV
2344	Clear	+	7	234	Co	TAC to TGC	Tyr to Cys	Missense	-	TS
2717	Ser	+	7	234	Co	TAC to TGC	Tyr to Cys	Missense	+	TS
2656	Endo	+	7	237	Co	ATG to ATT	Met to Ile	Missense	+	TV
3344	Endo	+	7	239 / 240	Co	AAC to AAC TTA	Leu ins	3 bp Ins	+	-
2659	Endo	+	7	242	Co	TGC to TAC	Cys to Tyr	Missense	+	TS
790	Mixed	+	7	242	Co	TGC to TTC	Cys to Phe	Missense	+	TV
2338	Endo	+	7	242	Co	TGC to TTC	Cys to Phe	Missense	+	TV
2724	Endo	+	7	242	Co	TGC to AGC	Cys to Ser	Missense	+	TV

2730	Ser	+	7	243	Co	ATG to GTG	Met to Val	Missense	+	TS
665	Ser	+	7	244	Co	GGC to AGC	Gly to Ser	Missense	+	TS
1752	Muc	+	7	245	Co	GGC to AGC	Gly to Ser	Missense	+	TS;CpG
1559	Ser	+	7	245	Co	GGC to GAC	Gly to Asp	Missense	+	TS;CpG
3540	Ser	+	7	248	Co	CGG to CAG	Arg to Glu	Missense	+	TS;CpG
802	Endo	+	7	248	Co	CGG to TGG	Arg to Trp	Missense	+	TS;CpG
249	Ser	+	7	248	Co	CGG to CAG	Arg to Gln	Missense	+	TS;CpG
3403	Undiff	+	7	249, 250	Co	AGG <u>CCC</u> to AGT <u>TCC</u>	Arg,Pro to Ser,Ser	Dble-Missense	+	TV,TS
2364	Ser	+	7	251, 252	Co	<u>ATC</u> <u>CTC</u> to ATC	Leu del	3 bp Del	+	-
1589	Ser	+	7	253	Co	ACC to CCC	Thr to Pro	Missense	+	TV
2651	Undiff	+	7	254 - 256	Co	<u>ATC</u> <u>ATC</u> <u>ACA</u> to A	frameshift	7 bp Del	-	-
2001	Ser	+	7	255	Co	ATC to AGC	Ile to Ser	Missense	-	TV
2337	Endo	+	7	258	Co	GAA to TAA	Glu to Stop	Nonsense	+	TV
2341	Ser	+	7	258	Co	GAA to TAA	Glu to Stop	Nonsense	-	TV
3362	Undiff	+	7	259	NC	GAC to TAC	Asp to Tyr	Missense	+	TV
3347	Ser	+	7	nt 14110	-	AGgt to AGtt	intron 7	5' splice jun	-	TV
2725	Ser	+	8	nt 14449	-	tagTG to agTG	intron 7	3' splice jun	+	TV
767	Ser	+	8	264	NC	CTA to TA	frameshift	1 bp Del	+	-
696	Ser	+	8	264, 265	NC	<u>CTA</u> <u>CTG</u> to CTG	Leu,Leu to Leu	3 bp Del	+	-
3364	Muc	+	8	266	NC	GGA to CGA	Gly to Arg	Missense	+	TV
ov45	Ser	+	8	266	NC	GGA to AGA	Gly to Arg	Missense	+	TS
2341	Ser	+	8	267	NC	CGG to CCG	Arg to Pro	Missense	-	TV
2332	Endo	+	8	267	NC	CGG to CCG	Arg to Pro	Missense	+	TV
2708	Mixed	-	8	271	Co	GAG to TAG	Glu to Stop	Nonsense	-	TV
2155	Ser	-	8	272	Co	GTG to ATG	Val to Met	Missense	+	TS
2732	Ser	-	8	272	Co	GTG to TTG	Val to Leu	Missense	+	TV
3346	Ser	+	8	273	Co	CGT to CAT	Arg to His	Missense	+	TS;CpG
3358	Undiff	+	8	273	Co	CGT to CAT	Arg to His	Missense	+	TS;CpG
3382	Endo	+	8	273	Co	CGT to CTT	Arg to Leu	Missense	+	TV
2715	Ser	-	8	273	Co	CGT to TGT	Arg to Cys	Missense	+	TS;CpG
693	Ser	+	8	273	Co	CGT to TGT	Arg to Cys	Missense	+	TS;CpG
700	Ser	-	8	273	Co	CGT to GGT	Arg to Gly	Missense	+	TV
2718	Ser	+	8	275	Co	TGT to TAT	Cys to Tyr	Missense	+	TS
ov 93	Ser	+	8	275	Co	TGT to GGT	Cys to Gly	Missense	+	TV
ov 164	Ser	+	8	275	Co	TGT to GGT	Cys to Gly	Missense	+	TV
2326	Mixed	+	8	276	Co	GCC to GTC	Ala to Val	Missense	+	TS
3385	Endo	+	8	280	Co	AGA to AGT	Arg to Ser	Missense	+	TV
2328	Ser	+	8	280	Co	AGA to ATA	Arg to Ile	Missense	+	TV
1751	Ser	+	8	281	Co	GAC to GAA	Asp to Glu	Missense	+	TV
2182	Endo	+	8	281	Co	GAC to GAG	Asp to Glu	Missense	-	TV
ov 72	Ser	+	8	281	Co	GAC to CAC	Asp to His	Missense	+	TV
3351	Ser	+	8	282	Co	CGG to TGG	Arg to Trp	Missense	+	TS;CpG
1756	Clear	+	8	282	Co	CGG to TGG	Arg to Trp	Missense	+	TS;CpG
1254	Ser	+	8	286	Co	GAA to GTA	Glu to Val	Missense	+	TV
3386	Ser	+	8	300	NC	<u>CCC</u> to <u>..CC</u>	frameshift	1 bp Del	+	-
3461	Endo	+	8	301	NC	CCA to <u>CCC</u> A	frameshift	1 bp Ins	-	-
2339	Ser	+	9	nt 14680	-	agCA to agCA	intron 8	3' splice jun	-	TS
1749	Undiff	+	9	311	NC	AAC to AA..	frameshift	1 bp Del	-	-
3402	Endo	+	9	320	NC	AAG to A..G	frameshift	1 bp Del	+	-
3394	Undiff	+	9	324	NC	GAT to G..T	frameshift	1 bp Del	+	-

* according to Cho et al. 1994

** Im p53: Immunostaining for p53

*** TS / TV: Transition / Transversion

Histopathology: Ser: Serous, Endo: Endometrioid, Undiff: Undifferentiated

Muc: Mucinous, Clear: Clear Cell, Mixed: Mixed Epithelial

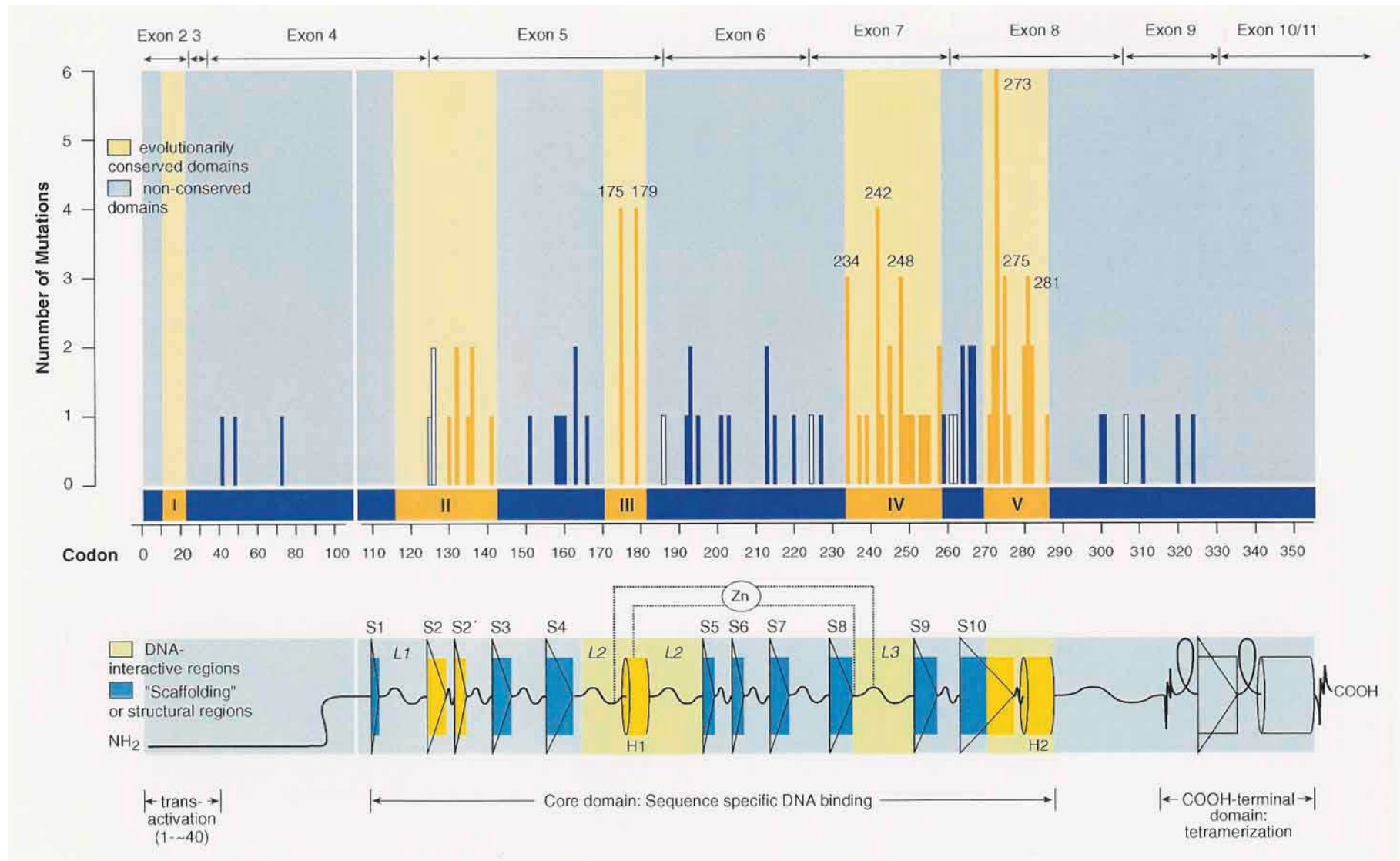
Among the cases with insertions, one had a nine basepair deletion and a six basepair insertion (case #2719). One case had a 3 bp insertion of TTA resulting in the insertion of the amino acid residue Leucin between codon 239 and 240 in exon 7 (#3344). A one basepair insertion (case #3461) at codon 301, exon 8 caused a frameshift with introduction of a premature stop at codon 305.

Eleven cases had deletions of 1-9 bp, four of which (cases # 2719, 2737, 767, 696) have been described previously (Wen et al. 1999). Of the newly identified deletions, four were 1 bp deletions, one in exon 8 (case # 3386) and three in exon 9 (case # 1749, 3402, 3394), all resulting in the introduction of a premature stop codon at codon 344. Three of these cases had p53 protein overexpression. One case had a 3 bp deletion in exon 7, resulting in the loss of a leucine residue (case #2364) and one case had a 2 bp deletion in exon 4, causing the introduction of a stop codon at codon 50 (case #3401). This case was negative in immunohistochemistry. A seven bp deletion in exon 7 (case #2651), affecting codons 254-256, resulted in a frameshift affecting the entire sequence between codon 256 and a premature stop at codon 344.

Furthermore, we identified 5 splice junction mutations (cases # 3391, 2658, 3355, 3373, 3347) in addition to three cases described in our previous study (Wen et al. 1999). Two of these affected the donor site at exon 4/intron 4 and exon 7/intron 7 respectively (Table 8). Both cases were negative for immunohistochemistry. Three splice site mutations involved the consensus acceptor site at intron 4/exon5 (2 cases) and intron 6/exon 7. These three cases had p53 protein overexpression (Table 8).

Four regions of the translated sequence of *p53* have been highly conserved throughout evolution and span codon 117-124 (II), 171-181 (III), 234-258 (IV) and 270-286 (V). These regions span a total of 79 codons. In 62% (62/100) of the cases, mutations were located in these highly conserved regions (Fig. 13). Region II, which spans part of exon 4 and exon 5, contained 10 mutations including 3 splice site mutations in intron 4 (10%). Region III contained 8 mutations (8%), region IV 23 mutations (23%) and region V a total of 21 mutations (21%). Thirty-eight percent of the mutations were found in non-conserved regions of the gene. The codons most frequently mutated were codons 175, 179, 234, 242, 248, 273, 275 and 281 which were each mutated in three or more different carcinomas (Fig. 13).

Fig. 13: p53 mutations in evolutionary highly conserved domains of the gene. The upper part of the figure shows the number of mutations in codons 36 through 324 of the *p53* gene. Mutations in evolutionary highly conserved regions are marked in yellow, mutations in non-conserved regions in dark blue and splice site mutations in white. The lower part of the figure shows the corresponding DNA interacting regions of the p53 protein.



Fourty-two mutations (42%) were classified as transition mutations, 46 (45%) as transversions, and 13% were deletions or insertions. We found 29 G:C to A:T transitions and 13 A:T to G:C transitions. Among the G:C to A:T transitions 16 (55%) were located in CpG sites, which are known to be potential sites of DNA methylation. Out of 46 transversions, we found 20 G:C to T:A mutations, 12 G:C to C:G, 8 T:A to A:T and 6 A:T to G:C mutations.

4.1.2 *p53* polymorphisms and intron alterations

A total number of 45 *p53* polymorphisms and intron alterations of unknown significance were found in 33 cases (19%). In 15/33 cases (46%) with polymorphisms or intron alterations additional *p53* mutations with an amino acid exchange had been identified. This accounted for 15% of the cases with mutations. Only 61/178 ovarian cancer cases (34%) were found to have a completely normal *p53* sequence with neither mutations nor other sequence alterations in the DNA segments which were analyzed.

The most frequent exon polymorphism was located in exon 4 at codon 72 (Fig. 14), and was found in 9 cases (5.1%). This CGC→CCC polymorphism at codon 72 results in an arginine to proline amino acid exchange (Harris et al. 1986, Matlashewski et al. 1987). In one case (#3379), an additional CCG to CCA (Pro/Pro) polymorphism was identified at codon 36 of exon 4 (Table 9 and 10).

A further exon polymorphisms, CGA→CGG (Arg/Arg), was identified in exon 6 at codon 213. Another silent mutation which was considered a polymorphism, occurred at codon 224 of exon 6 as a GAG→GAA (Glu/Glu) polymorphism without amino acid alteration. In exon 7 an ACC→ACA (Thr/Thr) polymorphism was identified at codon 231 (Table 9 and 10).

An intron 3 polymorphism (Fig. 15), which is known as a 16 bp repeat (Lazar et al. 1993) at nucleotide 11951, was found in 24 (14%) of the cases. Six (25%) of the cases were identified by SSCP as homozygote and 18 (75%) were heterozygote for this intron 3 alteration. Five cases were sequenced to confirm the polymorphism suspected by the SSCP alteration.

Eight *p53* sequence alterations were identified in intron sequences, flanking the exons 7, 10 and 11 (Table 9 and 10). In all of these cases, a shift in the SSCP bands was noticed without evidence of a mutation in the exon sequence. In intron 6 at position 13964, a g→c base exchange was identified in two cases. No normal tissue was available in these cases to verify the polymorphism.

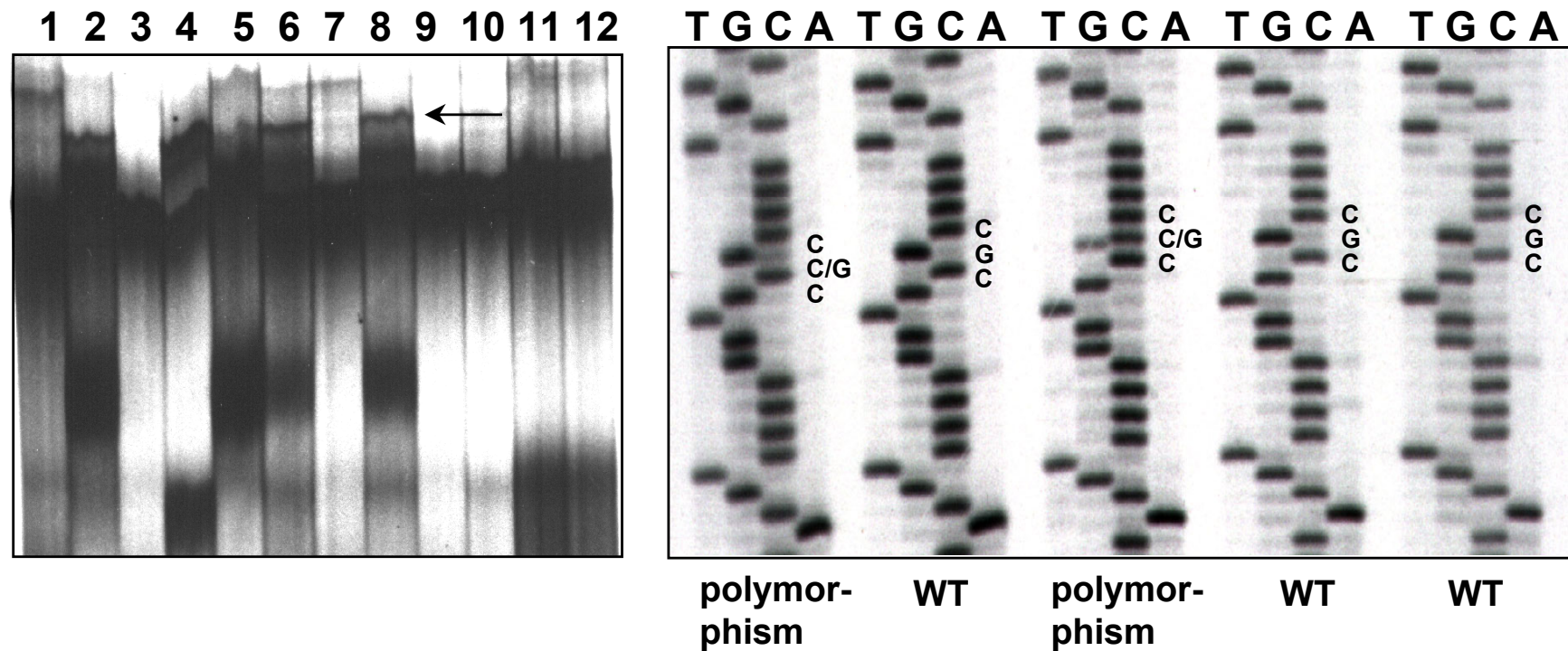


Fig. 14: CGC → CCC (Arg → Pro) polymorphism at codon 72 of the p53 gene

A: SSCP analysis of p53, exon 4 in ovarian carcinomas. DNA in lanes 2,4,5,6,and 8 shows band shifts suspicious for sequence alterations and was analyzed by DNA sequencing.

B: DNA sequence analysis of p53, exon 4 shows a CGC to CCC polymorphism at codon 72, resulting in an arginine to proline amino acid exchange.

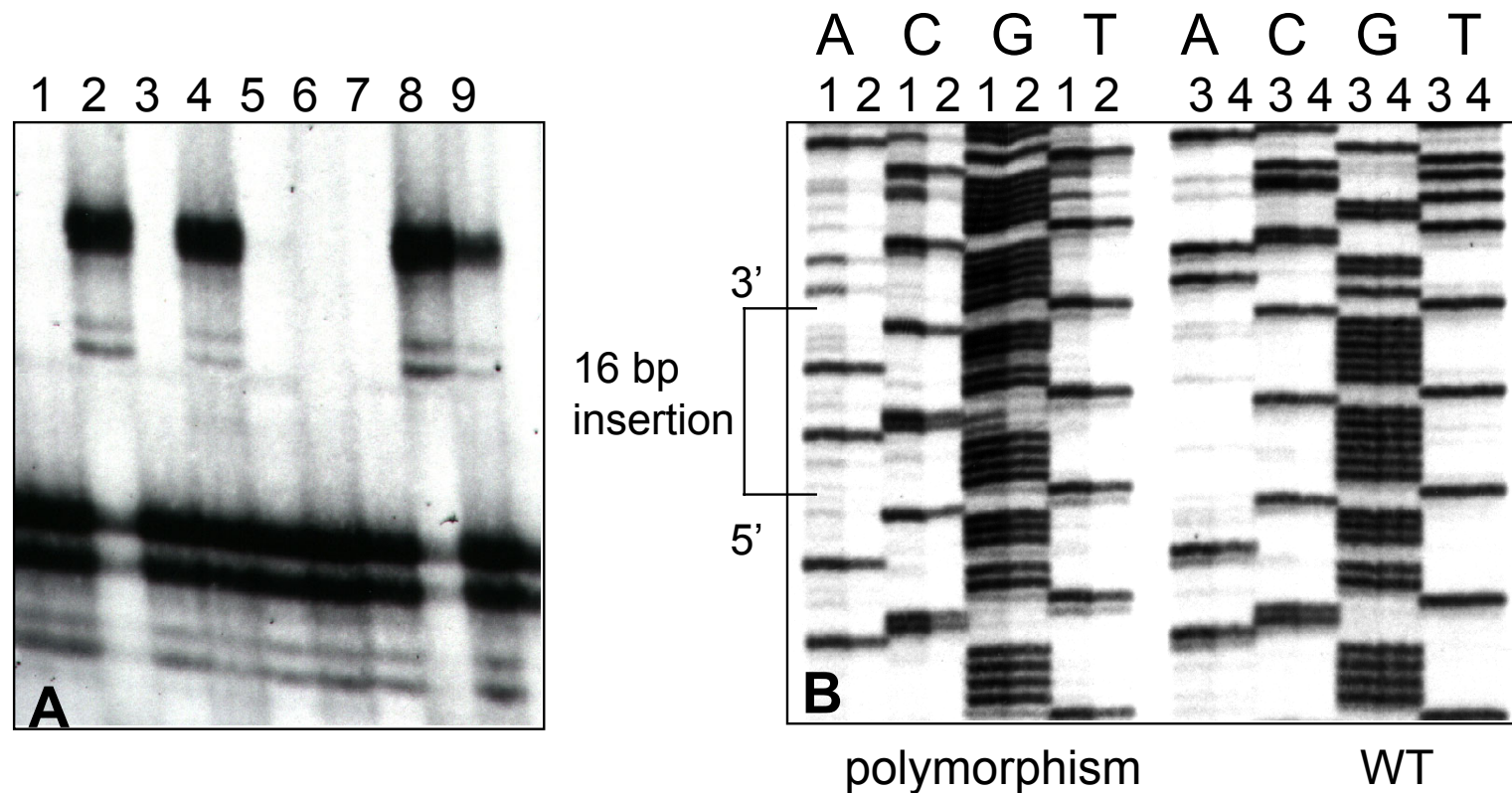


Fig. 15: Intron 3 polymorphism of the p53 gene

A: Single Strand Conformation Polymorphism (SSCP) of *p53*, exon 3 with the adjacent intron sequence shows a band shift in lanes 2,4,8 and 9 indicating the intron 3 polymorphism.

B: Wild type (lanes 3 and 4) and the polymorphism sequence (lanes 1 and 2) of *p53*, intron 3 with a 16 bp insertion (lanes 1 and 2) and adjacent sequence are shown as 5' to 3': GCTggggacctggagggtGGGGG

In intron 10 at position 17708, an a→t base exchange was found in 2 out of five cases which had shown SSCP alterations in exon 10. In 4 out of 9 cases which had shown an obvious band shift in the SSCP analysis for exon 11, a c→t base exchange at position 18550 was identified.

Multiple polymorphisms were identified in 11/178 (6%) of all ovarian cancer cases and 11/33 (33%) of the cases with polymorphisms. In case #3379, three polymorphisms were identified, two in exon 4 (codon 36 and codon 72) and one in intron 3. The other cases had two polymorphisms. Eight out of nine cases with exon 4 polymorphisms (89%) and 3/6 cases with intron 10 alterations (50%) had an additional intron 3 polymorphism.

4.1.3 Confirmation of *p53* polymorphisms in normal tissue DNA

In cases with exon 4, exon 6 or exon 7 polymorphisms, and in cases with intron 6 or intron 10 alterations, normal tissue of the ovarian cancer patients, which had been formalin fixed and paraffin embedded at the time of surgery, was sequenced at the same DNA site (Table 10). Normal tissue was available in 12/20 of these cases. In three cases with a codon 72 Arg→Pro polymorphism, the same sequence alteration was found in normal tissue. In two heterozygote cases, in which the CGC sequence was stronger than the CCC sequence and in one case with equally strong G and C band only, the CGC (arginin) sequence was identified in normal tissue. In two cases with a homozygote CGC→CCC polymorphism in the tumor, only CGC was identified in normal tissue. In the cases with exon 6, intron 6 and exon 7 polymorphisms no normal tissue was available

The intron 10 alteration at nucleotide 17708 was confirmed in one case, in which normal tissue was available. We have identified this alteration in two ovarian carcinoma cases, which had shown SSCP band shifts. We assume that this is an a→t polymorphism at nucleotide 17708, which has not been described so far. Furthermore, the intron 10 c→t sequence alteration at nucleotide 18550 was found in four ovarian carcinoma cases and could be confirmed in all three cases, in which normal tissue had been analyzed (Table 10). We therefore consider these intron alterations as two novel intron 10 polymorphisms.

4.1.4 *p53* protein overexpression

p53 protein overexpression, using a cut-point of ≥10% positively stained nuclei, was found in 62% (110/178) of the cases. The cut-off for *p53* overexpression was chosen as 10%, because we found frozen sections from proliferating normal

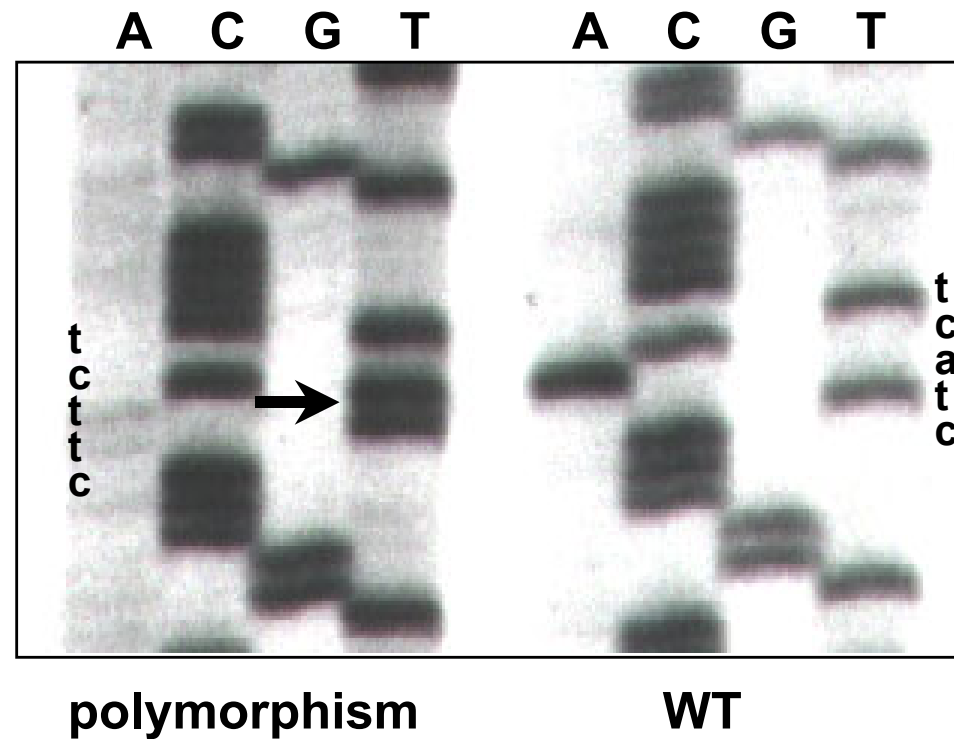


Fig. 16: Intron 10 polymorphism of the p53 gene at nucleotide 17708

A novel polymorphism of the *p53* gene was identified at nucleotide 17708 (a>t) of intron 10 by SSCP analysis and DNA sequencing in the ovarian cancer case #3402.

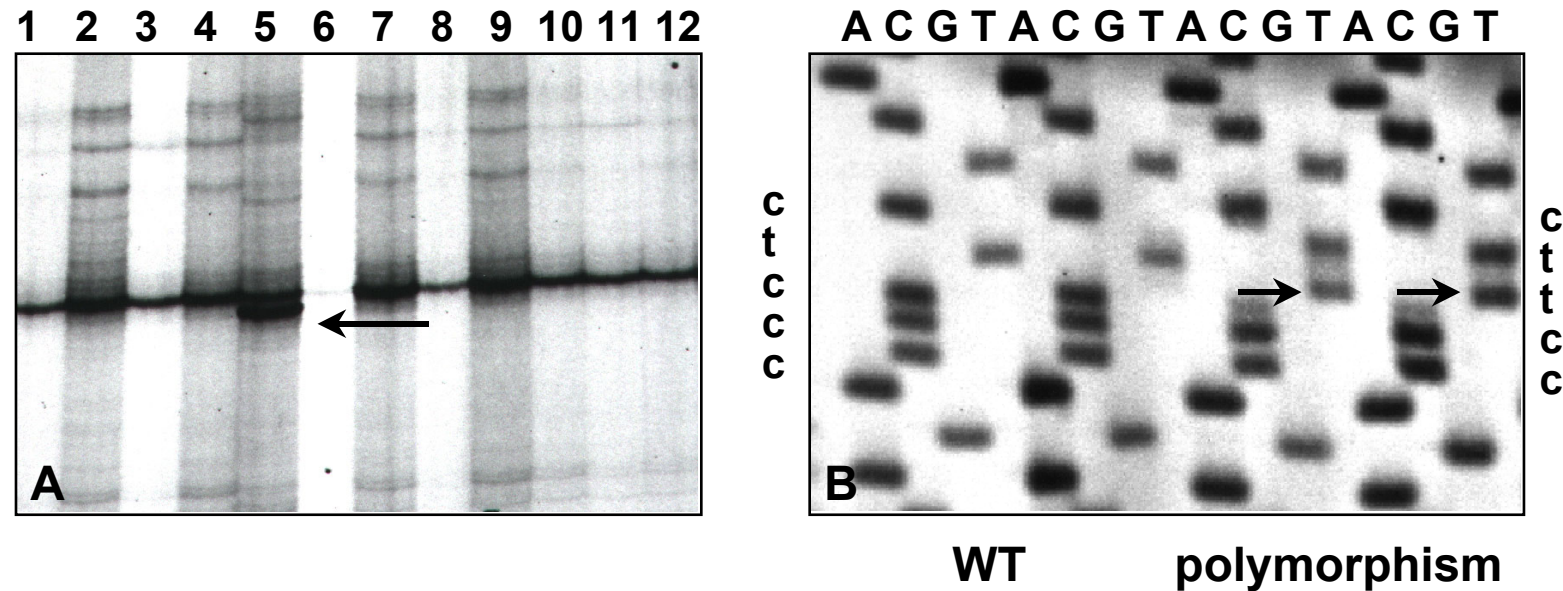


Fig. 17: Intron 10 polymorphism of the p53 gene at nucleotide 18550

A: SSCP analysis of *p53* exon 11 and flanking intron sequence in ovarian carcinomas. The band shift in lane 5 (case #3394) is suspicious for DNA sequence alterations.

B: DNA sequence analysis of *p53* exon 11/ intron 10 reveals a novel c>t polymorphism at nucleotide 18550 of intron 10 in the ovarian cancer cases #2660 and #3344. The polymorphism was confirmed in normal tissue DNA.

Table 9: p53 polymorphisms and overexpression in ovarian carcinomas

Case #	Histo-pathology	SSCP Result	p53 Mut	Exon/ Intron	Codon/ Nucleotide #	DNA Sequence	Amino Acid Sequence	Polymorphism Type	Immunostaining p53
1749	Undiff	+	+	Intron 3	nt 11951	gggtcgggaggtccag	-	16 bp repeat	-
1751*	Ser	+	+	Intron 3	nt 11951	gggtcgggaggtccag	-	16 bp repeat	+
1754	Ser	+	-	Intron 3	nt 11951	gggtcgggaggtccag	-	16 bp repeat	-
2341	Ser	+	+	Intron 3	nt 11951	gggtcgggaggtccag	-	16 bp repeat	-
2353	Ser	+	-	Intron 3	nt 11951	gggtcgggaggtccag	-	16 bp repeat	-
2364	Ser	+	+	Intron 3	nt 11951	gggtcgggaggtccag	-	16 bp repeat	+
2653*	Undiff	+	-	Intron 3	nt 11951	gggtcgggaggtccag	-	16 bp repeat	+
2660*	Ser	+	-	Intron 3	nt 11951	gggtcgggaggtccag	-	16 bp repeat	+
3348	Endo	+	-	Intron 3	nt 11951	gggtcgggaggtccag	-	16 bp repeat	-
3350*	Ser	+	-	Intron 3	nt 11951	gggtcgggaggtccag	-	16 bp repeat	-
3351	Ser	+	+	Intron 3	nt 11951	gggtcgggaggtccag	-	16 bp repeat	+
3355	Endo	+	+	Intron 3	nt 11951	gggtcgggaggtccag	-	16 bp repeat	+
3357	Endo	+	-	Intron 3	nt 11951	gggtcgggaggtccag	-	16 bp repeat	-
3359	Endo	+	-	Intron 3	nt 11951	gggtcgggaggtccag	-	16 bp repeat	+
3362	Undiff	+	+	Intron 3	nt 11951	gggtcgggaggtccag	-	16 bp repeat	+
3365	Endo	+	-	Intron 3	nt 11951	gggtcgggaggtccag	-	16 bp repeat	+
3370*	Muc	+	-	Intron 3	nt 11951	gggtcgggaggtccag	-	16 bp repeat	-
3376*	Ser	+	-	Intron 3	nt 11951	gggtcgggaggtccag	-	16 bp repeat	-
3377*	Ser	+	-	Intron 3	nt 11951	gggtcgggaggtccag	-	16 bp repeat	-
3379*	Ser	+	+	Intron 3	nt 11951	gggtcgggaggtccag	-	16 bp repeat	+
3381*	Endo	+	-	Intron 3	nt 11951	gggtcgggaggtccag	-	16 bp repeat	-
3385*	Endo	+	+	Intron 3	nt 11951	gggtcgggaggtccag	-	16 bp repeat	+
3402*	Endo	+	+	Intron 3	nt 11951	gggtcgggaggtccag	-	16 bp repeat	+
3403	Undiff	+	+	Intron 3	nt 11951	gggtcgggaggtccag	-	16 bp repeat	+
3379*	Ser	+	+	Exon 4	36	CCG to CCA	Pro / Pro	known PM	+
1751*	Ser	+	+	Exon 4	72	CGC to CCC	Arg to Pro	known PM	+
3350*	Ser	+	-	Exon 4	72	CGC to CCC	Arg to Pro	known PM	-
3354	Ser	+	+	Exon 4	72	CGC to CCC	Arg to Pro	known PM	+
3370*	Muc	+	-	Exon 4	72	CGC to CCC	Arg to Pro	known PM	-
3376*	Ser	+	-	Exon 4	72	CGC to CCC	Arg to Pro	known PM	-
3377*	Ser	+	-	Exon 4	72	CGC to CCC	Arg to Pro	known PM	-
3379*	Ser	+	+	Exon 4	72	CGC to CCC	Arg to Pro	known PM	+
3381*	Endo	+	-	Exon 4	72	CGC to CCC	Arg to Pro	known PM	-
3385*	Endo	+	+	Exon 4	72	CGC to CCC	Arg to Pro	known PM	+
2340	Ser	+	-	Exon 6	213	CGA to CGG	Arg / Arg	known PM	-
808	Clear	-	-	Exon 6	224	GAG to GAA	Glu / Glu	possible PM	-
3529	Ser	+	+	Intron 6	nt 13964	gcgca to gccca	-	possible PM	+
3390	Ser	+	-	Intron 6	nt 13964	gcgca to gccca	-	possible PM	-
2705	Mixed	+	-	Exon 7	231	ACC to ACA	Thr / Thr	possible PM	+
2653*	Undiff	+	-	Intron 10	nt 17708	ctact to ctct	-	possible PM	+
3402*	Endo	+	+	Intron 10	nt 17708	ctact to ctct	-	possible PM	+
2660*	Ser	+	-	Intron 10	nt 18550	ccctc to ccttc	-	possible PM	+
3344	Endo	+	+	Intron 10	nt 18550	ccctc to ccttc	-	possible PM	+
3394	Undiff	+	+	Intron 10	nt 18550	ccctc to ccttc	-	possible PM	+
3464	Ser	+	-	Intron 10	nt 18550	ccctc to ccttc	-	possible PM	+

* multiple p53 polymorphisms

Table 10: Normal tissue sequencing results for *p53* polymorphisms

Case #	Exon/ Intron	Codon/ Nucleotide #	Tumor DNA Sequence	Tumor Amino Acid Sequence	NI tissue DNA Sequence	NI tissue Amino Acid Sequence	Immuno- staining p53
3379	Exon 4	36	CCG to CCA	Pro / Pro	not available	-	+
1751	Exon 4	72	CGC to CCC	Arg to Pro	CGC	Arg	+
3350	Exon 4	72	CGC to CCC	Arg to Pro	CCC	Pro	-
3354	Exon 4	72	CGC to CCC	Arg to Pro	CGC	Arg	+
3370	Exon 4	72	CGC >> CCC*	Arg >> Pro	CGC	Arg	-
3376	Exon 4	72	CGC to CCC	Arg to Pro	not available	-	-
3377	Exon 4	72	CGC to CCC	Arg to Pro	CCC	Pro	-
3379	Exon 4	72	CGC / CCC	Arg / Pro	CGC	Arg	+
3381	Exon 4	72	CGC >> CCC	Arg >> Pro	CGC	Arg	-
3385	Exon 4	72	CGC to CCC	Arg to Pro	CCC	Pro	+
2340	Exon 6	213	CGA to CGG	Arg / Arg	not available	-	-
808	Exon 6	224	GAG to GAA	Glu / Glu	not available	-	-
3529	Intron 6	nt 13964	gcgca to gccca	-	not available	-	+
3390	Intron 6	nt 13964	gcgca to gccca	-	not available	-	-
2705	Exon 7	231	ACC to ACA	Thr / Thr	not available	-	+
2653	Intron 10	nt 17708	ctact to ctctt	-	ctact to ctctt	-	+
3402	Intron 10	nt 17708	ctact to ctctt	-	not available	-	+
2660	Intron 10	nt 18550	ccctc to ccttc	-	ccctc to ccttc	-	+
3344	Intron 10	nt 18550	ccctc to ccttc	-	not available	-	+
3394	Intron 10	nt 18550	ccctc to ccttc	-	ccctc to ccttc	-	+
3464	Intron 10	nt 18550	ccctc to ccttc	-	ccctc to ccttc	-	+

* base G stronger than C

tissues to show a small proportion of cells with p53 immunostaining, usually not more than a few percent. This cut-off value of 10% had shown the best sensitivity and specificity for *p53* mutations in our previous study (Wen et al. 1999). 22 (12%) cases had immunostaining <10% and 46 (26%) cases had no immunostaining of tumor cell nuclei and, together were considered to have normal p53 expression. None of the ovarian carcinomas had specific cytoplasmic staining. p53 immunostaining was not observed in the benign tissue of ovarian carcinomas including fibrous connective tissue, blood vessels and inflammatory cells. Seventy-five out of 178 (42%) cases were found to have high overexpression with a percentage of positively stained nuclei of more than 78%. This cut-point had been determined to be optimal as a predictor of clinical outcome in the statistical analysis of survival.

4.1.5 Comparison of p53 overexpression with *p53* mutations

p53 overexpression detected by immunohistochemical staining was significantly correlated with *p53* mutations ($p < 0.001$) detected by DNA sequence analysis. The percentage of cases with overexpression was 81% in ovarian carcinomas with *p53* mutation and 38% in cases with wildtype *p53*. The percentage of cases with p53 immunostaining varied according to the type of mutation. The correlation between protein overexpression and mutations was mainly due to the high proportion of missense mutations. 67 out of 71 (94%) of the cases with missense mutations showed p53 overexpression, while immunostaining $\geq 10\%$ was only seen in 1/7 (14%) of the cases with nonsense mutations, 8/13 (62%) of the cases with insertions or deletions and 4/8 (50%) of the cases with splice site mutations (Fig. 18 a,b).

Overall only 46% (13/28) of the ovarian carcinomas with nonmissense mutations had p53 overexpression, which is not significantly different from the frequency of overexpression in 30/79 tumors with wildtype *p53* sequence (38%) ($p = 0.43$). Nineteen percent (19/99) of the cases with *p53* mutations failed to show immunostaining, which is largely caused by nonmissense mutations.

4.1.6 *p53* polymorphisms and p53 protein overexpression

Ovarian cancer cases with normal p53 expression respectively p53 overexpression were distributed approximately equally among cases with exon 4 polymorphism ($p = 0.27$) and intron 3 polymorphisms ($p = 0.41$) (Table 11). Interestingly, though, out of eight cases with intron 6 or intron 10 sequence alterations, seven cases had p53 overexpression which is close to reaching statistical significance ($p = 0.086$) (Table 11).

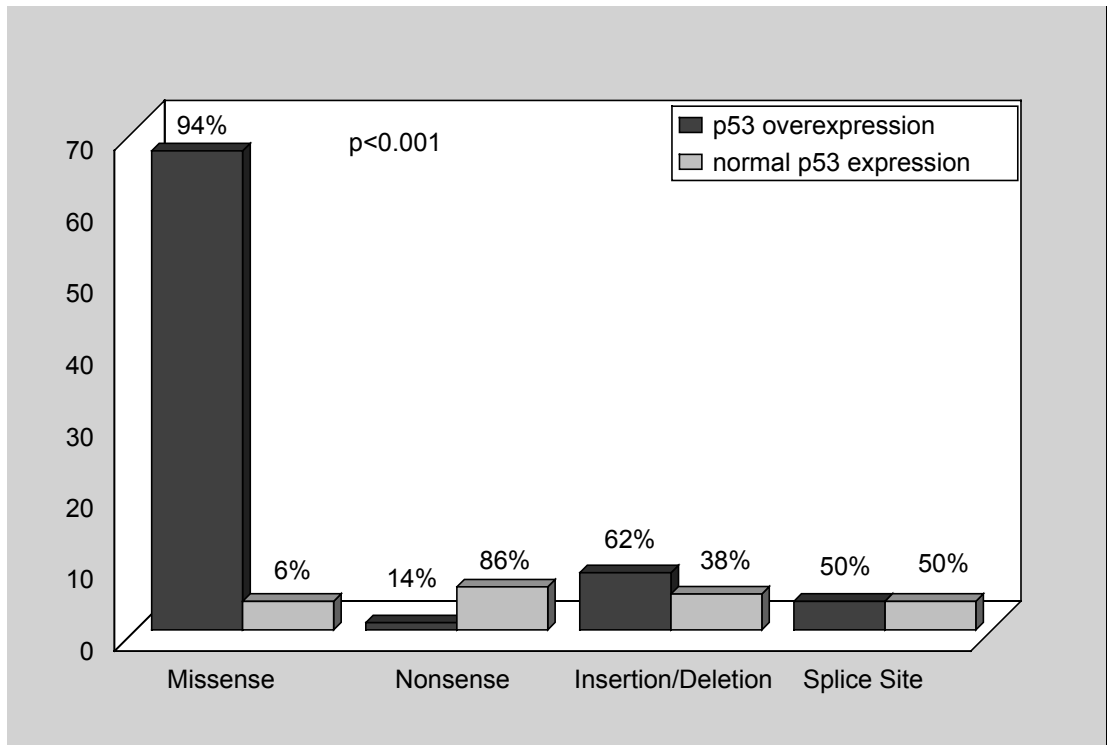


Fig. 18a: p53 protein overexpression according to type of *p53* mutation. Overexpression is found in a high percentage of cases with missense mutations, while the frequency of overexpression in nonmissense mutations is overall only 46%.

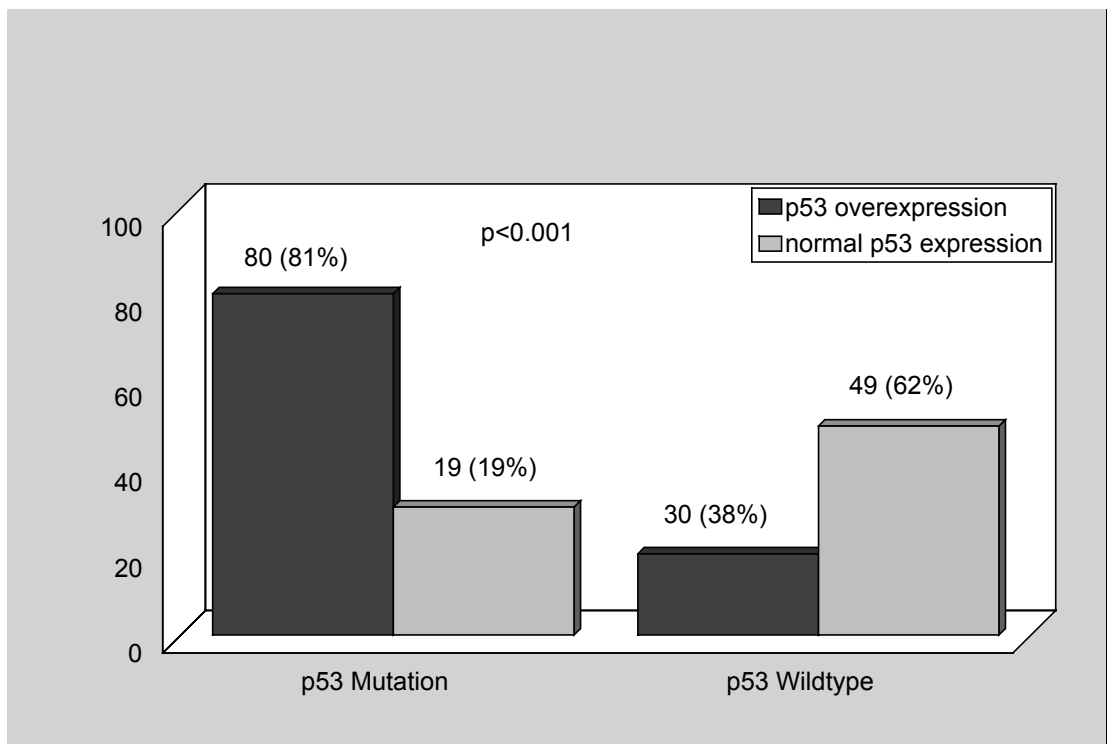


Fig. 18b: p53 protein overexpression according to *p53* mutation or wildtype *p53*. A high proportion of cases (38%) shows p53 protein accumulation (immunostaining in $\geq 10\%$ of the nuclei) despite *p53* wildtype sequence.

Table 11: p53 protein overexpression in ovarian cancer cases with p53 polymorphisms

<i>p53</i> Polymorphism	p53 Over- expression n (%)	Normal p53 Expression n (%)	Total n (%)	p- value
Exon 4 Codon 72				
Polymorphism CGC Arg →CCC Pro	4 (44)	5(56)	9 (5)	0.27
Normal Sequence CGC Arg	106 (63)	63 (37)	169 (95)	
Intron 3				
16 bp repeat Polymorphism	14 (54)	12 (46)	26 (15)	0.37
Normal Intron 3 Sequence	96 (63)	56 (37)	152 (85)	
Intron 6 / Intron 10				
Polymorphism	8 (89)	1 (11)	9 (5)	0.086
Normal Sequence	102 (60)	67 (40)	169 (95)	
Total	110 (62)	68 (38)	178 (100)	

4.1.7 Correlation of p53 alterations with histopathological and clinical data

p53 mutations were significantly more frequent in ovarian carcinomas with advanced FIGO stages III and IV ($p<0.001$), poor differentiation ($p<0.001$), residual tumor burden after debulking surgery ($p<0.04$), DNA-aneuploidy ($p=0.003$) and high S-phase-fraction as measured by image cytometry ($p<0.001$). Patients with p53 mutations also had a higher median age than patients with p53 wildtype ($p=0.041$). Overexpression of the p53 protein was correlated only with low grade of differentiation ($p<0.001$) and high S-phase-fraction ($p<0.001$) (Table 12).

4.1.8 p53 alterations and response to chemotherapy

Patients with p53 overexpressing tumors were significantly more often resistant or refractory to a platinum based chemotherapy (61%) than patients with non-overexpressing tumors (22%) ($p=0.001$) (Table 13, Fig. 19 A-D).

Table 12. Clinico-pathologic characteristics of patients with epithelial ovarian cancer

Characteristic	<u>p53 Mutation Analysis</u>			<u>p53 Protein Expression</u>			<u>p53 Alterations</u>		
	p53 Mutation	p53 Wildtype	P value*	Overex- pression	normal Expression	P value*	p53 Alteration	normal p53	P value*
Patients - no. (%)	99 (56)	79 (44)		110 (62)	68 (38)		132 (74)	46 (26)	
Median age - yrs	57	53	0.041**	57	52	0.06**	57	52	0.056**
Histological Subtype - no. (%)									
Serous	60 (61)	51 (65)	0.08	67 (61)	44 (65)	0.62	79 (60)	32 (70)	0.4
Mucinous	2 (2)	6 (8)		4 (4)	4 (6)		4 (3)	4 (9)	
Endometriod	18 (18)	12 (15)		20 (18)	10 (15)		24 (18)	6 (13)	
Clear Cell	1 (1)	5 (6)		2 (2)	4 (6)		4 (3)	2 (4)	
Brenner	1 (1)	0		1 (1)	0		1 (1)	0	
Undifferentiated	8 (8)	2 (3)		7 (6)	3 (4)		9 (7)	1 (2)	
Mixed Epithelial	7 (7)	3 (4)		7 (6)	3 (4)		9 (7)	1 (2)	
Unclassified	2 (2)	0		2 (2)	0		2 (2)	0	
Clinical stage - no. (%)									
FIGO I	11 (11)	25 (32)	0.001	18 (17)	18 (28)	0.11	21 (16)	15 (34)	0.005
FIGO II	3 (3)	5 (7)		4 (4)	4 (6)		5 (4)	2 (7)	
FIGO III	67 (70)	39 (51)		72 (67)	34 (52)		83 (64)	23 (52)	
FIGO IV	15 (16)	8 (10)		14 (13)	9 (14)		20 (16)	3 (7)	
Grade of Differentiation - no. (%)									
I (well)	7 (7)	21 (27)	< 0.001	8 (7)	20 (29)	< 0.001	11 (8)	17 (37)	< 0.001
II (moderate)	25 (25)	27 (34)		32 (29)	20 (29)		36 (27)	16 (35)	
III (poor)	67 (68)	31 (39)		70 (64)	28 (41)		85 (64)	13 (28)	
Residual Tumor - no. (%)									
No residual tumor	32 (39)	39 (56)	0.04	36 (40)	35 (56)	0.062	46 (41)	25 (60)	0.044
≤ 2 cm	29 (35)	19 (27)		32 (35)	16 (26)		37 (33)	11 (26)	
> 2 cm	22 (27)	12 (17)		23 (25)	11 (18)		28 (25)	6 (14)	
Lymph nodes - no. (%)									
Negative	9 (11)	15 (22)	0.2	13 (15)	11 (17)	0.5	16 (15)	8 (19)	0.24
Positive	20 (25)	17 (25)		20 (24)	17 (27)		24 (23)	13 (30)	
Not resected	50 (63)	37 (54)		52 (61)	35 (56)		65 (62)	22 (51)	
DNA-ploidy - no. (%) (n=102)									
Diploid	21 (39)	33 (69)	0.003	28 (48)	26 (59)	0.28	31 (44)	23 (74)	0.004
Aneuploid	33 (61)	15 (31)		30 (52)	18 (41)		40 (56)	8 (26)	
S-Phase-Fraction - no. (%) (n=102)									
low (< 5%)	4 (7)	22 (46)	< 0.001	6 (10)	20 (45)	< 0.001	9 (13)	17 (55)	< 0.001
intermediate (5% - 14.4%)	26 (48)	21 (44)		29 (50)	18 (41)		35 (49)	12 (39)	
high (≥ 14.5%)	24 (44)	5 (10)		23 (40)	6 (14)		27 (38)	2 (6)	
Treatment - no. (%) ***									
Cisplatin - Cyclophosphamide	27 (32)	27 (39)	0.43	34 (37)	20 (33)	0.55	39 (35)	15 (38)	0.98
Carboplatin - Cyclophosphamide	13 (16)	7 (10)		13 (14)	7 (12)		15 (14)	5 (13)	
Other regimens	25 (31)	16 (23)		26 (29)	15 (25)		31 (28)	10 (25)	
No chemotherapy	17 (21)	19 (28)		18 (20)	18 (30)		26 (23)	10 (25)	
No information - no.	17	10		19	8		21	6	

* Chi-Square test for two categories, Mantel-Haenszel test for three or more categories

** Wilcoxon test

*** Chemotherapy regimens are described in the methods section

Among patients with *p53* mutations, 56% (22/39) as opposed to only 35% (12/34) of the patients with wildtype *p53* were resistant or refractory to platinum based chemotherapy, but the result did not achieve statistical significance ($p=0.071$). However the response to chemotherapy was correlated with the type of mutation. If only patients with missense mutations were evaluated, only 10/29 (34%) were platinum sensitive as compared to 29/44 (66%) of patients with *p53* wildtype or nonmissense mutations ($p=0.008$) (Table 13). Overall, time to progression since chemotherapy was significantly shorter for patients with *p53* alterations than patients with normal *p53* ($p=0.037$) (Fig. 19).

Table 13: Response to platinum-based chemotherapy in correlation to *p53* alterations

Response to Chemotherapy	<u>Immunostaining</u>		<u><i>p53</i> Sequence</u>		<u>Type of Mutation</u>	
	neg	pos	WT	MUT	WT/Non Missense	Missense
	n (%)	n (%)	n (%)	n (%)	n(%)	n(%)
Sensitive	21 (78)	18 (39)	22 (65)	17 (44)	29 (66)	10 (34)
Resistant / Refractory	6 (22)	28 (61)	12 (35)	22 (56)	15 (34)	19 (66)
p-value		0.001		0.071		0.008
Total (100%)	27	46	34	39	44	29

Interestingly, out of 5 patients in our study who were treated with Taxol/Carboplatin, the only patient (case #3400) who was sensitive to treatment and had no evidence of disease 28 months after diagnosis of a poorly differentiated FIGO III ovarian carcinoma, had high overexpression of *p53* protein and a missense mutation in exon 5.

4.1.9 *p53* alterations as a predictor of time to progression and overall survival

Ovarian cancer patients with *p53* mutations had a significantly shorter time to progression ($p=0.029$) and overall survival ($p=0.014$) than patients with wildtype *p53* (Fig. 20A, Table 14, 15). In 61/99 (62%) tumors, the *p53* mutation was in an evolutionary highly conserved domain. If the clinical outcome of these was

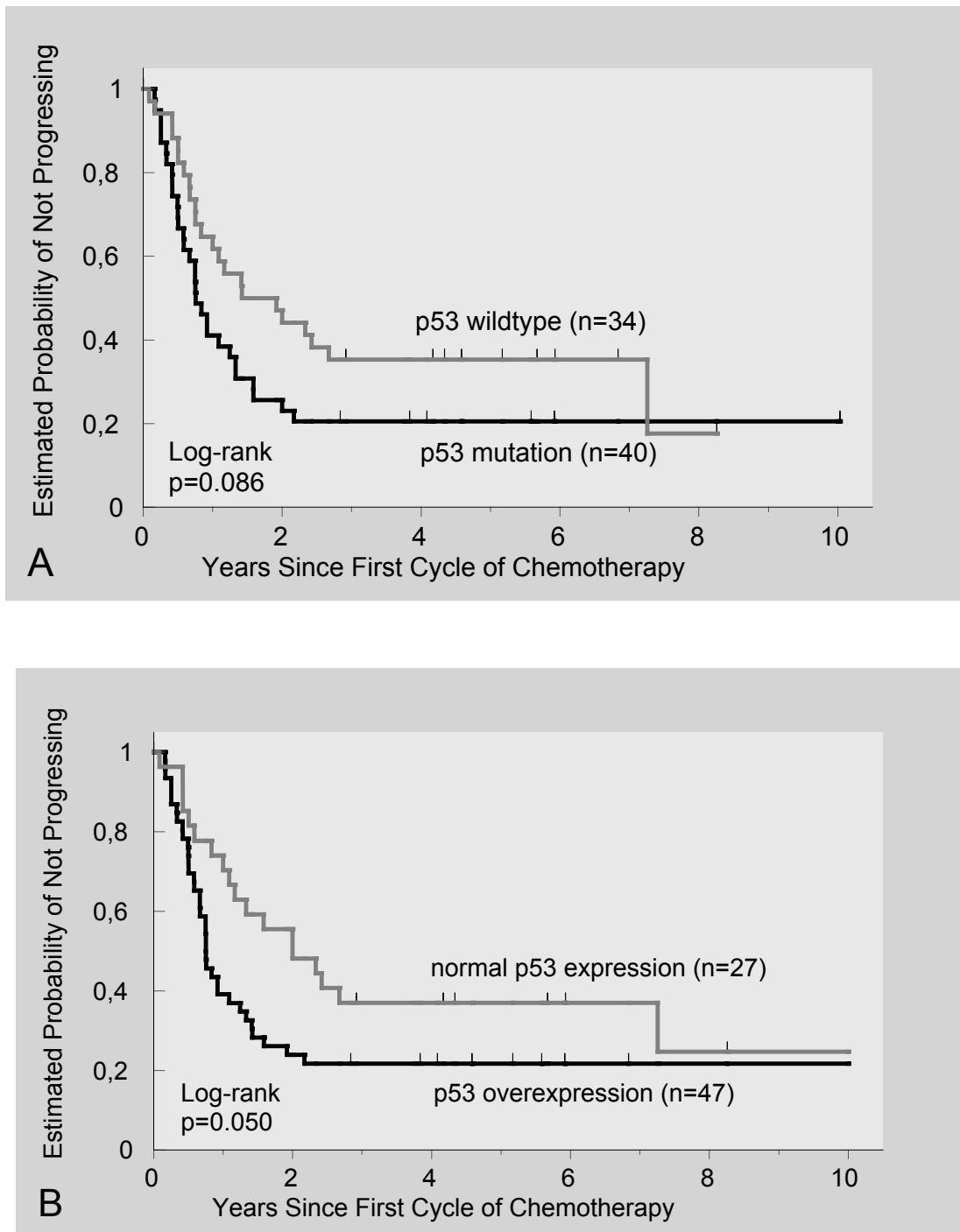


Fig. 19 A-B: Estimated probability of not progressing in epithelial ovarian cancer patients (n=74), who received platinum-based chemotherapy. **(A)** Ovarian carcinomas with *p53* mutations versus wildtype *p53*. **(B)** Ovarian carcinomas with *p53* proteinoverexpression versus normal *p53* expression.

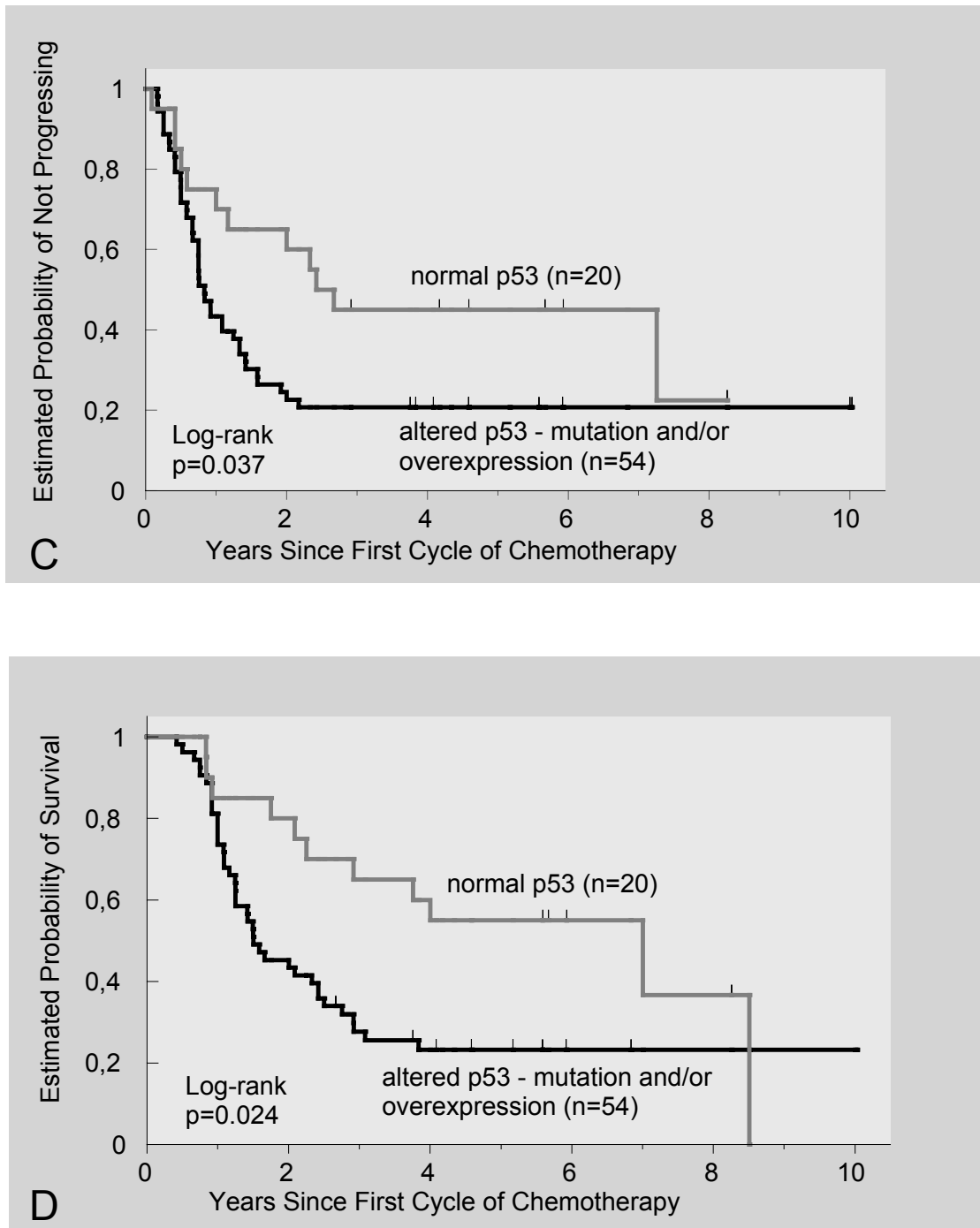


Fig. 19 C-D:: Estimated probability of (C) not progressing, and (D) overall survival respectively in epithelial ovarian cancer patients (n=74), who received platinum-based chemotherapy. Ovarian cancer with p53 alterations (mutation or overexpression or both) versus normal p53 status.

compared to patients with either wild-type *p53* or a mutation in a nonconserved domain, the difference in time to progression ($p=0.010$) and overall survival was even more significant ($p=0.007$) (Fig. 20B). Similar results were seen for *p53* mutations in DNA interacting regions (Fig. 20C). Furthermore, time to progression and overall survival were better in patients with normal *p53* expression as opposed to *p53* overexpression, but the results did not reach statistical significance ($p=0.071$, $p=0.056$ logrank) (Fig. 20D, Table 14, 15). In ovarian cancer cases with high *p53* overexpression (>78%) though, time to progression and overall survival were significantly shorter than in cases with low overexpression or normal *p53* expression ($p=0.043$, $p=0.020$ logrank). Overall, the most favourable prognosis in terms of overall survival was seen in patients who had wildtype *p53* sequence and normal *p53* expression as opposed to those, who had either one or both alterations of the *p53* gene and *p53* protein expression ($p=0.007$) (Fig. 20E,F).

4.1.10 Univariate and multivariable analysis of prognostic factors

Univariate analysis of time to progression identified *p53* mutations, *p53* alterations, residual disease, FIGO stage, histologic grade, age, lymph node status, and S-phase-fraction as prognostic factors. Multivariable analysis of time to progression identified only FIGO stage ($p=0.001$), residual disease ($p=0.005$) and age ($p=0.032$) as independent prognostic factors (Table 14).

Univariate analysis of overall survival identified residual disease, FIGO stage, age, grade, lymph node status and S-phase-fraction as prognostic factors besides *p53* mutation and *p53* alteration (Table 15). In multivariable analysis though, only residual disease ($p<0.001$), FIGO stage ($p=0.001$), grade ($p=0.009$), and patient age ($p=0.01$) were shown to be independent predictors of survival (Table 15).

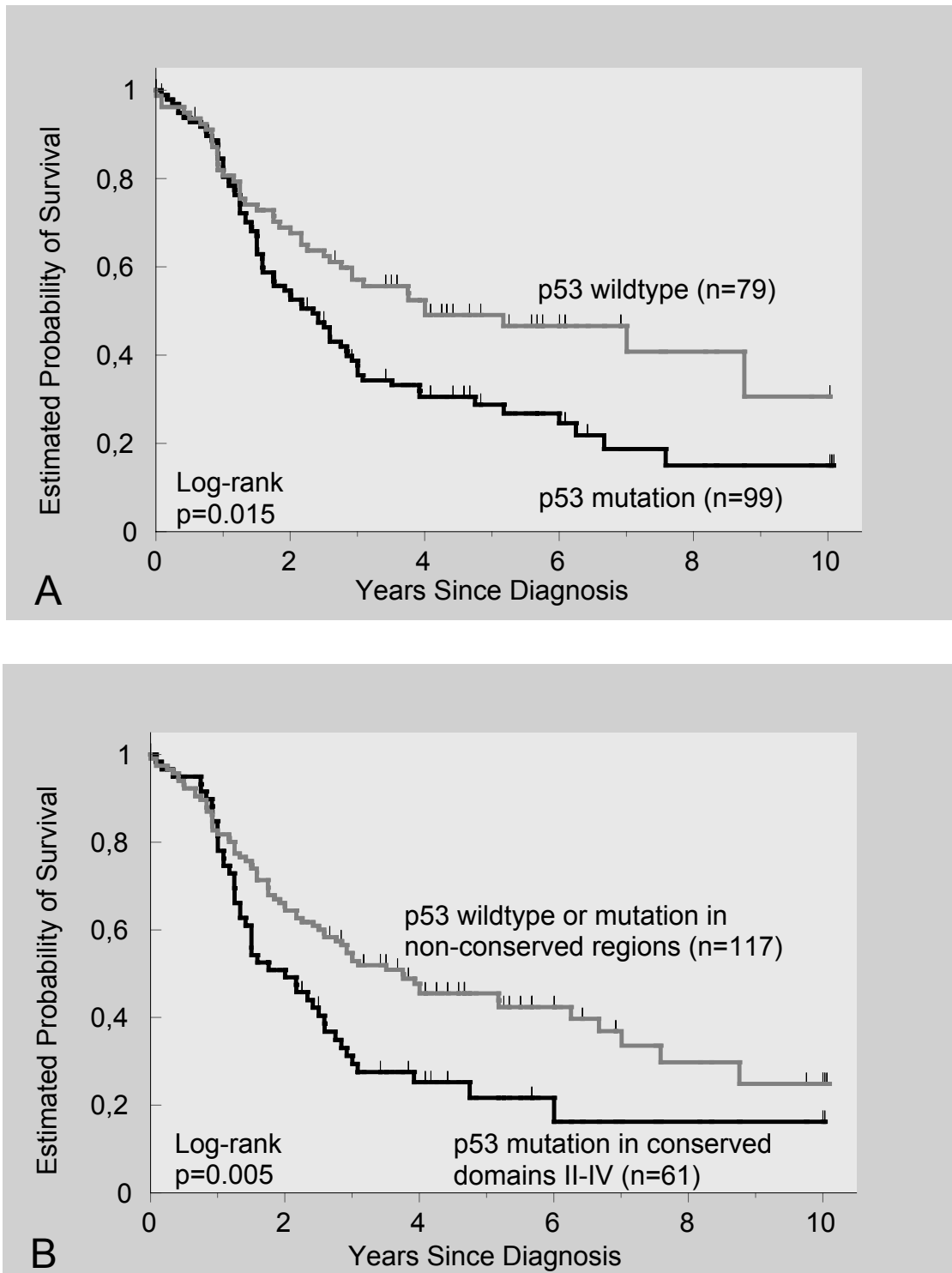


Fig. 20 A-B: Estimated probability of overall survival in patients with epithelial ovarian cancer (n=178) according to p53 alterations. (A) p53 mutations versus wildtype p53. (B) p53 mutations in evolutionary highly conserved domains versus wildtype p53 or mutations in non-conserved domains.

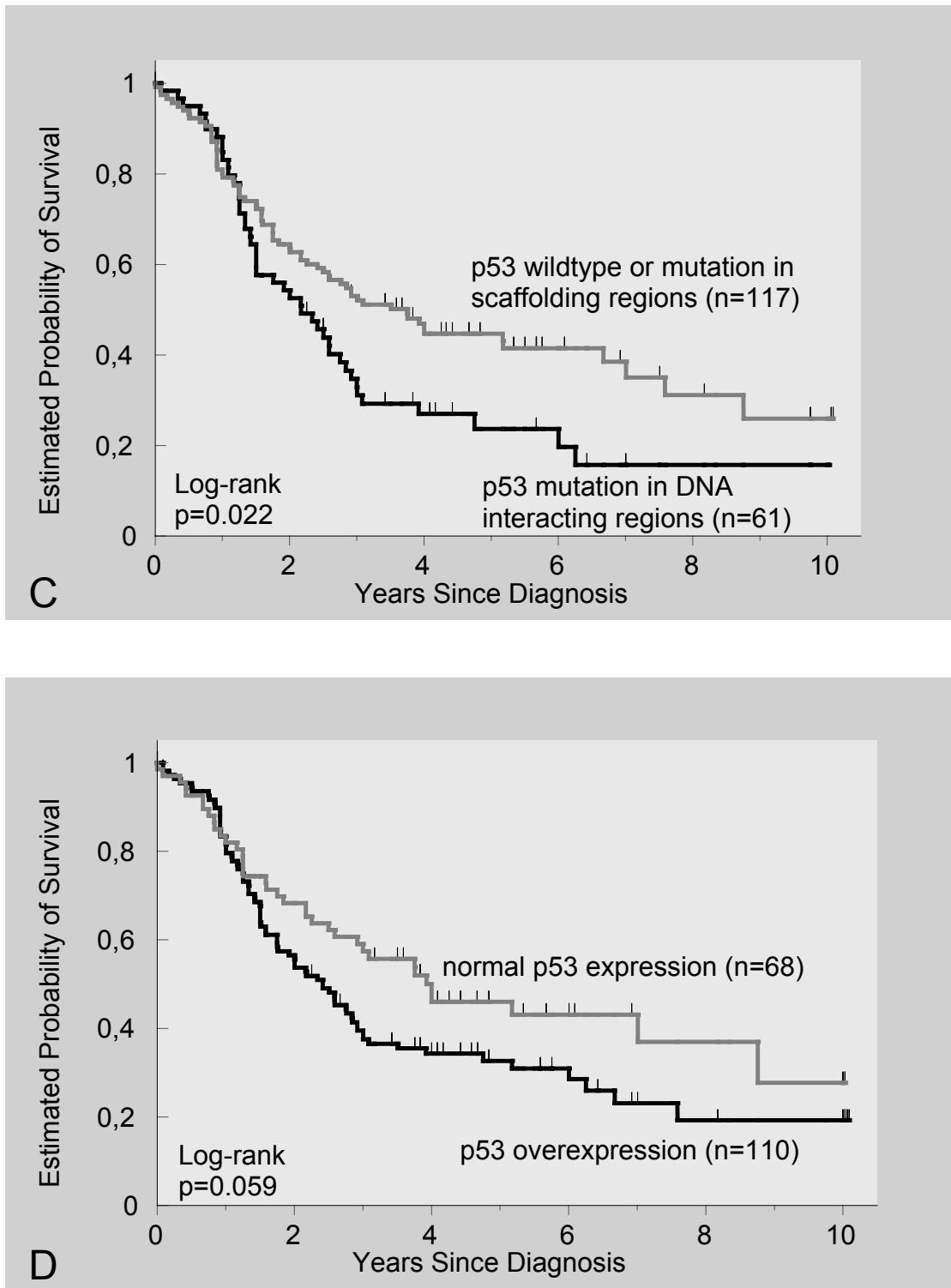


Fig. 20 C-D: Estimated probability of overall survival in epithelial ovarian patients (n=178) according to p53 alterations. (C) p53 mutations in DNA-interacting regions versus wildtype p53 or mutations in scaffolding regions of the p53 protein. (D) p53 protein overexpression versus normal expression of the p53 protein.

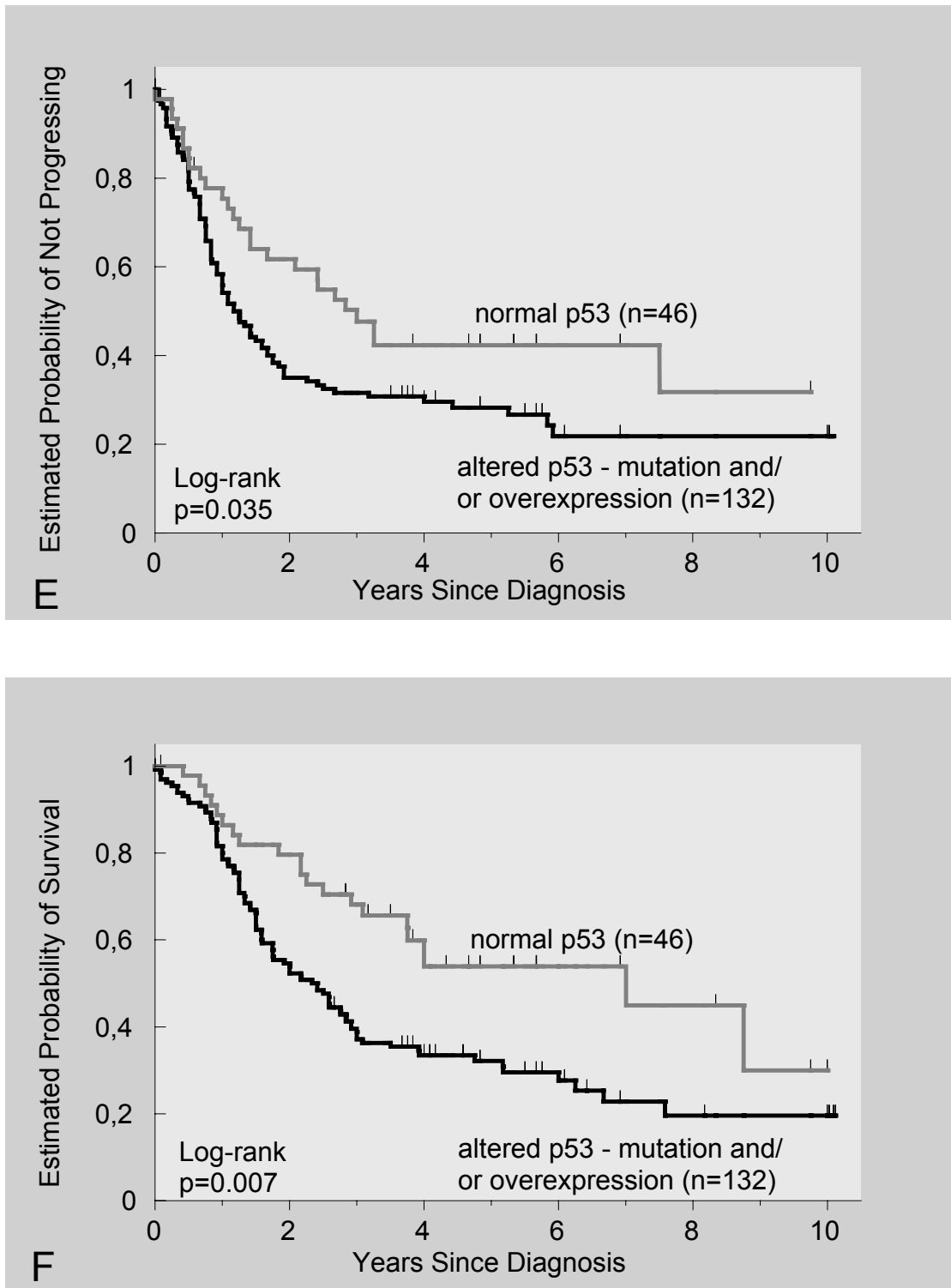


Fig. 20 E-F: Estimated probability of (E) not progressing, and (F) overall survival respectively in epithelial ovarian cancer patients (n=178). Ovarian cancer with p53 alterations (*p*53 mutation or p53 overexpression or both) versus normal p53 status.

Table 14: Multivariable proportional hazards Cox regression analysis for the identification of independent prognostic factors in time to progression of patients with ovarian carcinoma.

Variables	Univariate Analysis			Multivariable Analysis		
Variables in the Baseline Model *	Unadjusted Relative Risk	(95% CI)	p-value[1]	Adjusted Relative Risk	(95%CI)	p-value[2]
FIGO			< 0.001			0,001
I + II	1,00			1,00		
III + IV	6,08	(3.16, 11.71)		3,76	(1.70, 8.32)	
Residual Disease			< 0.001			0,005
None	1,00			1,00		
Any	3,89	(2.50, 6.06)		1,98	(1.19, 3.27)	
Histologic Grade			< 0.001			0,44
Well Differentiated	1,00			1,00		
Moderately	1,95	(0.99, 3.85)		1,23	(0.54, 2.81)	
Poorly	3,00	(1.58, 5.68)		1,52	(0.70, 3.34)	
The p53 Variables						
	Unadjusted Relative Risk	(95% CI)	p-value[1]	Adjusted Relative Risk	(95%CI)	p-value[2]
Immunostaining			0,071			0,67
No	1,00			1,00		
Yes	1,42	(0.96, 2.08)		1,10	(0.71, 1.69)	
Mutation			0,029			0,82
No	1,00			1,00		
Yes	1,51	(1.04, 2.20)		0,95	(0.62, 1.47)	
Alteration			0,030			0,59
No	1,00			1,00		
Yes	1,59	(1.03, 2.47)		1,15	(0.70, 1.90)	
Conserved Regions			0,010			0,47
Non Conserved/ WT p53	1,00			1,00		
Cons. Region II, III, IV, V	1,66	(1.14, 2.42)		1,17	(0.77, 1.79)	
% p53 IM (continuous)			0,13			0,40
0	1,00			1,00		
10	1,03	(0.99, 1.08)		0,98	(0.93, 1.03)	
20	1,07	(0.98, 1.16)		0,96	(0.87, 1.05)	
50	1,18	(0.95, 1.46)		0,90	(0.71, 1.14)	
Other Variables of Interest						
	Unadjusted Relative Risk	(95% CI)	p-value[1]	Adjusted Relative Risk	(95%CI)	p-value[2]
Age [0]			0,019			0,032
50	1,00			1,00		
60	1,19	(1.03, 1.38)		1,21	(1.02, 1.44)	
70	1,42	(1.06, 1.90)		1,46	(1.04, 2.06)	
Metastasis			0,057			0,63
None	1,00			1,00		
Any	1,82	(1.02, 3.23)		1,16	(0.63, 2.15)	
Lymph Node Status			< 0.001			0,31
Free of Tumor	1,00			1,00		
Infiltrated	4,84	(2.00, 11.73)		1,91	(0.76, 4.76)	
Not Resected	3,57	(1.54, 8.29)		1,84	(0.76, 4.44)	
Histology			0,18			0,37
Serous	1,00			1,00		
Other	0,76	(0.51, 1.14)		1,23	(0.78, 1.95)	
S-Phase			0,006			0,54
0.0 - 4.9%	1,00			1,00		
5.0 - 14.4%	1,76	(0.83, 3.77)		1,44	(0.54, 3.84)	
14.5% +	3,29	(1.51, 7.18)		1,79	(0.61, 5.25)	
Ploidy			1,00			0,45
Diploid	1,00			1,00		
Tetraploid / Aneuploid	1,00	(0.60, 1.68)		0,79	(0.43, 1.46)	

* Based on a previous analysis, FIGO, residual disease, and histologic grade were selected for the baseline model

[0] Age, in years, fit as a continuous variable.

[1] P-values based on the likelihood ratio of the univariate model with no other variables.

[2] P-values based on the likelihood ratio with the variables included in the baseline model: FIGO, residual disease, and histologic grade.

Table 15: Multivariable proportional hazards Cox regression analysis for the identification of independent prognostic factors in overall survival of patients with ovarian carcinoma.

Variables	Univariate Analysis			Multivariable Analysis		
Variables in the Baseline Model *	Unadjusted Relative Risk	(95% CI)	p-value[1]	Adjusted Relative Risk	(95%CI)	p-value[2]
FIGO			< 0.001			0,002
I + II	1,00			1,00		
III + IV	6,98	(3.51, 13.87)		3,59	(1.49, 8.66)	
Residual Disease			< 0.001			< 0.001
None	1,00			1,00		
Any	4,77	(3.00, 7.58)		2,44	(1.46, 4.09)	
Histologic Grade			< 0.001			0.009
Well Differentiated	1,00			1,00		
Moderately	3,99	(1.67, 9.50)		3,26	(1.13, 9.43)	
Poorly	5,95	(2.58, 13.71)		3,87	(1.37, 10.88)	
The p53 Variables	Unadjusted Relative Risk	(95% CI)	p-value[1]	Adjusted Relative Risk	(95%CI)	p-value[2]
Immunostaining			0.056			0.73
No	1,00			1,00		
Yes	1,45	(0.98, 2.14)		1,08	(0.70, 1.67)	
Mutation			0.014			0.49
No	1,00			1,00		
Yes	1,59	(1.09, 2.33)		0,86	(0.55, 1.33)	
Alteration			0.005			0.47
No	1,00			1,00		
Yes	1,88	(1.18, 3.00)		1,21	(0.72, 2.05)	
Conserved Regions			0.007			0.8
Non Conserved / WT	1,00			1,00		
Cons. Regions II,III,IV,V	1,70	(1.17, 2.47)		1,06	(0.69, 1.61)	
Im p53 (continuous)			0.056			0.64
0	1,00			1,00		
10	1,04	(1.00, 1.09)		0,99	(0.94, 1.04)	
20	1,09	(1.00, 1.19)		0,98	(0.89, 1.07)	
50	1,23	(0.99, 1.53)		0,95	(0.75, 1.20)	
Other Variables of Interest	Unadjusted Relative Risk	(95% CI)	p-value[1]	Adjusted Relative Risk	(95%CI)	p-value[2]
Age [0]			0.003			0.005
50	1,00			1,00		
60	1,26	(1.08, 1.46)		1,29	(1.08, 1.55)	
70	1,58	(1.17, 2.14)		1,67	(1.17, 2.40)	
Metastasis			0.062			0.6
None	1,00			1,00		
Any	1,77	(1.01, 3.10)		1,18	(0.64, 2.17)	
Lymph Node Status			0,001			0,54
Negative	1,00			1,00		
Positive	4,20	(1.82, 9.68)		1,54	(0.64, 3.71)	
Not Resected	3,13	(1.42, 6.87)		1,26	(0.54, 2.94)	
Histology			0.021			0.9
Serous	1,00			1,00		
Other	0,78	(0.52, 1.16)		1,03	(0.65, 1.64)	
S-Phase-Fraction			0.001			0.72
0.0 - 4.9%	1,00			1,00		
5.0 - 14.4%	2,75	(1.13, 6.68)		1,47	(0.43, 5.07)	
14.5% +	4,88	(1.95, 12.17)		1,68	(0.46, 6.19)	
DNA-Ploidy			0.24			0.37
Diploid	1,00			1,00		
Tetraploid / Aneuploid	1,38	(0.80, 2.37)		1,33	(0.71, 2.51)	

* Based on a previous analysis, FIGO, residual disease, and histologic grade were selected for the baseline model

[0] Age, in years, fit as a continuous variable.

[1] P-values based on the likelihood ratio of the univariate model with no other variables.

[2] P-values based on the likelihood ratio with the variables included in the baseline model: FIGO, residual disease, and histologic grade.

4.2 Alterations of the *mdm2* gene in ovarian cancer

4.2.1 Expression and absence of amplification of *mdm2* in ovarian carcinomas

Fifty-six ovarian cancer cases were analyzed by Southern hybridization for *mdm2* DNA-amplification. The osteosarcoma cell line SA1 which is known to have amplification and overexpression of *mdm2* was used as a control (Fig. 21). Fifty-two ovarian cancer cases did not show amplification of the *mdm2* gene, independently of *p53* mutations and/or overexpression. In four cases, the result could not be interpreted. All cases had been previously sequenced and analyzed for *p53* protein overexpression. In 21 of these cases, *p53* wildtype had previously been found. Thirteen of these 21 cases showed *p53* overexpression despite the wild type sequence. In 30 cases, *p53* was mutated, 26 of which also showed protein overexpression.

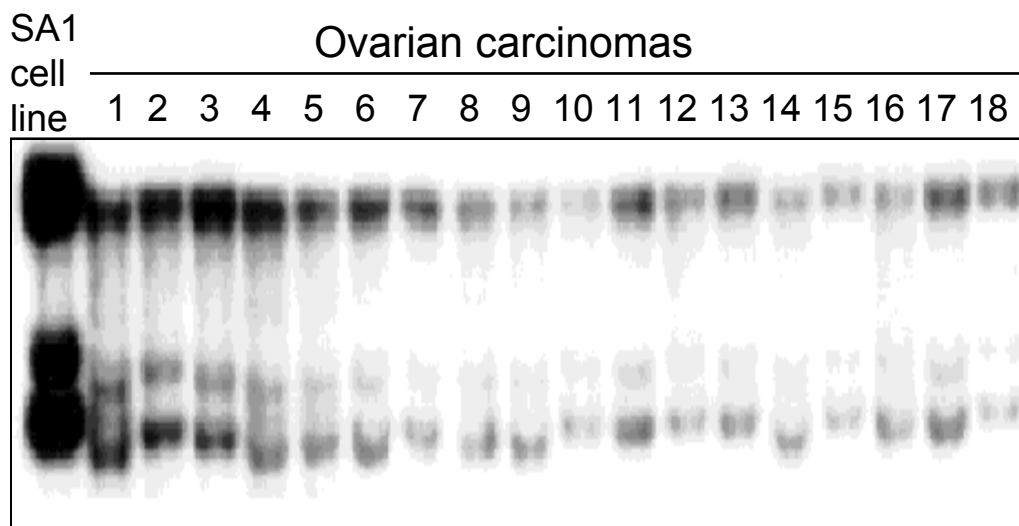


Fig. 21: Southern hybridization of genomic DNA with the *mdm2* cDNA probe. The sarcoma cell line SA1 which was used as a positive control shows amplification of *mdm2* DNA, while none of the ovarian cancer tissues shows DNA amplification.

mdm2-expression was also analyzed by Northern hybridization in 29 ovarian cancer cases (Fig. 22). Only the sarcoma cell line SA1 but none of the ovarian cancer cases showed overexpression of the *mdm2* gene. In the sarcoma cell line as well as all ovarian cancers, three different mRNA transcripts of 7.4 kb, 5.5 kb and 2.8 kb were seen. Ten ovarian cancer cases had previously been shown to have wildtype *p53*, of which six overexpressed *p53* as detected by immunohistochemistry. The remaining 19 cases had been identified to have a *p53* mutation, 16 of which also showed protein overexpression.

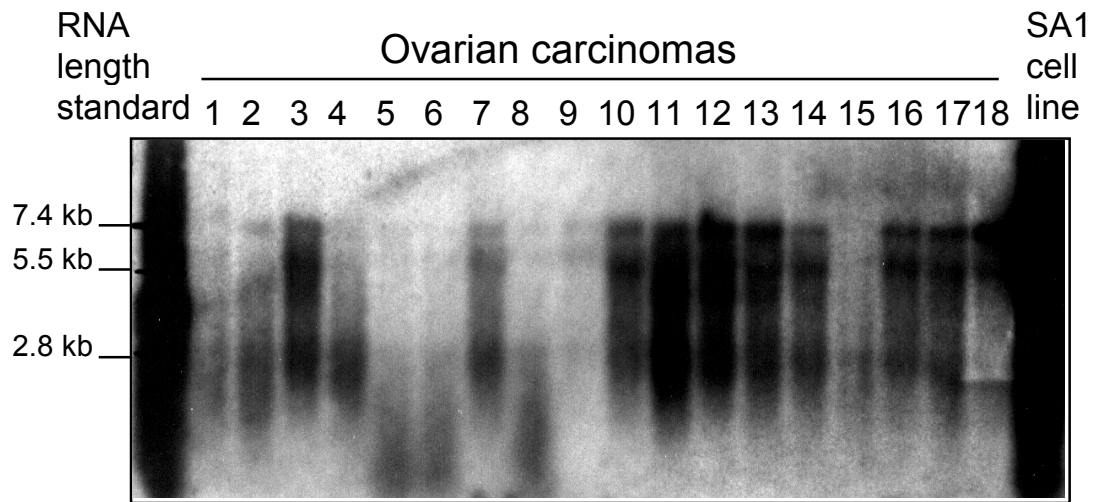


Fig. 22: Northern hybridization of total mRNA with the *mdm2* cDNA probe. The sarcoma cell line SA1 which was used as a positive control shows overexpression of *mdm2* RNA, while none of the ovarian cancer tissues shows *mdm2* overexpression.

4.2.2 *mdm2* alternative and aberrant RNA splicing in ovarian carcinomas

PCR analysis of the reverse transcribed mRNA revealed the presence of the expected full length (1473) bp product of *mdm2* as well as other, smaller products (Fig. 23). Among 92 cases analyzed, 76 (83%) had a full length 1473 bp RT-PCR product, in some cases only weakly expressed. Only 18 cases (20%) had exclusive expression of the normal *mdm2* full length cDNA, while 58 cases (63%) had both the 1473 bp product and smaller RT-PCR products (Table 16). Eight cases (9%) showed no *mdm2* expression despite repeated RT-PCR analysis.

Amplification of the human *β 2-Microglobulin* gene, a member of the immunoglobulin gene superfamily, which is represented on the surface of nearly all cells (Güssow et al. 1987), was used as a control for integrity and equal amounts of RNA respectively cDNA. PCR analysis of the *β 2-Microglobulin* showed strong expression in all normal ovarian tissues and all ovarian carcinomas (Fig. 24).

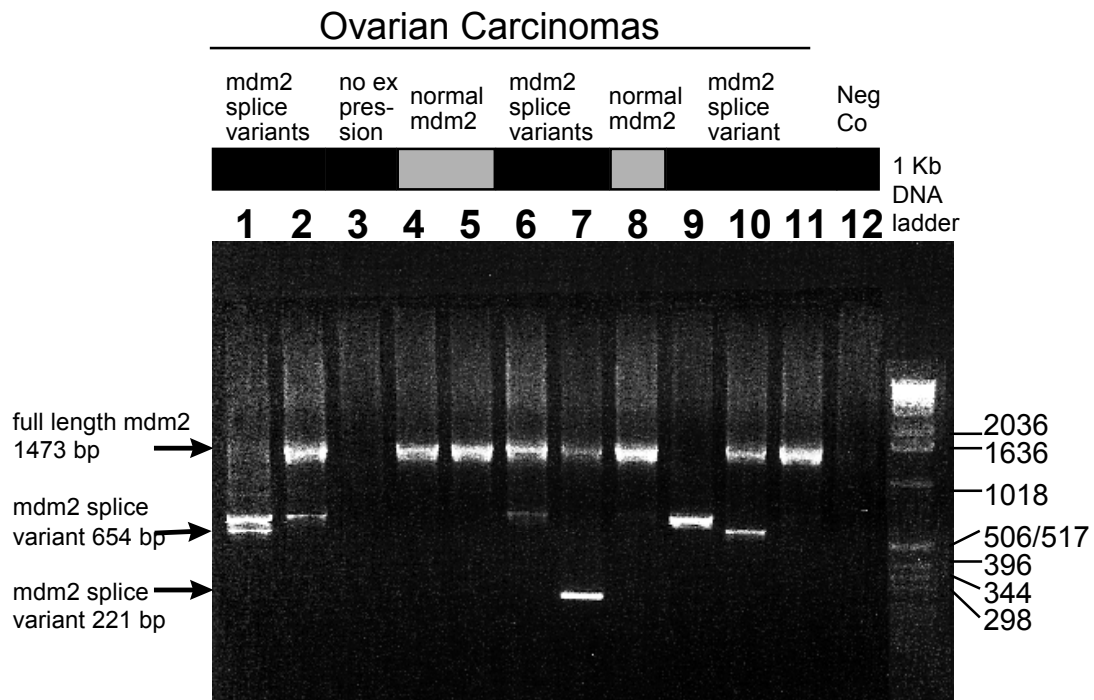


Fig. 23: *mdm2* RNA splice variants in ovarian carcinomas. Total RNA was ana-lyzed by RT-PCR, and PCR-products were separated on a 1.2% agarose gel. Cases in lanes 1,2,6,7,9, and 10 show splice variants of different sizes. The case in lane 3 shows no *mdm2* expression. (cDNA bands on the gel contain additional 53 bp of flanking primer sequence)

Table 16: *mdm2* RNA splicing in ovarian cancer as analyzed by reverse transcriptase PCR and DNA Sequencing

RT-PCR result in ovarian carcinomas	n (%)	n (%)
<u>normal <i>mdm2</i> only</u>	18 (20)	
<u>normal <i>mdm2</i> and splice variants</u>	58 (63)	
normal <i>mdm2</i> / <i>mdm2</i> -b		26 (28)
normal <i>mdm2</i> / <i>mdm2</i> -b / <i>mdm2</i> 221		1 (1)
normal <i>mdm2</i> / <i>mdm2</i> 221		8 (9)
normal <i>mdm2</i> / other splice variants		23 (25)
<u>splice variants only / no normal <i>mdm2</i></u>	8 (9)	
<i>mdm2</i> -b only		3 (3)
other splice variants only		5 (5)
<u>no <i>mdm2</i> expression</u>	8 (9)	
Total	92 (100)	

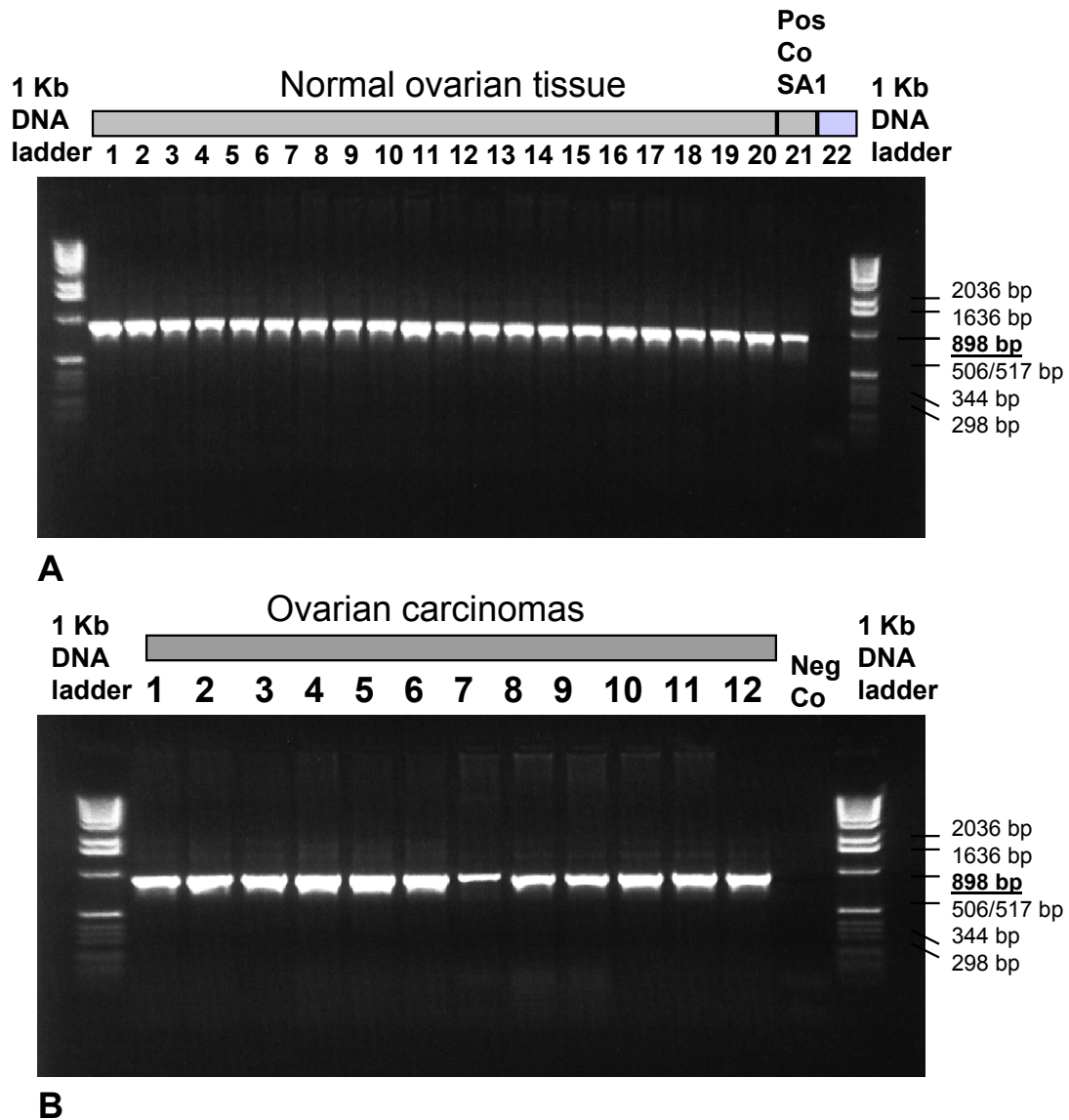


Fig. 24: A-B: RT-PCR for $\beta 2$ microglobulin as a positive control for quality and amount of RNA. (A) RNA was extracted from normal ovarian tissue. All cases show equal amplification of a 898 bp $\beta 2M$ PCR product. Lane 21 shows the PCR product of cDNA from the SA1 sarcoma cell line. Lane 22 is the negative control. **(B)** RT-PCR for $\beta 2$ microglobulin expression in ovarian cancer RNA. Except for case #2341 in lane 7 all cases show approximately equal expression of the $\beta 2$ microglobulin RNA.

Out of those cases which showed an approximately 700 bp band on the agarose gel, six ovarian cancer cases, one borderline tumor, and one normal ovarian tissue were sequenced and the 654 bp splice variant was confirmed. The typical approximately 290 bp band on the agarose gel was confirmed as the 221bp splice variant in 8 ovarian carcinomas, four tumors of borderline malignancy, one cystadenoma, and four normal ovarian tissues.

The *mdm2* splice variant which we found most frequently was a 654 base *mdm2* cDNA. We found this splice variant in 38 (41%) ovarian cancer cases. It comprises 654 bp of the open reading frame and splices out exon 4-11 (Fig. 23, Table 17). The 654 bases fragment misses a large portion of the mRNA, including 90% (81 of 90 amino acids) of the 3' end of the p53 binding domain, and the entirety of the nuclear localization signal and acidic domain (Fig. 25). This splice variant had been named *mdm2-b* by Sigalas et al. (1996) and was described as a 707 bp product, since he included the primer sequence which is outside the open reading frame of *mdm2* into the numbering (Sigalas et al. 1996). We named the fragment 654 bp, because we counted only those bases between the start and the stop codon, but not the primers.

Another splice variant, which has been named *mdm2-a* (Sigalas et al. 1996) splices out exon 4 through 9 and spans 888 basepairs of the open reading frame (Fig. 25, Table 17). This variant was seen in 4 cases (4 %). In both of these variants splicing takes place at the exon/intron boundary and the truncated RNA is in frame.

In contrast to this in a small splice variant of 221 bp, which was seen in 15 cases (16%), splicing did not take place at the exon/intron boundary. We identified three variations of this splice variant (Table 17).

We identified a total of 30 different splice variants. Fourteen of these (47%) were only seen in ovarian carcinomas, while seven were identified both in ovarian cancer and other histologies. Seven were seen only in borderline tumors or cystadenomas, and two splice variants were found exclusively in normal ovarian tissue. Most of these splice variants should be classified as aberrant splicing because they splice out parts of exon sequences (Table 17).

In only three splice variants of 888 bp (*mdm2-a*), 654 bp (*mdm2-b*) and 613 bp, donor and acceptor splice site were found at exon-intron boundaries. The *mdm2-a* splice variant splices out exon 4 through exon 9 and the *mdm2-b* splice variant splices out exon 4 through exon 11. In the 613 bp splice variant the entire exon 5 is spliced out the exon/intron boundaries as well as part of exon 9, exon 10, exon 11, and part of exon 12 (Table 17). In the splice variants of 446 bp, 397 bp, 391 bp, 365 bp, 357 bp, and 351 bp length, the donor splice site is at the exon/intron-boundary of exon 4, 5 or 6, while the acceptor splice site is an internal splice site in exon 12. The splice variants of 391 bp and 357 bp splice out exon 5-11 and part of exon 12, the splice variants of 397 bp and 351 bp splice out exon 6-11 and part of exon 12, and the splice variants of 446 bp and 365 bp splice out exon 7-11 and part of exon 12.

All other splice variants would be considered aberrant splicing since they have a donor splice site internally in exon 3-10 and an acceptor splice site internally in exon 12. Except for the *mdm2-a* splice variant, exon 11 is generally spliced out.

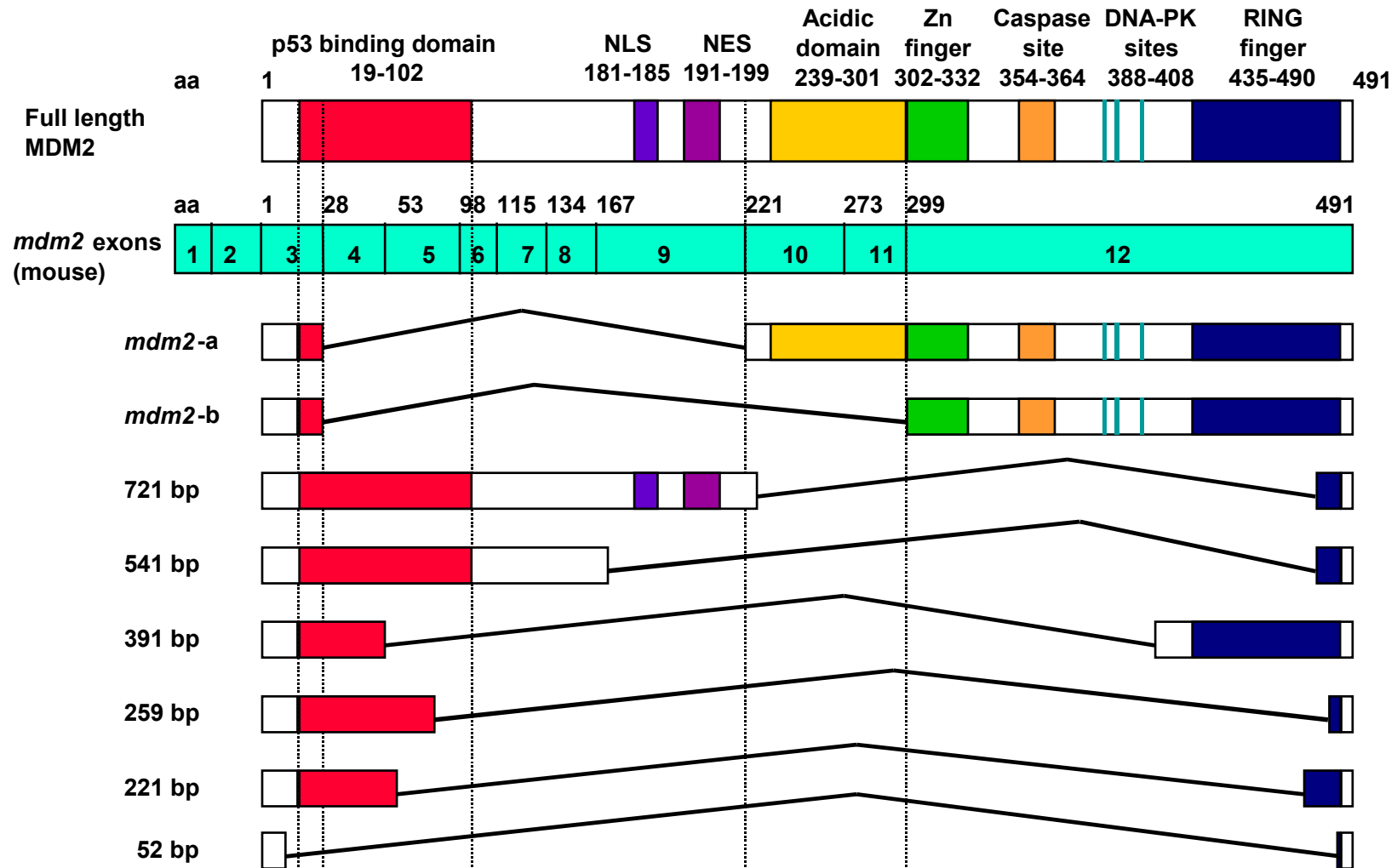


Fig. 25: Loss of functional regions in *mdm2* splice variants in comparison to the full length *mdm2* gene Above, functional domains of the MDM2 protein with corresponding amino acid residues are shown (according to Freedman et al. 1999). Below, splice variants of the *mdm2* gene are shown. Black lines indicate the missing part of the sequence.

Table 17: mdm2 RNA splice variants in ovarian cancer identified by RT-PCR and DNA sequencing. The table shows sizes of splice variants, splice sites and tissues in which the splice variant was identified. (First nucleotide of coding sequence is #312, last nucleotide of coding sequence is #1784). The length of the splice variants includes only the coding sequence but not the flanking primer sequence. (> indicates exon/intron boundary and < indicates intron/exon boundary)

Size of splice variant	p53 binding site	Donor splice site nucleotide #	Donor splice site exon	Splice site sequence		Acceptor splice site exon	Acceptor splice site (nucleotide #)	Overlap	Frame	Splice variant identified in			
				Donor	Acceptor					Ov Ca	LMP	Cystade - noma	NL Ovary
888	partial	392	ex 3 >	GAG ACC CTG	---- <u>G</u> AT CTT GAT	< ex 10	978	G	in frame	+	-	-	-
721	complete	1007	cryptic ex 10	AGT GAA <u>CAT TCA</u>	---- A ATG ATT	cryptic ex 12	1760	ATTCA	shift (+A..)	+	-	-	-
654	partial	392	ex 3 >	GAG ACC CTG	---- GAC TAT TGG	< ex 12	1212	G	in frame	+	+	-	+
613	partial	467 and 856	ex 4 > and cryptic ex 9	ATG AAA <u>GAG</u>	---- <u>G</u> AAA ATA	< ex 6	602	AGG	shift (+G)	-	-	+	-
	partial	856	cryptic ex 9	<u>CGA CAA AGA A</u>	---- GAC AAA GAA	cryptic ex 12	1581	GACAAAGAA	shift (+A)				
571	complete	879	cryptic ex 9	GAT AGT <u>ATT T</u>	---- C CCC	cryptic ex 12	1781	TATTT	shift (+T,+C)	+	-	-	-
565	complete	807	cryptic ex 8	AGA GCA ATT <u>A</u>	---- AAG AAA AGG	cryptic ex 12	1716	TA	shift (+A)	+	-	-	-
541	complete	827	cryptic ex 9	GAA <u>AAT TCA</u>	---- A ATG ATT GTG	cryptic ex 12	1760	AATTCA	shift (+A)	+	-	-	-
533	partial	407	cryptic ex 4	ACC <u>AAA GCC A</u>	---- AA CTG GAA	cryptic ex 12	1348	AAAGCCA	in frame	+	-	-	-
520	partial	596	cryptic ex 5	CTC <u>TGT GAA GAG</u>	---- TTT GAA AGG	cryptic ex 12	1550	TGTGAAGAG	in frame	-	-	+	-
461	partial	510	cryptic ex 5	AAA CGA <u>TTA T</u>	---- T TAT AGC AGC	cryptic ex 12	1523	ATTAT	shift (+TT)	+	-	-	-
446	complete	650	ex 6 >	AAT CAG <u>CAG</u>	---- <u>GA</u> CAT CTT ATG	cryptic ex 12	1678	CAGGA	shift (+GA)	-	+	-	-
442	partial	453	cryptic ex 4	AAA GAC ACT <u>T</u>	---- GAA GAC TAT	cryptic ex 12	1485	T	shift (+T)	-	-	-	+
421	complete	627	cryptic ex 6	ATC TAC AGG <u>A</u>	---- CAT CTT ATG	cryptic ex 12	1680	ACAGGA	shift (+A)	+	-	-	-
421	complete	683	cryptic ex 7	GTG AGT GAG	---- C CCA GTA TGT	cryptic ex 12	1736	G	shift (+C)	-	-	+	-
397	partial	601	ex 5 >	GAG <u>CAC AG</u>	---- <u>GA</u> CAT CTT ATG	cryptic ex 12	1678	ACAGGA	shift (+GA)	+	-	-	-
391	partial	467	ex 4 >	ATG AAA GAG	---- TTT GAA GGG	cryptic ex 12	1551	TGAAAGAG	in frame	+	-	+	-
378	partial	408	cryptic ex 4	CCA <u>AAG CCA</u>	---- <u>TCA</u> ACT TCT	cryptic ex 12	1504	AGCCAT	in frame	+	-	-	-
365	complete	651	ex 6 >	AAT CAG CAG G	---- <u>AATG</u> ATT GTG	cryptic ex 12	1760-	AAT	shift (+GA)	-	-	-	+

357	partial	467	ex 4 >	ATG <u>AAA GAG</u> ---- AGT GTG GAA	cryptic ex 12	1584	AAGAG	in frame	-	+	-	-
351	partial	601	ex 5 >	GAG CAC <u>AG</u> ---- <u>G AAT</u> AAG CCC	cryptic ex 12	1724	AGGAA	in frame	+	-	-	-
334	partial	597	cryptic ex 5	GTG AAA <u>GAG C</u> CCA GTA TGT AGA	cryptic ex 12	1737	GC	(shift+C)	-	+	-	-
282	partial	522	cryptic ex 5	GAT <u>GAG AAG C</u> ---- TA AAGAAA	cryptic ex 12	1714	AGAAGC	in frame	-	+	-	-
279	partial	514	cryptic ex 5	CGA TTA TAT <u>GA</u> ---- G AAG CTA AAG	cryptic ex 12	1712	A	in frame	+	-	-	+
267	partial	447	cryptic ex 4	GCA CAA AAA <u>G</u> ---- GT TGC ATT AGA	cryptic ex 12	1654	G	in frame	+	-	-	-
266	partial	410	cryptic ex 4	<u>AAG CCA TTG</u> ---- AA CCT TGT	cryptic ex 12	1618	AGCCATTG	shift (+AA)	+	-	-	-
259	partial	551	cryptic ex 5	<u>TGT TCA AAT GAT</u> ---- T GTG CTA ACT	cryptic ex 12	1766	TTCAAATGAT	shift (+T)	+	-	-	+
221	partial	483	cryptic ex 5	TAT CTT <u>G</u> ---- C CCA GTA	cryptic ex 12	1736	TG	shift (+GC)	+	+	+	+
221	partial	484	cryptic ex 5	TAT CTT <u>GGC</u> ---- <u>C</u> CA GTA	cryptic ex 12	1737	GCC	shift (+GC)	+	-	-	-
221	partial	491 484	cryptic ex 5	TAT CTT GG <u>C CAG TAT</u> ---- GT AGA CAA or TAT CTT GG ---- <u>CCA GTA</u> TGT AGA	cryptic ex 12	1744 1737	CCAGTAT	shift (+GT)	+	-	-	+
150	partial	455	cryptic ex 4	GAC <u>ACT TAT</u> ---- TTC CCC	cryptic ex 12	1779	ACTTAT	in frame	+	+	-	-
77	absent	338	cryptic ex 3	TCT GTA <u>CCT</u> ---- GC CCA GTA	cryptic ex 12	1735	CCT	shift (+GC)	+	-	-	-
52	absent	350	cryptic ex 3	GAT <u>GGT GCT</u> ---- A ACT TAT	cryptic ex 12	1772	GTGCT	shift (+A)	+	-	-	+

4.2.3 Loss of p53 binding sequence in *mdm2* splice variants

The binding site of the p53 protein has been suggested to be a region of approximately 84 amino-acids between aa 19-102 of the MDM2 protein (Chen et al. 1993). This corresponds to base 366-617 of the *mdm2* sequence. Out of 30 splice variants which had been identified in ovarian tumors and normal ovarian tissue, only 8 splice variants (27%) contained the complete p53 binding sequence, while 20 (67%) had only a partial sequence and 2 (7%) of the splice variants were missing the entire p53 binding site (Table 18, Fig. 25). The most frequent splice variant of 654 bp length (*mdm2*-b) contains only 9 out of 84 amino acids of the p53 binding site, while the 221 bp splice variant contains 39 amino acids of the binding site.

Table 18: Loss of p53 binding sequence in *mdm2* splice variants

p53 binding site in <i>mdm2</i> splice variants	n (%)	size of splice variant (bp)
Complete p53 binding site	8 (27%)	721,571, 565,541,446,421,421,365
Partial p53 binding site	20 (67%)	888,654,613,533,520,461,442,397,391,378, 357,351,334,282,279,267,266,259,221,150
Loss of p53 binding site	2 (7%)	77,52
30 (100%)		

4.2.4 *mdm2* splice sites and repeat sequences

Many of the splice variants show an interesting pattern of splicing, because the donor and acceptor sites are in regions of exact sequence homology (Fig. 26). For example in the 391 bp splice variant, which was seen in carcinomas as well as in benign tissues, the 3' end of the donor site ends with an eight base sequence of TGAAAGAG which is also found at the non-transcribed downstream acceptor splice site in exon 12 (Fig. 26). The acceptor splice site sequence would be tgaagagTTTGAAAGG. (The underlined sequence indicates the exact sequence match. The uppercase letters indicate the coding bases).

In the 221 bp splice variant, the splice site showed sequence overlaps with minor variations in different cases which are shown in Table 17 and Fig. 26. Similar sequence matches, mostly 2 to 10 bases long, were found in the majority of the splice variants.

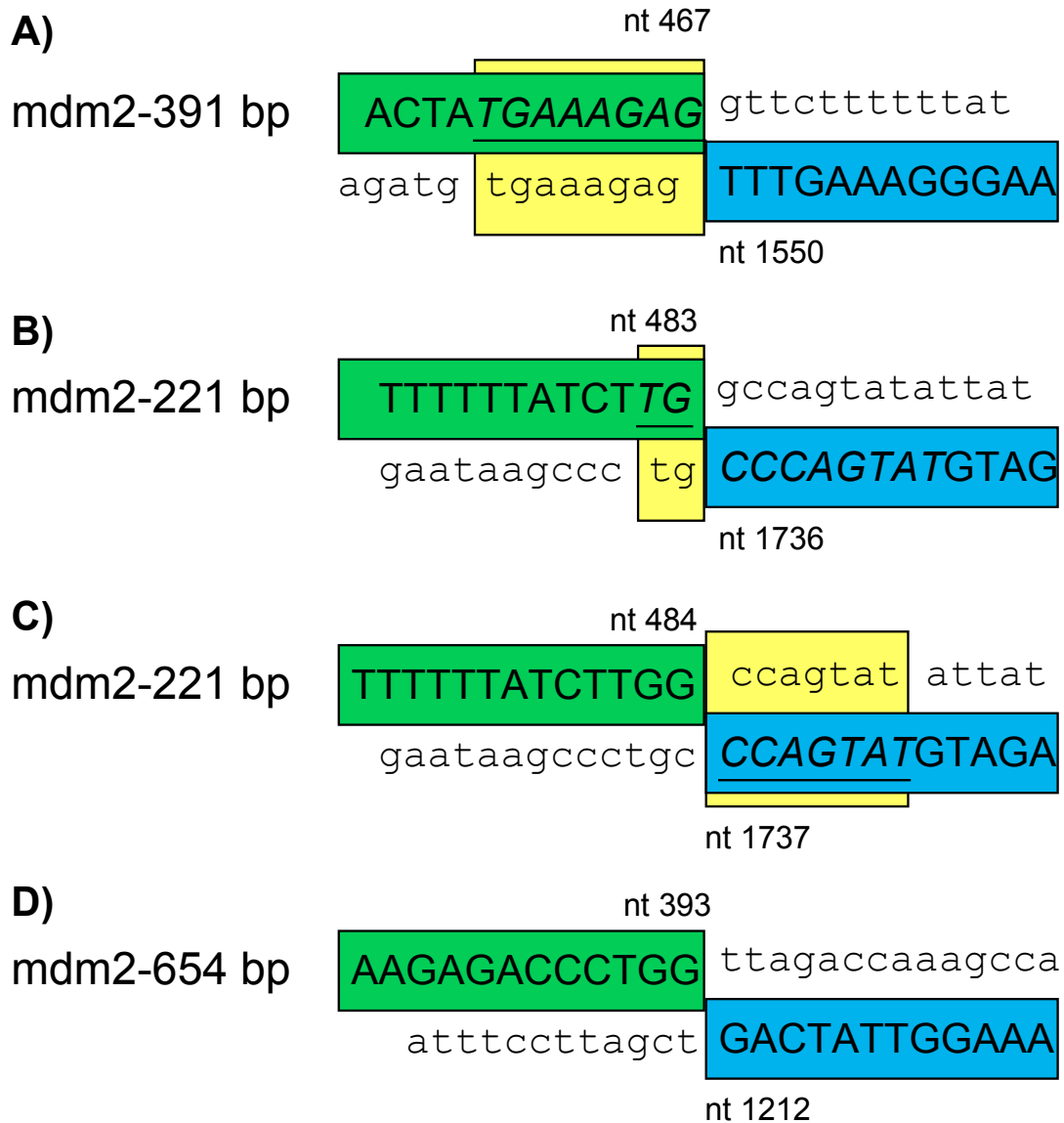


Fig. 26: A-D: Sequence overlaps in *mdm2* RNA splice variants. (A-C) Splice site sequences of the 391 bp and 221 bp *mdm2* splice variants show overlaps of several basepairs. The capital letters refer to transcribed bases that remain in the final mRNA products, while the lower case letters refer to untranscribed bases which are spliced out of the final mRNA product. The green boxes enclose the transcribed sequence at the donor site and the blue boxes enclose the transcribed sequence at the acceptor site. The yellow boxes indicate sequence homologies. **D)** As opposed to many of the aberrant splice variants which show overlapping sequences at the splice site, no such sequence homology is notable in the 654 bp *mdm2*-b splice variant which splices at exact exon/intron boundaries of exon 3 and exon 12.

Interestingly, the acceptor splice site of the 221 bp splice variant (nucleotide 1737) was shared by four different splice variants of 421 bp, 334 bp, 22 bp and 77 bp length (Table 17). The same phenomenon was observed for other splice variants which used the exact same sequence in exon 12 as acceptor site. The sequence match in all three cases comprises a CAGGA sequence. The 446 bp splice variant has the donor site at the exon 6/intron 6 boundary with an AAT CAG CAG gaa tca tcg sequence and splices into exon 12 at base 1678 with a ggc aaa aca gGA CAT CTT ATG sequence.

The 421 bp splice variant has a donor site in exon 6 with an ATC TAC AGg aac ttg gta sequence and splices into exon 12 at base 1678 with the same ggc aaa aca gGA CAT CTT ATG sequence. And the 397 bp splice variant has the donor site at the exon 5/intron 5 boundary with a GAG CAC AGg aaa ata tat sequence and splices into the identical acceptor site in exon 12 (Table 17). All three splice variants are out of frame. The donor sites were shared among the splice variants 888 (*mdm2*-a) and 654 (*mdm2*-b) (nucleotide 392), 613, 391, and 357 (nucleotide 467), and 397 and 351 (nucleotide 601).

Twelve of the thirty splice variants with a cDNA length between 888 and 150 bp were in frame, while all others were out of frame and therefore, either no protein or only a truncated protein will be synthesized.

4.2.5 *mdm2* alterations in ovarian cystadenomas and borderline tumors

RNA from six benign cystadenomas and nine ovarian tumors of low malignant potential (LMP) was analyzed by RT-PCR for *mdm2* alterations (Table 19 and 20, Fig. 27). Except for one cystadenoma which was completely lacking *mdm2* expression, all other cystadenomas showed the full length *mdm2* as well as splice variants (Table 19). None of the cases had only a full length *mdm2* transcript. The 221 bp splice variant, which had been described for ovarian carcinomas, was seen in one case. Four other cystadenomas, though, showed splice variants which had not been found before in the ovarian cancer cases. The length of these splice variants was 613, 520, 421 and 390 basepairs. The *mdm2*-b splice variant of 654 bp, which is frequent in ovarian carcinomas, was not seen in any of the cystadenomas.

Among the nine borderline ovarian tumors (Table 20), only one case was found to have only the full length *mdm2* cDNA and one case had no *mdm2* expression. The other seven cases showed *mdm2* alternative splicing, which was seen in six cases, in addition to the normal length *mdm2*, and in one case as the only *mdm2* cDNA.

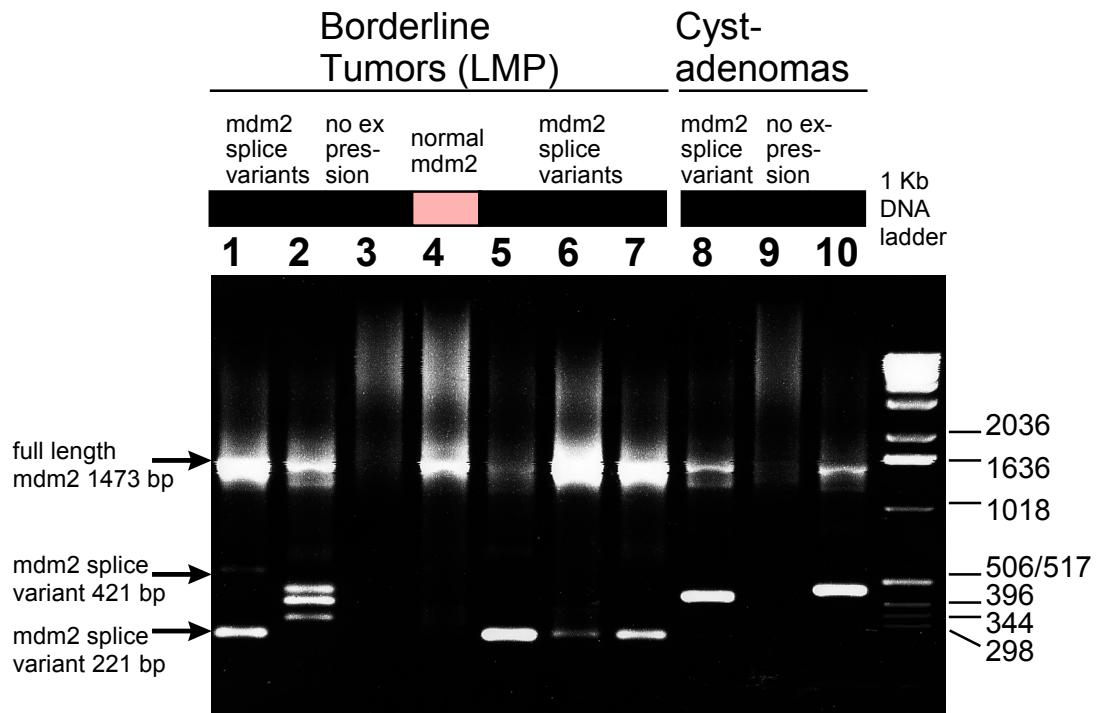


Fig. 27: *mdm2* RNA splice variants in ovarian cystadenomas and tumors of borderline malignancy. Total RNA was analyzed by RT-PCR and PCR-products were

separated on a 1.2% agarose gel. Cases in lanes 1, 2, 5-8, and 10 show splice variants of different sizes. The case in lane 3 shows no *mdm2* expression despite normal expression of the β 2-microglobulin control gene. (cDNA bands on the gel contain additional 53 bp of flanking primer sequence).

Table 19: *mdm2* alternative and aberrant splicing in benign ovarian cystadenomas

Case ID #	Diagnosis at surgery	full length <i>mdm2</i>	<i>mdm2</i> -b 654 bp	<i>mdm2</i> 221 bp	other splice variants
2305	serous cystadenoma	+	-	+	-
2539	serous cystadenoma	-	-	-	-
2771	serous cystadenoma	+	-	-	421
3456	serous cystadenoma	+	-	-	613
3457	mucinous cystadenoma	+	-	-	391
3462	serous cystadenoma	+	-	-	520
n (%)		5 (83)	0 (0)	1 (17)	4 (67)

Table 20: *mdm2* alternative and aberrant splicing in ovarian tumors of borderline malignancy

Case ID #	Diagnosis at surgery	full length <i>mdm2</i>	<i>mdm2</i> -b 654 bp	<i>mdm2</i> 221 bp	other splice variants
2434	serous borderline	+	-	+	-
3084	serous borderline	+	-	+	-
3453	serous borderline	+	-	-	-
3454	serous borderline	+	-	+	334, 150
3455	serous borderline	+	-	+	-
3458	mucinous borderline	+	-	-	357, 282
3459	serous borderline	-	-	-	-
3463	mucinous borderline	+	-	-	446
3465	serous borderline	-	+	+	-
n (%)		7(78)	1 (11)	5 (56)	3 (33)

The *mdm2*-b splice variant (654 bp) was seen in one (1/9) of the borderline ovarian tumors (11%). Five cases had the 221 bp splice variant, which is also frequent in ovarian carcinomas. Five splice variants of the sizes 446, 357, 334, 282 and 150 bp were found in three cases of borderline tumors. The 150 bp splice variant was also found in two ovarian carcinomas, while the other variants were only seen in the borderline tumors.

4.2.6 *mdm2* alterations in normal ovarian tissue

RNA from normal ovarian tissue was extracted and analyzed for *mdm2* splice products by RT-PCR (Fig. 28). The age of the patients, diagnosis at the time of surgery, menopausal status or day of menstrual cycle respectively are demonstrated in table 21. In nine cases the ovaries were removed in surgery for uterine fibroids. In one patient the ovarian tissue was snap frozen at the time of autopsy for liver failure. Two patients had ovarian cancer of the contralateral side, two patients had endometrioid cancer, and two had cervical cancer.

Only 9/20 (45%) of the normal ovarian tissues showed expression of only the full length *mdm2* cDNA, while 11/20 (55%) showed alternative splice products, in

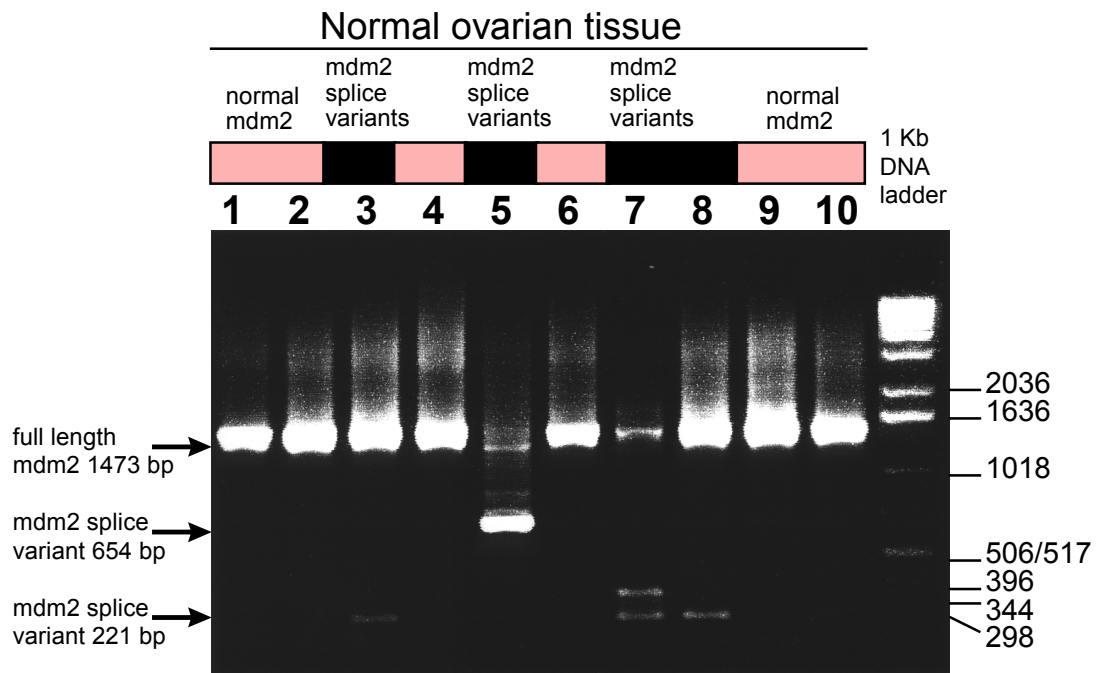


Fig. 28: *mdm2* RNA splice variants in normal ovarian tissue. Total RNA of ovarian tissue was analyzed by RT-PCR and PCR-products were separated on a 1.2% agarose gel. Cases in lanes 3, 5, 7, and 8 show splice variants of different sizes. (cDNA bands on the gel contain additional 53 bp of flanking primer sequence).

nine cases in addition to normal *mdm2*, and in two cases, which were lacking the full length *mdm2*, as the only *mdm2* cDNA.

The *mdm2*-b splice variant of 654 bp was found in one case of the normal ovarian tissues. The most frequent splice variant was the 221 bp *mdm2* cDNA, which was seen in 40% of normal ovarian tissues. The 259 bp splice variant was found in four cases (20%).

Interestingly, seven out of 12 patients who had undergone surgery for a benign disease, mostly uterine fibroids, had expression of only normal *mdm2*. In contrast, none of the six patients who had undergone surgery for a gynecological cancer had exclusively expression of the full-length *mdm2* in the normal ovarian tissue. In five of these cases we found one or several splice variants, besides the full-length *mdm2* expression, and in one case only two splice variants and no full length *mdm2* cDNA. This result reached statistical significance. The finding of *mdm2* RNA splicing in the unaffected normal ovary was significantly correlated with the diagnosis of a gynecological cancer, either in the contralateral ovary, or in the uterine cervix or endometrium ($p=0.017$).

Table 21: *mdm2* alternative and aberrant RNA splicing in normal ovarian tissue

Case ID #	Age of patient	Diagnosis at surgery / autopsy	Meno-pausal status	Day of menstrual cycle	full length <i>mdm2</i>	<i>mdm2</i> -b 654 bp	<i>mdm2</i> 221 bp	other splice variants
ov51	41	endometrial cancer	pre	12	+	-	+	365
ov56	48	unknown	?	?	+	-	-	-
ov63	54	endometrial cancer	post	-	+	-	+	279, 259
ov65	37	cervical cancer	pre	42	-	-	-	279, 259
ov97	39	unknown	pre	19	+	-	-	-
ov98	37	uterine fibroids	pre	7	+	-	-	-
ov105	40	uterine fibroids	pre	20	+	-	-	-
ov108	39	uterine fibroids	pre	10	+	-	+	-
ov119	61	uterine fibroids	post	-	+	-	-	-
ov120	37	uterine fibroids	pre	2 nd half	+	-	-	-
ov127	39	uterine fibroids	pre	23	+	-	-	-
ov172	41	uterine fibroids	pre	11	+	-	-	-
ov214	39	uterine fibroids	pre	?	+	-	+	-
402A	50	ovarian cancer Ia	?	?	+	-	+	-
2150	60	normal ovary	post	-	+	-	+	259
3106	43	cervical cancer	pre	?	+	-	+	52
3119	41	liver failure	pre	?	-	+	-	-
3294	42	normal ovary	pre	?	+	-	-	442
3539	-	contralateral	?	?	+	-	+	-
73595	50	ovarian cancer Ia uterine fibroids	post	-	+	-	-	-
n	-	-	-	-	18	1	8	6
(%)					(90)	(5)	(40)	(30)

4.2.7 In vitro expression of p53 and MDM2 splice variant proteins

Transient transfection of HeLa cells with the pcDNA3 expression vector containing the *mdm2* cDNA of interest was used for expression of MDM2 and p53 proteins (Fig. 29). The cDNA sequence had been inserted into the pcDNA3 plasmid such that it came under the control of the T7 RNA polymerase promoter (p_{T7}). The HeLa cells were previously infected with the recombinant vaccinia virus vTF7-3 which expresses the bacteriophage T7 RNA polymerase gene. During incubation, the

gene of interest is transcribed with high efficiency by T7 RNA polymerase (Panicali and Paoletti, 1982, Mackett et al. 1982, Moss and Flexner, 1987).

A full length *p53* cDNA, a full length *mdm2* cDNA, and three splice variants of 654 bp, 351 bp, and 52 bp were amplified by PCR using a primer pair designed for cloning the cDNA of interest into a pcDNA3 expression-vector. The pcDNA3 expression vector had been modified such that it contained a myc-epitope respectively a HA-epitope at the 3' end of the DNA-insert. The amplified DNA was ligated into the pcDNA3 vector and transformation of electro-competent *E. coli* bacteria was carried out through electroporation. The correct size of the insert was verified by digestion of the plasmid by the NcoI restriction enzyme. (Fig. 8b).

HeLa cells were infected with the vaccinia virus strain vTF7-3 and subsequently, transient transfection of the infected HeLa-cells with the expression vector plasmid was carried out through incubation with a DNA-liposome-complex (Fig. 9).

After harvesting the cells, proteins were analyzed by SDS-polyacrylamide gel electrophoresis. We were able to express the full length p53 protein (53 kDa), the full length MDM2 protein (90 kDa), and the protein of the *mdm2*-b-splice variant (40kDa) in vitro in HeLa-cells (Fig. 29). The clones containing the splice variants 351 bp and 52 bp did either not express a protein, or it was undetectable due to small amounts or rapid degradation.

Co-immunoprecipitation was carried out by transient transfection of vTF7-3 infected HeLa-cells with both the full length p53 cDNA and the *mdm2*-b splice variant cDNA, respectively with p53 and full length *mdm2* cDNA as a control, followed by SDS-PAGE and immunoprecipitation with the anti-myc respectively anti-HA-antibody. We were able to demonstrate that the full length MDM2 protein binds to the p53 protein (results not shown). However, co-expression and co-immuno-precipitation of the p53 protein and the *mdm2*-b splice variant protein were not successful so far. Further experiments will be needed to clarify, whether p53 binds to the *mdm2* splice variant proteins.

4.2.8 Correlation of *mdm2* and *p53* alterations

Out of 92 ovarian cancer cases analyzed for *mdm2* splice variants, 50 (54%) had *p53* mutations, and 52 (57%) had *p53* overexpression including 13 cases with wildtype *p53* sequence. No correlation was found between *p53* mutation status and

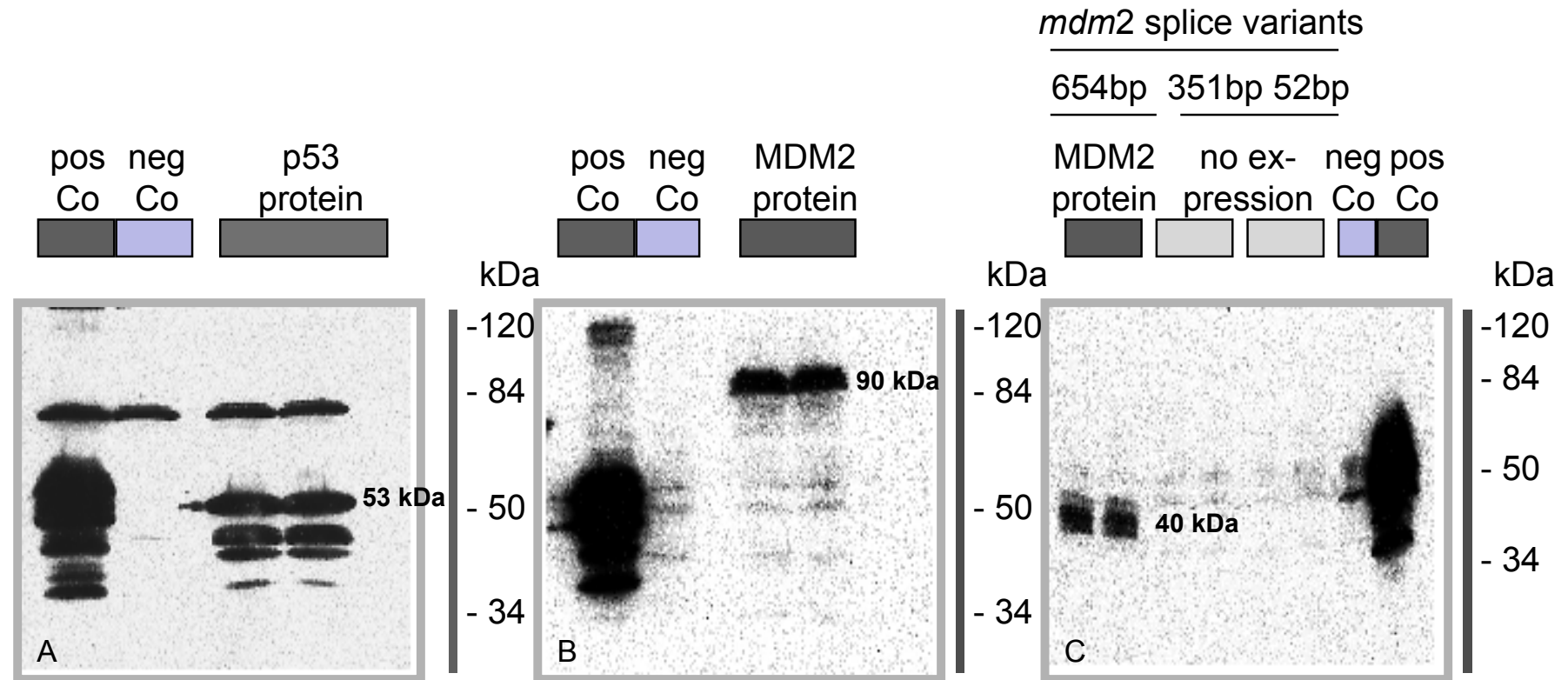


Fig. 29: Cytoplasmic expression of p53 and MDM2 proteins by transient transfection of pcDNA3 vector constructs into vaccinia virus infected HeLa cells

A: Expression of the full length p53 protein (53 kDa). **B:** Expression of the full length MDM2 protein (90 kDa).

C: Expression of a 40 kDa protein of the splice variant *mdm2*-b (654 bp). No protein could be expressed from the *mdm2* splice variants of 351 bp and 52 bp. Proteins were analyzed by Western blotting and anti-myc respectively anti-HA immunodetection.

mdm2 splicing. In cases with *p53* mutation, 22% (11/50) had no detectable full length *mdm2*, 72% (36/50) had splice variants, 48% (24/50) expressed the *mdm2*-b splice variant and 12% (6/50) expressed the 221 bp splice variant.

Out of 52 cases with *p53* protein overexpression, 7 (14%) had no detectable full length *mdm2*, 41 (79%) had splice variants, and 9 (17%) expressed the 221 bp *mdm2* variant. The only significant difference was seen for the *mdm2*-b splice variant which was present in 52% of the cases with *p53* overexpression but only in 28% of cases with no immunohistochemically detectable *p53* protein ($p=0.018$).

In cases with *p53* overexpression despite wildtype sequence, *mdm2* splicing was seen more frequently (11/13, 85%) than in cases with normal *p53* expression and wildtype *p53* sequence (19/29, 65%). However, the results did not reach statistical significance.

Table 22: *p53* alterations in comparison to *mdm2* RNA splicing

<i>p53</i> sequence / <i>p53</i> protein	no <i>mdm2</i> expression n (%)	full length <i>mdm2</i> n (%)	full length and splice variants n (%)	only splice variants n (%)	Total n (%)
wildtype/ normal expression	3 (10)	7 (24)	18 (62)	1 (3)	29 (32)
wildtype / overexpression	0 (0)	2 (15)	10 (77)	1 (8)	13 (14)
mutation / normal expression	2 (18)	3 (27)	3 (27)	3 (27)	11 (12)
mutation / overexpression	3 (8)	6 (15)	27 (69)	3 (8)	39 (42)
	8 (9)	18 (20)	58 (63)	8 (9)	92 (100)
					$p = 0.23$

4.2.9 Correlation of *mdm2* alterations with histopathological and clinical data

If *mdm2* results were classified into full length *mdm2*, altered, and no expression of *mdm2*, we did not find any correlation with clinical or histological characteristics of the ovarian tumors (Table 23). A comparison of the most frequent splice variants though, the 654 bp and the 221 bp variant, showed some interesting correlations.

Table 23: Clinico-pathologic characteristics of patients with ovarian cancer and mdm2 alterations

Characteristic	<u>mdm2 Alterations</u>				<u>Splice variant 654 bp (mdm2-b)</u>			<u>Splice variant 221 bp</u>		
	mdm2 full length	altered mdm2	no mdm2 expression	P value*	absent	present	P value*	absent	present	P value*
Patients - no. (%)	18 (20%)	66 (71%)	8 (9%)		54 (59%)	38 (41%)		77 (84%)	15 (16%)	
Median age - yrs	58	55	50		55	57		55	57	
Histological Subtype - no. (%)										
Serous	12 (67%)	25 (39%)	3 (38%)	0.10	24 (44%)	16 (43%)	0.90	35 (46%)	5 (36%)	0.50
Other	6 (34%)	40 (61%)	5 (62%)		30 (56%)	21 (57%)		42 (54%)	9 (46%)	
Clinical stage - no. (%)										
FIGO I	6 (33%)	19 (29%)	3 (38%)	0.50	20 (37%)	8 (21%)	0.066	20 (26%)	8 (53%)	0.017
FIGO II	2 (11%)	3 (5%)	0		4 (7%)	1 (3%)		4 (5%)	1 (6%)	
FIGO III	8 (44%)	36 (54%)	3 (38%)		24 (44%)	23 (61%)		41 (53%)	6 (40%)	
FIGO IV	2 (11%)	8 (12%)	2 (25%)		6 (11%)	6 (16%)		12 (16%)	0	
Grade of Differentiation - no. (%)										
I (well)	7 (39%)	11 (17%)	3 (37%)	0.41	17 (31%)	4 (10%)	0.04	17 (22%)	4 (27%)	0.31
II (moderate)	3 (17%)	23 (35%)	0		14 (26%)	12 (32%)		20 (26%)	6 (40%)	
III (poor)	8 (44%)	32 (48%)	5 (63%)		23 (43%)	22 (58%)		40 (52%)	5 (33%)	
Residual Tumor - no. (%)										
No residual tumor	13 (76%)	36 (58%)	5 (63%)	0.65	37 (76%)	17 (45%)	0.004	44 (59%)	10 (77%)	0.12
≤ 2 cm	2 (12%)	16 (26%)	2 (25%)		8 (16%)	12 (32%)		17 (23%)	3 (23%)	
> 2 cm	2 (12%)	10 (16%)	1 (13%)		4 (8%)	9 (24%)		13 (18%)	0	
Lymph nodes - no. (%)										
Negative	6 (35%)	13 (21%)	1 (13%)	0.89	14 (29%)	6 (16%)	0.45	17 (23%)	3 (23%)	0.99
Positive	4 (24%)	20 (32%)	3 (37%)		14 (29%)	13 (34%)		23 (31%)	4 (31%)	
Not resected	7 (41%)	29 (47%)	4 (50%)		21 (42%)	19 (50%)		34 (46%)	6 (46%)	
DNA-ploidy - no. (%) (n=88)										
Diploid	8 (44%)	33 (55%)	4 (57%)	0.51	26 (51%)	19 (51%)	0.97	36 (49%)	9 (60%)	0.45
Aneuploid	10 (56%)	30 (45%)	3 (43%)		25 (49%)	18 (49%)		37 (51%)	6 (40%)	
S-Phase-Fraction - no. (%) (n=88)										
low (< 5%)	5 (28%)	17 (27%)	1 (14%)	0.72	17 (33%)	6 (16%)	0.016	16 (22%)	7 (47%)	0.056
intermediate (5% - 14.4%)	8 (44%)	27 (43%)	5 (71%)		24 (47%)	16 (43%)		32 (44%)	8 (53%)	
high (≥ 14.5%)	5 (28%)	19 (30%)	1 (14%)		10 (20%)	15 (41%)		25 (34%)		
Treatment - no. (%) **										
Cisplatin - Cyclophosphamide	3 (17%)	14 (21%)	2 (25%)	1.0	9 (17%)	10 (26%)	0.19	16 (21%)	3 (20%)	0.66
Carboplatin - Cyclophosphamide	4 (22%)	13 (13%)	1 (12%)		9 (17%)	9 (24%)		16 (21%)	2 (13%)	
Other regimens	4 (22%)	12 (18%)	1 (12%)		12 (22%)	5 (13%)		14 (18%)	3 (20%)	
No chemotherapy	5 (28%)	21 (32%)	3 (38%)		16 (30%)	13 (34%)		25 (33%)	4 (27%)	
No information - no.	2 (11%)	6 (9%)	1 (12%)		8 (15%)	1 (3%)		6 (8%)	3 (20%)	

* Chi-Square test for two categories, Mantel-Haenszel test for three or more categories

** Chemotherapy regimens are described in the methods section

Presence of the 654 bp splice variant (*mdm2*-b) was significantly correlated with poor grade of differentiation ($p=0.04$), a residual tumor mass after surgery ($p=0.004$) and high S-phase fraction ($p=0.016$). It was also more frequent in tumors of advanced stage ($p=0.066$) (Table 23). The *mdm2*-b splice variant thus seems to be significantly associated with histologically and clinically more aggressive tumors.

As opposed to this the presence of the splice variant 221 bp was significantly correlated with early stage tumors ($p=0.017$), and was more frequently identified in grade I or II tumors, tumors without residual mass after surgery, and tumors with low S-phase fraction, though the latter results did not reach statistical significance (Table 23) (Table 23).

4.2.10 *mdm2* alterations and clinical outcome in ovarian cancer

mdm2 splice variant findings were furthermore compared with the response to a platinum based chemotherapy (Table 24). Details of chemotherapy regimen and evaluation of response were described in the methods section. If full length *mdm2* was present in the ovarian carcinomas, the majority of tumors (64%) were sensitive to

Table 24: Response to platinum-based chemotherapy in ovarian cancer depending on *mdm2* alternative splicing

<i>mdm2</i> transcript	<u>Chemotherapy-Response</u>				p-value
	Sensitive n (%)	Resistant n (%)	Refractory n (%)	Total n (%)	
<i>mdm2</i> full length present	27 (64)	3 (7)	12 (29)	42 (84)	p = 0.001
<i>mdm2</i> full length absent	2 (25)	5 (63)	1 (13)	8 (16)	
	29	8	13	50	
no <i>mdm2</i> expression	1 (25)	2 (50)	1 (25)	4 (8)	p=0.006
normal <i>mdm2</i> expression	8 (80)	0 (0)	2 (20)	10 (20)	
normal and splice variants	19 (59)	3 (9)	10 (31)	32 (64)	
only splice variants	1 (25)	3 (75)	0 (0)	4 (8)	
	29 (58)	8 (16)	13 (26)	50 (100)	

platinum-based chemotherapy (27/42), whereas in cases with no detectable full length transcript, only 2/8 cases were sensitive (25%), while the majority of cases was resistant or refractory ($p=0.001$) (Table 24). Similarly, presence of *mdm2* splicing in general was significantly correlated with poor response to chemotherapy ($p=0.006$) (Table 24).

mdm2 alterations were analyzed for their impact on the clinical outcome of the patients by log-rank statistical survival analysis (Fig. 30A-F). Presence or absence of alternative splicing as opposed to full length *mdm2* cDNA, absence of *mdm2*-expression, and the site of RNA splicing at exon-intron boundaries as opposed to cryptic exon splice sites, did not have a significant influence on survival after diagnosis of ovarian cancer (Fig. 30A,B). The size of the splice variants had some influence on survival but did not reach statistical significance (Fig. 30C,D). However, analysis of the splice variant 654 bp showed a trend to poor clinical outcome for patients with expression of this splice variant in the ovarian tumor ($p=0.17$, Fig. 30E). The only significant difference was seen for patients with expression of the 221 bp splice variant (Fig. 30F), who had a better survival prognosis than patients without expression of the 221 bp splice variant ($p=0.048$).

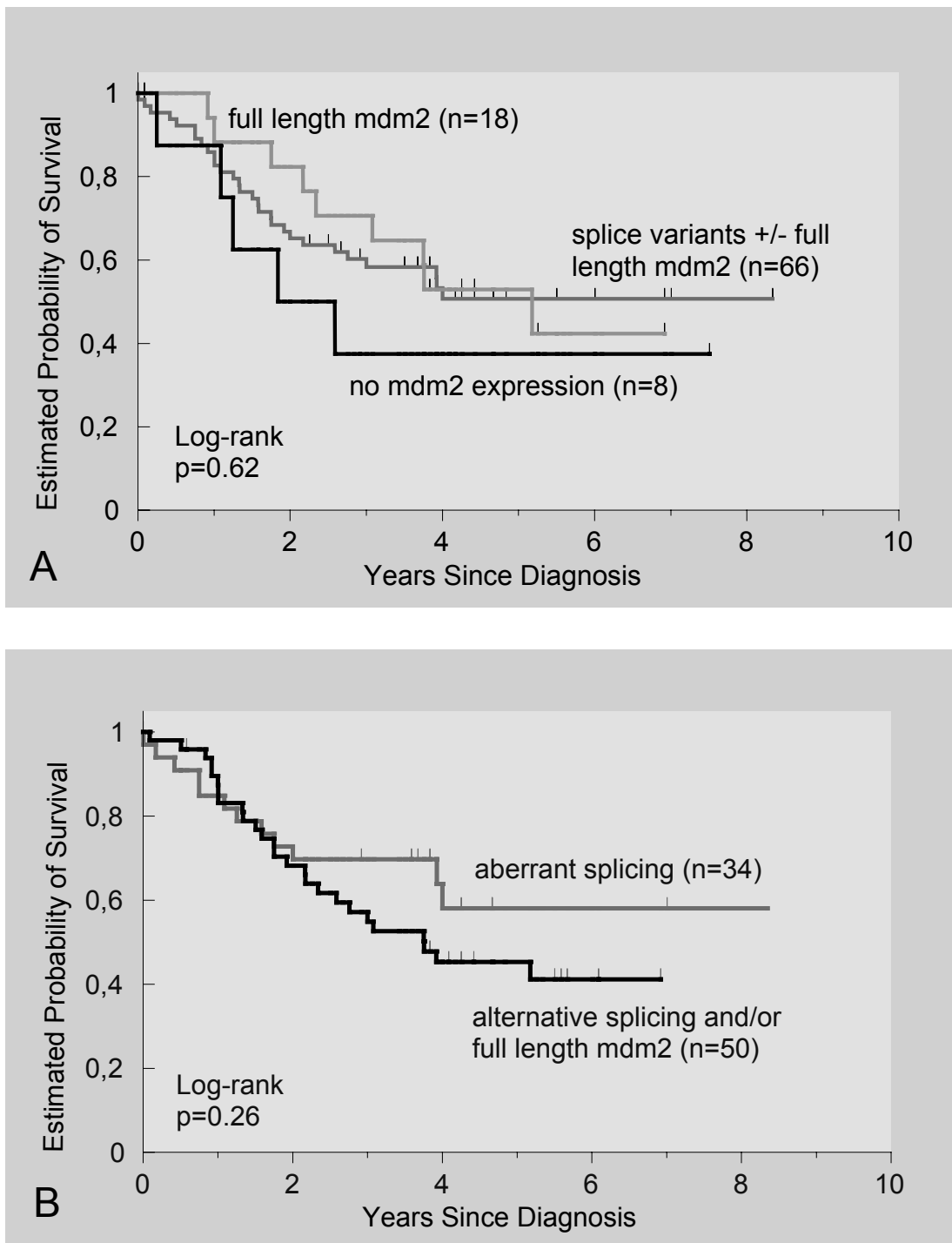


Fig. 30: A-B: Clinical outcome of ovarian cancer patients dependent on *mdm2* alternative RNA splicing (n=92) as analyzed by RT-PCR and DNA sequencing.
A) Overall survival in patients with expression of the full length *mdm2* RNA transcript, versus *mdm2* splice variants, versus absence of *mdm2* RNA expression.
B) Overall survival in patients with aberrant splicing in the donor and acceptor or only the acceptor site, versus patients with full length *mdm2* and/or alternative splicing at exon/intron boundary of exon 3 and 9 (*mdm2*-a, 888 bp) or exon 3 and 11 (*mdm2*-b, 654 bp).

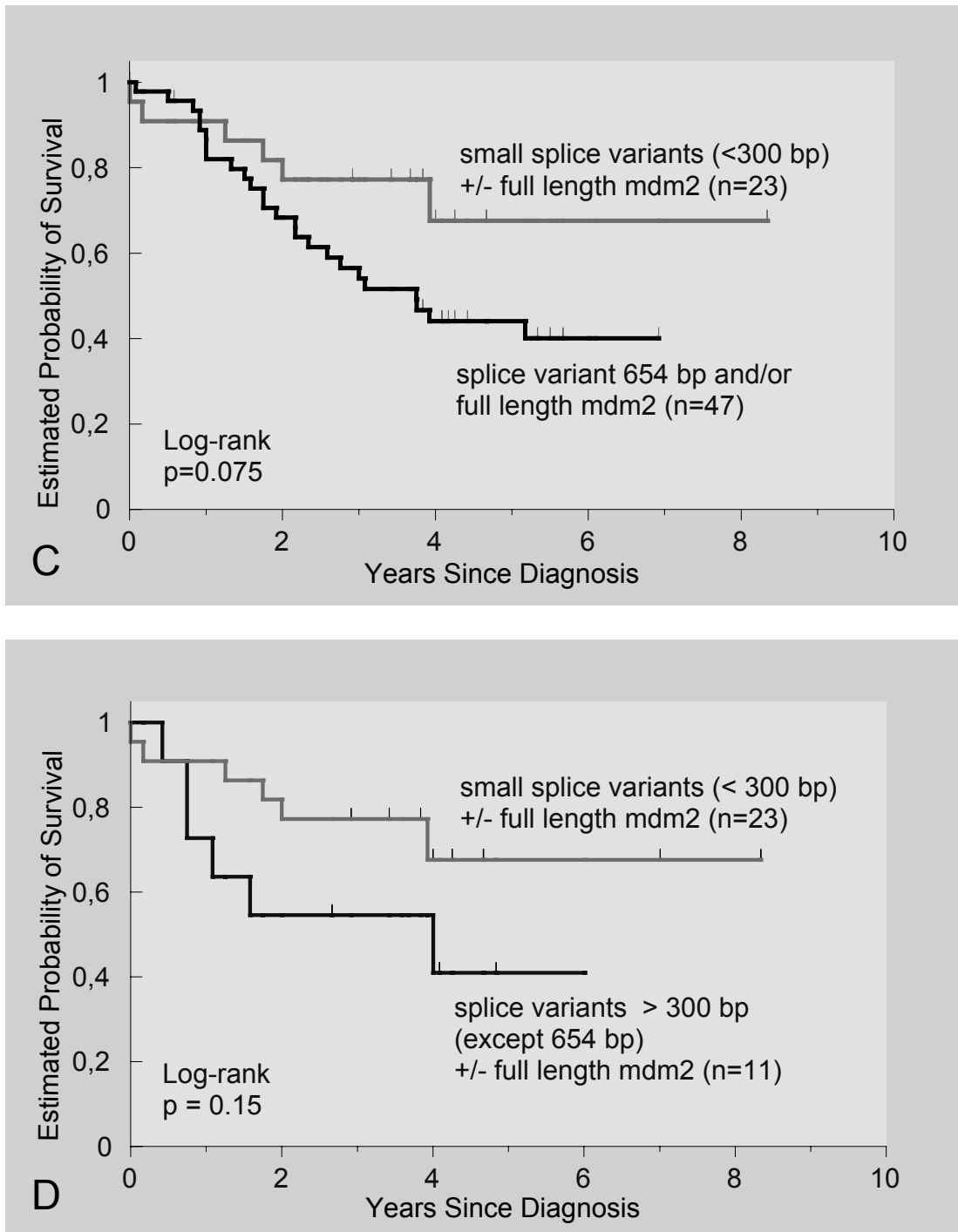


Fig.30 C-D: Clinical outcome of ovarian cancer patients dependent on *mdm2* RNA alternative splicing (n=92) as analyzed by RT-PCR and DNA sequencing.
C) Overall survival in patients with expression of small splice variants of <300 bp versus expression of the *mdm2*-b splice variant (654 bp) or full length *mdm2*
D) Overall survival in patients with expression of small splice variants (<300 bp) versus expression of *mdm2* splice variants of >300 bp in the presence or absence of the full length *mdm2* transcript. Cases with expression of the the *mdm2*-b splice variant (654 bp) were not included in this analysis.

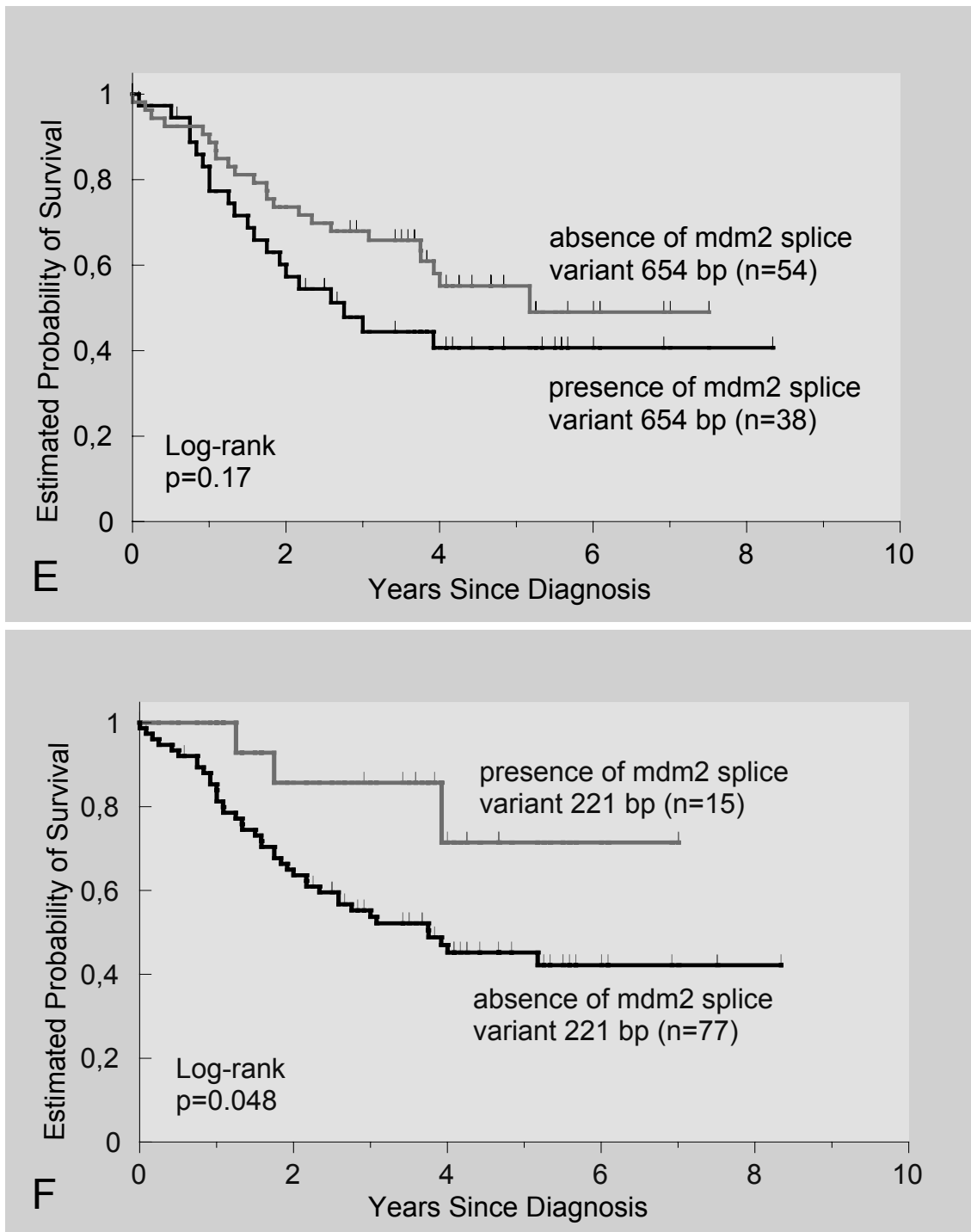


Fig.30 E-F: Clinical outcome of ovarian cancer patients dependent on *mdm2* RNA alternative splicing (n=92) as analyzed by RT-PCR and DNA sequencing.

E) Overall survival in patients with expression of the *mdm2*-b splice variant (654 bp) versus absence of the *mdm2*-b splice variant.

F) Overall survival in patients with expression of a small splice variant of 221 bp was correlated with early stage (FIGO I/II) and marginally significant with a better clinical outcome.

5. DISCUSSION

5.1 Alterations of the *p53* tumor suppressor gene in ovarian cancer

5.1.1 *p53* mutations

Our study includes a large cohort of primary ovarian carcinomas and addresses several issues relevant to *p53* sequence alterations and protein overexpression. First, we analyzed, as in our previous study (Wen et al. 1999), frozen tissue in order to avoid problems related to loss of antigenicity that is observed with immunohistochemistry in paraffin-embedded tissue. Secondly, we assessed the frequency of mutations throughout the entire coding region of the gene by analyzing exons 2-11 by SSCP and subsequent sequencing of cases with alterations, as opposed to most other studies which are limited to exons 5-8. Thirdly, information on adjuvant treatment was available and the results of the *p53* sequence analysis and immunohistochemistry were compared to the response to chemotherapy, in order to evaluate the role of *p53* for the sensitivity of platinum based chemotherapy. Finally, clinical follow-up information concerning outcome was available in 96% of the cases and information about the progression of the disease was available in 78% of the patients, which allows the evaluation of the prognostic relevance of *p53* alterations in a sufficient number of cases.

We found a total of 100 *p53* mutations in 99 out of 178 ovarian carcinomas (56%), which is higher than the percentage in most other studies. The frequency of *p53* mutations in studies using frozen tissues including our previous study is 50% and ranges from 20% to 73% (Mazars et al. 1991, Kihana et al. 1992, Kohler et al. 1993a, Milner et al. 1993, Sheridan et al. 1994, Fujita et al. 1994, Lee et al. 1995, Casey et al. 1996, Sakamoto et al. 1996, Skilling et al. 1996, Schuyer et al. 1998, Wen et al. 1999). In studies using paraffin-embedded tissues, the frequency of mutations was 47%, ranging from 26% to 79%. (Teneriello et al. 1993, Kupryjanczyk et al. 1993, Wertheim et al. 1994, Niwa et al. 1994, Zheng et al. 1995, Kappes et al. 1995).

Several studies have analyzed part of the *p53* coding region for mutations and found mostly between 20% and 52% mutations (Milner et al. 1993, Teneriello et al. 1993, Wertheim et al. 1994, Fujita et al. 1994, Niwa et al. 1994, Zheng et al. 1995, Kappes et al. 1995) with the exception of Kohler et al. (1993a) who found a percentage of 73% and Jacobs et al. (1992) who found 66% mutations. Three studies analysing exon 4-9 found 20-37% mutations (Kim et al. 1995, Lee et al. 1995, Sakamoto et al. 1996) and one study found 26% mutations in exon 4-8 (Niwa et al. 1994).

The mutations were located predominantly (92%) in exons 5-8 and their associated splice junctions. Eight mutations (8%) though, were found outside of exons 5-8. These eight mutations were located in exon 4 and the exon 4/intron 4 splice junction (4 mutations) and in exon 9 and the intron 8/exon 9 splice junction (4 mutations). These results demonstrate that the evaluation of codons 126 to 307 (182 codons) provided 92 of 100 (92%) of the mutations, while eight mutations (8%) could only be identified by evaluation of codons 1 to 125 and 308 to 393 (211 codons).

The percentage of mutations in studies analysing the entire coding region of *p53* is overall 59% (207/349) and varies from 52% to 79%, which is consistent with our own results (Kihana et al. 1992, Kupryjanczyk et al. 1993, 1995, Skilling et al. 1996, Casey et al. 1996, Wen et al. 1999). The frequency of mutations in exons 2-4 and 9-11 was reported to be between 0% and 20% with an overall average of 11% (24/258) (Kihana et al. 1992, Kupryjanczyk et al. 1993, 1995, Skilling et al. 1996, Casey et al. 1996, Wen et al. 1999). This means that studies analysing only exons 5-8 of the *p53* gene will miss approximately 11% of the mutations.

In our previous study (Wen et al. 1999) exons 2-11 were first screened by SSCP in 105 ovarian carcinomas and cases with suspicious band patterns were sequenced. Out of 50 cases with normal SSCP band patterns, 42 were subjected to complete sequence analysis of the open reading frame by automated sequencing (Wen et al. 1999, Wang-Gohrke et al. 1998). A total of 60 mutations (57%) were identified in this study with only 5% mutations outside exons 5-8. Skilling et al. (1996) identified 61% mutations in 64 cases with 34/39 mutations located in exon 5-8 and only 5 mutations (13%) outside these exons. Kihana et al. (1992) reported that two of 10 mutations (20%) identified in 14 ovarian carcinomas were outside exons 5-8, although the codon for one of the two mutations was not specified. Kupryjanczyk et al. (1993) analyzed 38 ovarian carcinomas and found 31 mutations in 30/38 tumors (79%) by PCR-SSCP and sequencing, which is the highest percentage so far reported in the literature. Three of these mutations were located outside exon 5-8.

Excluding nonsense and frameshift mutations, 222 of the 393 codons of the human *p53* gene have been described as the targets of at least 698 different mutations (Beroud et al. 1996). While some codons, such as codon 190, are the target of only one mutational event, others such as codon 179 have been the target of multiple mutational events. In our study, the codons most frequently mutated were codons 175, 179, 234, 242, 248, 273, 275, and 281, which were each mutated in three or more different carcinomas. No mutations have been identified in codons 92-112, the region which has been recently identified as the degradation signal in *p53*/MDM2 interaction (Gu et al. 2000).

In our study we identified 72% missense mutations. This is consistent with the results of most other authors who found between 62% and 85% missense mutations (Milner et al. 1993, Kupryjanczik et al. 1993, Niwa et al. 1994, Skilling et al. 1996, Casey et al. 1996, Righetti et al. 1996, Schuyer et al. 1998). Deletions are usually described in a percentage of 7%-13% (Kupryjanczik et al. 1993, Milner et al. 1993, Righetti et al. 1996, Schuyer et al. 1998, Wen et al. 1999), which is similar to our findings of 10% deletions. But some authors found deletions in a percentage as high as 22% by SSCP of exon 2-11 and sequencing (Skilling et al. 1996) and 27% of all mutations by sequencing exon 2-11 (Casey et al. 1996). Insertions have been found less often and have been described by Skilling et al. (1996) as 2.5%, Casey et al. (1996) as 6%, and Milner et al. (1993) as 3% of the mutations in ovarian cancer. Several studies with smaller case numbers do not describe insertions at all. We identified 3 insertions (3%), one of which was combined with a deletion. Splice junction mutations are considered rare mutations and so far only 12 splice junction mutations have been described in the ovarian cancer literature including our previous study, with a percentage of usually 1-5% (Kupryjanczik et al. 1993, Niwa et al. 1994, Skilling et al. 1996, Casey et al. 1996, Righetti et al. 1996, Schuyer et al. 1998). Including three previously published splice junction mutations (Wen et al. 1999) we found eight splice junction mutations accounting for 8% of all mutations identified, which is higher than in any of the other studies.

5.1.2 *p53* mutations in evolutionary highly conserved domains

The majority of mutations in this study (61/99 carcinomas, 62%) were located within highly conserved domains of *p53* (domains II, III, IV and V) (Cho et al. 1994, Soussi and May, 1996). These domains are almost equivalent to the loop-sheet-helix (domains II and V), loop 2 (domain III), and loop 3 (domain IV) regions of *p53* (Cho et al. 1994, Soussi and May, 1996). The loop-sheet-helix is responsible for direct DNA interactions with the major groove; loop 3 is responsible for direct interactions with the minor groove of DNA, and loop 2 and 3 together are responsible for maintaining the needed 3-dimensional conformation (Cho et al. 1994, Prives 1994, Soussi and May, 1996, Arrowsmith and Morin, 1996). Mutations in these conserved domains have been observed to confer more aggressive behavior in patients with breast carcinomas or colon carcinomas than mutations in other regions of *p53* (Bergh et al. 1995, Goh et al. 1995). Similarly, in our study, comparisons of overall survival for women with mutations in highly conserved domains together did show a statistically significant difference in survival compared to those with mutations in non-conserved regions or wildtype *p53* sequence ($p = 0.007$).

5.1.3 *p53* polymorphisms and intron alterations

Several *p53* constitutional polymorphisms have been reported. These are located in codon 21 (exon 2) (Ahuja et al. 1990), codon 36 (exon 4) (Felix et al. 1994), codon 72 (exon 4) (Harris et al. 1986, Matlashewski et al. 1987), codon 213 (exon 6) (Carbone et al. 1991), intron 1 (Ito et al. 1994), intron 2 (Pleasant and Hansen 1994, DiCioccio and Piver 1996, Ge et al. 1998, Verselis and Li, 2000), intron 3 (Lazar et al. 1993) and intron 6 (Peller et al. 1995).

p53 polymorphisms can cause abnormal bands in single-strand conformation polymorphism (SSCP) analysis, which is widely used as a screening technique for *p53* mutations and can therefore be mistaken for mutations, if they are not confirmed by DNA sequencing (Carbone et al. 1991).

Among the 178 ovarian carcinomas, which were analyzed by SSCP and DNA sequencing, we identified 100 mutations (Table 8) and 45 polymorphisms in exons 4, 6, and 7, and in the intron sequences, which were flanking exons 3, 6, 10, and 11. We observed four polymorphisms in codon 36 (CCG to CCA), codon 213 (CGA to CGG), codon 224 (GAG to GAA), and codon 231 (ACC to ACA). The frequency of each of these polymorphisms was 0.6% in our study cohort. The codon 36 polymorphism was first described by Felix et al. 1994 and was present in the heterozygous state in 4% of 100 individuals. Carbone et al. (1991) first described the polymorphism at codon 213 (CGA→CGG), which doesn't result in an amino acid exchange but causes the loss of a Taq I restriction site. It was found in a frequency of 3.2% in lung cancer and breast cancer and caused an SSCP alteration (Carbone et al. 1991). The sequence alterations at codon 224 (exon 6) and 231 (exon 7) have not been previously described in the literature. They may be polymorphisms or silent mutations since they do not result in an amino acid exchange. But in these cases, no normal tissue DNA was available, so that we could not verify whether this is a polymorphism.

Five percent (9/178) of all the cases had a CCG→CCC polymorphism at codon 72 resulting in an arginine to proline amino acid exchange. Codon 72 of the *p53* gene has been described to be the site of a primary structure polymorphism with an amino acid residue which could be an arginine, proline or cysteine (Harris et al 1986, Matlashewski et al. 1987). The majority of Caucasian individuals express the arginine-containing *p53* protein as opposed to African-Americans who express predominantly the proline-containing *p53* protein (Weston et al. 1992, Sjölander et al. 1995). We therefore considered the arginine-72 *p53* as the normal sequence and the proline-72 *p53* as the polymorphic sequence.

Overall, the percentage of polymorphisms identified in our study seems low compared to the literature. This may be due to the fact that this cancer cohort was not systematically screened for *p53* polymorphisms. Only cases with SSCP band alterations were sequenced. Therefore polymorphisms, which do not cause SSCP alterations, may have been missed.

The codon 72 *p53* polymorphism is presently discussed to play a role for cancer predisposition. In breast cancer patients, a significant increase in the codon 72 proline allele frequency was observed, which was most pronounced in highly differentiated breast cancer (Själänder et al. 1996). In ovarian cancer, probands homozygous for the arginine allele have been found to develop ovarian cancer at an earlier age and have a survival advantage compared to arginine/proline heterozygote and proline homozygote patients (Buller et al. 1997). When a loss of heterozygosity occurred in patients with invasive ovarian cancer, the proline allele was lost preferentially and tumors which retained a proline allele were significantly more prone to mutation than tumors without a proline allele (Buller et al. 1997).

Storey et al. described a significant overrepresentation of homozygous arginine-72 *p53* in human papilloma-virus-associated cervical carcinoma compared with the normal population which makes individuals homozygous for arginine 72 about seven times more susceptible to HPV associated tumorigenesis than heterozygotes (Storey et al. 1998). They conclude that the arginine-encoding allele represents a significant risk factor in the development of human papilloma-virus-associated cervical carcinoma. This finding was corroborated in two independent studies (Zehbe et al 1999, Agorastos et al. 2000), however, refuted by others (Helland et al. 1998, Hildesheim et al. 1998; Josefsson et al. 1998, Lanham et al. 1998). Inter-laboratory variation in *p53* genotyping may have contributed to the inconsistent findings across studies (Makni et al. 2000). Makni et al. observed odds ratios of 8.0 (95% CI: 2.3-28.5) for the Arg/Arg genotype and cervical cancer when they excluded individuals which were differently genotyped in three independent laboratories (Makni et al. 2000). Recently a differential effect of the *p53* codon 72 variants on interaction of mutant *p53* with p73 has been published (Marin et al. 2000). The binding of the arginine isoform to p73 tended to be stronger than that observed for the proline isoform, with a neutralizing effect on p73-induced apoptosis. The presented data also suggested the codon 72 polymorphism to modify the response of selected tumor cells to chemotherapy. In some tumors, such as squamous cell cancers, the authors found evidence for preferential mutation and expression of the arginine form of *p53* in arginine/proline heterozygotes (Marin et al. 2000).

Compared to the expected frequency of the arginine and the proline allele, the arginine allele was clearly overrepresented in our study population which consisted

predominantly of caucasian individuals. A correlation between the proline allele and p53 overexpression was not identified.

Various intron alterations of unknown significance have been found in the *p53* gene. A polymorphism in intron 3, which consists of a single repeat of 16 nucleotides starting at nucleotide 11951 of the *p53* gene, was first described by Lazar et al. (1993) and was identified in its heterozygote form in 28% of 82 individuals in lymphocyte DNA. The polymorphism was not associated with a predisposition to breast cancer. We found this 16 bp repeat polymorphism in 14% of the ovarian cancer cases. The presence of the polymorphism was not associated with a higher percentage of p53 overexpression, but was found in eight of nine cases with the codon 72 proline polymorphism. According to Sjölander et al. (1995), significant ethnic differences have been found for the codon 72 and the intron 3 16 bp repeat polymorphism (Sjölander et al. 1995). The most common finding in a northern european population was the codon 72 arginine allele combined with absence of the 16 bp repeat polymorphism and was therefore considered the „wild-type,, haplotype (Sjölander et al. 1995).

The biological significance of the intron 3 16 bp repeat polymorphism remains unclear. Homozygosity of the *p53* intron 3 polymorphism was suspected to be highly associated with sporadic ovarian cancer by Runnebaum et al. (1995). The authors found an overall frequency of 24.1% heterozygous and 1.7% homozygous PIN 3 polymorphism in normal controls, while the frequency was 30.6% and 11.3% respectively in ovarian cancer patients, which was a 6.7 fold increase of the homozygotes in ovarian cancer (Runnebaum et al. 1995). However, no such association was observed by others in 82 ovarian carcinomas (Lancaster et al. 1995). The frequency of this polymorphism in our study cohort was lower than that mentioned by Runnebaum et al. (1995). In a study of breast cancer patients and normal controls, no significant difference was found for the frequency of the 16 bp repeat polymorphism (Sjölander et al. 1996).

Further intron polymorphisms have been described in the literature to be associated with cancer predisposition. An intron 6 polymorphism, a G to A transition at position 61, has been found significantly more frequently in ovarian carcinomas as compared to normal controls (Mavridou et al. 1998). This was confirmed in a second study, where an association of this intron 6 polymorphism and the strongly linked 16 bp polymorphism in intron 3 with ovarian cancer has been established, however, only in women not carrying *BRCA1* or *BRCA2* germline mutations (Wang-Gohrke et al. 1999). Furthermore Peller et al. (1995) described a 8bp polymorphic sequence in intron 6 of the *p53* gene, which was identified in the heterozygotic form in 32% of normal blood samples. Patients with gastric cancer and breast cancer demonstrated a

higher incidence of heterozygosity (50%). Therefore the authors suggested an association between this polymorphism and cancer predisposition and susceptibility (Peller et al. 1995).

We describe three intron alterations, which to our knowledge have not been described in the literature. One g→c alteration was identified in intron 6 at position 13964 of the *p53* gene in two ovarian cancer cases. Both cases had shown SSCP band shifts. In one case, a *p53* mutation was identified. Since no normal tissue was available in these two cases, we can not prove that this is a polymorphism, but we found this alteration in only 1% of the cancer cases, while the other cases, which were sequenced because of SSCP band shifts, revealed the normal sequence at this location.

We identified two new polymorphisms in intron 10, which have not previously been described. An a→t polymorphism was found at position 17708 of the *p53* gene in two cases in the flanking region of exon 10. In one of the cases, normal tissue was available and DNA sequencing confirmed the polymorphism. In three other ovarian cancer cases which showed only a weak SSCP band shift in the exon 10 and flanking intron region, a normal sequence at nucleotide 17708 was identified.

The other intron 10 polymorphism was found in the flanking sequence of exon 11. Four out of eight cases with SSCP band shifts revealed the polymorphic sequence, a c→t nucleotide exchange at position 18550 of the *p53* gene. In three out of these four cases, the polymorphic sequence could be confirmed in normal cervical tissue of the patient. We therefore conclude, that both intron 10 sequence alterations are polymorphisms. Since none of the cases with intron 10 alterations had a mutation in exon 10 or exon 11, we assume that the SSCP band shift was caused by the polymorphism. These two polymorphisms have not been described in the literature so far.

Interestingly, out of eight cases with intron 6 or intron 10 alterations, seven showed *p53* overexpression, though *p53* mutations and *p53* wildtype, respectively, were evenly distributed among these cases. Though the case number was very small, the result almost reached statistical significance. Intron polymorphisms may affect transcription and splicing processes and may therefore cause alterations in protein expression, stability and/or activity. For variations in *p53* introns functional relevance has been suggested (Beenken et al. 1991; Avigad et al. 1997). The actual allele frequencies and possible association with *p53* overexpression of the here newly identified intron alterations need to be clarified by screening larger case numbers.

The biological significance of *p53* polymorphisms is unclear at this point, since conflicting results regarding cancer predisposition have been reported. But there is increasing evidence, that some polymorphisms or defined constellations of polymorphisms (haplotypes) may be important for processes relevant for cancer risk

and treatment outcome, as has been suggested for the codon 72 polymorphism as intragenic modifier of mutant p53 behaviour (Marin et al. 2000). It might therefore be worthwhile, to screen a large cohort of patients with ovarian cancer in comparison to unaffected individuals for several *p53* polymorphisms to possibly define risk and prognostic factors for ovarian carcinoma.

5.1.4 p53 protein overexpression

Several investigators have used frozen ovarian carcinoma specimens for immunohistochemical analysis of p53 and found p53 overexpression in 32% - 84% with an average percentage of 51% (Marks et al. 1991, Kihana et al. 1992, Eccles et al. 1992, Kohler et al. 1993a, Kiyokawa et al. 1994, Henriksen et al. 1994, Sheridan et al. 1994, Lee et al. 1995, Casey et al. 1996, Skilling et al. 1996, Buttitta et al. 1997, Geisler et al. 1997, 2000, Schuyer et al. 1998, Wen et al. 1999). We found p53 overexpression in 62% of the cases. A few authors have performed both immunohistochemical and mutation analysis (Marks et al. 1991, Kihana et al. 1992, Sheridan et al. 1994, Lee et al. 1995, Casey et al. 1996, Skilling et al. 1996, Buttitta et al. 1997, Wen et al. 1998). Only four of the latter studies involved more than 50 carcinomas (Casey et al. 1996, Skilling et al. 1996, Buttitta et al. 1997, Wen et al. 1999).

Many studies have used formalin-fixed, paraffin-embedded material for immunohistochemistry. In those studies, which analyzed more than 50 cases of FIGO I-IV ovarian carcinomas, the frequency of p53 overexpression ranged from 26% to 70% with an overall frequency of 48% (Bosari et al. 1993, Sheridan et al. 1994, Inoue et al. 1994, Niwa et al. 1994, Hartmann et al. 1994, Kupryjanczyk et al. 1994, van der Zee et al. 1995, Klemi et al. 1995, Herod et al. 1996, Reles et al. 1996, Viale et al. 1997, Dong et al. 1997, Eltabakkah et al. 1997, Röhlke et al. 1997, Anttila et al. 1999, Ferrandina et al. 1999, Werness et al. 1999). In one study, p53 overexpression was identified immunohistochemically in only 14% of the cases (Marx et al. 1998).

With the exception of four studies (Kupryjanczyk et al. 1993, Casey et al. 1996, Lee et al. 1995, Teneriello et al. 1993), three of which were of a small number of cases, the frequency of p53 overexpression is consistently higher than the frequency of p53 mutations. Our observations of a 62% immunostaining rate and a 56% mutation rate for p53 were consistent with these generalizations.

5.1.5 Correlation of p53 overexpression with *p53* mutations

A strong correlation was observed between p53 immunostaining and *p53* mutations ($p < 0.001$), but this was mainly an effect of the high rate of immunostaining of missense mutations (94%). However, only 46% of nonmissense mutations were identified by immunostaining and this percentage was not significantly different from the percentage of staining in wildtype *p53* cases (38%) ($p=0.43$). Therefore it can be concluded that immunohistochemistry is not suitable for the detection of nonmissense mutations, which is consistent with the findings of other authors (Casey et al. 1996, Skilling et al. 1996, Schuyer et al. 1998). The low rate of immunostaining in cases with nonmissense mutations is assumed to be caused by alteration and truncation of the protein due to introduction of a stop codon in nonsense mutations, frameshifts caused by deletions or insertions, and alterations of transcribed RNA in splice site mutations. Since the antibody used for immunohistochemistry (DO-7) recognizes an epitope near the amino-terminus of the protein between amino acid 19 and 26, one would expect the antibody to have the potential to recognize nearly all of the mutant p53 proteins. But p53 protein may not only be qualitatively altered but also quantitatively reduced, possibly because of destruction of the messenger RNA as a result of sequence changes.

A high percentage of cases with wildtype p53 sequence (38%) showed overexpression of the p53 protein. Since this can not be explained by sequence alterations, the stabilization and accumulation of a presumably normal p53 protein is most likely caused by other genes interacting with *p53*. Alterations of the *mdm2* gene, which downregulates p53 in an autoregulatory feedback and promotes degradation of the p53 protein (Kubbatat et al. 1997, Haupt et al. 1997, Kubbutat et al. 1999) may play an important role in these cases. In fact, we found *mdm2* alternative splicing in a high percentage of cases with p53 overexpression despite wild-type *p53* sequence, and p53 overexpression was significantly correlated with the presence of a 654 bp splice variant (*mdm2*-b), which has lost most of the p53 binding sequence (see chapter 5.2.8).

5.1.6 *p53* alterations and response to chemotherapy

Cell culture experiments have shown that the sensitivity of tumor cells to various chemotherapeutic agents depends on the efficient induction of apoptosis mediated by a functional p53 protein and that loss of p53 can enhance resistance to chemotherapy (Lowe et al. 1993, Vasey et al. 1996, Vikhanskaya et al. 1997).

The wildtype *p53*-expressing A2780 human ovarian cancer cell line acquired cross resistance to Cisplatin and Doxorubicin by transfection with a dominant negative mutant *p53* gene, while it retained sensitivity to Taxol (Vasey et al. 1996). In another

study (Vikhanskaya et al. 1997), Cisplatin caused strong induction of p53, WAF1 and Bax in the Cisplatin sensitive A2780 cell line, while there was no such effect in a Cisplatin resistant cell line A2780-DX3, which furthermore showed a significant proportion of potentially inactive p53 protein located in the cytoplasm instead of the nucleus.

However, some of the studies using cell culture experiments report contradictory results. In a panel of cell lines, cisplatin was more efficient against mutant/null *p53* cell lines than wildtype cell lines, while the novel platinum analogue DACH-aceto-Pt was considerably more toxic in wild-type *p53* cell lines (Hagopian et al. 1999). Similarly, in isogenic A2780 human ovarian cancer cell lines that differ only in *p53* function by transfection of HPV-16 E6, the *p53*-deficient cell line was more sensitive to cisplatin and the novel platinum agent ZD0473 (Pestell et al. 2000).

Recently, genetic suppressor elements (GSEs) have been identified which correspond to various regions within the *p53* gene and can act as dominant negative peptides or antisense RNA molecules (Gallagher et al. 1997). A synthetic peptide, representing the predicted amino acid sequence of this GSE, conferred resistance to Cisplatin when introduced into A2780 cells and inhibited the sequence specific DNA binding activity of p53 protein in vitro. This indicates that inactivation of p53 function confers Cisplatin resistance in these ovarian tumor cells.

The hypothesis that ovarian cancer cells with functional p53 are more sensitive to Cisplatin is furthermore supported by the findings of gene therapy studies. Introduction of wildtype *p53* via adenovirus gene transfer into A2780/CP cisplatin resistant cells significantly sensitized these cells to platinum cytotoxicity, indicating that *p53* was involved in resistance to cisplatin (Song et al. 1997).

Further strong evidence for the importance of a functional p53 protein for the efficacy of Cisplatin and Carboplatin is given by a database of the National Cancer Institute on drug activity in cell lines (Weinstein et al. 1997). This database compares activity patterns of chemotherapeutic agents and possible targets or modulators of activity in the cells, such as oncogenes, tumor-suppressor genes, drug-resistance-mediating transporters and others for more than 60.000 compounds against a panel of 60 human cancer cell lines. The results show a strong correlation between *p53* wildtype sequence respectively *p53* function in a yeast based assay and efficacy of Cisplatin and Carboplatin (Weinstein et al. 1997). As opposed to this, antimitotic tubulin-active agents such as Taxol show a strong negative correlation between *p53* wildtype as well as p53 function and activity of the drug (Weinstein et al. 1997).

Since a dysfunctional p53 can not mediate the apoptotic process, tumors with *p53* mutations or altered p53 protein may become resistant to platinum-based chemotherapy (Lowe et al. 1994). In our study in a subgroup of 72 patients, who

received Cisplatin or Carboplatin / Cyclophosphamide combination therapy, we found a significant correlation between p53 protein overexpression and resistance to platinum-based chemotherapy ($p=0.001$). If all *p53* mutations were taken into account, there was only a trend but not a significant association with treatment response ($p=0.071$). Interestingly though, we found that missense mutations, when compared to wildtype *p53* or other mutations, were correlated with a high percentage of chemotherapy resistance in this cohort ($p=0.008$). This is consistent with the results of two other studies which have demonstrated a correlation between p53 alterations and resistance to platinum-based chemotherapy in ovarian cancer (Righetti et al. 1996, Buttitta et al. 1997). One study analyzed p53 overexpression and mutations in 32 cases of ovarian cancer FIGO stage III and IV and found a higher frequency of chemotherapy-resistance both in p53 overexpressing tumors and in tumors with missense mutations (Righetti et al. 1996). Another study, analysing 33 cases of advanced ovarian cancer FIGO III and IV found a significant association between chemotherapy-resistance and p53 immunostaining, as well as SSCP alterations (Buttitta et al. 1997). These results are further supported by two immunohistochemical studies. p53 overexpression was found to be associated with poor response to either paclitaxel/platinum or cyclophosphamide/ platinum chemotherapy in 54 stage III and IV patients with results approaching statistical significance (Goff et al. 1998). A higher frequency of early tumor progression was found in 28/59 patients who had received either cisplatin and treosulfan or treosulfan alone (Petty et al. 1998). In one immunohistochemical study, a dose-dependent response to platinum-based chemotherapy was found only in p53 negative, but not in p53 positive tumors (Marx et al. 1998). And a more recent study, which analyzed 168 primary stage III-IV ovarian carcinomas showed p53 overexpression to be significantly correlated with resistance to a platinum based chemotherapy in those patients who underwent pathologic assessment of response (Ferrandina et al. 1999). However, three other studies using immunohistochemistry (van der Zee et al. 1995, Herod et al. 1996, Viale et al. 1997) and one study using temperature gradient gel electrophoresis and immunohistochemistry (Röhlke et al. 1997) did not find a difference in treatment response between patients with or without p53 alterations.

Interestingly, missense mutations seem to have a different effect on p53 function in terms of apoptosis than other mutations. Recently, it was shown that certain types of mutations such as the p53His175 mutant and the p53His179 mutant substantially reduce the rate of etoposide-induced apoptosis, whereas other mutations had a much milder effect (Blandino et al. 1999). This suggests that certain types of mutation may have a selective gain of function, which may compromise the efficacy of cancer chemotherapy.

Recently, small synthetic molecules have been identified which not only promote the stability of wild-type p53 protein but also allow mutant p53 to maintain an active conformation (Foster et al. 1999). Further work on these compounds may open new perspectives to overcome an impaired p53 function in combination with chemotherapy.

In contrast to these findings, sensitivity to Taxol appears to be increased through the absence of functional p53 protein because of increased G2M arrest and p53 independent apoptosis (Wahl et al. 1996, Vikhanskaya et al. 1998). Interestingly, though numbers are very small, the only patient in our study who was sensitive to Taxol/Carboplatin had high overexpression of p53 protein and a missense mutation in exon 5, while three out of four patients with resistant or refractory disease were immunohistochemically negative and two had wild type p53 sequence.

5.1.7 p53 alterations as a predictor of time to progression and overall survival

To date, only p53 protein overexpression but not *p53* mutations have been shown to be a predictor of poor clinical outcome in ovarian cancer. Several studies have found a correlation between p53 overexpression and shortened survival (Bosari et al. 1993, Henriksen et al. 1994, Hartmann et al. 1994, van der Zee et al. 1995, Klemi et al. 1995, Levesque et al. 1995, Herod 1996, Viale et al. 1997, Eltabakkah 1997, Geisler et al. 1997, 2000, Röhlke et al. 1997, Anttila et al. 1999, Werness et al. 1999), but only few studies have identified p53 as an independent prognostic factor for overall survival (Klemi et al. 1995, Herod et al. 1996, Geisler et al. 1997, 2000, Röhlke et al. 1997) respectively recurrence-free survival (Anttila et al. 1999) in multivariate analysis. However, p53 protein expression was not a significant predictor of poor outcome in seven other studies (Marks et al. 1991, Kohler et al. 1993a, Kupryjanczyk et al. 1993, Sheridan et al. 1994, Niwa et al. 1994, Reles et al. 1996, Ferrandina et al. 1999, Wen et al. 1999). Only five studies found a correlation between p53 overexpression and time to recurrence (van der Zee et al. 1995, Levesque et al. 1995, Röhlke et al. 1997, Werness et al. 1999, Anttila et al. 1999).

p53 overexpression is relatively rare in tumors of low malignant potential but has been identified in 13% of advanced (stage II and III) borderline ovarian tumors and was found to be strongly associated with increased probability of recurrence or progression (Gershenson et al. 1999).

Seven of eight studies though which analyzed *p53* sequence alterations and clinical follow-up data did not find a significant correlation between *p53* mutations and shortened relapse-free or overall survival (Mazars et al. 1991, Kohler et al. 1993a, Kupryjanczyk et al. 1993, Niwa et al. 1994, Sheridan et al. 1994, Buttitta et al. 1997,

Skomedal et al. 1997). Only our previous study found *p53* mutations to be associated with shortened overall survival, but the results reached only marginal statistical significance ($p=0.049$) (Wen et al. 1999).

Most of the *p53* studies examined either *p53* expression or *p53* mutations but not both in study populations of limited size. In our study *p53* overexpression reached only marginal statistical significance as a predictor of poor clinical outcome ($p=0.056$). *p53* mutations and especially those, which were located in highly conserved domains, were clearly correlated with poor overall survival ($p=0.014$ and $p=0.007$). An association between *p53* mutations and overexpression was observed ($p<0.001$) and the most favourable prognosis with a significantly longer time to progression and overall survival was seen in patients with neither *p53* mutation nor overexpression ($p=0.035$, $p=0.007$).

Summarizing these results, we analyzed *p53* protein expression and *p53* sequence alterations in the entire coding region of the gene in 178 frozen ovarian cancer tissues with complete clinical follow-up information. We could demonstrate that *p53* mutations and especially those in evolutionary conserved domains correlate with shortened time to progression and shortened overall survival. Most importantly, evaluation of adjuvant treatment showed that *p53* overexpression as well as *p53* missense mutations were correlated with resistance to platinum-based chemotherapy. This provides further clinical evidence, that the sensitivity of ovarian cancer cells for Cis- or Carboplatin depends on the efficient induction of apoptosis mediated by a functional *p53* protein.

5.2 Alterations of the *mdm2* gene in ovarian cancer

5.2.1 *mdm2* expression and absence of amplification in ovarian cancer

Since *mdm2* is upregulated by p53 in response to DNA damage and subsequently inhibits p53 function and promotes p53 protein degradation, it seemed interesting to analyze *mdm2* alterations in ovarian cancer cases with known p53 mutations and overexpression.

We analyzed the *mdm2* gene by Southern and Northern hybridization but we found neither DNA amplification nor RNA overexpression in any of the 56 ovarian carcinomas analyzed, independently of *p53* status. Since accumulation of mutant p53 protein has been shown to depend on a lack of *mdm2* induction (Haupt et al. 1997, Kubbutat et al. 1997) one would expect that p53 protein accumulation despite wildtype p53 might induce *mdm2* overexpression. Vice versa in cases with p53 mutation but undetectable p53 expression a possible mechanism might be the rapid degradation of p53 through higher levels of MDM2. But none of the p53 alterations in ovarian cancer cases caused *mdm2* alterations detectable by Southern or Northern analysis.

This is consistent with findings in other epithelial tumors. Though *mdm2* has been found to be amplified in more than 30% of sarcomas and amplification was correlated with overexpression of the MDM2 protein (Oliner et al. 1992), amplification in epithelial tumors is rare (as reviewed by Momand and Zambetti 1997). In breast cancer, gene amplification was noted in only 1.7-7.7% (McCann et al. 1995, Marchetti et al. 1995a, Quesnel et al. 1994), and in HPV negative cervical cancer in 2% (Ikenberg et al. 1995). In ovarian cancer, amplification has not been found in any case (Foulkes et al. 1995). MDM2 protein overexpression is rare in ovarian cancer (Foulkes et al. 1995), but has more recently been described in 40% of borderline ovarian tumors (Palazzo et al. 2000).

RNA overexpression was found in sarcomas which showed amplification of the gene (Oliner et al. 1992) and in 6% of non-small cell lung carcinomas (Marchetti et al. 1995b) but is generally rare in epithelial tumors. In ovarian cancer, absence of *mdm2* expression was identified in 18/90 ovarian carcinomas (22%), while 66% showed weak expression and 12% showed strong expression (Tanner et al. 1997). Absence of *mdm2* expression was found to be an independent predictor of poor survival in FIGO III and IV ovarian cancer patients (Tanner et al. 1997) and in non-small cell lung cancer (Ko et al. 2000). Low levels as opposed to high levels of *mdm2* mRNA were found, furthermore, to be associated with poor clinical outcome in soft tissue sarcomas (Taubert et al. 2000).

We found three RNA transcripts of approximately 7.4 kb, 5.5 kb, and 2.8 kb by Northern blot analysis in the ovarian cancer cases. In sarcomas and lung cancers, only a single 5.5 kb transcript had been observed (Oliner et al. 1992, Marchetti et al. 1995b) while in mammary epithelial cell lines, multiple messenger RNAs, ranging in size from 4.5 to 12.5 kilobases, were found. (Gudas et al. 1995). These different sizes of RNA transcripts may be the result of alternative splicing which has been described when *mdm2* was originally cloned and more recently in ovarian and bladder carcinomas (Oliner et al. 1992, Sigalas et al. 1996).

5.2.2 *mdm2* alternative and aberrant splicing in ovarian carcinomas

PCR analysis of the reverse transcribed mRNA and sequencing of the cDNA products revealed numerous *mdm2* splice variants, which were present either instead of, or in addition to, the full length *mdm2* transcript in ovarian cancer tissue. Only 20% of the ovarian carcinomas expressed exclusively the full length *mdm2* RNA and some cases (9%) had no expression while the majority of cases (72%) expressed splice variants. We identified 30 different splice variants and the sizes ranged from 52 bp to 888 bp.

Alternative splicing has been previously described for the *mdm2* gene (Oliner et al. 1992) but only few splice variants were identified in ovarian cancer (Sigalas et al. 1996). The results were not analyzed with regard to *p53* sequencing and immunohistochemistry. Alternative splicing is a common occurrence in a number of different genes and can create isoforms of proteins with extensive sequence overlap but different functions. This has been well described for example for the troponin T gene of rat muscle which exists in an α and β form depending on splice variants (Lewin, 1994). These splice variants include alternatively, either the α or the β exon besides three other exons which are identical in both mRNA transcripts. Another example is the *APC* (adenosis polyposis coli) gene, a tumor suppressor gene altered early in colon carcinogenesis, which is expressed both with and without exon 1 at equivalent levels in brain, heart, and skeletal muscle in humans and mice (Santoro et al. 1997). The resulting APC proteins with different amino-terminal domains potentially have different functions in interaction with other proteins. The expression of APC isoforms is dependent on tissue differentiation indicating that alternative splicing occurs in response to tissue dependent signals as well as signals to differentiate (Santoro et al. 1997).

In ovarian cancer we observed alternative and aberrant splicing. In some of the splice variants, the splice site was located at the exon-intron boundaries, but in others splicing took place within the exon sequence and should therefore be classified as

aberrant splicing. Aberrant splicing, in contrast to alternative splicing, is the splicing of mRNA which is misdirected and does not occur at *de facto* splice sites. Both the tumor susceptibility gene 101 (*TSG 101*) and the fragile histidine triad gene (*FHIT*) mRNAs show evidence of alternative and aberrant splicing (Gayther et al. 1997).

In ovarian cancer, deletions of several hundred basepairs of the *TSG 101* gene, a putative tumor suppressor gene, have been found in 40% of the cases and are thought to be due to aberrant splicing. The breakpoints of these deletions were located at genuine or cryptic splice sites therefore most likely being the result of aberrant splicing (Gayther et al. 1997).

Deletions of the *FHIT* gene which is also thought to be a tumor suppressor gene, occurred in 42% of ovarian carcinomas at exon/intron boundaries and were suspected to be due to alternative splicing (Gayther et al. 1997). Evidence of both alternative and aberrant splicing was furthermore described in breast (Negrini et al. 1996), lung (Fong et al. 1997), head and neck tumors (Virgilio et al. 1996).

In this investigation of malignant, as well as benign ovarian tumors, and normal tissue, we found evidence of expression of normal *mdm2* (1473 bp) coexisting with both alternative and aberrant splicing. We found alternative splicing at the exon/intron boundary in two variants (888 bp, 654 bp) which were missing exon 4-9 and exon 4-11, respectively. These two splice variants had been described previously in ovarian carcinomas but not in normal ovarian tissue and had been named *mdm2-a* and *mdm2-b* (Sigalas et al. 1996). Both variants were found to have transforming ability in NIH 3T3 cells (Sigalas et al. 1996). We found the 654 bp splice variant in almost half of the ovarian carcinomas, but also infrequently in borderline tumors (1/9), and even in one normal ovarian tissue (1/20). The presence of this variant is therefore strongly, but not exclusively, associated with carcinomas.

All other RNA transcripts of 721 bp to 52 bp size resulted from aberrant splicing. Exon 10 and 11 were spliced out completely in all but one of these splice variants and the cryptic acceptor splice site was consistently located within exon 12. The donor splice sites were located at the exon/intron boundaries of exon 4, exon 5, or exon 6 in seven of the splice variants but in the majority of variants within the sequence of exon 3 to exon 9. In one splice variant of 613 bp, the complete exon 5 as well as parts of exon 9, 10 and 11 were deleted, while exon 6, 7 and 8 were contained. All splice variants except, for the 888 bp and the 721 bp variant, completely lose the acidic domain which was suggested to be involved in the regulation of ribosome metabolism (as reviewed by Piette et al. 1997).

Only 13/30 splice variants were spliced in frame. This means that no protein can be synthesized from the 5' RNA fragment. Among the splice variants, which were in frame, all had spliced out the putative nuclear localization signal which is thought to

be located at aa 181-185 (Fakharzadeh et al. 1991), and the nuclear export signal (NES) which is thought to be located at aa 191-199 (Fig. 5, Fig. 24, Table 17). This suggests that even if these RNA transcripts were translated into truncated proteins, there is no function of these MDM2 variants in the nucleus, especially no possible MDM2/p53 interaction. Most importantly though, the majority of splice variants (22/30) lack part or all of the p53 binding sequence at the N-terminal end of the protein, therefore most likely being unable to inhibit and degrade p53 protein. Some of the splice variants splice out the zinc-finger-like sequence which is as yet of unknown function. Other splice variants have lost part or all of the RING finger motif, which was shown to specifically bind to RNA and suggested to play a role for cell cycle regulation (Elenbaas et al. 1996, Argentini et al. 2000).

Furthermore, different *mdm2* transcripts containing or skipping exon 2 according to different promoters have also been described. Translational enhancement of *mdm2* involved a preferential increase in *mdm2* transcription that was initiated from an internal p53-responsive promoter region of the gene (Landers et al. 1994).

Occurrence of multiple MDM2 proteins has been noted in different tissues and is thought to result from alternative splicing. Protein variants of sizes between 78 kD and 12 kD have been found in non-small cell lung cancer and oral squamous cell carcinomas (Maxwell, 1994, Ralhan et al. 2000). The p74 protein, which lacks the N-terminus and does not bind to p53 (Olson et al. 1993) is expressed in response to UV light in a p53-dependent manner (Saucedo et al. 1999). Both internal initiation at AUG codon 50 and alternate splicing can give rise to p76 in cells (Saucedo et al. 1999). A p76 MDM2 protein was found to antagonize the ability of MDM2 to stimulate the degradation of p53 and lead to an increase in the level of p53 (Perry et al. 2000).

Since most of the *mdm2* splice variants lack various functional domains of the gene such as the p53 binding site and the nuclear localization signal, the purpose of the alternative splicing remains unclear. But the fact that splicing is found in the majority of ovarian carcinomas and splice variants of identical sequence occur throughout this cancer cohort as well as in benign tissues suggests that these splice variants have distinct, as yet unknown functions and are not only a by-product of RNA processing.

5.2.3 Loss of p53 binding sequence in *mdm2* splice variants

The MDM2 protein binds to p53, inhibits its function and promotes rapid degradation of the p53 protein (Momand et al. 1992, Haupt et al. 1997, Kubbutat et al. 1997). The p53 binding domain has been located to an N-terminal region of aa 19-102 which is critical for stable interaction with p53 protein in vitro (Chen et al. 1993).

Out of 30 splice variants in ovarian tumors, 20 (67%) were partially and 2 (7%) completely missing the sequence coding for the p53 binding region at aa 19-102. Mapping experiments of the MDM2/p53 interaction domain had shown that N-terminal deletions in MDM2 mutants or internal deletions affecting part or all of this entire region resulted in significantly reduced or absent binding to p53 protein (Chen et al. 1993). Similar binding regions were found by Oliner et al. (1993) who identified a protein sequence of codons 1-118 of MDM2 to be able to interact with full length p53 (Oliner et al. 1993). Other experiments located the p53 binding domain to amino acids 14- 154 (Leng et al. 1995).

Further experiments, though, suggested that amino acid sequences outside of the region between residues 19 and 102 contribute to MDM2/p53 binding, since the smallest mutant that could bind to p53 protein contained amino acids 1 to 294 (Chen et al. 1993). The MDM2 protein sequences which were suggested to be additionally necessary for a stable MDM2/p53 interaction may comprise either amino acids 102 to 294 or 294 to 491 (Chen et al. 1993). Other studies though, showed that the N-terminal 154 amino acids of MDM2 are sufficient for p53 binding in vivo (Leng et al. 1995).

Furthermore, p53 binding can not only be prevented by large deletions but also by point mutations in the *mdm2* sequence (Freedman et al. 1997). Though the wild-type (1-115) fragment of MDM2 was clearly able to bind specifically to p53, two MDM2 mutants with an amino acid exchange at residue 58 and 77, respectively, did not show any detectable level of binding to p53. By binding to conformation-dependent antibodies it was shown that these two MDM2 mutants are not grossly misfolded. Site directed mutagenesis yielded mutations of two additional amino acids of MDM2 (D68 and V75) that prevented binding to p53 in vitro. In a functional assay MDM2 with the point mutations also failed to regulate p53 dependent transactivation of target genes, which is consistent with the assumption that a physical interaction between the two proteins is required for MDM2's inhibition of p53 activity (Freedman et al. 1997).

Given these experimental results, most of the splice variants which we found in ovarian cancers would be expected to be unable to bind p53. Only eight splice variants contained the complete p53 binding sequence. All of these were spliced with a frame shift so that only a 5' portion of 316 to 696 basepairs could potentially code for a protein that binds to p53, comprising 105 to 232 amino acids of the N-terminal portion of the protein. These splice variants, though containing the entire p53 binding sequence, still lack additional supportive protein sequences which may be required for MDM2/p53 interaction.

In mapping experiments (Chen et al. 1993) the smallest MDM2 mutant that could bind to p53 comprised aa 1-294, while two smaller mutants comprising aa 1-222

and 6-204 were unable to bind to p53. In ovarian cancer five *mdm2* splice variants have previously been identified that were all lacking part of the p53 binding sequence (Sigalas et al. 1996). Interestingly though, the smallest of the splice variants which retained the largest part of the p53 binding domain consisting of a 5' portion of 225 basepairs of the coding region was clearly shown to bind to p53 in co-immunoprecipitation experiments (Sigalas et al. 1996). This is in contradiction to the hypothesis that a complete p53 binding sequence plus additional protein sequences are required for binding (Chen et al. 1993).

Recently, a highly conserved *mdm2* exon α has been identified in human and dog DNA (Veldhoen et al. 1999). The exon is located between exon 4 and 5 of *mdm2* and codes for additional 29 amino acids. Expression of exon α disrupts in vitro translation of the p53 binding domain of MDM2. The putative MDM2 α protein lacks the N-terminus of MDM2 and shows little if any binding capacity to p53 (Veldhoen et al. 1999).

Nevertheless, among the splice variants identified in this ovarian tumor cohort, those which were found most frequently were all missing a large portion of the p53 binding sequence making a MDM2/p53 interaction probably impossible. Some rare splice variants contained the full binding sequence, but these sequences are probably still too short to allow a stable MDM2/p53 interaction. Therefore, we assume that the splice variants which we see in ovarian tumors do not play a role for p53 inhibition, but may possibly fulfill other as yet unknown functions.

5.2.4 *mdm2* splice sites and repeat sequences

The pattern of splicing in many of the variants was interesting since the splice donor and acceptor sites were in regions of exact sequence homology. A sequence of up to 10 bp as for example TTCAAATGAT in the 259 bp splice variant was found at the 3' end of the donor site as well as at the untranscribed end of the downstream acceptor splice site. The pattern of deletions between short direct repeats was similar to data from a DNA polymerase delta (pol 3) in *Saccharomyces cerevisiae* (Tran et al. 1996). A mutation of pol 3 caused an approximately 1000-fold increase in 7-61 deletions between repeat sequences. To clarify whether the deletions in *mdm2* cDNA could also result from genomic deletions in the DNA sequence, we performed PCR at the expected site of loss, but did not identify any deletions in genomic *mdm2* DNA (data not shown).

Interestingly several splice variants, though different in length shared either an identical cryptic acceptor site sequence or donor site sequence. This has been observed for three donor sites and two acceptor sites, each of which are identical for

two, three or four splice variants. An identical donor site had been described previously for *mdm2*-a (888 bp) and *mdm2*-b (654 bp) (Sigalas et al. 1996). Similar observations have been made for splice variants of the *TSG101* gene sharing proximal or distal breakpoints in ovarian cancer (Gayther et al. 1997).

5.2.5 *mdm2* alterations in ovarian cystadenomas and borderline tumors

In ovarian cystadenomas and ovarian tumors of borderline malignancy alternative and aberrant splicing of *mdm2* was also frequent, but the pattern of splicing was different from ovarian carcinomas. Expression of full length *mdm2* was usually present except for three cases, two of which had no detectable *mdm2* mRNA at all. Besides full length *mdm2*, expression of small splice variants was frequent. The 221 bp splice variant was even notable in 5/9 LMP tumors (56%) as opposed to 16% of the ovarian carcinomas. The *mdm2*-b splice variant though, which is not only frequent in ovarian cancer (41%) but also correlated with poor grade of differentiation and other unfavourable prognostic criteria, was rarely seen in borderline tumors (1/9) and in no case of cystadenomas.

Little is known about *mdm2* splicing in benign tumors of the ovary and nothing about LMP tumors. Only five cases of benign ovarian tumors have been analyzed for splice variants and one out of these was described to have alternative splicing without mentioning the exact size of the splice variant (Sigalas et al. 1996).

Our results clearly show that the *mdm2*-b splice variant predominantly, but not exclusively, occurs in ovarian carcinomas, while small splice variants are frequently seen coexisting with the full length transcript in tumors of borderline malignancy and benign ovarian tumors. This suggests that the *mdm2*-b splice variant is either involved directly in carcinogenesis or that RNA processing is indirectly affected by alterations of other cell cycle related genes, leading to *mdm2* alterations.

5.2.6 *mdm2* alterations in normal ovarian tissue

Surprisingly, *mdm2* alternative splicing also occurred in normal ovarian tissue. Full length *mdm2* was, like in ovarian cancer, missing in 2/20 cases (10%). In almost half of the cases small splice variants were noted besides the full length transcript. This is in contrast to previous reports which only found the full length *mdm2* transcript in normal tissue (Sigalas et al. 1996).

mdm2 is thought to be expressed under normal conditions only during, but not after embryonic development. During early embryogenesis, the expression of *xmdm2*, the xenopus laevis homolog of *mdm2*, increases from oocyte stage I/II to reach its maximum in oocyte stage V/VI in unfertilized eggs and then becomes undetectable by

Northern blot analysis in various differentiated normal tissues after embryonic development (Marechal et al. 1997). Since p53 is stored as a cytoplasmic pool until fertilization, *xm2* expression is possibly independent of transcriptional activation by p53 (Marechal et al. 1997). In the normal ovarian tissue cases of our study, *mdm2* expression patterns did not correlate with pre- or postmenopausal status. Therefore, presence or absence of oocytes does not seem to have an influence on *mdm2* expression and *mdm2* splicing.

Alternative splicing in normal tissue is well known under physiological conditions, for example for muscle proteins such as troponin, but has also been noted for other genes which are typically involved in tumorigenesis. Aberrant splicing in up to 50% of normal tissue or cells including peripheral blood, immortalized B-cell lines and lung parenchyma has been described for the *TSG 101* gene (Gayther et al. 1997, Lin et al. 1998). Some of the splice variants were found more frequently in normal cells and the spectrum of splice variants seemed to differ between tumor and normal samples (Gayther et al. 1997). Deletions that are thought to result from alternative splicing were also found for the *FHIT* gene in normal lymphocytes (Druck et al. 1997). However, concerning other genes which are involved in tumorigenesis, alternative splicing still remains to be a rare phenomenon in normal cells. In normal peripheral blood samples, no mis-splicing of *BRCA1*, *BRCA2*, *BRUSH1*, *hMSH2*, IGF2 receptor *PGDB* or *RB* was seen (Gayther et al. 1997).

In our study 221 bp splice variant was found in 40% of the normal ovaries. This is interesting since this variant is rare in ovarian carcinomas and if present, is associated with a more favourable outcome in terms of survival. Remarkably, the splice variant *mdm2-b* which seems to be clearly associated with a more aggressive type of ovarian carcinomas, was found in abundance and as the sole transcript in the normal ovary of one woman who died of liver failure. Generally, presence or absence of splicing in normal ovarian tissue was not related to age, day of menstrual cycle or menopause. Interestingly though, if the uterus and ovaries had been removed for a benign disease, *mdm2* splicing was rare as opposed to those cases in which the contralateral ovary or the uterus had been affected by cancer.

The presence of *mdm2* splice variants in normal ovarian tissue suggests that *mdm2* splicing is not generally associated with malignant transformation of cells. It remains unclear though, which possible function a splice variant of 221 bp could have that splices out most of the functional regions of the gene and in addition is spliced out of frame. The fact that it occurs predominantly in normal tissue and borderline tumors raises the question whether it is a waste product of RNA processing in an otherwise normally functioning *mdm2* gene. Interestingly though, a distinct pattern of splice variants in normal tissue as opposed to ovarian cancer is notable.

5.2.7 In vitro expression of p53 and MDM2 proteins

Full length MDM2, p53 and *mdm2* splice variant sequences were cloned into the pcDNA3 expression vector and transient transfection of vaccinia virus infected HeLa cells with the vector construct was used to express MDM2 and p53 proteins. We were able to express the full length MDM2 and p53 protein as well as a 40 kD protein from the *mdm2*-b (654 bp) splice variant. Two smaller splice variants, both spliced in frame, did not express a protein detectable on Western blot, possibly due to degradation of the protein. Most of the splice variants were not suitable for these experiments at all because of out of frame splicing.

We attempted to analyze binding of the splice variants to p53 by co-immunoprecipitation experiments and were able to show binding between full length MDM2 and full length p53, which is a requirement for further binding experiments (data not shown). The co-immunoprecipitation experiments of p53 and *mdm2* splice variants though, could not be successfully completed yet. Mapping studies have already shown that the N-terminal region between aa 19 and 102 is most likely necessary for p53 binding (Chen et al. 1993). Co-immunoexpression experiments have shown that *mdm2*-b and other splice variants which lack a major portion of the p53 binding site are unable to bind p53 (Sigalas et al. 1996).

Different sizes of MDM2 proteins have been noted previously in cells and have been suggested to stem from alternative splicing. Besides the normal size MDM2 protein of 90 kD, four additional polypeptides (p85, p76, p74, and p58-p57) were identified in mouse cells (Olson et al. 1993). Antibody binding experiments revealed that p76/74 have lost the N-terminal epitopes and the p58/p57 protein is missing the carboxy-terminus epitope (Olson et al. 1993). Similar sizes of proteins of 76/78 kD, 57/59 kD and 46 kD which were identified in non small cell lung cancer were associated with different nuclear substructures and may potentially interact with transcription factors other than p53 (Maxwell, 1994). The presence of distinct MDM2 proteins of 54kD-68kD was also confirmed in breast epithelial cells (Gudas et al. 1995). In oral carcinomas three isoforms of MDM2 (90 kD, 76 kD, and 57 kD) were identified and showed differential compartmentalization in the cells (Ralhan et al. 2000).

The splice variants though, which we found by RT-PCR and sequencing, were mostly much smaller in size. One of the larger variants of 654 bp codes for an approximately 40kD protein, but we were unable to express smaller proteins which may have been too unstable.

5.2.8 Correlation of *mdm2* and *p53* alterations

p53 mutations often lead to accumulation of the altered protein due to a prolonged half-life. However, protein accumulation was also seen in 38% of the ovarian carcinomas which had the wildtype *p53* sequence. Since MDM2 promotes nuclear export and degradation of the *p53* protein, our hypothesis was that cases with *p53* protein overexpression in the absence of mutation might have *mdm2* alterations, which cause accumulation of normal *p53* protein. In fact, in this group we found *mdm2* alterations in 11/13 cases (85%). Cases with *p53* mutation and *p53* overexpression also had a high proportion of abnormal *mdm2* (71%). Cases without normal *p53* expression, regardless of whether they had a wildtype or mutated *p53* sequence, had a lower percentage of *mdm2* alterations (63%), but the results did not reach statistical significance.

p53 mutations were not correlated with any form of *mdm2* alternative or aberrant splicing. However, *p53* protein overexpression was found significantly more often in cases with the *mdm2*-b splice variant. Wildtype *p53* protein stabilization through *mdm2* splicing has also been found in glioblastomas (Kraus et al. 1999). This is consistent with findings in MDM2 mutant experiments. Expression of the MDM2 mutant (Δ 222-437) not only failed to target degradation of *p53*, but also resulted in a significant elevation of *p53* levels (Kubbutat et al. 1997). Since these cells express endogenous full length MDM2, it was suggested that the MDM2 mutant can, at significantly high levels of overexpression, act in a dominant negative manner, protecting *p53* from degradation by endogenous MDM2 protein (Kubbutat et al. 1997).

These results are corroborated by recent findings about p76 MDM2, a protein which lacks the first 49 amino acids of p90 MDM2. Overexpression of p76 MDM2 was shown to antagonize the ability of MDM2 to stimulate the degradation of *p53* and lead to an increase in the levels and activity of *p53* (Perry et al. 2000). Furthermore, the *mdm2*-P2 promoter which is a transcriptional target of *p53*, was found overexpressed in oral carcinomas which both overexpressed MDM2 and *p53* proteins despite wild-type *p53* sequence. The authors suggest that enhanced translation of *mdm2*-P2 transcripts may represent an important mechanism of overexpression, subsequent stabilization and functional inactivation of *p53* (Ralhan et al. 2000).

Although we observed expression of both full length and splice variant *mdm2*, especially the *mdm2*-b splice variant is present in abundant quantity in many cases of ovarian cancer. It may therefore, have a dominant negative effect even if it coexists with the full length *mdm2* transcript. Since this splice variant has lost the *p53* binding ability, it may cause accumulation of the *p53* protein despite *p53* wildtype sequence.

5.2.9 Correlation of *mdm2* alterations with histopathological and clinical data

The *mdm2*-b splice variant (654 bp) was not only the most frequent *mdm2* alteration in ovarian cancers and rare in borderline tumors as well as normal tissues. It was also significantly correlated with more aggressive tumors of high grade, high S-phase fraction and presence of residual tumor after surgery. All of this is contributing to a poorer outcome of these tumors in terms of survival. This confirms the results of a previous study in which *mdm2* splice variants were associated with poor differentiation and advanced stage (Sigalas et al. 1996).

These findings indicate that this specific form of *mdm2* splicing plays a role in tumorigenesis and tumor progression. Similar observations were made for astrocytic neoplasms. *mdm2* splice variants, predominantly *mdm2*-b, were significantly more often found in glioblastomas than in lower grade astrocytomas (Matsumoto et al. 1998). The *mdm2*-b splice variant, as well as other variants, were found to have transforming ability in NIH 3T3 cells (Sigalas et al. 1996).

Given that most of the splice variants lack a major part of the p53 binding domain, we assume that they cannot inhibit p53 function. But since p53 itself is dysfunctional through mutations in most of the ovarian cancer cases, this does not lead to a more stable p53 function for cell cycle control and apoptosis. Mechanisms which cause *mdm2* splicing though might be an attempt to disrupt MDM2/p53 interaction in a cell that has undergone DNA damage in order to prevent *mdm2* mediated p53 inhibition and degradation.

5.2.10 *mdm2* alterations and clinical outcome in ovarian cancer

Absence of the full length *mdm2* transcript and presence of splice variants was significantly associated with increased resistance to platinum-based chemotherapy in ovarian cancer. This is, though numbers are small, an interesting but unexpected result. Current knowledge about platinum based chemotherapy and cell cycle regulation suggests that a functional p53 is necessary to induce apoptosis (Lowe et al. 1993). Resistance to chemotherapy has been found in our study and by others more frequently in tumors with p53 overexpression and p53 missense mutations. A functional MDM2 would inhibit p53 and therefore, potentially make the tumor less prone to undergo apoptosis after treatment with chemotherapy. In contrast, *mdm2* splice products which have lost p53 binding ability, might indirectly contribute to p53 stability and enhance its function. Recent experiments with fibroblasts from *p53/mdm2* null mice have shown, that loss of *mdm2* can induce the p53-dependent apoptotic pathway in vivo (de Rozières et al. 2000).

However, the opposite was suggested by our results. Tumors with functional *mdm2* were more sensitive to chemotherapy than those with splice variants. Among tumors resistant to platinum based chemotherapy is a high percentage of cases with *p53* alterations. Mutant *p53* though, does not induce *mdm2* in the same manner as wildtype *p53*, possibly leading to undetectable amounts of *mdm2* full length transcript. The underlying regulatory mechanisms for this result remains presently unclear. Further studies would be needed to clarify whether chemotherapy-sensitivity actually depends on a functional *mdm2*, or whether the above described findings are indirectly influenced by *p53* alterations.

In terms of prognosis, no correlation was found between presence of full length *mdm2* nor presence of *mdm2* alterations in general, and clinical outcome. A trend though, towards poorer outcome was noted in cases that expressed the *mdm2*-b splice variant, which also correlated with clinical and histopathological indicators of poor prognosis such as grading and residual tumor after surgery. The clinical correlations of *mdm2*-b though, suggest that this splice variant is associated with tumorigenesis and tumor progression.

Interestingly, presence of the splice variant 221 bp, which was more frequently seen in benign and normal tissues, was significantly associated with better outcome. Though this splice variant has lost most of the important functional domains, we assume that its occurrence is associated with a relatively intact cell cycle regulation and less aggressive tumors. However, further studies will be necessary to clarify whether alternative and aberrant splicing of *mdm2* is important in tumorigenesis and progression of ovarian cancer, or whether these transcripts are merely a product of altered mRNA splicing fidelity that occurs more commonly and in a different pattern in tumors as compared to normal tissues.

Summarizing these results, we could demonstrate that *mdm2* alternative and aberrant RNA splicing is frequent in ovarian tumors as well as normal ovaries. Distinct splicing patterns were identified in ovarian carcinomas as opposed to benign tumors and normal tissue. The most frequent of the splice variants, *mdm2*-b, correlates with *p53* protein accumulation in ovarian cancer as well as features of biologically more aggressive tumors.

6. SUMMARY AND CONCLUSIONS

Background: The *p53* tumor suppressor gene, the ‘guardian of the genome’ (Lane, 1992), is involved in key responses to genotoxic stress and plays a central role in the maintenance of genomic stability. Activation of *p53* in response to DNA damage is associated with a rapid increase in its level and with an increased ability of *p53* to bind DNA and mediate transcriptional activation. Upon low or repairable levels of DNA damage, *p53* mediates delay or arrest of replication to give the cell the opportunity to repair the damage before its fixation and propagation. Upon high or irreparable DNA damage, *p53* promotes apoptosis. Mutations of the gene which inactivate some or all of *p53*’s functions provide a selective advantage for clonal expansion of neoplastic cells.

Functional *p53* must be tightly regulated and the *mdm2* (murine double minute 2) gene plays an important role in this regulation. The transcription of the *mdm2* oncogene is induced by the *p53* gene after DNA damage. The MDM2 protein then binds to *p53* and downregulates it in an autoregulatory feedback loop. MDM2 inhibits *p53* transcriptional activity, promotes nuclear export to the cytoplasm and rapid degradation of the *p53* protein. It, therefore, plays a crucial role as a regulator of *p53* in early embryonic development and for recovery of cellular proliferation after repair of DNA damage.

The aim of this study was to analyze the frequency and type of *p53* and *mdm2* alterations in ovarian cancer and to correlate the results with clinico-pathological variables, response to chemotherapy and clinical outcome of the patients.

Methods: 178 cases of primary epithelial ovarian cancer, snap frozen and stored at -80°C, were used in this study. Mutations of the entire *p53* coding sequence (exons 2-11) were analyzed by SSCP (Single Strand Conformation Polymorphism) and DNA-sequencing. *p53* protein expression was analyzed immunohistochemically with the monoclonal Ab DO7 in frozen tissue sections. *p53* was considered to be overexpressed, if more than 10% of the nuclei in the sections showed immunostaining. Clinical follow-up of the ovarian cancer patients was documented up to 12 years. In the total cohort, the median time of follow-up was 31 months and among the survivors, 52 months. 74 patients who received Cis- or Carboplatin in combination with Cyclophosphamide were evaluated for platinum-sensitivity.

Analysis of the *mdm2* gene for alternative splicing was performed by using PCR amplification of full length *mdm2* cDNAs. Total RNA was reverse transcribed into cDNA, and then the cDNA was amplified by nested PCR. Cases with RT-PCR products other than the full length *mdm2* cDNA were cloned into a pCR 2.1 vector and

sequenced or the PCR products were directly sequenced. *p53* and *mdm2* splice variant cDNAs were cloned into a pcDNA3 expression vector. p53 and MDM2 full length and *mdm2* splice variant proteins were expressed in vitro by transient transfection of the pcDNA3 constructs into HeLa-cells. The HeLa cells had been previously infected with the vTF7-3 virus, a recombinant vaccinia virus encoding bacteriophage T7 RNA polymerase.

Results: *p53* mutations were seen in 56% (99/178) of the ovarian cancer cases of which 72% were missense mutations. *p53* overexpression (> 10% positively stained nuclei) was seen in 62% (110/178) of cases. 62% of the *p53* mutations were located in the evolutionary highly conserved domains of the gene. *p53* mutations were significantly correlated with shortened time to progression ($p=0.028$) and poor overall survival of the patients ($p=0.015$). Comparing clinical outcome of patients with mutations in highly conserved domains with those who had either wildtype *p53* or a mutation in a nonconserved domain, the difference in time to progression ($p=0.007$) and overall survival was even more obvious ($p=0.005$). Furthermore, time to progression and overall survival were seen to be shorter in patients with *p53* overexpression as compared to normal *p53* expression, but the results only reached marginal statistical significance ($p=0.073$, $p=0.058$). Patients with *p53* overexpression ($p=0.001$) or *p53* missense mutations ($p=0.008$) were significantly more often platinum resistant than patients without *p53* alterations. Overall, the most favorable prognosis in terms of overall survival was seen in patients who had wildtype *p53* sequence and normal *p53* expression, as opposed to those who had either one or both alterations of the *p53* gene and protein ($p=0.007$).

Besides *p53* mutations 45 sequence alterations were identified and considered polymorphisms. The codon 72 arginine→proline polymorphism was identified in 5% (9/178) of the cases. Furthermore, alterations were found at codon 36 (exon 4), codon 213 (exon 6), codon 224 (exon 6), and codon 231 (exon 7). The 16 basepair repeat polymorphism of intron 3 was identified in 14% (24/178) of the cases. Three novel intron alterations were identified by sequencing the introns 6 and 10. A g→c nucleotide exchange at position 13964 in intron 6 was found in two cases. An a→t polymorphism was found at nucleotide 17708 of intron 10 in a frequency of 1.1% and a c→t polymorphism at nucleotide 18550 of intron 10 in a frequency of 2.3%. Both intron 10 polymorphisms were confirmed in normal tissue of the patients. Most of the cases (7/8) with intron 6 or intron 10 polymorphisms showed *p53* over-expression.

The *mdm2* gene was neither amplified nor overexpressed in any of the ovarian cancer cases. An mRNA transcript of 7.4 kb, 5.5 kb and 2.8 kb was seen at normal levels in all ovarian carcinomas. However, *mdm2* alternative or aberrant splicing was

seen in 66/92 (72%) of the ovarian carcinomas, 7/9 (78%) of borderline tumors, 5/6 (83%) of benign ovarian cystadenomas and 11/20 (55%) of the normal ovarian tissues. A total of 30 splice variant sequences were identified. 67% of these had a partial and 7% a complete loss of the p53 binding site. 28/30 splice variants do not splice at exon/intron boundaries but use cryptic splice sites within exons and were therefore considered aberrant splice variants.

A 654 bp splice variant (*mdm2*-b) was expressed in 41% of ovarian carcinomas, but only in 1/9 (11%) borderline tumors, none of the benign cystadenomas, and 1/20 (5%) normal ovaries. This splice variant splices out exon 4-11, including 90% (81 of 90 amino acids) of the 3' end of the p53 binding domain as well as the nuclear localization signal (NLS) and the nuclear export signal (NES). Expression of this splice variant in ovarian carcinomas was significantly correlated with poor grade of differentiation ($p=0.004$), residual tumor after surgery ($p=0.004$), and high S-phase fraction ($p=0.016$) of ovarian carcinoma. Presence of *mdm2*-b was furthermore correlated with p53 protein overexpression ($p=0.018$). A small splice variant of only 221 bp, which has lost most of the functional *mdm2* domains was present in only 16% of the ovarian carcinomas but in 5/9 (56%) of borderline tumors, 1/6 of the cystadenomas, and interestingly also in 8/20 (40%) of the normal ovarian tissues. The 221 bp splice variant was correlated with early stage of ovarian cancer (FIGO I and II) and longer overall survival ($p=0.048$).

The absence of the full length *mdm2* transcript respectively, the presence of *mdm2* splice variants in general were correlated with a higher proportion of ovarian carcinomas, which were resistant or refractory against a platinum-based chemotherapy but were not correlated with survival.

Depending on the diagnosis for which the patient underwent surgery, different *mdm2* RNA splicing patterns were seen in normal ovarian tissue. The presence of splice variants in the unaffected normal ovary was significantly correlated with the diagnosis of gynecological cancer, either in the contralateral ovary or in the uterine cervix or endometrium ($p=0.017$).

Conclusions: *p53* mutations are present in more than 50% of epithelial ovarian carcinomas and are associated with early progression and shortened overall survival. Mutations in evolutionary conserved domains correlate with significantly shorter survival, compared to mutations in nonconserved regions and *p53* wildtype sequence. *p53* protein overexpression reached only marginal statistical significance as a predictor of clinical outcome. With multivariable analysis however, *p53* alterations were not an independent prognostic factor. Evaluation of adjuvant treatment showed that *p53* overexpression as well as *p53* missense mutations were correlated with resistance to

platinum-based chemotherapy. This provides further clinical evidence that the sensitivity of ovarian cancer cells for Cis- or Carboplatin depends on the efficient induction of apoptosis mediated by a functional p53 protein.

mdm2, which inhibits p53's transcriptional activity and downregulates it in an autoregulatory feedback-loop by promoting nuclear export and rapid degradation of the protein, was found to be frequently altered in ovarian carcinomas. *mdm2* alternative and aberrant splicing was found in the majority of ovarian carcinomas and borderline tumors, but also in cystadenomas and normal ovarian tissue. A distinct difference in patterns of splice variants was notable in comparing benign and malignant tissues. While the *mdm2*-b splice variant was found in nearly 50% of the ovarian carcinomas and was associated with more advanced and histologically more aggressive tumors, smaller size variants were typically seen in early stage ovarian carcinomas and benign tissues.

The *mdm2* splice variants mostly lack part, or all of the p53 binding sequence. *mdm2* alterations appear to stabilize p53 protein and may cause p53 accumulation in the absence of *p53* mutation. If these results are corroborated by other investigators, alterations of *mdm2* may be considered to be an important step in carcinogenesis and may have important implications for the response to chemotherapy and clinical course of ovarian carcinomas.

Since most of the *mdm2* splice variants lack various functional domains of the gene, such as the p53 binding site and the nuclear localization signal, the purpose of the alternative splicing remains unclear. But the fact that splicing is found in the majority of ovarian carcinomas and splice variants of identical sequence occur throughout this cancer cohort and in benign tissues, suggests that these splice variants have distinct, as yet unknown functions and are not simply a by-product of RNA processing.

References

- Agorastos, T., Lambropoulos, A.F., Constantinidis, T.C., Kotis, A., and Bontis, J.N. P53 codon 72 polymorphism and risk of intra-epithelial and invasive cervical neoplasia in Greek women. *Eur. J. Cancer Prev.* 9: 113-118, 2000
- Ahuja, H.G., Testa, M.P., and Cline, M.J. Variation in the protein coding region of the human p53 gene. *Oncogene* 5: 1409-1410, 1990
- Angelopoulou, K., Levesque, M.A., Katsaros, D., Shipman, R., and Diamandis, E.P. Exon 5 of the p53 gene is a target for deletions in ovarian cancer. *Clin. Chem.* 44: 72-77, 1998
- Aunoble, B., Sanches, R., Didier, E., and Bignon, Y.-J. Major oncogenes and tumor suppressor genes involved in epithelial ovarian cancer (Review). *Int. J. Oncol.* 16: 567-576, 2000
- Anttila, M.A., Ji, H., Juhola, M.T., Saarikoski, S.V., and Syrjänen, K.J. The prognostic significance of p53 expression quantitated by computerized image analysis in epithelial ovarian cancer. *Int. J. Gynecol. Pathol.* 18: 42-51, 1999
- Argentini, M., Barboule, N., and Wasylyk, B. The contribution of the RING finger domain of MDM2 to cell cycle progression. *Oncogene* 19: 3849-3857, 2000
- Arrowsmith, C., and Morin, P. New insights into p53 function from structural studies. *Oncogene* 12: 1379-1385, 1996
- Averette, H.E., Janicek, M.F., and Menck, H.R. The national cancer data base report of ovarian cancer. *Cancer* 76: 1096-1103, 1995
- Avigad, S., Barel, D., Blau, O., Malka, A., Zoldan, M., Mor, C., Fogel, M., Cohen, I.J., Stark, B., Goshen, Y., Stein, J., and Zaizov, R. A novel germ line p53 mutation in intron 6 in diverse childhood malignancies. *Oncogene* 14: 1541-1545, 1997
- Bakalkin, G., Yakovleva, T., Selivanova, G., Magnusson, K.P., Szekely, L., Kiseleva, E., Klein, G., Terenius, L., and Wiman, K.G. p53 binds single-stranded DNA ends and catalyzes DNA renaturation and strand transfer. *Proc. Natl. Acad. Sci. USA* 91: 413-417, 1994
- Baylin, S.B. Tying it all together: epigenetics, genetics, cell cycle, and cancer. *Science* 277: 1948-1949, 1997
- Beenken, S.W., Karsenty, G., Raycroft, L., and Lozano, G. An intron binding protein is required for transformation ability of p53. *Nucleic Acids Res.* 19: 4747-4752, 1991
- Berchuck, A., Schildkraut, J.M., Marks, J.R., and Futreal, P.A. Managing hereditary ovarian cancer risk. *Cancer* 86: 2517-24, 1999
- Bergh, J., Norberg, T., Sjogren, S., Lindgren, A., and Holmberg, L. Complete sequencing of the p53 gene provides prognostic information in breast cancer patients, particularly in relation to adjuvant systemic therapy and radiotherapy. *Nature Med.* 1: 1029-1034, 1995

- Beroud, C., Verdier, F., and Soussi, T. p53 gene mutation: software and database. *Nucl. Acids Res.* 24: 147-150, 1996
- Blandino, G., Levine, A.J., and Oren, M. Mutant gain of function: differential effects of different p53 mutants on resistance of cultured cells to chemotherapy. *Oncogene* 18: 477-485, 1999
- ten Bokkel Huinink, W., Gore, M., Carmichael, J., Gordon, A., Malfetano, J., Hudson, I., Broom, C., Scarabelli, C., Davidson, N., Spaczynski, M., Bolis, G., Malmström, H., Coleman, R., Fields, S.C., and Heron, J.-F. Topotecan versus paclitaxel for the treatment of recurrent epithelial ovarian cancer. *J. Clin. Oncol.* 15: 2183-2193, 1997
- Bosari, S., Viale, G., Radaelli, U., Bossi, P., Bonoldi, E., and Coggi, G. p53 accumulation in ovarian carcinomas and its prognostic implications. *Human Pathol.* 24: 1175-1179, 1993
- Brown, C.R., Doxsey, S.J., White, E., and Welch, W.J. Both viral (adenovirus E1B) and cellular (hsp 70, p53) components interact with centrosomes. *J. Cell. Physiol.* 160: 47-60, 1994
- Buckbinder, L.R., Talbott, S., Velasco-Miguel, I., Takenaka, B., Faha, B., Seizinger, B.R., and Kley, N. Induction of the growth inhibitor IGF-binding protein 3 by p53. *Nature* 377: 646-649, 1995
- Buller, R.E., Sood, A., Fullenkamp, C., Sorosky, J., Powills, K., and Anderson, B. The influence of the p53 codon 72 polymorphism on ovarian carcinogenesis and prognosis. *Cancer Gene Therapy* 4: 239-245, 1997
- Burghardt, E., Girardi, F., Lahousen, M., Tamussino, K., and Stettner, H. Patterns of pelvic and paraaortic lymph node involvement in ovarian cancer. *Gynecol. Oncol.* 40: 103-106, 1991
- Buttitta, F., Marchetti, A., Gadducci, A., Pellegrini, S., Morganti, M., Carnicelli, V., Cosio, S., Gagettti, O., Genazzani, A.R., and Bevilacqua, G. p53 alterations are predictive of chemoresistance and aggressiveness in ovarian carcinomas: a molecular and immunohistochemical study. *Br. J. Cancer* 75: 230-235, 1997
- Cahilly-Snyder, L., Yang-Feng, T., Francke, U., and George, D. Molecular analysis and chromosomal mapping of amplified genes isolated from a transformed mouse 3T3 cell line. *Somat. Cell. Mol. Genet.* 13: 235-244, 1987
- Canman, C.E., Lim, D.-S., Cimprich, K.A., Taya, Y., Tamai, K., Sakaguchi, K., Appella, E., Kastan, M.B., and Siliciano, J.D. Activation of the ATM kinase by ionizing radiation and phosphorylation of p53. *Science* 281: 1677-1679, 1998
- Carbone, D., Chiba, I., and Mitsudomi, T. Polymorphism at codon 213 within the p53 gene, *Oncogene* 6: 691-692, 1991
- Casey, G., Lopez, M., Ramos, J., Plummer, S., Arboleda, M., Shaughnessy, M., Karlan, B., and Slamon, D. DNA sequence analysis of exons 2 through 11 and immunohistochemical staining are required to detect all known p53 alterations in human malignancies. *Oncogene* 13: 1971-1981, 1996

- Chen, C.-Y., Oliner, J.D., Zhan, Q., Fornace, A.J.Jr., Vogelstein, B., and Kastan, M.B. Interactions between p53 and MDM2 in a mammalian cell cycle checkpoint pathway. *Proc. Natl. Acad. Sci.* *91*: 2684-2688, 1994
- Chen, J., Marechal, V., and Levine, A. Mapping of the p53 and mdm-2 interaction domains. *Mol. Cell. Biol.* *13*: 4107-4114, 1993
- Chen, J., Lin, J., and Levine, A.J. Regulation of transcription functions of the p53 tumor suppressor by the mdm-2 oncogene. *Mol. Med.* *1*: 142-152, 1995
- Chen, J., Wu, X., Lin, J., and Levine, A. Mdm-2 inhibits the G1 arrest and apoptosis functions of the p53 tumor suppressor protein. *Mol. Cell. Biol.* *16*: 2445-2452, 1996
- Chen, L., Agrawal, S., Zhou, W., Zhang, R., and Chen, J. Synergistic activation of p53 by inhibition of MDM2 expression and DNA damage. *Proc. Natl. Acad. Sci. USA* *95*: 195-200, 1998
- Chen, X., Ko, L.J., Jayaraman, L., and Prives, C. p53 levels, functional domains, and DNA damage determine the extent of the apoptotic response of tumor cells. *Genes Dev.* *10*: 2438-2451, 1996
- Cho, Y., Gorina, S., and Pavletich, N. Crystal structure of a p53 tumor suppressor-DNA complex: Understanding tumorigenic mutations. *Science* *265*: 346-355, 1994
- Chuaqui, R.F., Zhuang, Z., and Merino, M.J. Molecular genetic events in the development and progression of ovarian cancer in humans. *Mol. Med. Today* *3*: 207-13, 1997
- Clement, P.B. Histology of the ovary. *Am. J. Surg. Pathol.* *11*: 277, 1987
- Cobleigh, M.A., Vogel, C.L., Tripathy, D., Robert, N.J., Scholl, S., Fehrenbacher, L., Wolter, J.M., Paton, V., Shak, S., Lieberman, G., and Slamon, D.J. Multinational study of the efficacy and safety of humanized anti-HER2 monoclonal antibody in women who have HER2-overexpressing metastatic breast cancer that has progressed after chemotherapy for metastatic disease. *J. Clin. Oncol.* *17*: 2639-2648, 1999
- Conklin, D.S., Galaktionov, K., and Beach, D. 14-3-3 proteins associate with cdc25 phosphatases. *Proc. Natl. Acad. Sci. USA* *29*: 7892-7896, 1995
- Cordon-Cardo, C., Latres, E., Drobnjak, M., Oliva, M., Pollack, D., Woodruff, J., Marechal, V., Chen, J., Brennan, M., and Levine, A. Molecular abnormalities of mdm2 and p53 genes in adult soft tissue sarcomas. *Cancer Res.* *54*: 794-799, 1994
- Counts, J.L., and Goodman, J.I. Alterations in DNA methylation may play a variety of roles in carcinogenesis. *Cell* *83*: 13-15, 1995
- Cox, D.R. Regression models and life-tables, *J. R. Stat. Soc. [B]* *34*: 187-220, 1972
- Cross, S.M., Sanchez, C.A., Morgan, C.A., Schimke, M.K., Ramel, S., Idzerda, R.L., Raskind, W.H., and Reid, B.J. A p53 dependent mouse spindle checkpoint. *Science* *267*: 1353-1356, 1995

- Dang, C.V. c-Myc target genes involved in cell growth, apoptosis, and metabolism. *Mol. Cell. Biol.* 19: 1-11, 1999
- DiCioccio, R.A., Werness, B.A., Allen, H.J., and Piver, M.S. Correlation of TP53 mutations and p53 expression in ovarian tumors. *Cancer Genet. Cytogenet.* 105: 93-102, 1998
- DiCioccio, R.A., and Piver, M.S. A polymorphism in intron 2 of the TP53 gene. *Clinical Genetics* 50: 108-109, 1996
- Dong, Y., Walsh, M.D., McGuckin, M.A., Cummings, M.C., Gabrielli, B.G., Wright, G.R., Hurst, T., Khoo, S.K., and Parsons, P.G. Reduced expression of Retinoblastoma Gene product (pRB) and high expression of p53 are associated with poor prognosis in ovarian cancer. *Int. J. Cancer* 74: 407-415, 1997
- Druck, T., Hadaczek, P., Fu, T.-B., Ohta, M., Siprashvili, Z., Baffa, R., Negrini, M., Kastury, K., Veronese, M.L., Rosen, D., Rothstein, J., McCue, P., Cotticelli, M.G., Inoue, H., Croce, C.M., and Huebner, K. Structure and expression of the human FHIT gene in normal and tumor cells. *Cancer Res.* 57: 504-512, 1997
- Easton, D.F., Ford, D., and Bishop, D.T. Breast and ovarian cancer incidence in BRCA1-mutation carriers. Breast Cancer Linkage Consortium. *Am. J. Hum. Genet.* 56: 265-271, 1995
- Eccles, D., Breet, L., Lessells, A., Gruber, L., Lane, D., Steel, C., and Leonard, R. Overexpression of the p53 protein and allele loss at 17p13 in ovarian carcinoma. *Br. J. Cancer* 65: 40-44, 1992
- Eisenkop, S.M., Friedman, R.L., and Wang, H.J. Complete cytoreductive surgery is feasible and maximizes survival in patients with advanced epithelial ovarian cancer: a prospective study. *Gynecol. Oncol.* 69: 103-108, 1998
- El-Deiry, W.S., Kern, S.E., Pietenpol, J.A., Kinzler, K.W., and Vogelstein, B. Definition of a consensus binding site for p53. *Nature Genet.* 1: 45-49, 1992
- El-Deiry, W.S., Tokino, T., Velculescu, V.E., Levy, D.B., Parsons, R., Trent, J.M., Lin, D., Mercer, W.E., Kinzler, K.W., and Vogelstein, B. WAF1, a potential mediator of p53 tumor suppression. *Cell* 75: 817-825, 1993
- El-Deiry, W.S. Regulation of p53 downstream genes. *Sem. Cancer Biol.* 8: 345-357, 1998
- Elenbaas, B., Dobbelsstein, M., Roth, J., Shenk, T., and Levine, A.J. The MDM2 oncoprotein binds specifically to RNA through its RING finger domain. *Mol. Med.* 2: 439-451, 1996
- Eltabakkah, G.H., Belinson, J.L., Kennedy, A.W., Biscotti, C.V., Casey, G., Tubbs, R.R., and Blumenson, L.E. p53 overexpression is not an independent prognostic factor for patients with primary ovarian epithelial cancer. *Cancer* 80: 892-898, 1997
- Fakharzadeh, S.S., Trusko, S.P., and George, D.L. Tumorigenic potential associated with enhanced expression of a gene that is amplified in a mouse tumor cell line. *EMBO J.* 10: 1565-1569, 1991

- Fathalla, M.F. Incessant ovulation - a factor in ovarian neoplasia? *Lancet* 2: 163, 1971
- Felix, C., Brown, D., Mitsudomi, T., Ikagaki, N., Wong, A., Wasserman, R., Womer, R., and Biegel, J. Polymorphism at codon 36 of the p53 gene. *Oncogene* 9: 327-328, 1994
- Ferrandina, G., Fagotti, A., Salerno, M.G., Natali, P.G., Mottolise, M., Maneschi, F., De Pasqua, A., Benedetti-Panici, P., Mancuso, S., and Scambia, G. p53 overexpression is associated with cytoreduction and response to chemotherapy in ovarian cancer. *Br. J. Cancer* 81: 733-740, 1999
- Fong, K., Biesterveld, E., Vermani, A., Wistuba, I., Sekido, Y., Bader, S., Ahmadian, M., Ong, S., Rassool, F., Zimmerman, P., Giaccone, G., Gazdar, A., and Minna, J. FHIT and FRA3B 3p14.2 allele loss are common in lung cancer and preneoplastic bronchial lesions and are associated with cancer related FHIT cDNA splicing aberrations. *Cancer Res.* 57: 2256-2267, 1997
- Ford, D., Easton, D.F. The genetics of breast and ovarian cancer. *Br. J. Cancer* 72: 805-812, 1995
- Ford, D., Easton, D.F., Stratton, M., Narod, S., Goldgar, D., Devilee, P., Bishop, D.T., Weber, B., Lenoir, G., Chang-Claude, J., Sobol, H., Teare, M.D., Struwing, J., Arason, A., Scherneck, S., Peto, J., Rebbeck, T.R., Tonin, P., Neuhausen, S., Barkardottir, R., Eyfjord, J., Lynch, H., Ponder, B.A., Gayther, S.A., and Zelada-Hedman, M. Genetic heterogeneity and penetrance analysis of the BRCA1 and BRCA2 genes in breast cancer families. The Breast Cancer Linkage Consortium. *Am. J. Hum. Genet.* 62: 676-689, 1998
- Foster, B.A., Coffey, H.A., Morin, M.J., Rastinejad, F. Pharmacological rescues of mutant p53 conformation and function. *Science* 286: 2507-2510, 1999
- Foulkes, W., Stamp, G., Afzal, S., Lalani, N., McFarlane, C., Trowsdale, J., and Campbell, I. MDM2 overexpression is rare in ovarian carcinoma irrespective of TP53 mutation status. *Br. J. Cancer* 72: 883-888, 1995
- Freedman, D.A., Epstein, C.B., Roth, J.C., and Levine, A.J. A genetic approach to mapping the p53 binding site in the mdm2 protein. *Mol. Med.* 3: 248-259, 1997
- Freedman, D.A., Wu, L., and Levine, A.J. Functions of the MDM2 oncoprotein. *Cell. Mol. Life Sci.* 55: 96-107, 1999
- Fujita, M., Enomoto, T., Inoue, M., Tanizawa, O., Ozaki, M., Rice, J., and Nomura, T. Alteration of the p53 tumor suppressor gene occurs independently of K-ras activation and more frequently in serous adenocarcinoma than in other common epithelial tumors of the human ovary. *Jpn. J. Cancer Res.* 85: 1247-1256, 1994
- Fukasawa, K., Choi, T., Kuriyama, R., Rulong, S., and Vande Woude, G.F. Abnormal centrosome amplification in the absence of p53. *Science* 271: 1744-1747, 1996
- Gallagher, W.M., Cairney, M., Schott, B., Roninson, I.B., and Brown, R. Identification of p53 genetic suppressor elements which confer resistance to cisplatin. *Oncogene* 14: 185-193, 1997

- Gayther, S.A., Barski, P., Batley, S.J., Li, L., de Foy, K.A.F., Cohen, S.N., Ponder, B.A.J., and Caldas, C. Aberrant splicing of the TSG101 and FHIT genes occurs frequently in multiple malignancies and in normal tissues and mimics alterations previously described in tumours. *Oncogene* 15: 2119-2126, 1997
- Ge, H., Wong, M.P., Lam, W.K., Lee, J., Fu, K.H., Yew, W.W., and Lung, M.L. p53 intron 2 genotypes detected in normal specimens and lung carcinomas in Hong Kong. *Oncol. Rep.* 5: 1265-1267, 1998
- Geisler, J.P., Geisler, H.E., Wiemann, M.C., Givens, S.S., Zhou, Z., and Miller, G.A. Quantification of p53 in epithelial ovarian cancer. *Gynecol. Oncol.* 66: 435-438, 1997
- Geisler, J.P., Geisler, H.E., Miller, G.A., Wiemann, M.C., Zhou, Z., and Crabtree, W. p53 and bcl-2 in epithelial ovarian carcinoma: their value as prognostic indicators at a median follow-up of 60 months. *Gynecol. Oncol.* 77: 278-282, 2000
- Gershenson, D.M., Deavers, M., Diaz, S., Tortolero-Luna, G., Miller, B.E., Bast, R.C., Mills, G.B., and Silva, E.G. Prognostic significance of p53 expression in advanced-stage ovarian serous borderline tumors. *Clin. Cancer Res.* 5: 4053-4058, 1999
- Goff, B.A., Ries, J.A., Els, L.P., Coltrera, M.D., and Gown, A.M. Immunophenotype of ovarian cancer as predictor of clinical outcome: evaluation at primary surgery and second-look procedure. *Gynecol. Oncol.* 70: 378-385, 1998
- Goh, H., Yao, J., and Smith, D. p53 point mutation and survival in colorectal cancer patients. *Cancer Res.* 55: 5217-5221, 1995
- Gottlieb, E., and Oren, M. p53 facilitates pRb cleavage in IL-3-deprived cells: novel proapoptotic activity of p53. *EMBO J.* 17: 3587-3596, 1998
- Gottlieb, E. and Oren, M. p53 and apoptosis. *Sem. Cancer Biol.* 8: 359-368, 1998
- Graeber, A., Osmanian, C., Jacks, T., Housman, D., Koch, C., Lowe, S., and Graccia, A. Hypoxia-mediated selection of cells with diminished apoptotic potential in solid tumors. *Nature* 379, 88-91, 1996
- Greenblatt, M., and Harris, C. Mutations in the p53 tumor suppressor gene: clues to cancer etiology and molecular pathogenesis. *Cancer Res.* 54: 4855-4878, 1994
- Gu, J., Chen, D., Rosenblum, J., Rubin, R.M., and Yuan, Z.-M. Identification of a sequence element from p53 that signals for Mdm2 targeted degradation. *Mol. Cell. Biol.* 20: 1243-1253, 2000
- Gudas, J.M., Nguyen, H., Klein, R.C., Katayose, D., Seth, P., and Cowan, K.H. Differential expression of multiple MDM2 messenger RNAs and proteins in normal and tumorigenic breast epithelial cells. *Clin. Cancer Res.* 1: 71-80, 1995
- Güssow, D., Rein, R., Ginjaar, I., Hochstenbach, F., Seemann, G., Kottman, A., and Ploegh, H.L. The human β 2-Microglobulin gene. Primary structure and definition of the transcriptional unit. *J. Immunol.* 139: 3132-3138, 1987

- Guidos, C.J., Williams, C.J., Grandal, I., Knowles, G., Huang, M.T.F., and Danska, J.S. V(D)J recombination activates a p53-dependent DNA damage checkpoint in scid lymphocyte precursors. *Genes Dev.* 10: 2038-2054, 1996
- Gurnani, M., Lipari, P., Dell, J., Shi, B., and Nielsen, L.L. Adenovirus-mediated p53 gene therapy has greater efficacy when combined with chemotherapy against human head and neck, ovarian, breast and prostate cancer. *Cancer Chemother. Pharmacol.* 44:143-151, 1999
- Hall, J., Lee, M., Newman, B., Morrow, J., Huey, B., and King, M.C. Linkage of early onset familial breast cancer to chromosome 17q21. *Science* 250: 1684-1689, 1990
- Halpern, J. Maximally selected chi square statistics for small samples. *Biometrics* 38: 1017-1023, 1982
- Hagopian, G.S., Mills, G.B., Khokhar, A.R., Bast, R.C., and Siddik, Z.H. Expression of p53 in Cisplatin-resistant ovarian cancer cell lines: Modulation with the novel platinum analogue (1R,2R-Diaminocyclohexane)(trans-diacetato)(dichloro)-platinum (IV). *Clin. Cancer Res.* 5: 655-663, 1999
- Harlow, E., Williamson, N.M., Ralston, R., Helfman, D.M., and Adams, T.E. Molecular cloning and in vitro expression of a cDNA clone for human cellular antigen p53. *Mol. Cell. Biol.* 5: 1601-1610, 1985
- Harris, N., Brill, E., Shohat, O., Prokocimer, M., Wolf, D., Arai, N., and Rotter, V. Molecular Basis for heterogeneity of the human p53 protein. *Mol. Cell. Biol.* 6: 4650-4656, 1986
- Hartmann, L., Podratz, K., Keeney, G., Kamel, N., Edmonson, J., Grill, J., Su, J., Katzmann, J., and Roche, P. Prognostic significance of p53 immunostaining in epithelial ovarian cancer. *J. Clin. Oncol.* 12: 64-69, 1994
- Haupt, Y., Rowan, S., Shaulian, E., Vousden, K.H., and Oren, M. Induction of apoptosis in HeLa cells by trans-activation-deficient p53. *Genes Dev.* 9: 2170-2183, 1995
- Haupt, Y. and Oren, M. p53-mediated apoptosis: mechanisms and regulation. *Behring Inst. Mitt.* 97: 32-59, 1996
- Haupt, Y., Maya, R., Kazaz, A., and Oren, M. Mdm2 promotes the rapid degradation of p53. *Nature* 397: 296-299, 1997
- Helland, A., Langerod, A., Johnsen, H., Olsen, O.A., Skovlund, E., and Borresen-Dale, A.-L. p53 polymorphism and risk of cervical carcinoma. *Nature* 396: 530-531, 1998
- Henriksen, R., and Oberg, K. p53 expression in epithelial ovarian neoplasms: relationship to clinical and pathological parameters, Ki-67 expression and flow cytometry. *Gynecol. Oncol.* 53(3): 301-306, 1994
- Hermeking, H., Lengauer, C., Polyak, K., He, T.C., Zhang, L., Thiagalingam, S., Kinzler, K.W., and Vogelstein, B. 14-3-3 σ is a p53-regulated inhibitor of G2/M progression. *Mol. Cell* 1: 3-11, 1997

- Herod, J., Eliopoulos, A., Warwick, J., Niedobitek, G., Young, L., and Kerr, D. The prognostic significance of Bcl-2 and p53 expression in ovarian carcinoma. *Cancer Res.* 56: 2178-2184, 1996
- Hildesheim, A., Schiffman, M., Brinton, L.A., Fraumeni, J.F., Herrero, R., Bratti, M.-C., Schwartz, P., Mortel, R., Barnes, W., Greenberg, M., McGowen, L., Scott, D.R., Martin, M., Herrera, J.E., and Carrington, M. P53 polymorphism and risk of cervical carcinoma. *Nature* 396: 530-531, 1998
- Hirai, M., Kelsey, L.S., Maneval, D.C., Vaillancourt, M., and Talmadge, J.E. Adenovirus p53 purging for human breast cancer stem cell products. *Acta Haematol.* 101: 97-105, 1999
- Holschneider, C.H., and Berek, J.S. Ovarian Cancer: Epidemiology, Biology, and Prognostic Factors. *Sem. Surg. Oncol.* 19: 3-10, 2000
- Hollstein, M., Rice, K., Greenblatt, M.S., Soussi, T., Fuchs, R., Sorlie, T., Hovig, E., Smith-Sorensen, B., Montesano, R., and Harris, C.C. Database of p53 gene somatic mutations in human tumors and cell lines. *Nucleic Acids Res.* 22: 3551-3555, 1994
- Howes, K.A., Ransom, N., Papermaster, D.S., Lasudry, J.G.H., Albert, D.M., and Windle, J.J. Apoptosis or retinoblastoma: Alternative fates of phosphoreceptors expressing the HPV-16 E7 gene in the presence or absence of p53. *Genes Dev.* 8: 1300-1310, 1994
- Hsieh, J.-K., Chan, F.S.G., O'Connor, D.J., Mitnacht, S., Zhong, S., and Lu, X. RB regulates the stability and the apoptotic function of p53 via MDM2. *Mol. Cell* 3: 181-193, 1999
- Ikenberg, H., Matthay, K., Schmitt, B., Bauknecht, T., Kiechle-Schwarz, M., Göppinger, A., and Pfeleiderer, A. p53 Mutation and MDM2 amplification are rare even in Human Papillomavirus- negative cervical carcinomas. *Cancer* 76: 57-66, 1995
- Inoue, M., Fujita, M., Enomoto, T., Morimoto, H., Monden, T., Shimano, T., and Tanizawa, O. Immunohistochemical analysis of p53 in gynecologic tumors. *Am. J. Clin. Pathol.* 102 (5): 665-670, 1994
- Israeli, D., Tessler, E., Haupt, Y., Elkeles, A., Wilder, S., Amson, R., Telerman, A., and Oren, M.A. Novel p53-inducible gene PAG608, encodes a nuclear zinc finger protein whose overexpression promotes apoptosis. *EMBO J.* 16: 4384-4392, 1997
- Ito, T., Seyama, T., Hayashi, T.E.A. Hae III polymorphism in intron 1 of the human p53 gene. *Hum. Genet.* 92, 222-, 1994
- Jacobs, I.J., Kohler, M.F., Wiseman, R.W., Marks, J.R., Whitaker, R., Kerns, B.A.J., Humphrey, P., Berchuck, A., Ponder, B.A.J., and Bast, R.C. Jr. Clonal origin of epithelial ovarian carcinoma: Analysis by Loss of Heterozygosity, p53 mutation, and x-chromosome inactivation. *J. Natl. Cancer Inst.* 84: 1793-1798, 1992
- Jones, S.N., Roe, A.E., Donehower, L.A., and Bradley, A. Rescue of embryonic lethality in Mdm2-deficient mice by absence of p53. *Nature* 378: 206-208, 1995

- Josefsson, A.M., Magnusson, P.K.E., Ylitalo, N., Quarforth-Tubbin, P., Ponten, J., Adami, H.O., and Gyllensten, U.B. P53 polymorphism and risk of cervical carcinoma. *Nature* 396: 530-531, 1998
- Kanamori, Y., Kigawa, J., Minagawa, Y., Irie, T., Oishi, T., Shimada, M., Takahashi, M., Nakamura, T., Sato, K., Terakawa, N. A newly developed adenovirus-mediated transfer of a wild-type p53 gene increases sensitivity to cis-diamminedichloroplatinum (II) in p53-deleted ovarian cancer cells. *Eur. J. Cancer* 34: 1802-1806, 1998
- Kaplan, E.L., and Meier, P. Nonparametric estimation from incomplete observations. *J. Am. Stat. Assoc.* 53, 457-481, 1958
- Kappes, S., Milde-Langosch, K., Kressin, P., Passlack, B., Dockhorn-Dworniczak, B., Rohlke, P., and Loning, T. p53 mutations in ovarian tumors, detected by temperature-gradient gel electrophoresis, direct sequencing and immunohistochemistry. *Int. J. Cancer* 64: 52-59, 1995
- Kastan, M., Zhan, Q., el-Deiry, W., Carrier, F., Jacks, T., Walsh, W., Plunkett, B., Vogelstein, B., and Fornace, A.J. A mammalian cell cycle checkpoint pathway utilizing p53 and GADD45 is defective in ataxia-teleangiectasia. *Cell* 71: 587-597, 1992
- Kihana, T., Tsuda, H., Teshima, S., Okada, S., Matsuura, S., and Hirohashi, S. High incidence of p53 gene mutation in human ovarian cancer and its association with nuclear accumulation of p53 protein and tumor DNA aneuploidy. *Jpn. J. Cancer Res.* 83: 978-984, 1992
- Kim, J.W., Cho, Y.H., Kwon, D.J., Kim, T.E., Park, T.C., Lee, J.M., and Namkoong, S.E. Aberrations of the p53 tumor suppressor gene in human epithelial ovarian carcinoma. *Gynecol. Oncol.* 57: 199-204, 1995
- Kim, J., Hwang, E.S., Kim, J.S., You, E.H., Lee, S.H., and Lee, J.H. Intraperitoneal therapy with adenoviral-mediated p53 tumor suppressor gene for ovarian cancer model in nude mouse. *Cancer Gene Ther.* 6: 172-178, 1999
- Kiyokawa, T. Alteration of p53 in ovarian cancer: Its occurrence and maintenance in tumor progression. *J. Gynecol. Pathol.* 13: 311-318, 1994
- Klemi, P., Pylkkanen, L., Kiilholma, P., Kuruvinen, K., and Joensuu, H. p53 protein detected by immunohistochemistry as a prognostic factor in patients with epithelial ovarian carcinoma. *Cancer* 76(7): 1201-1208, 1995
- Ko, J.L., Cheng, Y.W., Chang, S.L., Su, J.M., Chen, C.Y., and Lee, H. MDM2 mRNA expression is a favorable prognostic factor in non-small-cell lung cancer. *Int. J. Cancer* 89: 265-270, 2000
- Kohler, M., Marks, J., Wiseman, R., Jacobs, I., Davidoff, A., Clarke-Pearson, D., Soper, J., Bast, R., and Berchuck, A. Spectrum of mutation and frequency of allelic deletion of the p53 gene in ovarian cancer. *J. Natl. Cancer Inst.* 85(18): 1513-1519, 1993a
- Kohler, M., Kerns, B., and Berchuck, A. Mutation and overexpression of p53 in early stage epithelial ovarian cancer. *Obstet. Gynecol.* 81: 643-650, 1993b

- Kondo, S., Barnett, G.H., Hara, H., Morimura, T., and Takeuchi, J. MDM2 protein confers the resistance of a human glioblastoma cell line to cisplatin-induced apoptosis. *Oncogene 10*: 2001-2006, 1995
- Kosary, C.L. FIGO stage, Histology, Histologic Grade, Age and Race as Prognostic Factors in Determining Survival for Cancers of the Female Gynecological System: An Analysis of 1973-1987 SEER Cases of Cancers of the Endometrium, Cervix, Ovary, Vulva and Vagina. *Sem. Surg. Oncol. 10*: 31-46, 1994
- Kraus, A., Neff, F., Behn, M., Schuermann, M., Muenkel, K., and Schlegel, J. Expression of alternatively spliced mdm2 transcripts correlates with stabilized wild-type p53 protein in human glioblastoma cells. *Int. J. Cancer 80*: 930-934, 1999
- Kubbutat, M., Jones, S., and Vousden, K. Regulation of p53 stability by mdm2. *Nature 387*: 299-303, 1997
- Kubbutat, M., and Vousden, K.H. Keeping an old friend under control: regulation of p53 stability. *Mol. Med. Today 4*: 250-256, 1998
- Kubbutat, M.H.G., Ludwig, R.L., Levine, A.J., and Vousden, K.H. Analysis of the degradation function of Mdm2. *Cell Growth Diff. 10*: 87-92, 1999
- Kupryjanczyk, J., Thor, A., Beauchamp, R., Merritt, V., Edgerton, S., Bell, D., and Yandell, D. p53 gene mutations and protein accumulation in human ovarian cancer. *Proc. Natl. Acad. Sci. USA 90*: 4961-4965, 1993
- Kupryjanczyk, J., Bell, D., Dimeo, D., Yandell, D., Scully, R., and Thor, A. p53 expression in ovarian borderline tumors and stage I carcinomas. *Am. J. Clin. Pathol. 102(5)*: 671-676, 1994
- Kupryjanczyk, J., Bell, D., Dimeo, D., Beauchamp, R., Thor, A., and Yandell, D. p53 gene analysis of ovarian borderline tumors and stage I carcinomas. *Human Pathol. 26*: 387-392, 1995
- Kurman, R.J. (Editor) *Blaustein's Pathology of the Female Genital Tract*. 3rd edition. Springer-Verlag New York-Berlin-Heidelberg-London-Paris-Tokyo 1987 page 560-505
- Kussie, P.H., Gorina, S., Marechal, V., Elenbaas, B., Moreau, J., Levine, A.J., and Pavletich, N.P. Structure of the MDM2 oncoprotein bound to the p53 tumor suppressor transactivation domain. *Science 274*: 948-953, 1996
- Laemmli, U.K. Cleavage of structural proteins during the assembly of the head of bacteriophage T4. *Nature 227*: 680-685, 1970
- Lancaster, J.M., Brownlee, H.A., Wiseman, R.W., and Taylor, J. p53 polymorphism in ovarian and bladder cancer. *Lancet 182*: 346, 1995
- Landers, J., Haines, D., Strauss III J., and George, D. Enhanced translation: A novel mechanism of mdm2 oncogene overexpression identified in human tumor cells. *Oncogene 9*: 2745-2750, 1994

- Landers, J.E., Cassel, S.L., and George, D.L. Translational enhancement of mdm2 oncogene expression in human tumor cells containing a stabilized wild-type p53 protein. *Cancer Res.* 57: 3562-3568, 1997
- Landis, S.H., Murray, T., Bolden, S., and Wingo, P.A. Cancer Statistics 1998. *CA Cancer J. Clin.* 48: 6 - 29, 1998
- Lane, D.P. p53, guardian of the genome. *Nature* 358: 15-16, 1992
- Lanham, S., Campbell, I., Watt, P., and Gornall, R. P53 polymorphism and risk of cervical cancer. *Lancet* 352: 1631, 1998
- Laplace-Marieze, V., Presncau, N., Sylvain, V., Kwiatkowski, F., Lortholary, A., Hardouin, A., and Bignon, Y.J. Systematic sequencing of the BRCA-1 coding region for germ-line mutation detection in 70 French high risk families. *Int. J. Oncol.* 14: 971-977, 1999
- Lausen, B., and Schumacher, M. Maximally selected rank statistics. *Biometrics* 48: 73-86, 1992
- Lazar, V., Hazard, F., Bertin, F., Janin, N., Bellet, D., and Bressac, B. Simple sequence repeat polymorphism within the p53 gene. *Oncogene* 8: 1703-1705, 1993
- Lee, J., Kang, Y., Park, S., Kim, B., Lee, E., Lee, K., Kavanagh, J., and Wharton, J. p53 mutation in epithelial ovarian carcinoma and borderline ovarian tumor. *Cancer Genet. Cytogenet.* 85: 43-50, 1995
- Lee, S., Elenbaas, B., Levine, A., and Griffith, J. p53 and its 14 kDa C-terminal domain recognize primary DNA damage in the form of insertion/deletion mismatches. *Cell* 81: 1013-1020, 1995
- Leng, P., Brown, D.R., Shivakumar, C.V., Deb, S., and Deb, S.P. N-terminal 130 amino acids of MDM2 are sufficient to inhibit p53-mediated transcriptional activation. *Oncogene* 10: 1275-1282, 1995
- Levesque, M., Katsaros, D., Yu, H., Zola, P., Sismondi, P., Giardina, G., and Diamandis, E. Mutant p53 protein overexpression is associated with poor outcome in patients with well or moderately differentiated ovarian carcinoma. *Cancer* 75: 1327-1338, 1995
- Levine, A.J. p53, the cellular gatekeeper for growth and deviation. *Cell* 88: 323-331, 1997
- Levkau, B., Koyama, H., Raines, E.W., Clurman, B.E., Herren, B., Orth, K., and Ross, J.M.R.R. Cleavage of p21cip1/waf1 and p27kip1 mediates apoptosis in endothelial cells through activation of cdk2: role of a caspase cascade. *Mol. Cell* 1: 553-563, 1998
- Lewin, B. *Genes*. Oxford University Press Inc., New York, 688-689, 1994
- Li, F.P., and Fraumeni, J.F. Jr. Soft-tissue sarcoma, breast cancer, and other neoplasms. A familial syndrome? *Ann. Intern. Med.* 71: 747-752, 1969
- Lin, P.M., Liu, T.C., Chang, J.G., Chen, T.P., and Lin, S.F. Aberrant TSG101 transcripts in acute myeloid leukemia. *Br.J. Haematol.* 102: 753-758, 1998

- Lin, Y., Ma, W., and Benchimol, S. Pidd, a new death-domain-containing protein, is induced by p53 and promotes apoptosis. *Nature Gen.* 26: 124-127, 2000
- Linke, S., Clarkin, K., DiLeonardo, A., Tsou, A., and Wahl, G. A reversible, p53-dependent G0/G1 cell cycle arrest induced by ribonucleotide depletion in the absence of detectable DNA damage. *Genes Dev.* 10: 934-937, 1996
- Lowe, S.W., Ruley, H.E., Jacks, T., and Housman, E. p53-dependent apoptosis modulates the cytotoxicity of anticancer agents. *Cell* 74: 957-967, 1993
- Lowe, S.W., Bodis, S., McClatchey, A., Remington, L., Ruley, H.E., Fisher, D.E., Housman, D.E., and Jacks, T. p53 status and the efficacy of cancer therapy in vivo. *Science* 266: 807-810 1994
- Lu, H., Fisher, R.P., Bailey, P., and Levine, A.J. The CDK7-cycH-p36 complex of transcription factor IIH phosphorylates p53, enhancing its sequence-specific DNA binding activity in vitro. *Mol. Cell. Biol.* 17: 5923-5934, 1997
- Lu, W., Pochampally, R., Chen, L., Traidej, M., Wang, Y., and Chen, J. Nuclear exclusion of p53 in a subset of tumors requires MDM2 function. *Oncogene* 19: 232-240, 2000
- Lukas, J., Groshen, S., Saffari, B., Niu, N., Reles, A., Wen, H.-W., Felix, J., Jones, L.A., Hall, F.L., and Press, M.F. WAF1/CIP1 Gene polymorphism and expression in carcinomas of the breast, ovary, and endometrium. *Am. J. Pathol.* 150: 167-175, 1997
- Lund, B., Hansen, O.P., Theilade, K., Hansen, M., and Nejlit, J.P. Phase II study of gemcitabine (2,2-difluorodeoxycytidine) in previously treated ovarian cancer patients. *J. Natl. Cancer Inst.* 86: 152- 156, 1994
- Lynch, H.T., Harris, R.E., Guirgis, H.A., Maloney, K., Carmody, L.L., and Lynch, J.F. Familial association of breast/ovarian carcinoma. *Cancer* 41: 1543-1549, 1978
- Mackett, M., Smith, G.L., and Moss, B. Vaccinia Virus: A selectable eukaryotic cloning and expression vector. *Proc. Natl. Acad. Sci. USA* 79: 7415-7419, 1982
- Makar, A.P., Baekelandt, M., Tropé, C.G., and Kristensen, G.B. The prognostic significance of residual disease, FIGO substage, tumor histology, and grade in patients with FIGO stage III ovarian cancer. *Gynecol. Oncol.* 56: 175-180, 1995
- Maki, C.G., and Howley, P.M. Ubiquitination of p53 and p21 is differentially affected by ionizing and UV radiation. *Mol. Cell. Biol.* 17: 355-363, 1997
- Makni, H., Franco, E.L., Kaiano, J., Villa, L.L., Labrecque, S., Dudley, R., Storey, A., and Matlashewski, G.J. P53 polymorphism in codon 72 and risk of human papilloma-induced cervical cancer: effect of inter-laboratory variation. *Int. J. Cancer* 87: 528-533, 2000
- Mantel, N., and Haenszel, W. Statistical aspects of the analysis of data from retrospective studies of disease. *J. Natl. Cancer Inst.* 22: 719-748, 1959

- Marchetti, A., Buttitta, F., Girlando, S., Palma, P.D., Pellegrini, S., Fina, P., Doglioni, C., Bevilacqua, G., and Barbareschi, M. mdm2 gene alterations and mdm2 protein expression in breast carcinomas. *J. Pathol.* 175: 31-38, 1995a
- Marchetti, A., Buttitta, F., Pellegrini, S., Giorgio, M., Chella, A., Angeletti, C.A., and Bevilacqua, G. mdm2 gene amplification and overexpression in non-small cell lung carcinomas with accumulation of the p53 protein in the absence of p53 gene mutations. *Diagn. Mol. Pathol.* 4: 93- 97, 1995b
- Marechal, V., Elenbaas, B., Taneyhill, L., Piette, J., Mechali, M., Nicolas, J.-C., Levine, A.J., and Moreau, J. Conservation of structural domains and biochemical activities of the MDM2 protein from *Xenopus laevis*. *Oncogene* 14: 1427-1433, 1997
- Marin, C.M., Jost, C.A., Brooks, L.A., Irwin, M.S., O'Nions, J., Tidy, J.A., James, N., McGregor, J.M., Harwood, C.A., Yulug, I.G., Vousden, K.H., Allday, M.J., Gusterson, B., Ikawa, S., Hinds, P.W., Crook, T., and Kaelin, W.G. A common polymorphism acts as an intragenic modifier of mutant p53 behaviour. *Nature Gen.* 25: 47-54, 2000
- Markman, M., Rothman, R., Hakes, T., Reichman, B., Hoskins, W., Rubin, S., Jones, Walmadrones, L., and Lewis, J.L.Jr. Second-line platinum-therapy in patients with ovarian cancer previously treated with cisplatin. *J. Clin. Oncol.* 9: 389-393, 1991
- Marks, J., Davidoff, A., Kerns, B., Humphrey, P., Pence, J., Dodge, R., Clarke-Pearson, D., Iglehart, J., Bast, R., and Berchuck, A. Overexpression and mutation of P53 in epithelial ovarian cancer. *Cancer Res.* 52: 2979-2984, 1991
- Marx, D., Meden, H., Ziemck, T., Lenthe, T., Kuhn, W., and Schauer, A. Expression of the p53 tumor suppressor gene as a prognostic marker in platinum-treated patients with ovarian cancer. *Eur. J. Cancer* 34: 845-850, 1998
- Matlashewski, G., Lamb, P., Pim, D., Peacock, J., Crawford, L., and Benchimol, S. Isolation and characterization of a human p53 cDNA clone: expression of the human p53. *EMBO J.* 3: 3257-3262, 1984
- Matlashewski, G.J., Tuck, S., Pim, D., Lamb, J., Schneider, J., and Crawford, L.V. Primary structure polymorphism at amino acid residue 72 of human p53. *Mol. Cell. Biol.* 7: 961-963, 1987
- Matsumoto, R., Tada, M., Nozaki, M., Zhang, C.L., Sawamura, Y., and Abe, H. Short alternative splice transcripts of the mdm2 oncogene correlate to malignancy in human astrocytic neoplasms. *Cancer Res.* 58: 609-613, 1998
- Mavridou, D., Gornall, R., Campbell, I.G., and Eccles, D.M. TP53 intron 6 polymorphism and the risk of ovarian and breast cancer. *Br. J. Cancer* 77: 676-678, 1998
- Mazars, R., Pujol, P., Maudelonde, T., Jeanteur, P., and Theillet, C. p53 mutations in ovarian cancer: A late event ? *Oncogene* 6: 1685-1690, 1991
- Maxwell, S. Selective Compartmentalization of Different mdm2 Proteins within the Nucleus. *Anticancer Res.* 14: 2541-2548, 1994

- May, P., and May, E. Twenty years of p53 research: structural and functional aspects of the p53 protein. *Oncogene 18*: 7621-7636, 1999
- McCann, A., Kirley, A., Carney, D., Corbally, N., Magee, H., Keating, G., and Dervan, P. Amplification of the MDM2 gene in human breast cancer and its association with MDM2 and p53 protein status. *Br. J. Cancer 71*: 981-985, 1995
- McGuire, W.P., Hoskins, W.J., Brady, M.F., Kucera, P.R., Partridge, E.E., Look, K.Y., Clarke-Pearson, D.L., and Davidson, M. Cyclophosphamide and cisplatin compared with paclitaxel and cisplatin in patients with stage III and IV ovarian cancer. *New Engl. J. Med. 334*: 1-6, 1996
- McGuire, W.P., and Ozols, R.F. Chemotherapy of advanced ovarian cancer. *Semin. Oncol. 25*: 340-348, 1998
- Meden, H., Marx, D., Rath, W., Kron, M., Fattahi-Meibodi, A., Hinney, B., Kuhn, W., and Schauer, A. Overexpression of the oncogene c-erbB2 in primary ovarian cancer: evaluation of the prognostic value in a Cox proportional hazards multiple regression. *Int. J. Gynecol. Pathol. 13*: 45-53, 1994
- Miki, Y., Swensen, J., Shattuck-Eidens, D., Futreal, P.A., Harshman, K., Tartigian, S., Lin, Q., Cochran, C., Bennett, L.M., and Ding, W. A strong candidate for the breast ovarian cancer susceptibility gene BRCA1. *Science 266*: 66-71, 1994
- Miller, R., and Siegmund, D. Maximally selected chi square statistics. *Biometrics 38*: 1011-1016, 1982
- Milner, B., Allan, L., Eccles, D., Kitchener, H., Leonard, R., Kelly, K., Parkin, D., and Haites, N. p53 gene mutation is a common genetic event in ovarian carcinoma. *Cancer Res. 53*: 2128-32, 1993
- Miyashita, T., Krajewski, S., Krajewska, M., Wang, H., Liebermann, D., Hoffman, B., and Reed, J.C. Tumor suppressor p53 is a regulator of bcl-2 and bax gene expression in vitro and in vivo. *Oncogene 9*: 1799-1805, 1994
- Miyashita, T., and Reed, J. Tumor suppressor p53 is a direct transcriptional activator of the human bax gene. *Cell 80*: 293-299, 1995
- Moll, U., LaQuaglia, J., Benard, J., and Riou, G. Wild-type p53 undergoes cytoplasmic sequestration in undifferentiated neuroblastomas but not in undifferentiated tumors. *Proc. Natl. Acad. Sci. USA 92*: 4407-4411, 1995
- Mok, S., Lo, K., and Taso, S. Direct cycle sequencing of mutated alleles detected by PCR single-strand conformation polymorphism analysis. *Biotechniques 14 (5)*: 790-794, 1993
- Momand, J., Zambetti, G., Olson, D., George, D., and Levine, A. The mdm-2 oncogene product forms a complex with the p53 protein and inhibits p53 mediated transactivation. *Cell 69*: 1237-1245, 1992
- Momand, J. and Zambetti, G. Mdm-2: „Big Brother,, of p53. *J. Cell. Biochem. 64*: 343-352, 1997

- Montes de Oca Luna, R., Tabor, A.D., Eberspaecher, H., Hulboy, D.L., Worth, L.L., Colman, M.S., Finlay, C.A., and Lozano, G. The organization and expression of the mdm2 Gene. *Genomics* 33: 352-357, 1996
- Morgenbesser, S.D., Williams, B.O., Jacks, T., and DePinho, R.A. p53 dependent apoptosis produced by Rb-deficiency in the developing mouse lens. *Nature* 371: 72-74, 1994
- Moss, B., and Flexner, C. Vaccinia virus expression vectors. *Annu. Rev. Immunol.* 5: 305-324, 1987
- Mujoo, K., Maneval, D.C., Anderson, S.C., and Gutterman, J.U. Adenoviral-mediated p53 tumor suppressor gene therapy of human ovarian carcinoma. *Oncogene* 12: 1617-1623, 1996
- Nagata, S. Apoptosis by death factor. *Cell* 88: 355-365, 1997
- Narod, S.A., Risch, H., Moslehi, R., Dorum, A., Neuhausen, S., Olsson, H., Provencher, D., Radice, P., Evans, G., Bishop, S., Brunet, J.-S., and Ponder, A.J. Oral contraceptives and the risk of hereditary ovarian cancer. *N. Engl. J. Med.* 339: 424-428, 1998
- Negrini, M., Monaco, C., Vorechovsky, I., Ohta, M., Druck, T., Baffa, R., Huebner, K., and Croce, C. The FHIT gene at 3p14.2 is abnormal in breast carcinomas. *Cancer Res.* 56: 3173-3179, 1996
- Nielsen, L.L., and Maneval, D. p53 tumor suppressor gene therapy for cancer. *Cancer Gene Ther.* 5: 52-63, 1998
- Nielsen, L.L., Lipari, P., Dell, J., Gurnani, M., and Hajian, G. Adenovirus-mediated p53 gene therapy and paclitaxel have synergistic efficacy in models of human head and neck, ovarian, prostate and breast cancer. *Clin. Cancer Res.* 4: 835-846, 1998
- Niwa, K., Itoh, M., Murase, T., Itoh, N., Mori, H., and Tamaya, T. Alteration of p53 gene in ovarian carcinoma: Clinicopathological correlation and prognostic significance. *Br. J. Cancer* 70: 1191-1197, 1994
- Oberosler, P., Hloch, P., Ramsperger, U., and Stahl, H. p53-catalyzed annealing of complementary single-stranded nucleic acids. *EMBO J.* 12: 2389-2396, 1993
- Ogawa, N., Fujiwara, T., Kagawa, S., Nishizaki, M., Morimoto, Y., Tanida, T., Hizuta, A., Yasuda, T., Roth, J.A., and Tanaka, N. Novel combination therapy for human colon cancer with adenovirus-mediated wild-type p53 gene transfer and DNA-damaging chemotherapeutic agent. *Int. J. Cancer* 73: 367-370, 1997
- Oliner, J., Kinzler, K., Meltzer, P., George, D., and Vogelstein, B. Amplification of a gene encoding a p53-associated protein in human sarcomas. *Nature* 358: 80-83, 1992
- Oliner, J., Pietsenpol, J., Thiengalingam, S., Gyuris, J., Kinzler, K., and Vogelstein, B. Oncoprotein MDM2 conceals the activation domain of tumour suppressor p53. *Nature* 362: 857-860, 1993

- Olson, D.C., Marechal, V., Momand, J., Chen, J., Romocki, C., and Levine, A.J. Identification and characterization of multiple mdm-2 proteins and mdm-2-p53 protein complexes. *Oncogene* 8: 2353-2360, 1993
- Oltvai, Z.N., Millman, C.L., and Korsmeyer, S.J. Bcl-2 heterodimerizes in-vivo with a conserved homolog, bax, that accelerates programmed cell death. *Cell* 74: 609-619, 1993
- Palazzo, J.P., Monzon, F., Burke, M., Hyslop, T., Dunton, C., Barusevicius, A., Capuzzi, D., and Kovatich, A.J. Overexpression of p21WAF1/CIP1 and MDM2 characterizes serous borderline ovarian tumors. *Hum. Pathol.* 31: 698-704, 2000
- Panicali, D., and Paoletti, E. Construction of poxviruses as cloning vectors: Insertion of the thymidine kinase gene from herpes simplex virus into the DANN of infectious vaccinis virus. *Proc. Natl. Acad. Sci. USA* 79: 4927-4931, 1982
- Peller, S., Kopilova, Y., Slutzki, S., Halevy, A., Kvitko, K., and Rotter, V. A novel polymorphism in intron 6 of the human p53 gene: A possible association with cancer predisposition and susceptibility. *DNA Cell Biol.* 14: 983-990, 1995
- Perry, M.E., Mendrysa, S.M., Saucedo, L.J., Tannous, P., and Holubar, M. p76 (MDM2) inhibits the ability of p90 (MDM2) to destabilize p53. *J. Biol. Chem.* 275: 5733-5738, 2000
- Pestell, K.E., Hobbs, S.M., Titley, J.C., Kelland, L.R., and Wlton, M.I. Effect of p53 status on sensitivity to platinum complexes in a human ovarian cancer cell line. *Mol. Pharmacol.* 57: 503-511, 2000
- Petru, E., Lahousen, M., Tamussino, K., Pickel, H., Stranzl, H., Stettner, H., and Winter, R. Lymphadenectomy in stage I ovarian cancer. *Am. J. Obstet. Gynecol.* 170: 656-662, 1994
- Pettersson, F. Annual report on the results of treatment in gynecologic cancer: statements of the results obtained in patients, 1982 to 1986, inclusive 3- and 5-year survival up to 1990. *Int. J. Gynecol. Oncol.* 21 (suppl.), 1991
- Petty, R., Evans, A., Duncan, I., Kurbacher, C., and Cree, I. Drug resistance in ovarian cancer - the role of p53. *Pathol. Oncol. Res.* 4: 97-102, 1998
- Picksley, S.M., Vojtesek, B., Sparks, A., and Lane, D. Immunochemical analysis of the interaction of p53 with MDM2-fine mapping of the MDM2 binding site on p53 using synthetic peptides. *Oncogene* 9: 2523-2529, 1994
- Piette, J., Neel, H., and Maréchal, V. Mdm2: keeping p53 under control. *Oncogene* 15: 1001-1010, 1997
- Piver, M.S., Jishi, M.F., Tsukada, Y., and Nava, G. Primary peritoneal carcinoma after prophylactic oophorectomy in women with a family history of ovarian cancer. A report of the Gilda Radner Familial Ovarian Cancer Registry. *Cancer* 71: 2751-2755,

- Pleasant, L.M., and Hansen, M.F. Identification of a polymorphism in intron 2 of the p53 gene. *Human Genetics* 93: 607-608, 1994
- Polyak, K., Xia, Y., Zweier, J.L., Kinzler, K.W., and Vogelstein, B. A model for p53 induced apoptosis. *Nature* 389: 300-305, 1997
- Pomerantz, J., Schreiber-Agus, N., Liégeois, N.J., Silverman, A., Alland, L., Chin, L., Potes, J., Chen, K., Orlow, I., Lee, H.-W., Cordon-Cardo, C., and DePinho, R.A. The Ink4a tumor suppressor gene product, p19Arf, interacts with MDM2 and neutralizes MDM2's inhibition of p53. *Cell* 92: 713-723, 1998
- Prives, C. How loops, beta sheets and alpha helices help us to understand p53. *Cell* 78: 543-546, 1994
- Pützer, B.M. The role of tumor suppressor gene therapy for anticancer treatment. *Tumordiagn. Ther.* 21: 1-7, 2000
- Qin, X.-Q., Livingston, D.M., Kaelin, W.G.Jr., and Adams, P.D. Deregulated transcription factor E2F-1 expression leads to S-phase entry and p53-mediated apoptosis. *Proc. Natl. Acad. Sci. USA* 91: 10918-10922, 1994
- Quesnel, B., Preudhomme, C., Fournier, J., Fenaux, P., and Peyrat, J. MDM2 gene amplification in human breast cancer. *Eur. J. Cancer* 30A: 982-984, 1994
- Ralhan, R., Sandhya, A., Meera, M., Bohdan, W., and Nootan, S.K. Induction of MDM2-P2 transcripts correlates with stabilized wild-type p53 in betel- and tobacco-related human oral cancer. *Am. J. Pathol.* 157: 587-596, 2000
- Reisman, D., and Loging, W.T. Transcriptional regulation of the p53 tumor suppressor gene. *Sem. Cancer Biol.* 8: 317-324, 1998
- Reles, A., Schmider, A., Press, M.F., Schönborn, I., Friedmann, W., Huber-Schumacher, S., Strohmeyer, T., and Lichtenegger, W. Immunostaining of p53 protein in ovarian carcinoma: correlation with histopathological data and clinical outcome. *J. Cancer Res. Clin. Oncol.* 122: 489-494, 1996
- Reles, A., Wein, U., Lichtenegger, W. Transvaginal color Doppler sonography and conventional sonography in the preoperative assessment of adnexal masses. *J. Clin. Ultrasound* 25: 217-225, 1997
- Reles, A., Wein, U., Lübke, M., Lichtenegger, W. Transvaginale Farbdopplersonographie in der präoperativen Diagnostik von Adnextumoren. Diagnostische Wertigkeit im Vergleich zu konventionellen Sonographiekriterien. *Geb. Frauenheilk.* 58: 93-99, 1998
- Reles, A.E., Gee, C., Schellschmidt, I., Schmider, A., Unger, M., Friedmann, W., Lichtenegger, W., and Press, M.F. Prognostic Significance of DNA Content and S-Phase Fraction in Epithelial Ovarian Carcinomas Analyzed by Image Cytometry. *Gynecol. Oncol.* 71: 3-13, 1998
- Reles, A., Wen, H.W., Schmider, A., Gee, C., Runnebaum, I.B., Kilian, U., Jones, L.A., El-Naggar, A., Minguillon, C., Schönborn, I., Reich, O., Kreienberg, R., Lichtenegger, W., Press, M.F. Correlation of p53 mutations with resistance to platinum-based

- chemotherapy and shortened survival in ovarian cancer. *Clin. Cancer Res.* in press, 2001
- Righetti, S.C., Della Torre, G., Pilotti, S., Ménard, S., Ottone, F., Colnaghi, M.I., Pierotti, M.A., Lavarino, C., Cornarotti, M., Oriana, S., Böhm, S., Bresciani, G.L., Spatti, G., and Zunino, F. A comparative study of p53 gene mutations, protein accumulation, and response to cisplatin-based chemotherapy in advanced ovarian carcinoma. *Cancer Res.* 56, 689-693, 1996
- Röhlke, P., Milde-Langosch, K., Weyland, C., Pichlmeier, U., Jonat, W., and Loning, T. p53 is a persistent and predictive marker in advanced ovarian carcinomas: multivariate analysis including comparison with Ki67 Immunoreactivity. *J. Cancer Res. Clin. Oncol.* 123: 496-501, 1997
- Roth, J., Dobbelstein, M., Freedman, D.A., Shenk, T., and Levine, A.J. Nucleo-cytoplasmic shuttling of the hdm2 oncoprotein regulates the levels of the p53 protein via a pathway used by the human immunodeficiency virus rev protein. *EMBO J.* 17: 554-564, 1998
- de Rozières, S., Maya, R., Oren, M. and Lozano, G. The loss of mdm2 induces p53-mediated apoptosis. *Oncogene* 19: 1691-1697, 2000
- Runnebaum, I.B., Tong, X.W., König, R., Hong, Z., Körner, K., Atkinson, E.N., Kreienberg, R., and Kieback, D.G. p53-based blood test for p53PIN3 and risk for sporadic ovarian cancer. *Lancet* 345: 994, 1995
- Sakaguchi, K., Herrera, J.E., Saito, S., Miki, T., Bustin, M., Vassilev, A., Anderson, C.W., and Appella, E. DNA damage activates p53 through a phosphorylation-acetylation cascade. *Genes Dev.* 12: 2831-2841, 1998
- Sakamoto, T., Nomura, N., Mori, H., and Wake, N. Poor correlation with Loss of Heterozygosity on chromosome 17p and p53 mutations in ovarian cancers. *Gynecol. Oncol.* 63: 173-179, 1996
- Sanger, F., Nicklen, S., and Coulson, A. DNA sequencing with chain-terminating inhibitors. *Proc. Nat. Acad. Sci.* 74: 5463-5467, 1977
- Santoro, I., and Groden, J. Alternative splicing of the APC gene and its association with terminal differentiation. *Cancer Res.* 57: 488-494, 1997
- Saucedo, L.J., Myers, C.D. and Perry, M.E. Multiple Murine Double Minute Gene 2 (MDM2) proteins are induced by ultraviolet light. *J. Biol. Chem.* 274: 8161-8168, 1999
- Scambia, G., Masciullo, V., Benedetti-Panici, P., Marono, M., Ferrandino, G., Todaro, N., Bellacosa, A., Jain, S.K., Neri, O., Pifanelli, A., and Mancuso, S. Prognostic significance of ras/p21 alterations in human ovarian cancer. *Br. J. Cancer* 75: 1547-1553, 1997
- Schmider, A. Immunhistochemische Bestimmung der Überexpression des Tumorsuppressorgens p53, seines Mediatorgens WAF1/CIP1 und des Onkogens c-neu beim Ovarialkarzinom, unter besonderer Berücksichtigung der Alterationen des p53 Tumorsuppressorgens. Diss., Berlin, p. 95-99, 1999

- Schmider, A., Gee, C., Friedmann, W., Lukas, J.J., Press, M.F., Lichtenegger, W., and Reles, A. p21 (WAF1/CIP1) Protein Expression Is Associated with Prolonged Survival but not with p53 Expression in Epithelial Ovarian Carcinoma. *Gynecol. Oncol.* 77: 237-242, 2000
- Schuyer, M., Henzen-Logmans, S.C., van der Burg, M.E.L., Fieret, E.J.H., Klijn, J.G.M., Foekens, J.A., and Berns, E.M.J.J. High prevalence of codon 213ARG→STOP mutations of the TP53 gene in human ovarian cancer in the southwestern part of the Netherlands. *Int. J. Cancer* 5: 65-68, 1998
- Schwartz, D., and Rotter V. p53-dependent cell cycle control: response to genotoxic stress. *Sem. Cancer Biol.* 8: 325-336, 1998
- Scully, R.E. Tumors of the ovary and maldeveloped gonads. *Atlas of Tumor Pathology*, 2nd series, fascicle 16. Washington, DC, Armed Forces Institute of Pathology, 1979
- Sheridan, E., Silcocks, P., Hancock, B., and Goyns, M. P53 mutation in a series of epithelial ovarian cancers from the U.K. and its prognostic significance. *Eur. J. Cancer* 11: 1701-1704, 1994
- Shieh, S.Y., Ikeda, M., Taya, Y., and Prives, C. DNA damage-induced phosphorylation of p53 alleviates inhibition by MDM2. *Cell* 91: 325-334, 1997
- Shieh, S.-Y., Taya, Y., and Prives, C. DNA damage-inducible phosphorylation of p53 at N-terminal sites including a novel site, Ser20, requires tetramerization. *EMBO J.* 18: 1815-1823, 1999
- Siddik, Z.H., Mims, B., Lozano, G., and Thai, G. Independent pathways of p53 induction by Cisplatin and X-Rays in a Cisplatin-resistant Ovarian Tumor Cell Line. *Cancer Res.* 58: 698-703, 1998
- Sigalas, I., Calvert, A., Anderson, J., Neal, D., and Lunec, J. Alternatively spliced mdm2 transcripts with loss of p53 binding domain sequences: transforming ability and frequent detection in human cancer. *Nature Med.* 2: 912-917, 1996
- Siliciano, J.D., Canman, C.E., Taya, Y., Sakaguchi, K., Appella, E., and Kastan, M.B. DNA damage induces phosphorylation of the amino terminus of p53. *Genes Dev.* 11: 3471-3481, 1997
- Skilling, J., Sood, A., Niemann, T., Lager, D., and Buller, R. An abundance of p53 null mutations in ovarian carcinoma. *Oncogene* 13: 117-123, 1996
- Skomedal, H., Kristensen, G.B., Abeler, V.M., Borresen-Dale, A.-L., Tropé, C., and Holm, R. TP 53 protein accumulation and gene mutation in relation to overexpression of mdm2 protein in ovarian borderline tumours and stage I carcinomas. *J. Pathol.* 181: 158-165, 1997
- Själänder, A., Birgander, R., Kivelä, A., and Beckman, G. p53 polymorphisms and haplotypes in different ethnic groups. *Hum. Hered.* 45: 144-149, 1995
- Själänder, A., Birgander, R., Hallmans, G., Cajander, S., Lenner, P., Athlin, L., Beckman, G., and Beckman, L. p53 polymorphisms and haplotypes in breast cancer. *Carcinogenesis* 17: 1313-1316, 1996

- Slamon, D.J., Godolphin, W., Jones, L.A., Holt, J.A., Wong, S.G., Keith, D.E., Levin, W.J., Stuart, S.G., Udove, J., and Ullrich, A. Studies of the HER-2/neu proto-oncogene in human breast and ovarian cancer. *Science* 244: 707-712, 1989
- Slatko, B. Thermal cycle dideoxy DNA sequencing. *Methods Mol. Biol.* 58: 413-423, 1996
- Slebos, R.J., Lee, M.H., Plunkett, B.S., Kesis, T.D., Williams, B.O., Jacks, T., Hedrick, L., Koston, M.B., and Cho, K.R. p53-dependant G1 arrest involves pRB-related proteins and is disrupted by the human papillomavirus 16E7 oncoprotein. *Proc. Natl. Acad. Sci. USA* 91: 5320-5324, 1994
- Smith, M.L., Chen, I.-T., Zhan, Q., Bae, I., Chen, C.-Y., Gilmer, T.M., Kastan, M.B., O'Connor, P.M., and Fornace, A.J.Jr. Interaction of the p53-regulated protein GADD45 with proliferating cell nuclear antigen. *Science* 266: 1376-1380, 1994
- Song, K., Li, Z., Seth, P., Cowan, K.H., and Sinha, B.K. Sensitization of cis-Platinum by a recombinant adenovirus vector expressing wild-type p53 gene in human ovarian carcinomas. *Oncology Res.* 9: 603-609, 1997
- Sood, A.K., Skilling, J.S., and Buller, R.E. Ovarian cancer genomic instability correlates with p53 frameshift mutations. *Cancer Res.* 57: 1047-1049, 1997
- Soussi, T., Caron de Fromentel, C., and May, E. Structural aspects of the p53 protein in relation to gene evolution. *Oncogene* 5: 945-952, 1990
- Soussi, T., and May, P. Structural aspects of the p53 protein in relation to gene evolution: A second look. *J. Mol. Biol.* 260: 623-637, 1996
- Spinardi, L., Mazars, R., and Theillet, C. Protocols for an improved detection of point mutations by SSCP. *Nucleic Acids Research* 19 (14): 4009, 1991
- Stewart, N., Hicks, G.G., Paraskevas, F., and Mowat, M. Evidence for a second cell cycle block at G2/M by p53. *Oncogene* 10: 109-115, 1994
- Stommel, J.M., Marchenko, N.D., Jimenez, G.S., Moll, U.M., Hope, T.J., and Wahl, G.M. A leucine-rich nuclear export signal in the p53 tetramerization domain: regulation of subcellular localization and p53 activity by NES masking. *EMBO J.* 18: 1660-1672, 1999
- Storey, A., Thomas, M., Kalita, A., Harwood, C., Gardiol, D., Mantovani, F., Breuers, J., Leigh, I.M., Matlashewski, G., and Banks, L. Role of p53 polymorphism in the development of human papilloma-virus-associated cancer. *Nature* 393: 229-234, 1998
- Suh, S.I., Cho, J.W., Baek, W.K., Suh, M.H., Carson, D.A. Lack of mutation at p16INK4A gene but expression of aberrant p16INK4A RNA transcripts in human ovarian carcinoma. *Cancer Lett.* 153: 175-182, 2000
- Tanner, B., Hengstler, J.G., Laubscher, S., Meinert, R., Oesch, F., Weikel, W., Knapstein, P.G., and Becker, R. mdm2 mRNA expression is associated with survival in ovarian cancer. *Int. J. Cancer* 74: 438-442, 1997
- Tao, W.K. and Levine A.J. P19 (ARF) stabilizes p53 by blocking nucleo-cytoplasmic shuttling of Mdm2. *Proc. Natl. Acad. Sci. USA*, 96: 6937-6941, 1999

- Taubert, H., Koehler, T., Meye, A., Bartel, F., Lautenschläger, C., Borchert, S., Bache, M., Schmidt, H., and Wurl, P. mdm2 mRNA level is a prognostic factor in soft tissue sarcoma. *Mol. Med.* 6: 50-59, 2000
- Teneriello, M., Ebina, M., Linnoila, R., Henry, M., Nash, J., Park, R., and Birrer, M. p53 and Ki-ras gene mutations in epithelial ovarian neoplasms. *Cancer Res.* 53: 3103-3108, 1993
- Thut, C.J., Goodrich, J.A., and Tjian, R. Repression of p53-mediated transcription by MDM2: a dual mechanism. *Genes Dev.* 11: 1974-1986, 1997
- Tortolero-Luna, G., Follen Mitchell, M., and Rhodes-Morris, H.E. Epidemiology and screening of ovarian cancer. *Obstet. Gynecol. Clin. North. Am.* 21: 1-23, 1994
- Tran, H., Gordenin, D., and Resnick, M. The prevention of repeat-associated deletions in *saccharomyces cerevisiae* by mismatch repair depends on size and origin of deletions. *Genetics* 143: 1579-1587, 1996
- Unger, T., Juven-Gershon, T., Moallem, E., Berger, M., Sionov, R.V., Lozano, G., Oren, M., and Haupt, Y. Critical role for Ser20 of human p53 in the negative regulation of p53 by Mdm2. *EMBO J.* 18: 1805-1814, 1999
- Utrera, R., Collavin, L., Lazarevic, D., Delia, D., and Schneider, C. A novel p53 inducible gene coding for a microtubule-localized protein with G2-phase-specific expression. *EMBO J.* 17: 5015-5025, 1998
- Vasey, P.A., Jones, N.A., Jenkins, S., Dive, C., and Brown, R. Cisplatin, Camptothecin, and Taxol sensitivities of cells with p53-associated multidrug resistance. *Mol. Pharmacol.* 50: 1536-1540, 1996
- Veldhoen, N., Metcalfe, S., and Milner, J. A novel exon within the mdm2 gene modulates translation initiation in vitro and disrupts the p53-binding domain of mdm2 protein. *Oncogene* 18: 7026-7033, 1999
- Verselis, S.J., Li, F.P. Common polymorphism in p53 intron 2, IVS2+38G>C. *Hum. Mutat.* 16: 181, 2000
- Viale, G., Maisonneuve, P., Bonoldi, E., Di Bacco, A., Bevilacqua, P., Panizzoni, A., Radaelli, U., and Gasparini, G. The combined evaluation of p53 accumulation and of Ki-67 (MIB1) labelling index provides independent information on overall survival of ovarian carcinoma patients. *Annals Oncol.* 8: 469-476, 1997
- Vikhanskaya, F., Clerico, L., Valenti, M., Stanzione, M.S., Broggin, M., Parodi, S., and Russo, P. Mechanism of resistance to Cisplatin in a human ovarian-carcinoma cell line selected for resistance to Doxorubicin: possible role of p53. *Int. J. Cancer* 72: 155-159, 1997
- Vikhanskaya, F., Vignati, S., Beccaglia, P., Ottoboni, C., Russo, P., D'Incalci, M., and Broggin, M. Inactivation of p53 in a human ovarian cancer cell line increases the sensitivity to Paclitaxel by inducing G2/M Arrest and Apoptosis. *Exp. Cell Res.* 241: 96-101, 1998

- Virgilio, L., Shuster, M., Gollin, S., Veronese, M., Ohta, M., Huebner, K., and Croce, C. FHIT gene alterations in head and neck squamous cell carcinomas. *Proc. Natl. Acad. Sci. USA* 93: 9770-9775, 1996
- Vogelstein, B. Clinical implication of basic research: Cancer therapy meets p53. *New Engl. J. Med.* 331: 49-50, 1994
- Wahl, A.F., Donaldson, K.L., Fairchild, C., Lee, F.Y.F., Foster, S.A., Demers, G.W., and Galloway, D.A. Loss of normal p53 function confers sensitization to Taxol by increasing G2/M arrest and apoptosis. *Nature Med.* 2: 72-79, 1996
- Waldmann, T., Kinzler, K.W., and Vogelstein, B. p21 is necessary for the p53-mediated G1 arrest in human cancer cells. *Cancer Res.* 55: 5187-5190, 1995
- Wang, P., Reed, M., Wang, Y., Mayr, G., Stenger, J.E., Anderson, M.E., Schwedes, J.F., and Tegtmeier, P. p53 domains: structure, oligomerization, and transformation. *Mol. Cell. Biol.* 14, 5182-5191, 1994
- Waterman, M.J.F., Stravridi, E.S., Waterman, J.L.F., and Halazonetis, T.D. ATM-dependent activation of p53 involves dephosphorylation and association with 14-3-3 proteins. *Nature Genet.* 19: 175-178, 1998
- Wang, H., Zeng, X., Oliver, P., Le, L.P., Chen, J., Chen, L., Zhou, W., Agrawal, S., and Zhang, R. MDM2 oncogene as a target for cancer therapy: An antisense approach. *Int. J. Oncol.* 15: 653-660, 1999
- Wang, X.W., Yeh, H., Schaeffer, L., Roy, R., Moncollin, V., Egly, J.-M., Wang, Z., Friedberg, E.C., Evans, M.K., Taffe, B.G., Bohr, V.A., Weeda, G., Hoeijmakers, J.H.J., Forrester, K., and Harris, C. p53 modulation of TFIIH-associated nucleotide excision repair activity. *Nature Gen.* 10: 188-195, 1995
- Wang, X.W., Vermeulen, W., Courson, J.D., Gibson, M., Lupold, S.E., Forrester, K., Xu, G., Elmore, L., Yeh, H., Hoeijmakers, J.H.J., and Harris, C. The XPB and XPD helicases are components of the p53-mediated apoptosis pathway. *Genes Dev.* 10: 1219-1232, 1996
- Wang, X.W., and Harris, C.C. p53 Tumor-suppressor gene: Clues to molecular carcinogenesis. *J. Cell. Physiol.* 173: 247-255, 1997
- Wang-Gohrke, S., Hees, S., Pochon, A., Wen, W.H., Reles, A., Press, M.F., Kreienberg, R., and Runnebaum, I.B. Genomic semi-automated cycle sequencing as a sensitive screening technique for p53 mutations in frozen tumor samples. *Oncol. Rep.* 5: 65-68, 1998
- Wang-Gohrke, S., Weikel, W., Risch, H., Vesprini, D., Abrahamson, J., Lerman, C., Godwin, A., Moslehi, A., Olipade, O., Brunet, J.-S., Stickeler, E., Kieback, D.G., Kreienberg, R., Weber, B., Narod, S.A., and Runnebaum, I.B. Intron variants of the p53 gene are associated with increased risk for ovarian cancer but not in carriers of BRCA1 or BRCA2 germline mutations. *Br. J. Cancer* 81: 179-183, 1999

- Weinstein, J.N., Myers, T.G., O'Connor, P.M., Friend, S.H., Fornace, A.J.Jr., Kohn, K.W., Fojo, T., Bates, S.E., Rubinstein, L.V., Anderson, N.L., Buolamwini, J.K., van Osdol, W.W., Monks, A.P., Scudiero, D.A., Sausville, E.A., Zaharevitz, D.W., Bunow, B., Viswanadhan, V.N., Johnson, G.S., Wittes, R.E., and Paull, K.D. An Information-Intensive Approach to the Molecular Pharmacology of Cancer. *Science* 275: 343-349, 1997
- Wen, H.W., Reles, A., Runnebaum, I.B., Sullivan-Halley, J., Bernstein, L., Jones, L.A., Felix, J.C., Kreienberg, R., El-Naggar, A., and Press, M.F. p53 mutations and expression in ovarian cancers: Correlation with overall survival. *Int. J. Gyn. Pathol.* 18: 29-41, 1999
- Werness, B.A., Freedman, A.N., Piver, M.S., Romero-Gutierrez, M., and Petrow, E. Prognostic significance of p53 and p21waf1/cip1 immunoreactivity in epithelial cancers of the ovary. *Gynecol. Oncol.* 75: 413-418, 1999
- Wertheim, I., Muto, M., Welch, W., Bell, D., Berkowitz, R., and Mok, S. p53 gene mutations in human borderline epithelial ovarian tumors. *J. Natl. Cancer Inst.* 86: 1549-51, 1994
- Weston, A., Perrin, L.S., Forrester, K., Hoover, R.N., Trump, B.F., Harris, C.L., and Caparaso, N.E. Allelic frequency of a p53 polymorphism in human lung cancer. *Cancer Epidemiol. Biomarkers Prev.* 1: 481-483, 1992
- Whittemore, A.S., Harris, R., and Itnyre, J. Collaborative Ovarian Cancer Group. Characteristics relating to ovarian cancer risk: collaborative analysis of 12 US case-control studies. II. Invasive epithelial ovarian cancers in white women. *Am. J. Epidemiol.* 136: 1184-1203, 1992
- Whittemore, A.S., Gong, G., and Itnyre, J. Prevalance and contribution of BRCA1 mutations in breast cancer and ovarian cancer: results from three U.S. population-based case-control studies of ovarian cancer. *Am. J. Hum. Genet.* 60: 496-504, 1997
- Wills, K.N., Maneval, D.C., Menzel, P., Harris, M.P., Sutjipto, S., Vaillancourt, M.-T., Huang, W.M., Johnson, D.E., Anderson, S.C., Wen, S.F. et al. Development and characterization of recombinant adenoviruses encoding p53 for gene therapy of cancer. *Human Gene Ther.* 5: 1079-1088, 1994
- Wong, Y.F., Chung, T.K., Cheung, T.H., Nobori, T., Yu, A.L., Yu, J., Batova, A., Lai, K.W., Chang, A.M. Methylation of p16INK4A in primary gynecologic malignancy. *Cancer Lett.* 136: 231-235, 1999
- Woo, R.A., McLure, K.G., Lees-Miller, S.P., Rancourt, D.E., and Lee, P.W.K. DNA-dependent protein kinase acts upstream of p53 in response to DNA damage. *Nature* 394: 700-704, 1998
- Wooster, R., Bignell, G., Lancaster, J., Swift, S., Seal, S., Mangion, J., Collins, N., Gregory, S., Gumbs, C., and Micklem, G. Identification of the breast cancer susceptibility gene BRCA2. *Nature* 378: 789-791, 1995
- Xiong, Y., Hannon, G.J., Zhang, H., Casso, D., Kobayashi, R., and Beach, D. p21 is a universal inhibitor of cyclin kinases. *Nature* 366: 701-704, 1993

- Yin, Y., Terauchi, Y., Solomon, G.G., Aizawa, S., Rangarajan, P.N., Yazaki, Y., Kadowaki, T., and Barrett, J.C. Involvement of p85 in p53-dependent apoptotic response to oxidative stress. *Nature* 391: 707-710, 1998
- Yonish-Rouach, E., Resnitzky, D., Lotem, J., Sachs, L., Kimchi, A., and Oren, M. Wild-type p53 induces apoptosis of myeloid leukemic cells that is inhibited by interleukin-6. *Nature* 352: 345-347, 1991
- van der Zee, A.G., Hollema, H., Suurmeijer, A.J., Krans, M., Sluiter, W.J., Willemse, P.H., Aalders, J.G., and de Vries, E.G. Value of P-glycoprotein, glutathione S-transferase pi, c-erbB-2, and p53 as prognostic factors in ovarian carcinomas. *J. Clin. Oncol.* 13: 70-78, 1995
- Zhan, Q., Antinore, M.J., Wang, X.W., Carrier, F., Smith, M.L., Harris, C.C., Fornace, A.J. Association with Cdc2 and inhibition of Cdc2/Cyclin B1 kinase activity by the p53-regulated protein Gadd45. *Oncogene* 18: 2892-900, 1999
- Zhang, H., Hannon, G., and Beach, D. p21-containing cyclin kinases exist in both active and inactive states. *Gene Dev.* 8: 1750-1758, 1994
- Zhang, Y., Xiong, Y., and Yarbrough, W.G. ARF promotes MDM2 degradation and stabilizes p53: ARF-INK4a locus deletion impairs both the Rb and p53 tumor suppression pathways. *Cell* 92: 725-734, 1998
- Zheng, J., Benedict, W., Xu, H., Hu, S., Kim, T., Velicescu, M., Wan, M., Cofer, K., and Dubeau, L. Genetic disparity between morphologically benign cysts contiguous to ovarian carcinomas and solitary cystadenomas. *J. Natl. Cancer Inst.* 87: 1146-1153, 1995
- Zauberman, A., Barak, Y., Ragimov, N., Levy, N., and Oren, M. Sequence-specific DNA binding by p53: identification of target sites and lack of binding to p53-MDM2 complexes. *EMBO J.* 12: 2799-2808, 1993
- Zehbe, I., Voglino, G., Wilander, E., Genta, F., and Tommasino, M. Codon 72 polymorphism of p53 and its association with cervical cancer. *Lancet* 354: 218-219, 1999

DANKSAGUNG

Die vorliegende Arbeit entstand an der Frauenklinik der Charité Campus Virchow-Klinikum der Medizinischen Fakultät der Humboldt-Universität zu Berlin und dem Norris Comprehensive Cancer Center der University of Southern California, Los Angeles, USA.

Mein herzlicher Dank gilt Herrn Professor Dr. med. Werner Lichtenegger, Geschäfts-führender Direktor der Klinik für Frauenheilkunde und Geburtshilfe der Charité, für seine Unterstützung der wissenschaftlichen Untersuchungen dieser Arbeit. Unter seiner Leitung wurde die Frauenklinik der Charité Campus Virchow-Klinikum zu einem national und international bekannten Zentrum für die operative Therapie und Chemotherapie des Ovarialkarzinoms.

Ganz besonders möchte ich Herrn Professor Michael F. Press, MD, PhD, Leiter des pathologisch-molekulargenetischen Labors im Norris Comprehensive Cancer Center der University of Southern California, Los Angeles, USA danken. Durch seine wissenschaftlichen Arbeiten über genetische Alterationen in Mamma- und Ovarialkarzinomen wurde ich auf dieses interessante Thema aufmerksam. In einer über Jahre bestehenden Kollaboration entstand die inhaltliche Konzeption für die vorliegende Studie, die ich im Rahmen eines Fellowships an der USC Los Angeles in seinem Labor durchgeführt habe.

Frau Professor Susan Groshen, PhD am Department of Preventive Medicine des Norris Cancer Center und Conway Gee, Doktorand, möchte ich ganz besonders für die hervorragende statistische Arbeit danken. Durch die anspruchsvolle Analyse der molekulargenetischen Daten in Zusammenhang mit dem follow-up der Patientinnen konnte die klinische Relevanz der Studie dargestellt werden.

Bei allen Mitarbeitern des Labors von Prof. Press und anderen Wissenschaftlern des Norris Cancer Center möchte ich mich für ihre Unterstützung in technischen und inhaltlichen Fragen bedanken, insbesondere Wen H. Wen, PhD, Jason Lukas, PhD, Dorothy Hong, Ning Niu, und Bahman Saffari, MD, PhD. Herrn Ulf Grawunder PhD, möchte ich ganz besonders für seine Hilfe bei der Proteinexpression danken. Herrn Prof. Dr. Ingo Runnebaum, UFK Freiburg, danke ich für seinen Beitrag zur Sequenzierung ausgewählter Fälle.

Ganz herzlich möchte ich auch Frau Dr. Annette Schmider und Frau Uta Kilian danken, die im Rahmen ihrer Promotion einen wichtigen Beitrag zur Erhebung der klinischen Verlaufsdaten und der Labordaten geleistet haben. Für die Unterstützung beim Aufbau einer Tumorgewebebank danke ich Frau Dr. Minguillon und den MTAs

des histologischen Labors der Universitätsfrauenklinik Charlottenburg und der Charité Campus Virchow-Klinikum.

Der Alexander von Humboldt-Stiftung bin ich zu großem Dank verpflichtet, da sie durch ein Feodor-Lynen-Stipendium meinen Forschungsaufenthalt in USA ermöglicht hat. Ich möchte außerdem der Forschungskommission der Medizinischen Fakultät der Humboldt-Universität ganz herzlich danken, daß sie meine wissenschaftliche Tätigkeit durch ein "Rahel Hirsch" Habilitationsstipendium unterstützt hat.

Berlin im April 2001

Dr. Angela Reles

EIDESSTATTLICHE VERSICHERUNG

Gemäß der Habilitationsordnung der Charité

Hiermit erkläre ich, an Eides statt:

- daß keine staatsanwaltlichen Ermittlungsverfahren gegen mich anhängig sind
- daß weder früher noch gleichzeitig ein Habilitationsverfahren durchgeführt oder angemeldet wurde
- daß die vorgelegte Habilitationsschrift ohne fremde Hilfe verfaßt und die beschriebenen Ergebnisse selbst gewonnen wurden
- daß die Zusammenarbeit mit anderen Wissenschaftlerinnen oder Wissenschaftlern und technischen Hilfskräften sowie die Literatur vollständig angegeben sind
- daß mir die geltende Habilitationsordnung bekannt ist

Berlin, den 28.3.2001

Dr. Angela Reles